

AD-A063 795

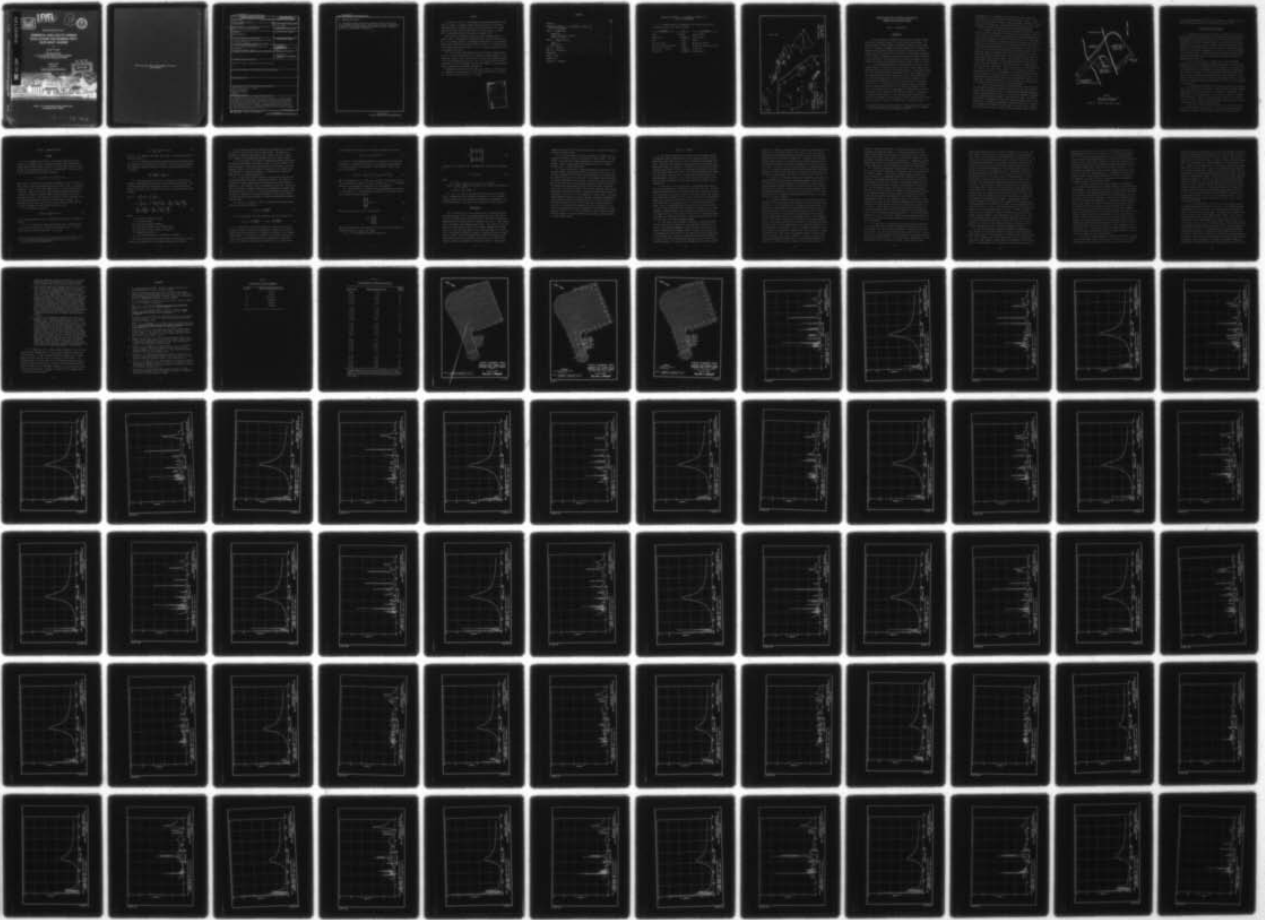
ARMY ENGINEER WATERWAYS EXPERIMENT STATION VICKSBURG MISS F/G 8/3  
NUMERICAL ANALYSIS OF HARBOR OSCILLATIONS FOR BARBERS POINT DEE--ETC(U)  
SEP 78 D L DURHAM  
WES-TR-H-78-20

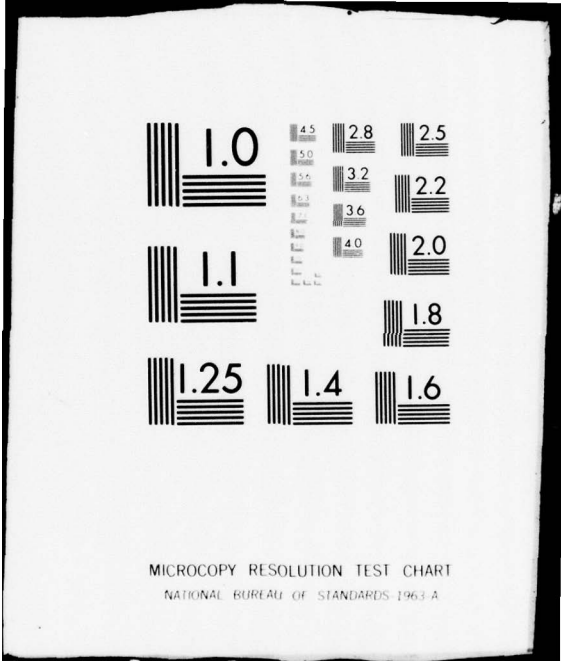
UNCLASSIFIED

NL

1 OF 3

AD  
A063 795





MICROCOPY RESOLUTION TEST CHART  
NATIONAL BUREAU OF STANDARDS-1963-A

T. R. H-78-20

NUMERICAL ANALYSIS OF HARBOR OSCILLATIONS FOR BARBERS POINT DEEP-DRAFT HARBOR

SEPT. 1978

AD A063795

DDC FILE COPY



LEVEL

12  
B.S.



TECHNICAL REPORT H-78-20

# NUMERICAL ANALYSIS OF HARBOR OSCILLATIONS FOR BARBERS POINT DEEP-DRAFT HARBOR

by

Donald L. Durham

Hydraulics Laboratory

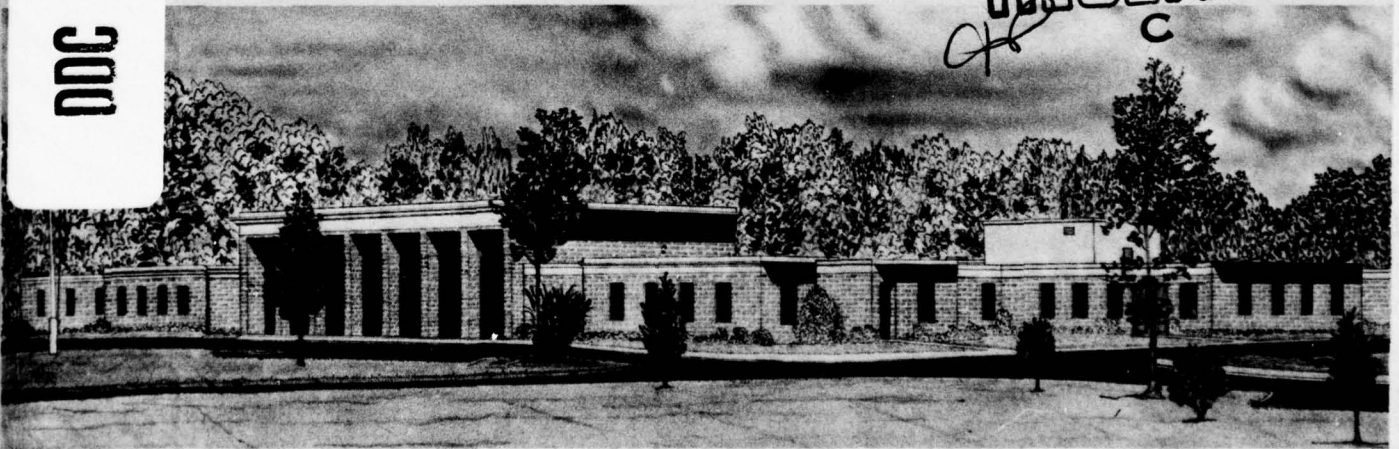
U. S. Army Engineer Waterways Experiment Station  
P. O. Box 631, Vicksburg, Miss. 39180

September 1978

Final Report

Approved For Public Release; Distribution Unlimited

DDC  
RECEIVED  
JAN 26 1979  
C



Prepared for U. S. Army Engineer Division, Pacific Ocean  
Fort Shafter, Hawaii 96858

79 01 26 025

2 . . .

Destroy this report when no longer needed. Do not return  
it to the originator.

Unclassified

SECURITY CLASSIFICATION OF THIS PAGE (When Data Entered)

REPORT DOCUMENTATION PAGE		READ INSTRUCTIONS BEFORE COMPLETING FORM
1. REPORT NUMBER Technical Report H-78-20	2. GOVT ACCESSION NO.	3. RECIPIENT'S CATALOG NUMBER
4. TITLE (and Subtitle) NUMERICAL ANALYSIS OF HARBOR OSCILLATIONS FOR BARBERS POINT DEEP-DRAFT HARBOR	9	5. TYPE OF REPORT & PERIOD COVERED Final report, 1 Jan-1 Apr 78
7. AUTHOR(s) Donald L. / Durham	10	6. PERFORMING ORG. REPORT NUMBER
9. PERFORMING ORGANIZATION NAME AND ADDRESS U. S. Army Engineer Waterways Experiment Station Hydraulics Laboratory P. O. Box 631, Vicksburg, Mississippi 39180		8. CONTRACT OR GRANT NUMBER(s)
11. CONTROLLING OFFICE NAME AND ADDRESS U. S. Army Engineer Division, Pacific Ocean Building 230 Fort Shafter, Hawaii 96858		10. PROGRAM ELEMENT, PROJECT, TASK AREA & WORK UNIT NUMBERS
14. MONITORING AGENCY NAME & ADDRESS (if different from Controlling Office) 14 WES-TR-H-78-20		12. REPORT DATE 14 September 1978
		13. NUMBER OF PAGES 205
		15. SECURITY CLASS. (of this report) Unclassified
		15a. DECLASSIFICATION/DOWNGRADING SCHEDULE
16. DISTRIBUTION STATEMENT (of this Report) Approved for public release; distribution unlimited.		
17. DISTRIBUTION STATEMENT (of the abstract entered in Block 20, if different from Report)		
18. SUPPLEMENTARY NOTES		
19. KEY WORDS (Continue on reverse side if necessary and identify by block number) Barbers Point, Hawaii -- Harbor Deep draft harbors Harbor oscillations Harbors Mathematical models		
20. ABSTRACT (Continue on reverse side if necessary and identify by block number) A hybrid finite element numerical model was used to calculate harbor resonance for a proposed deep-draft harbor at Barbers Point, Oahu, Hawaii. The numerical model calculates forced harbor oscillations for harbors of arbitrary shape and variable depth. A numerical finite element grid with 2,334 elements was used to compute wave-height amplification factors and normalized maximum current velocities associated with the harbor's response to incident waves from 20 sec to 27 min.		

(Continued)

DD FORM 1 JAN 73 1473 EDITION OF 1 NOV 65 IS OBSOLETE

Unclassified  
SECURITY CLASSIFICATION OF THIS PAGE (When Data Entered)

038-100

JOB

Unclassified

SECURITY CLASSIFICATION OF THIS PAGE(When Data Entered)

20. ABSTRACT (Continued)

can → The numerical model calculations identified resonant oscillations of the proposed deep-draft harbor. Based on model results, inferences as to potential ship movement, navigation problems, and harbor circulation were made for the resonant oscillations.

Unclassified

SECURITY CLASSIFICATION OF THIS PAGE(When Data Entered)

PREFACE

A request for the U. S. Army Engineer Waterways Experiment Station (WES) to conduct a numerical harbor oscillation study of a proposed deep-draft harbor at Barbers Point, Oahu, was made by the U. S. Army Engineer Division, Pacific Ocean (POD), in a letter dated 13 August 1976. Funds were authorized by POD on 23 December 1977.

This study was conducted during the period 1 January 1977 to 1 April 1977 in the Hydraulics Laboratory, WES, under the direction of Mr. H. B. Simmons, Chief of the Hydraulics Laboratory, Dr. R. W. Whalin, Chief of the Wave Dynamics Division (WDD), and Mr. C. E. Chatham, Chief of the Harbor Wave Action Branch. Mr. D. L. Durham conducted the study and prepared this report.

Mr. R. R. Bottin (WDD) prepared the finite element numerical grid. Mr. K. A. Turner (WDD) developed the computer plotting programs for the frequency response curves and assisted in reduction and computer graphics of the numerical model results. Mr. J. R. Houston (WDD) assisted in conversion of computer programs to a CDC-7600 computer at the Air Force Weapons Laboratory at Kirtland, New Mexico.

Commander and Director of WES during the conduct of the study and the preparation and publication of this report was COL John L. Cannon, CE. Technical Director was Mr. F. R. Brown.

ACCESSION for	
NTIS	Video Version <input checked="" type="checkbox"/>
DDC	Ball Search <input type="checkbox"/>
UNANNOUNCED	<input type="checkbox"/>
JUSTIFICATION	
BY	
ELECTRONICALLY SIGNED	
DATE	
INITIAL	
A	

CONTENTS

	<u>Page</u>
PREFACE . . . . .	1
CONVERSION FACTORS, U. S. CUSTOMARY TO METRIC (SI)	
UNITS OF MEASUREMENT . . . . .	3
PART I: INTRODUCTION . . . . .	5
Background . . . . .	5
Harbor Oscillation Problem . . . . .	8
Purpose of Study . . . . .	10
PART II: NUMERICAL MODEL . . . . .	11
Theory . . . . .	11
Application . . . . .	15
PART III: RESULTS . . . . .	17
PART IV: CONCLUSIONS . . . . .	24
REFERENCES . . . . .	26
TABLES 1 AND 2	
PLATES 1-173	
APPENDIX A: NOTATION	



CONVERSION FACTORS, U. S. CUSTOMARY TO METRIC (SI)  
UNITS OF MEASUREMENT

U. S. customary units of measurement used in this report can be converted to metric (SI) units as follow:

<u>Multiply</u>	<u>By</u>	<u>To Obtain</u>
acres	4046.856	square metres
cubic feet	0.02831685	cubic metres
feet	0.3048	metres
feet per second	0.3048	metres per second
feet per second per second	0.3048	metres per second per second
miles (U. S. statute)	1.609344	kilometres
square feet	0.09290304	square metres

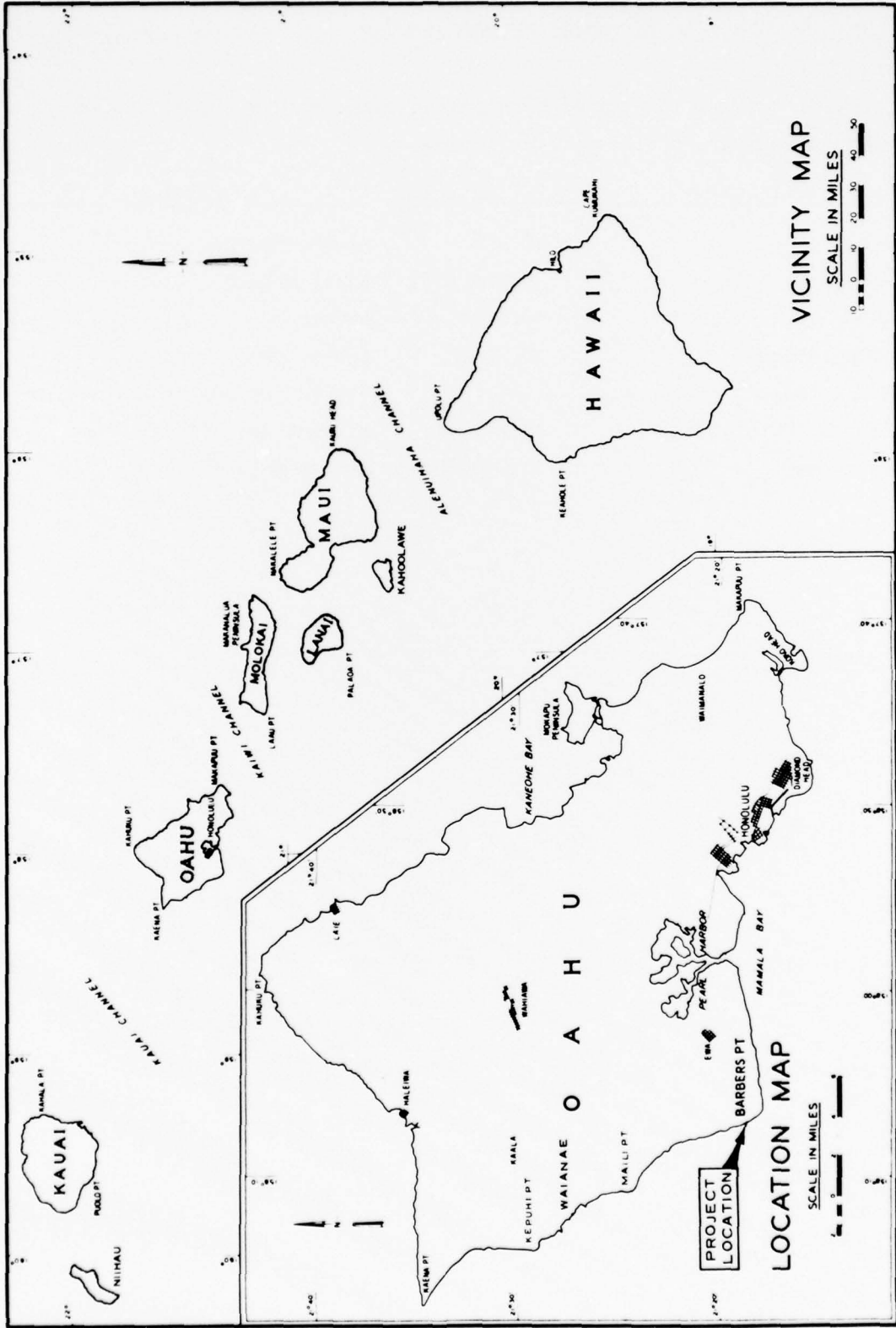


Figure 1. Location of Barbers Point Harbor

NUMERICAL ANALYSIS OF HARBOR OSCILLATIONS FOR  
BARBERS POINT DEEP-DRAFT HARBOR

PART I: INTRODUCTION

Background

1. Oahu's economy is integrated with the other islands of Hawaii and with the national economy of the continental United States. The local and State economy depends on waterborne commerce as the primary source of transport. Although waterborne commerce will continue to be centered around Honolulu Harbor, the projected volume of waterborne commerce for Oahu reveals a need to provide a second harbor at Barbers Point by 1995 to accommodate containerized cargo that cannot be handled by Honolulu Harbor and thus provide the facilities necessary to accommodate an efficient and uninterrupted flow of goods in and out of Oahu.<sup>1</sup>

2. The existing barge harbor at Barbers Point is located at the southern extent of the west coast of the Island of Oahu, Hawaii, and is approximately 16 miles\* west of Honolulu (Figure 1). This existing harbor is an L-shaped area which was dredged in the coral formation of the flat coastal plain by private interests in 1960. The existing harbor has horizontal dimensions of 520 ft by 700 ft with a depth of 21 ft. The entrance has dimensions of 1100 ft by 220 ft with a controlling depth of 22 ft. The construction of a deep-draft harbor at Barbers Point was authorized by Section 301 of the River and Harbor Act of 1965.<sup>1</sup> The authorized plan of improvement, as described in the Chief of Engineers report dated 5 October 1964, provides for a 450-ft-wide, 42-ft-deep entrance channel to a 38-ft-deep, 46-acre harbor basin which could accommodate a 633-ft-long C-4 class vessel and met the 1965 commerce needs for a harbor at Barbers Point. A hydraulic model

---

\* A table of factors for converting U. S. customary units of measurement to metric (SI) units is presented on page 3.

investigation<sup>2</sup> of the Barbers Point Harbor Project was conducted in 1967-1968 by the Look Laboratory of the University of Hawaii. These model studies indicated a nearly trapezoidal shaped, 38-ft-deep, 77-acre basin with a 450-ft-wide, 42-ft-deep entrance channel was a most effective harbor and would adequately serve the 1968 shipping needs.

3. Because of the long time interval between authorization of the project in 1965 and changes in the economic and environmental conditions of the project area as well as in Corps water resource planning policies, a post-authorization study<sup>1</sup> was conducted by the U. S. Army Engineer District, Honolulu, to assess the past basic planning decisions for Barbers Point deep-draft harbor and to provide a harbor project which could respond to these changes. This post-authorization study indicated a need<sup>3</sup> for a basin which is larger than the original design of the deep-draft harbor for Barbers Point and would be capable of accommodating the Enterprise class (720 ft long) container vessels as well as future 900-ft-long container ships. Using concepts resulting from the 1968 hydraulic model study<sup>2</sup> of the original deep-draft harbor design, a new harbor plan (Figure 2) was developed by the U. S. Army Engineer Division, Pacific Ocean (POD). This plan provides for an entrance channel 4,280 ft long, 450 ft wide, and 42 to 38 ft deep with a 94-acre harbor basin 38 ft deep. The alignment of the entrance channel allows the incorporation of a major portion of the existing barge harbor. The proposed harbor configuration can provide approximately 4,400 lin ft of docks with a 4,800-ft-long section of the northwest and southeast sides of the entrance channel and basin having wave absorbers.

4. With the post-authorization study indicating a need and design for a harbor basin which is larger than previously analyzed and model-tested,<sup>2</sup> POD requested that the U. S. Army Engineer Waterways Experiment Station (WES) determine the effects of the basin enlargement on surging in the proposed deep-draft harbor. From historical data, the existing barge harbor has experienced long-period surging problems of about 2-min wave periods. Therefore, the proposed deep-draft harbor can be expected to be subjected to long-period wave energy of at least 2 min. The natural oscillation periods, in particular the fundamental oscillation, of

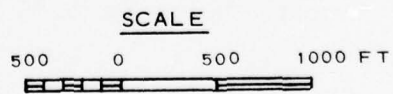
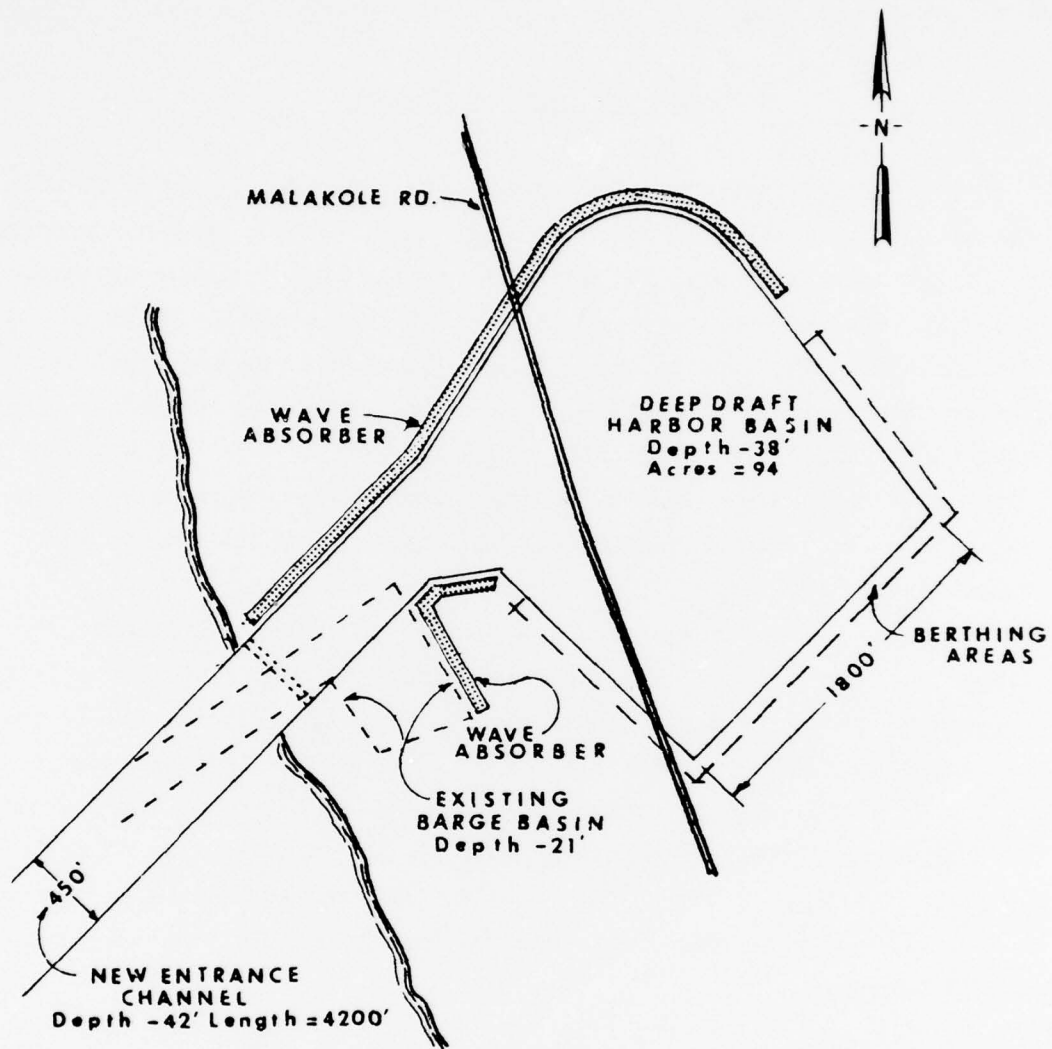


Figure 2. Proposed deep-draft harbor

the proposed deep-draft harbor need to be defined to determine potential harbor resonance especially near oscillation periods of 2 min.

#### Harbor Oscillation Problem

5. A harbor excited by long waves with a period close to its natural oscillation period experiences a resonant reaction that may produce wave heights in the harbor far greater than the incident wave heights. Generally, the vertical movement of water in the harbor is still only a few tenths of a foot due to the very small incident long-wave heights. However, the horizontal movement of water may cover a much greater distance (up to two orders of magnitude) as a result of the long wavelength of the incident waves. Such horizontal water movements cause surge and sway motion of moored ships that may hamper unloading operations and damage mooring facilities.

6. A few of the harbors on the west coast of the continental United States and in the Hawaiian Islands have histories of ship motion problems resulting from resonant harbor oscillations. It is likely that the long-period waves responsible for exciting harbor oscillations permeate the Pacific Basin. Lack of modern harbor development may prevent the occurrence of significant problems for most coastal areas of the Pacific. Many places that have a problem may merely tolerate it through ignorance of possible remedial measures with the result that the problem goes unreported.

7. The generating mechanism of the very small amplitude long waves that excite harbors is still unknown. However, Munk's surf-beat theory<sup>4</sup> suggested an attractive explanation of the origin of these waves. Surf beats result from the superposition of two trains of waves of slightly different period. The beats are an amplitude modulation of a shorter period wave train. Swell, for example, almost always exhibits an irregular beating up to several minutes in period.

8. Carr<sup>5</sup> argued that local surf beat could not cause the long-period waves known to excite harbors. Although the surf-beat process produces a long-period vertical water motion, the really important

factor of long-period horizontal water motion is lacking in surf beats. Severe harbor surging also is known to occur during otherwise calm seas with identical long-period wave activity reported along hundreds of miles of a coastline. Carr maintained that such activity is not compatible with long-period wave generation by local surf beat.

9. True long-period wave trains may be generated from surf beats through nonlinear processes in the surf zone. Munk<sup>4</sup> estimated that beaches reflected 1 percent of the energy incident upon them in the form of these long-period waves. It is perhaps these waves reflected from distant shores of the Pacific which cause oscillation problems in harbors on the west coast of the continental United States and in the Hawaiian Islands. Long-period wave activity would then increase after distant storms of the south or west Pacific Ocean created large swell conditions and the resulting surf beat generated long-period wave trains in the surf zone which reflected off shorelines. Wilson<sup>6</sup> has noted that oscillations in Los Angeles and Long Beach Harbors have seasonal fluctuations of frequency and intensity which are greatest during the summer months and least during the winter. He noted that such a pattern is almost identical with that found for Table Bay Harbor, Cape Town, South Africa, and suggests that the storms in the Southern Hemisphere are responsible for the long-period waves.

10. Evidence that long-period wave trains exist from time to time as a general ocean condition and are not generated by local surf beats comes from a harbor study for San Nicholas Bay, Peru.<sup>7</sup> It was concluded from horizontal water velocity measurements that long-period waves affecting San Nicholas Harbor were progressive waves unassociated with the concurrent swell waves. In addition, a recent study<sup>8</sup> of prototype wave energy in the Los Angeles and Long Beach Harbors indicates ship movement in the sheltered East Channel of Los Angeles Harbor was correlated with long-period (2.2 and 6.5 min) harbor oscillations. Furthermore, observed energy levels in long-period harbor oscillations within the harbors were correlated with energy levels in incident long-period waves.

### Purpose of Study

11. The purpose of this study is to investigate harbor oscillations excited by long waves with periods from 20 sec to 10-15 min (fundamental mode) using a finite element numerical model. The new harbor configuration (known as Plan 3 in "Design Memorandum No. 1, Plan Formulation"<sup>1</sup>) of the proposed deep-draft harbor at Barbers Point was studied to ensure that the expansion would not cause undesirable oscillations in the existing barge harbor or characteristic oscillations of its own that were undesirable.

12. The amplification peaks predicted by the numerical model may be much larger than the peaks which actually occur in nature, since the model neglects all dissipative processes except radiation of energy by a harbor. However, the model adequately predicts the relative severity of various modes of oscillation. Therefore, the results could be used to compare oscillation characteristics in the vicinity of the barge harbor with the proposed deep-draft harbor installed with oscillations characterizing only the existing barge harbor, provided such information is available. In addition, model results for currents in areas of the proposed deep-draft harbor, as well as the barge harbor, can be used to indicate docking areas which may have potential ship motion problems. Ship movement associated with slow-drift oscillation of the ship mooring system to amplitude modulation of swell cannot be detected from results of this numerical model.



## PART II: NUMERICAL MODEL

### Theory

13. The response,  $\eta(x,y,\omega)^*$ , of the proposed deep-draft harbor (Figure 2) at Barbers Point to long-wave excitation was determined by using a hybrid finite element numerical model developed recently by Chen and Mei at the Massachusetts Institute of Technology.<sup>9</sup> The model solves the following generalized Helmholtz equation:

$$\nabla \cdot [h(x,y)\nabla\phi(x,y)] + \frac{\omega^2}{g} \phi(x,y) = 0 \quad (1)$$

where  $\phi(x,y)$  is the velocity potential defined by  $U(x,y) = -\nabla\phi(x,y)$ , with  $U(x,y)$  being a two-dimensional velocity vector and  $\omega$  an angular frequency,  $h(x,y)$  is the water depth, and  $g$  is the acceleration due to gravity. Equation 1 governs small amplitude undamped oscillations of water in a basin of arbitrary shape and variable depth forced by periodic long waves. This equation is derived from the linearized long-wave equation assuming irrotational flow and harmonic motion. The boundary condition along the shoreline and/or harbor perimeter is that the normal component of the velocity be equal to zero.

14. The Helmholtz equation:

$$\nabla^2\phi(x,y) + \frac{\omega^2}{gh} \phi(x,y) = 0 \quad (2)$$

is the governing equation for a constant-depth ocean region outside the basin.

15. For a harbor in a semi-infinite ocean with a straight coastline, there is an incident, reflected, and scattered wave. The scattered wave has a velocity potential  $\phi_s$  given by

---

\* For convenience, symbols and unusual abbreviations are listed and defined in the Notation (Appendix A).

$$\phi_s = \sum_{n=0}^{\infty} \alpha_n H_n(kr) \cos n\theta \quad (3)$$

where  $\alpha_n$  are unknown coefficients and  $H_n(kr)$  are Hankel functions of the first order  $n$ .

16.  $\phi_s$  satisfies the radiation condition that the scattered wave must behave as an outgoing wave at infinity. This condition is known as the Sommerfeld radiation condition and may be expressed mathematically as follows:

$$\lim_{r \rightarrow \infty} \sqrt{r} \left( \frac{\partial}{\partial r} - ik \right) \phi_s = 0 \quad (4)$$

17. Chen and Mei used a calculus of variations approach and obtained a Euler-Lagrange formulation of the boundary value problem. The following functional with the property that it is stationary with respect to arbitrary first variations of  $\phi(x,y)$  was constructed by Chen and Mei:

$$\begin{aligned} F(\phi) = & \iint 1/2 \left[ h(\nabla\phi)^2 - \frac{\omega^2}{g} \phi^2 \right] dA \\ & + 1/2 \oint \left[ h(\phi_R - \phi_I) \frac{\partial(\phi_R - \phi_I)}{\partial n_a} \right] da - \oint \left[ h\phi_a \frac{\partial(\phi_R - \phi_I)}{\partial n_a} \right] da \\ & - \oint \left[ h\phi_a \frac{\partial\phi_I}{\partial n_a} \right] da + \oint \left[ h\phi_I \frac{\partial(\phi_R - \phi_I)}{\partial n_a} \right] da \end{aligned} \quad (5)$$

where

$A$  = the region inside the harbor

$\oint$  = the line integral

$\phi_R$  = far field velocity potential

$\phi_I$  = velocity potential of the incident wave

$n_a$  = unit normal vector outward from region  $A$

$a$  = boundary of region  $A$

$\phi_a$  = total velocity potential evaluated on boundary  $a$

18. Proof was given by Chen and Mei that the stationarity of this functional is equivalent to the original boundary value problem.

19. The integral equation obtained from extremizing the functional is solved by utilizing the finite element method. This method is a technique of numerical approximation that involves dividing a domain into a number of nonoverlapping subdomains which are called elements.

20. The solution of the problem is approximate within each element by suitable interpolation functions in terms of a finite number of unknown parameters. These unknown parameters are the values of the field variable  $\phi(x,y)$  at a finite number of points which are called nodes. The relations for individual elements are combined into a system of equations for all unknown parameters.

21. In the region outside the basin, the velocity potentials are solved analytically in terms of unknown coefficients. The region is considered a single element with an "interpolation function" given by Equation 3. The infinite series is terminated at some finite value such that the addition of further terms does not significantly influence the calculated values of  $\phi(x,y)$ . The resulting equation is combined with the system of equations for unknown parameters at nodal points within the basin and this complete system is solved using Gaussian elimination matrix methods.

22.  $\eta(x,y)$  is related to  $\phi(x,y)$  through the linearized dynamic free surface boundary condition

$$\eta(x,y) = - \frac{1}{g} \frac{\partial \phi(x,y)}{\partial t} \quad (6)$$

23. The horizontal velocity components have the following form:

$$u(x,y) = - \frac{g}{\omega} \frac{\partial \eta(x,y)}{\partial x} \quad ; \quad v(x,y) = \frac{-g}{\omega} \frac{\partial \eta(x,y)}{\partial y} \quad (7)$$

24. The hybrid finite element method (so named by Chen and Mei because the method involves the combination of analytical and finite element numerical solutions) is a steady-state solution of the boundary value problem. The response of a harbor to an arbitrary forcing function can be easily determined within the framework of a linearized theory. For example, an arbitrary incident wave at the harbor mouth

in the absence of the harbor can be Fourier decomposed as follows:

$$b_0(t) = \int_{-\infty}^{\infty} b(\omega) e^{-i\omega t} d\omega \quad (8)$$

If  $\eta(x,y,\omega)$  is the response amplitude at any point  $(x,y)$  inside the harbor due to an incident plane wave of unit amplitude and frequency  $\omega$ , then the response of the harbor to the arbitrary incident wave  $b_0(t)$  is given by

$$\xi(x,y,t) = R_e \left[ \int_{-\infty}^{\infty} b(\omega) \eta(x,y,\omega) e^{-i\omega t} d\omega \right] \quad (9)$$

where the operation  $R_e[ ]$  takes the real part of the bracketed quantity. Therefore, as soon as  $\eta(x,y,\omega)$  is known for all  $\omega$ , the harbor response to an arbitrary incident wave can be calculated.

25. Velocities<sup>10</sup> are calculated using the expressions in Equation 7. The slope of  $\eta$  may be obtained at any point  $(x,y)$  within an element through the matrix equation

$$\begin{bmatrix} \frac{\partial \eta}{\partial x} \\ \frac{\partial \eta}{\partial y} \end{bmatrix} = G(\eta)^e \quad (10)$$

where the matrix vector  $(\eta)^e$  is defined as

$$(\eta)^e = \begin{bmatrix} \eta_i \\ \eta_j \\ \eta_k \end{bmatrix} \quad (11)$$

and the coordinates of the three nodes  $(i,j,k)$  forming the elements are defined as  $(x_i, y_i)$ ,  $(x_j, y_j)$ , and  $(x_k, y_k)$ .

26.  $G$  is the element slope matrix defined as

$$G = \begin{bmatrix} \frac{\partial N_i}{\partial x} & \frac{\partial N_j}{\partial x} & \frac{\partial N_k}{\partial x} \\ \frac{\partial N_i}{\partial y} & \frac{\partial N_j}{\partial y} & \frac{\partial N_k}{\partial y} \end{bmatrix} \quad (12)$$

and matrix  $N$  is known as the "interpolation" function and is defined as

$$N = (N_i, N_j, N_k) \quad (13)$$

where

$$N_i = [(x_k y_j - x_j y_k) + (y_k - y_j)x + (x_j - x_k)y] / 2\Delta$$

$N_j, N_k$  = similar expressions obtained by the cyclical permutation of  $i, j, \text{ and } k$

$\Delta$  = area of the element  $A^e$

27. The  $(\eta)^e$  matrix is known from the finite element computations. Together with the interpolation function  $N$ , the horizontal velocity at any point  $(x,y)$  within an element can be determined. Velocities presented in this report were calculated at element centers.

#### Application

28. The surface area of the proposed (Plan 3) deep-draft harbor including entrance channel and existing barge harbor was discretized using 2,334 elements with 1,277 nodal points. The finite element grid approximating the proposed harbor is presented in Plate 1. The elements are all triangular and frequently equilateral. The lengths of the triangle sides were selected such that the largest elements had lengths equal to or less than one-eighth of the local wavelength for a 20-sec wave. Such element lengths were judged to provide sufficient accuracy<sup>11</sup> for this study. Smaller dimensions were selected for elements along docking facilities and wave absorbers as well as in the vicinity of changes in depth and alignment of channels and basins. These smaller

elements were chosen to allow spatial resolution of geometric changes or variations in water depths.

29. The water depths in the entrance channel and basins were represented by discrete values at the centroid of each element. For each element, the chosen water depth represented an average value over the element. These discrete depths were taken from Plate 2 of "Design Memorandum No. 1, Plan Formulation."<sup>1</sup>

30. Waves incident from a direction parallel to the axis of the entrance channel (approximately S45°W) with periods from 15 sec to 27 min were considered in this study. Wave amplitudes at each nodal point and current velocities at the centroid of each element were calculated for various increments in wave period. The initial values for the wave period increment over specified period ranges are presented in Table 1. For example, wave amplitudes and current velocities were calculated every 1 sec for the period range of 20 to 68 sec. Resonant peaks within each period range were defined by considering incident wave periods in increments of 0.02 sec to 0.1 sec depending on period range. The finite element numerical model has several important advantages compared with other numerical harbor oscillation models (i.e. Lee and Raichlen<sup>12</sup>). The numerical model allows a variable depth and excellent geometric resolution. Furthermore, the computational time requirement for the model is substantially less than computational times required by other numerical models.<sup>11</sup> It is the only numerical harbor oscillation model presently available that can economically calculate resonance effects in large complex harbors.

### PART III: RESULTS

31. The harbor response is calculated for each incident wave by the numerical harbor oscillation model with results available for wave amplitude at each nodal point and current velocity at each element centroid. These data from the large finite element grid for Barbers Point deep-draft harbor are voluminous. Therefore, 30 node points and element centroids were chosen for which wave amplitudes and current velocities for each incident wave were saved. These nodes and elements were chosen such that their locations were in harbor areas of major interest for ship docking and navigation. The location and station number for the 30 node points and element centroids are presented in Plates 2 and 3, respectively.

32. For each of the 30 node points, a wave-height amplification factor was determined for wave periods from 15 sec to 27 min. The wave-height amplification factor is defined at any point inside the harbor as the wave height at that point divided by twice the incident wave height. This traditional definition results from the fact that the standing wave height for a straight coast with no harbor would be twice the incident wave height due to the superposition of the incident and reflected waves. Plots of wave-height amplification factors versus wave period for each of the 30 node points are presented in Plates 4-63. For convenience of graphic display, the wave periods have been divided into two ranges of 15 sec to 70 sec and 70 sec to 27 min. Thus, each elevation station or node point has plots of wave-height amplification factors over each of the two wave period ranges.

33. For each of the 30 element centroids, a normalized maximum current velocity was determined for each wave period from 15 sec to 27 min. The normalized maximum current velocity at any point in the harbor is defined as the maximum current velocity over one period of the standing wave (oscillation) in the harbor divided by the amplitude of the incident wave. Since the numerical harbor oscillation model is based on the linearized long-wave equation, the velocities have no vertical variation. In addition, the mathematical form of the current

velocity of a harmonic, long-period wave is directly proportional to the amplitude of the long-period wave in the harbor. Hence, the current velocity associated with the harbor oscillation can be normalized for convenience by the incident wave amplitude. Therefore, the normalized maximum current velocity at any point in the harbor multiplied by the incident wave amplitude in feet gives maximum current velocity in feet per second. For each of the 30 velocity stations or element centroids, plots of the normalized maximum current velocity versus wave period are presented in Plates 64-123 with each velocity station having plots over the two wave period ranges of 15 sec to 70 sec and 70 sec to 27 min.

34. Based on the frequency (wave period) response curves for wave-height amplification factors and normalized maximum current velocity, the wave periods of peak responses can be determined. These peak responses represent resonant effects of the harbor response to incident long-period wave energy. The wave periods of the more important resonant peaks between 20 sec and 27 min are listed in Table 2. For each resonant peak, the maximum wave-height amplification factor in the harbor also is listed in Table 2.

35. The most prominent characteristic of the deep-draft harbor's response is the main resonant peak occurring at a period of 799.0 sec. This peak is a very broad peak in its response over wave periods. Its broadness is characterized by the wave-height amplification response being larger than 1.0 over the wave period range of 9 min to 27 min. This broad response over wave period is characteristic of the forced harbor response whose period is approximately equal to the fundamental period of the natural oscillation of the harbor. The broad characteristic of this resonant peak is very important in determining the harbor response since it allows amplification of incoming wave energy over a very broad band of wave periods. For this resonant response the deep-draft harbor is experiencing a "pumping mode" type oscillation in which the water-surface level inside the deep-draft harbor rises and falls almost uniformly. This type of movement in the water surface can be detected by comparing the magnitude of the wave-height amplification factors at elevation stations 1 through 18 for the wave period of



799.0 sec. Minimal differences in wave-height amplification exist throughout the deep-draft harbor. In contrast, comparison of wave-height amplification along the axis of the entrance channel (elevation stations 9-23) shows a major decrease in wave-height amplification as the mouth of the entrance channel is approached. A comparison of wave-height amplification in the barge harbor (elevation stations 24-30) indicates only small or minor differences throughout the barge harbor.

36. Contours of wave-height amplification factors over the entire grid are an excellent technique of representing the modal configuration of a harbor response. This graphic technique depicts very well the spatial variation of wave-height amplification throughout the harbor. Contours of wave-height amplification for the 799.0-sec incident wave are presented in Plate 124. Contours of wave-height amplification for other resonant peaks (listed in Table 2) are presented in Plates 125-148. For the 799.0-sec harbor oscillation, contours of wave-height amplification vividly indicate the changes in wave-height amplification in the deep-draft harbor, entrance channel, and barge harbor without considering individually the changes at each elevation station. The "pumping mode" effect of the deep-draft harbor is illustrated in these contours by the water-surface elevations changing nearly simultaneously throughout the basin and having nearly the same relative magnitude of 7.5 to 8.5. A large change in water-surface elevation exists in the entrance channel as evidenced by rapid changes in relative magnitudes (7.0 to 2.0) of wave-height amplification factors. In the barge harbor, changes (4.0 to 5.0) in relative magnitudes of wave-height amplification are less than in the entrance channel and are nearly the same over much of the basin.

37. At any point in the harbor, horizontal velocities (Equation 7) can be calculated from the pressure gradients associated with the spatial changes of the water-surface elevations or wave-height amplification factors. For each of the resonant peaks, listed in Table 2, vector plots of the normalized maximum current velocities throughout the harbor are plotted in Plates 149-173. The velocities are represented by arrows whose centers lie at the element centroids. Water particles move

horizontally back and forth in a direction parallel to the arrows. The total length of the two vectors is equal to twice the velocity magnitude. Since the velocities have been normalized by the amplitude of the incident wave, the velocities are in units of feet per second per foot of incident wave amplitude. For the 799.0-sec harbor oscillation, the velocity vector plot in Plate 149 indicates strong velocities (25 to 30 fps/ft of incident wave amplitude) in the entrance channel and much smaller velocities in the deep-draft harbor. Normalized velocities in the deep-draft harbor vary from 0.5 to 1.0 fps/ft along the NE and SE berthing areas and 2 to 10 fps/ft along the SW berthing area. In the barge harbor, normalized velocities vary from 2.5 to 15 fps/ft with velocities near the entrance channel having magnitudes greater than 20 fps/ft. These normalized velocities appear upon first inspection to be extremely large. However, to obtain absolute velocity magnitudes, these normalized velocities must be multiplied by the amplitude of the incident wave. For long-period waves (greater than 25- to 30-sec wave periods) excluding tsunamis, the incident wave energy and/or amplitude is extremely low and generally not known. Durham et al.<sup>8</sup> measured incident long-period wave energy at the breakwater of Los Angeles and Long Beach Harbors and estimated such energy to be approximately of the order of  $10^{-4}$  sq ft or less. Using these estimates, the associated wave heights would be approximately 0.01 ft or less. Therefore, maximum velocities for the 799-sec oscillation, excited by such incident wave energy, could be expected to have magnitudes less than 0.50 fps. However, for extreme energy levels in incident long-period waves, such as a tsunami, this broad resonant peak of 799.0 sec (13.32 min) has the potential to produce not only relatively large fluctuations in water-surface elevations but large velocities throughout the harbor.

38. The 799.0-sec harbor oscillation produces a "pumping mode" type response in the deep-draft harbor and has an average wave-height amplification factor of approximately 7.5 throughout the deep-draft harbor. Such a response over a large surface area of 94 acres produces a relatively large exchange of water between the deep-draft harbor and the ocean. A rough estimate of the total water volume exchanged during one

complete cycle (799.0 sec or 13.32 min) of this harbor oscillation is approximately  $60 \times 10^6$  cu ft of water for a 1-ft incident wave amplitude. For incident wave amplitudes of 0.01 ft, the exchanged water volume would be approximately 600,000 cu ft which is still a significant amount of water. Such volume transports of water should benefit the flushing and circulation of the deep-draft harbor (provided such long-period wave energy exists to excite this harbor oscillation). It is anticipated from Reference 8 that such small energy levels exist practically all the time. Consequently, it is reasonable to assume an exchange of water of approximately 600,000 cu ft every 13.32 min due to the response of the 799.0 sec mode of oscillation to the background long-period energy level of about  $10^{-4}$  ft<sup>2</sup>.

39. Detailed information about ship movement in the deep-draft harbor cannot be obtained from the resonant response of the harbor without knowledge of the incident wave spectrum and the moored ship response as a function of wave amplitude and period. However, general information concerning potential ship motion within the deep-draft harbor can be inferred from resonant responses of the harbor and available information<sup>8</sup> concerning moored ship motion. Although the precise degrees of ship movement cannot be inferred, potential surge and sway motion can be inferred from velocity patterns in each berthing area. Velocity vectors parallel to the berths can potentially cause surge movement while vectors perpendicular can cause sway movement. The amount of such movement depends upon the mooring response of ship and incident wave energy. Except for extreme levels of incident wave energy, the ship movement in the deep-draft harbor for the 799.0-sec oscillation will be dominated by surge movement which should be relatively small along the NE and SE berthing areas with an increase in surge movement along the SW berthing area. In the barge harbor, both surge and sway motion may exist and could be substantially larger for barges and smaller vessels than ship movement in the deep-draft harbor.

40. For each resonant response of the deep-draft harbor, the contours of wave-height amplification factors and vector plots of normalized maximum current velocity can be utilized to deduce information

similar to the above information for the 799.0-sec resonant oscillation. The other resonant peaks have responses over a much narrower wave period band than the fundamental (799.0 sec) harbor response. The resonant peak at the 145.0-sec wave period is slightly broader than the remaining peaks but is much smaller in response amplitude in the deep-draft harbor. However, for the barge harbor, this resonant peak has wave-height amplification factors equal to those of the 799.0-sec harbor response. All remaining resonant peaks, especially resonant peaks below 100.0-sec wave periods, are extremely narrow and sharp and will amplify only small amounts of incoming wave energy. Therefore, these very sharp resonant peaks are probably not important in deep-draft loading and unloading operations. The first five resonant peaks in Table 2 have relatively simple oscillation patterns with resonant peaks below 100.0 sec producing more complex patterns. For the deep-draft harbor, 129.5-sec and 81.9-sec resonant oscillations produce wave-height amplifications of 9.5 to 11.0. Very narrow peaks at 45.85, 40.805, 23.0, and 22.48 sec produce amplifications of 12 to 20 in the deep-draft harbor. The remaining resonant peaks produce amplification factors of 9 or less in the deep-draft harbor.

41. For the barge harbor, the first four resonant peaks produce wave-height amplification factors of 4.5 to 5.5. The largest amplification factors of 14.5 and 15.03 in the barge harbor are produced by the 81.9- and 19.4-sec resonant peaks. The remaining 19 resonant peaks, which are very narrow, produce amplification factors of 2 or less in the barge harbor with the exceptions of 63.0-, 35.92-, 34.92-, 23.0-, 22.48-, and 19.6-sec peaks which produce maximum amplifications of 6.3, 10.22, 12.93, 7.74, 5.0, and 8.46, respectively. Since the barge harbor has experienced 2-min oscillations in past history, resonant peaks at 145.0, 129.5, and 107.2 sec can be expected to be excited by incident long-period wave energy. In addition, resonant peaks near the first (1 min) and second (30 sec) harmonics of the 2-min oscillations may also be excited. Such oscillations, including the relatively large 81.9-sec oscillation, have the potential to produce ship movement (surge and sway) which for smaller vessels such as barges, may be adverse to cargo

handling. If the response of the existing barge harbor without the construction of the deep-draft harbor were known, a comparison of the harbor response from this study with the existing barge harbor response would be very beneficial in evaluating the relative effects of construction of the deep-draft harbor on the response in the barge harbor.

#### PART IV: CONCLUSIONS

42. Investigation of the response of the proposed Barbers Point deep-draft harbor by use of a hybrid finite-element variable depth numerical model has resulted in the following conclusions:

- a. Twenty-five resonant peaks ranging in period from 19.4 to 799.0 sec were identified.
- b. The deep-draft harbor is characterized by a predominant resonant peak at 799.0 sec (13.32 min). This peak exhibits amplification factors from 7.5 to 8.5 throughout the deep-draft harbor and represents a "pumping mode" type of harbor response. This peak has a half-width (width of the frequency band for which the response is at least half the peak response) of about 4-5 min; consequently, it will respond to a wide range of wave periods.
- c. Flushing and circulation in the deep-draft harbor should be aided by the characteristic (799.0 sec) resonant peak. This "pumping mode" will aid in flushing the harbor by exchanging water between the harbor and the ocean. The magnitude of this exchange is not possible to assess; however, it was shown that it is reasonable to expect water exchange of 600,000 cu ft per wave period (every 13.32 min).
- d. Resonant peaks were identified at periods of 145.0, 129.5, 107.2, and 81.9 sec. These peaks are all close enough to observed oscillations in the existing barge harbor of about 2 min to potentially be excitable. However, the bandwidth of the 129.50- and the 81.90-sec peaks (maximum wave-height amplification of 10.92 and 14.45, respectively) is so small that they probably pose little potential problem. Only incident energy within a very narrow frequency band would be amplified by these modes with their maximum response containing little energy. The 145.0- and 107.2-sec peaks are slightly broader in bandwidth and, consequently, will respond to a broader bandwidth of incident excitation. However, their maximum wave-height amplification is only 4.35 and 5.50, respectively. Therefore, it is concluded that these four resonant peaks probably do not pose a serious threat to day-to-day operation of the proposed deep-draft harbor.
- e. The other 20 resonant peaks identified range in period from 63.00 to 19.40 sec, and nine of these peaks (56.55, 45.85, 40.805, 35.92, 34.92, 23.0, 22.48, 19.6, and 19.4) have wave-height amplification factors between 8.5 and 19.62. All nine of these peaks are relatively narrow in bandwidth and probably do not pose a serious potential

hazard to deep-draft loading and unloading. Any future expansions and modifications of the deep-draft harbor should consider these peaks during the design phase.

- f. Nine resonant peaks occur between 19.40 sec and 23.40 sec with five of these having amplification factors below 3.75. However, the resonant peaks at 23.0, 22.48, 19.6, and 19.4 sec have amplification factors of 19.62, 13.75, 8.46, and 15.03, respectively. The background energy level of the ocean will certainly be greater in this frequency range than for longer period waves since frequency dispersion from swell will undoubtedly transfer energy to these wave periods. Since some smaller shallow-draft ships (such as banana-boats) respond to energy in these relatively low wave periods, there may be some potential for occasional mooring problems for smaller ships (e.g. RoRo). However, if such problems arise, they can probably be handled by special mooring methods or by mooring in locations where velocities from these resonant modes are minimal.
- g. A potential for flooding is indicated as a result of the response of the proposed deep-draft harbor to incident tsunami energy. The predominant resonant peak of 13.32 min (Item b above) with an amplification factor of 7.5 to 8.5 throughout most of the deep-draft harbor could create a situation wherein the harbor's response to incident tsunami energy is such that water elevations will rise above the docks, flood dockside facilities, and inundate adjacent low-lying areas. This potential flooding situation should be studied further to quantify the potential hazard from a tsunami similar to the 1946 Aleutian tsunami which had its major energy centered near this resonant frequency. There have been at least four occurrences (1868, 1946, 1952, and 1957) of tsunamis recorded since about 1837 in the vicinity of Honolulu with periods around 13 min and wave heights approximately 1 ft or higher.

43. To summarize, all 25 resonant peaks between 19.40 sec and the characteristic "pumping mode" of the proposed deep-draft harbor have been identified. It has been determined that probably none of these peaks will pose a serious threat to operation of the harbor. The "pumping mode," 13.32 min, will aid in flushing the harbor and improving water quality of the harbor. However, the broad response (half-width of about 5 min) of the harbor centered at 13.32 min poses a very serious potential threat to damage of property from a tsunami similar to the 1946 Aleutian tsunami.<sup>13</sup>

#### REFERENCES

1. U. S. Army Engineer District, Honolulu, "Design Memorandum No. 1, Plan Formulation," Jul 1976, Honolulu, Hawaii.
2. "Study of Proposed Barbers Point Harbor, Hawaii; Harbor Model Investigation," Technical Report No. 8, Apr 1970, Look Laboratory of Ocean Engineering, University of Hawaii, College of Engineering, Center for Engineering Research, Honolulu, Hawaii.
3. U. S. Army Engineering District, Honolulu, Letter referred PODED-P to Dr. R. W. Whalin, 13 Aug 1976.
4. Munk, W. H., "Surf Beats," Transactions, American Geophysical Union, Vol 30, No. 6, Dec 1949, pp 849-854.
5. Carr, J. H., "Long Period Waves or Surges in Harbors," Transactions, American Society of Civil Engineers, Vol 118, 1953, pp 588-603.
6. Wilson, B. W. et al., "Wave and Surge-Action Study for Los Angeles-Long Beach Harbors," Vol II, Jul 1968, Science Engineering Associates, San Marino, Calif.
7. Keith, J. M. and Murphy, E. J., "Harbor Study for San Nicolas Bay, Peru," Journal, Waterways and Harbors Division, American Society of Civil Engineers, Vol 96, No. WW2, May 1970, pp 251-273.
8. Durham, D. L. et al., "Los Angeles and Long Beach Harbors Model Study; Analyses of Wave and Ship Motion Data," Technical Report H-75-4, Report 3, Jul 1976, U. S. Army Engineer Waterways Experiment Station, CE, Vicksburg, Miss.
9. Chen, H. S. and Mei, C. C., "Oscillations and Wave Forces in an Offshore Harbor (Applications of the Hybrid Finite Element Method to Water-Wave Scattering)," Report No. 190, 1974, Massachusetts Institute of Technology, Cambridge, Mass.
10. Crosby, L. G., Durham, D. L., and Chatham, C. E., Jr., "Expansion of Port Hueneme, California; Hydraulic Model Investigation," Technical Report H-75-8, Apr 1975, U. S. Army Engineer Waterways Experiment Station, CE, Vicksburg, Miss.
11. Houston, J. R., "Numerical Modeling of Resonant Oscillations in Deep Draft Harbors," Research Report H-76-1, Jul 1976, U. S. Army Engineer Waterways Experiment Station, CE, Vicksburg, Miss.
12. Lee, J.-J. and Raichlen, F., "Wave Induced Oscillations in Harbors with Connected Basins," Report No. KH-R-20, Dec 1969, W. M. Keck Laboratory of Hydraulics and Water Resources, California Institute of Technology, Pasadena, Calif.
13. Loomis, H. G., "Tsunami Wave Runup Heights in Hawaii," Report HIG-76-5/NOAA-JTRE-161, May 1976, Hawaii Institute of Geophysics, University of Hawaii, Honolulu, Hawaii.



Table 1

Initial Wave Period Increments

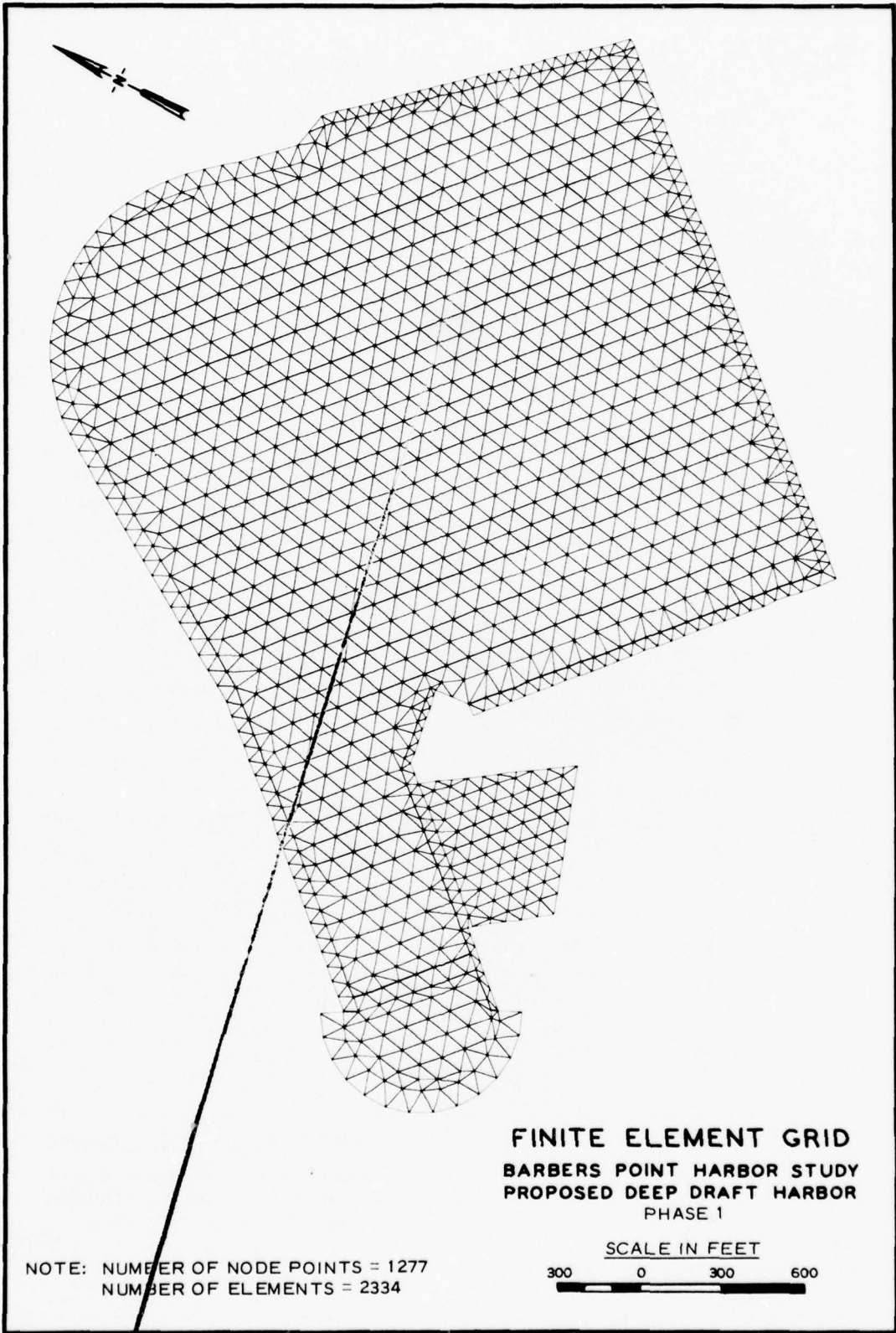
<u><math>\Delta T</math>, sec</u>	<u>Range of Wave Periods, sec</u>
1	15-68
2	70-100
2.5	102.5-200
5	205-360
10	370-720
20	740-1620

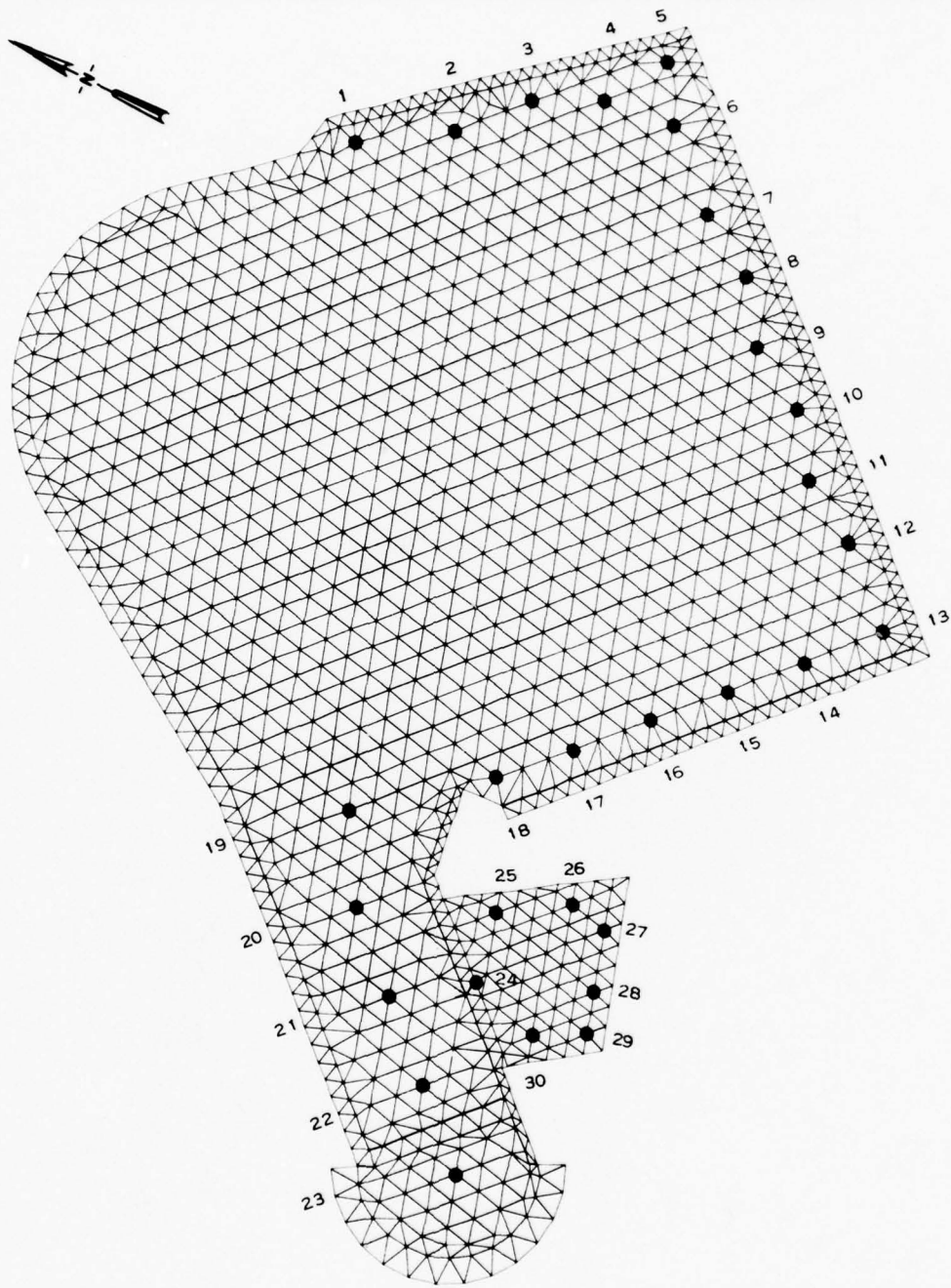
Table 2

Peak Responses of Harbor Oscillations

<u>Period, sec</u>	<u>Maximum Amplification</u>	<u>Nearest Gage*</u>
799.00	8.58	5
145.00	4.35	26
129.50	10.92	13
107.20	5.50	27
81.90	14.45	27
63.00	6.30	27
58.60	5.99	5
56.55	8.63	13
45.85	11.51	5
40.805	13.71	15
35.92	10.22	29
34.92	12.93	29
33.05	3.00	D.D.
30.34	6.00	5
29.42	4.00	3
26.82	6.00	D.D.
23.40	3.50	5
23.00	19.62	13
22.48	13.75	5
22.02	3.75	5
21.12	3.00	D.D.
20.78	3.00	1
20.14	3.00	18
19.60	8.46	28
19.40	15.03	29

\* Maximum amplification values in this table do not agree exactly with those plotted in Plates 4-123 because selected gages did not necessarily coincide exactly with amplification peaks.



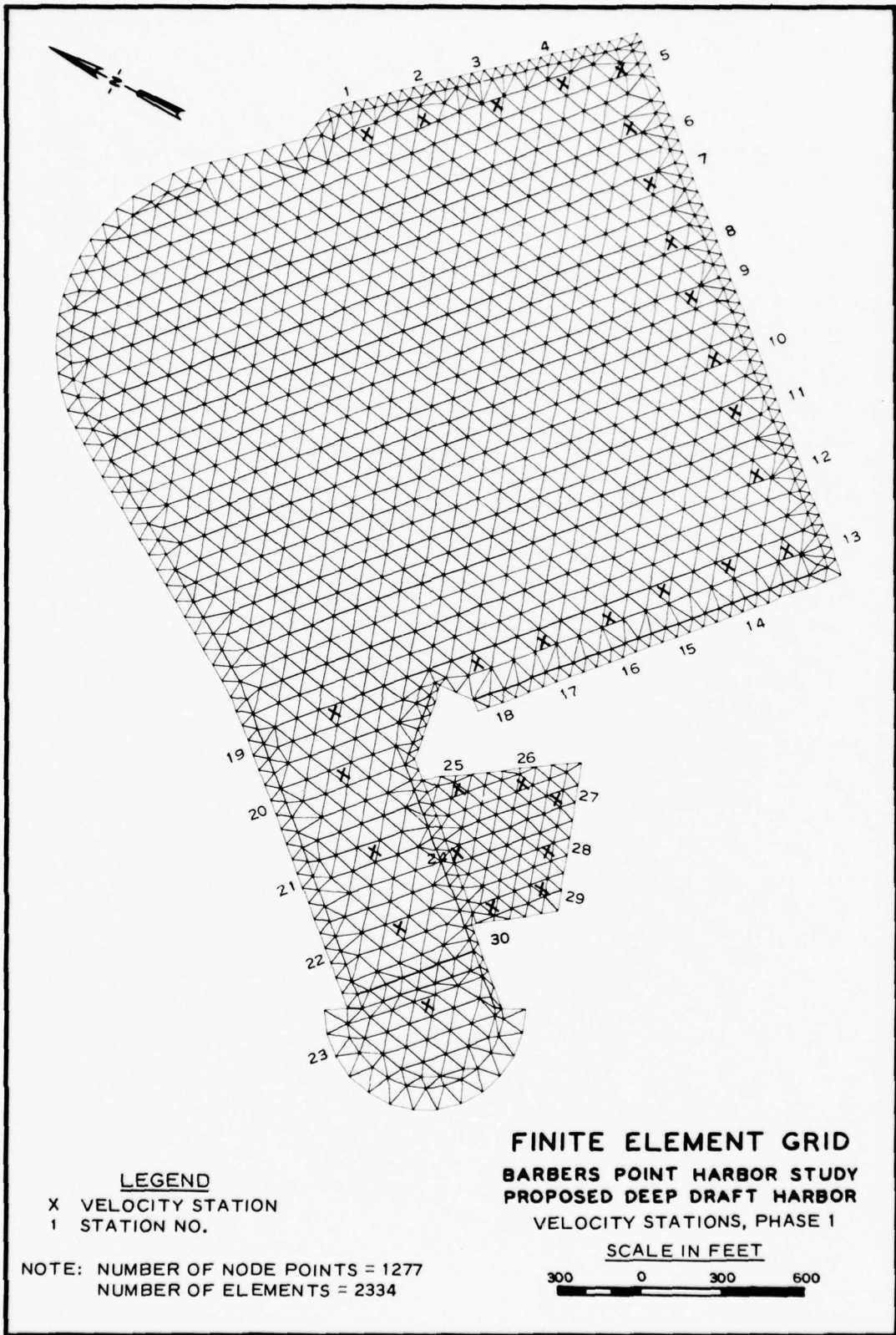


**LEGEND**  
 ● ELEVATION STATION  
 1 STATION NO.

NOTE: NUMBER OF NODE POINTS = 1277  
 NUMBER OF ELEMENTS = 2334

**FINITE ELEMENT GRID**  
**BARBERS POINT HARBOR STUDY**  
**PROPOSED DEEP DRAFT HARBOR**  
 ELEVATION STATIONS, PHASE 1

SCALE IN FEET  
 300 0 300 600



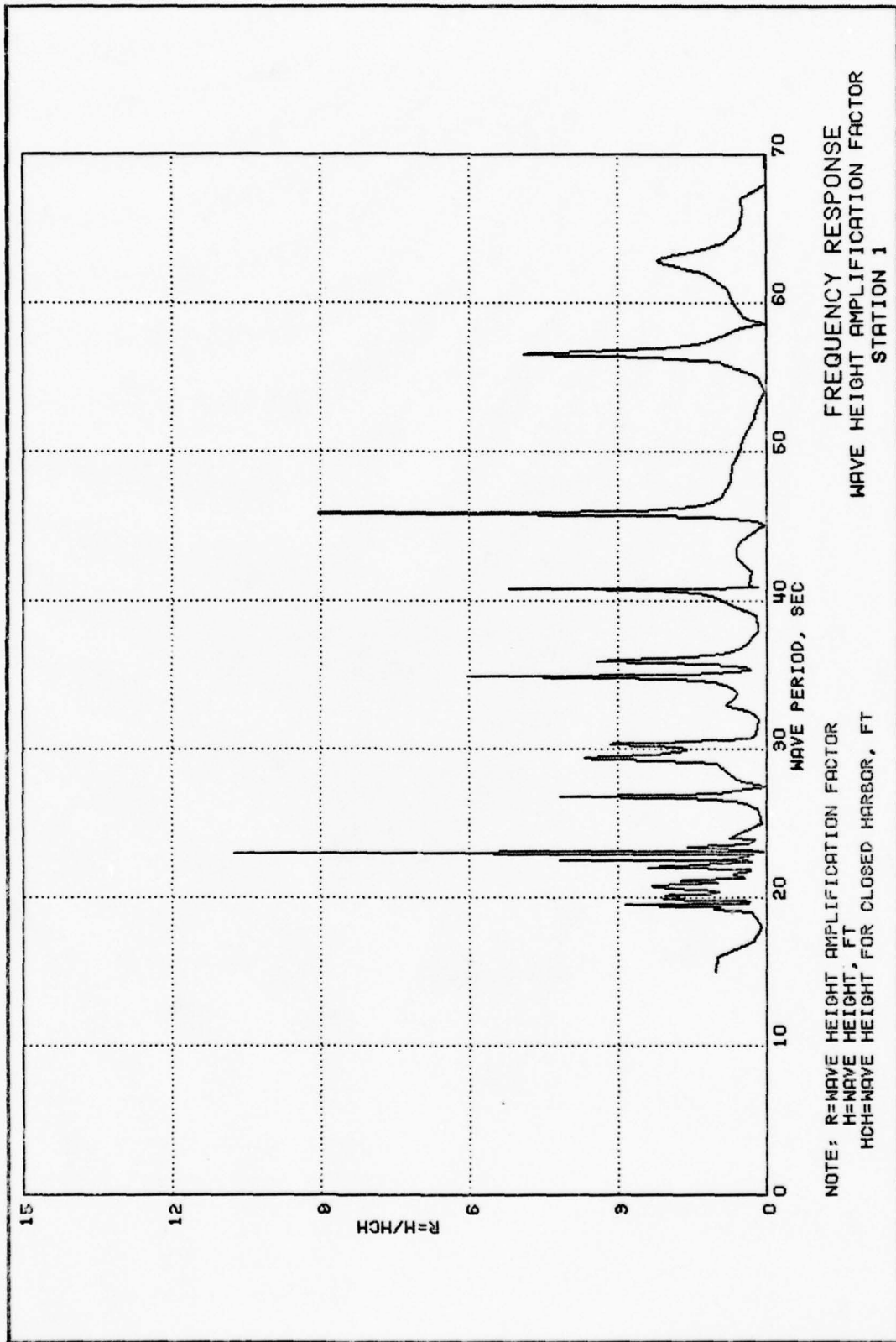


PLATE 4

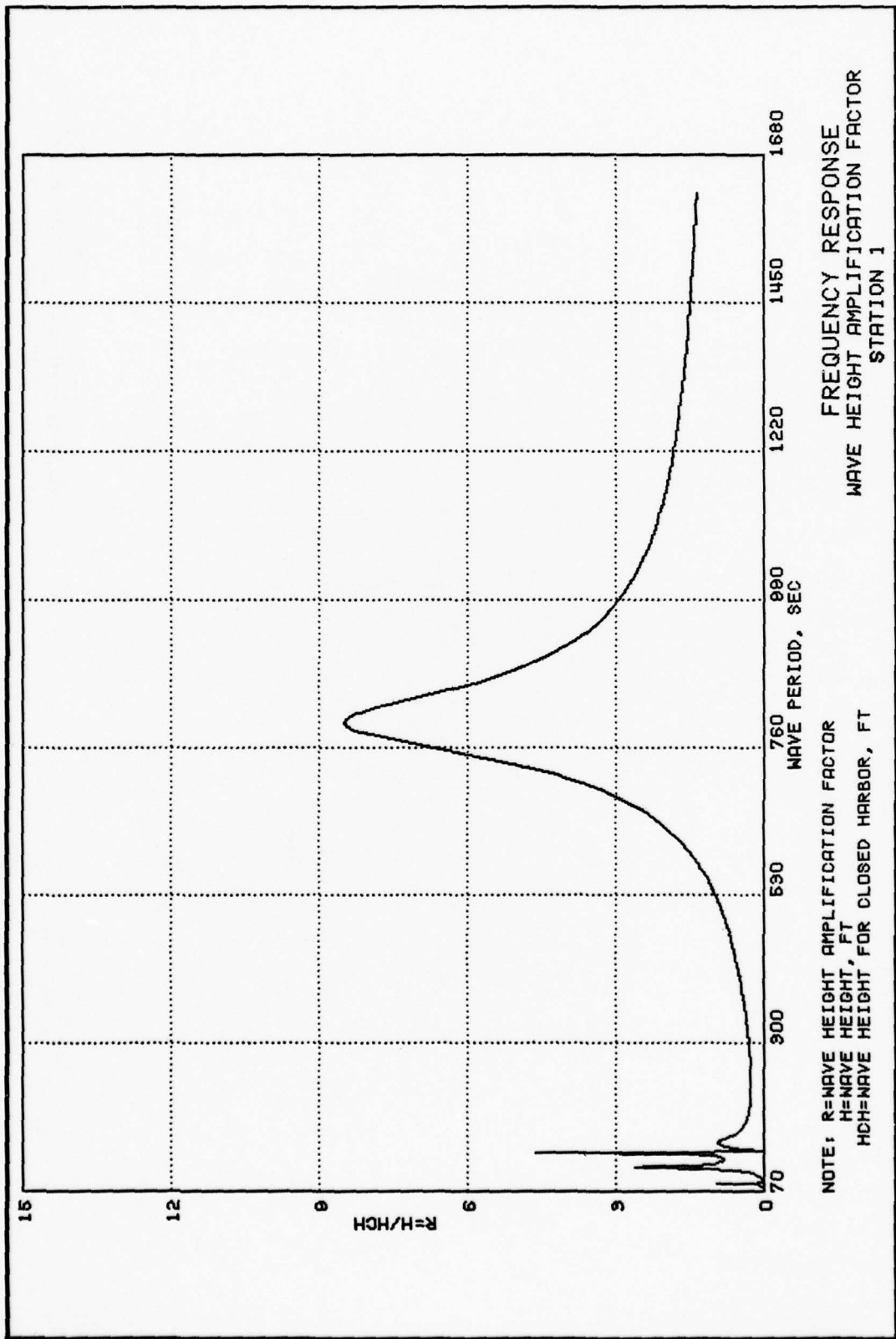


PLATE 5

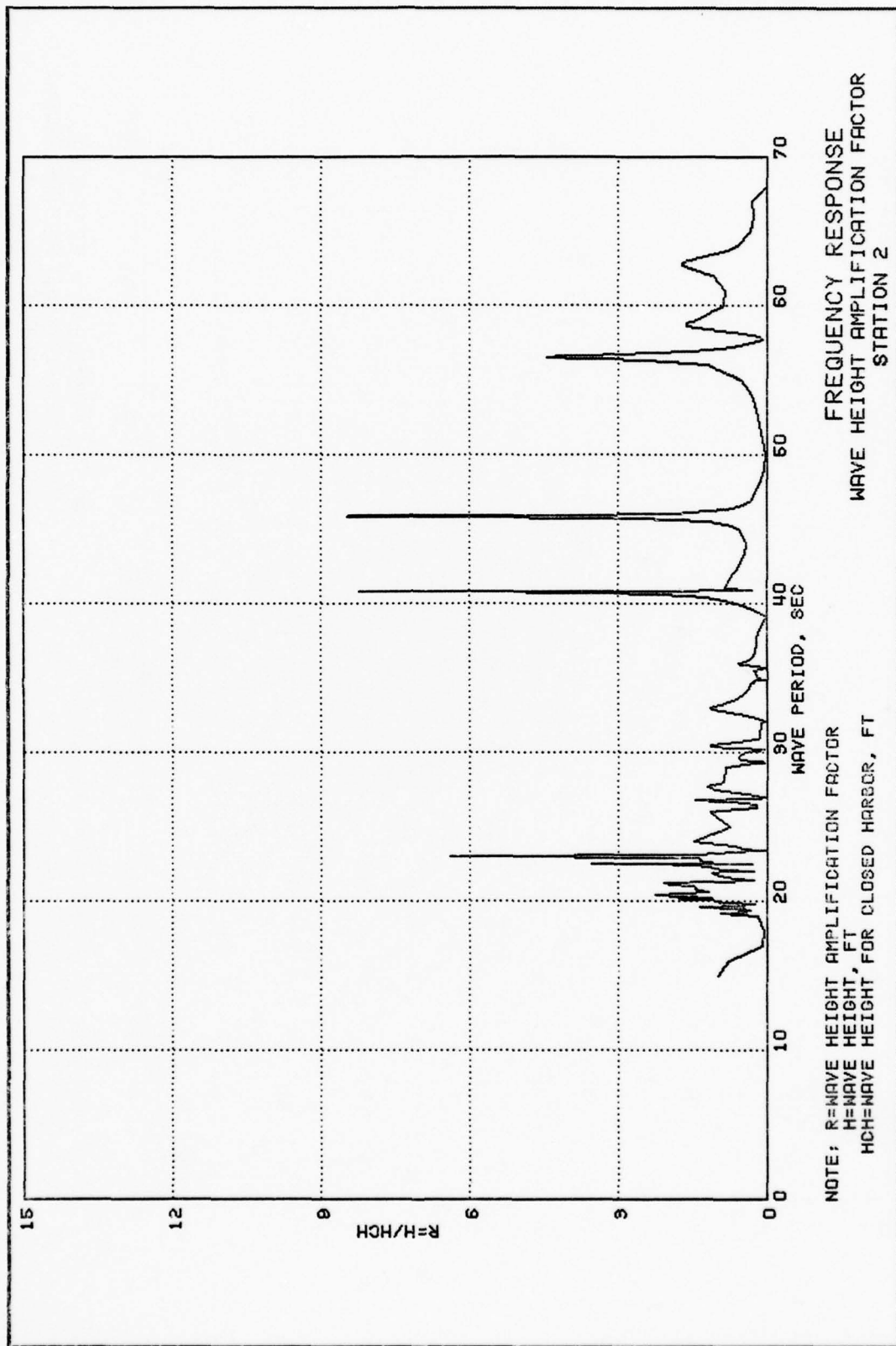
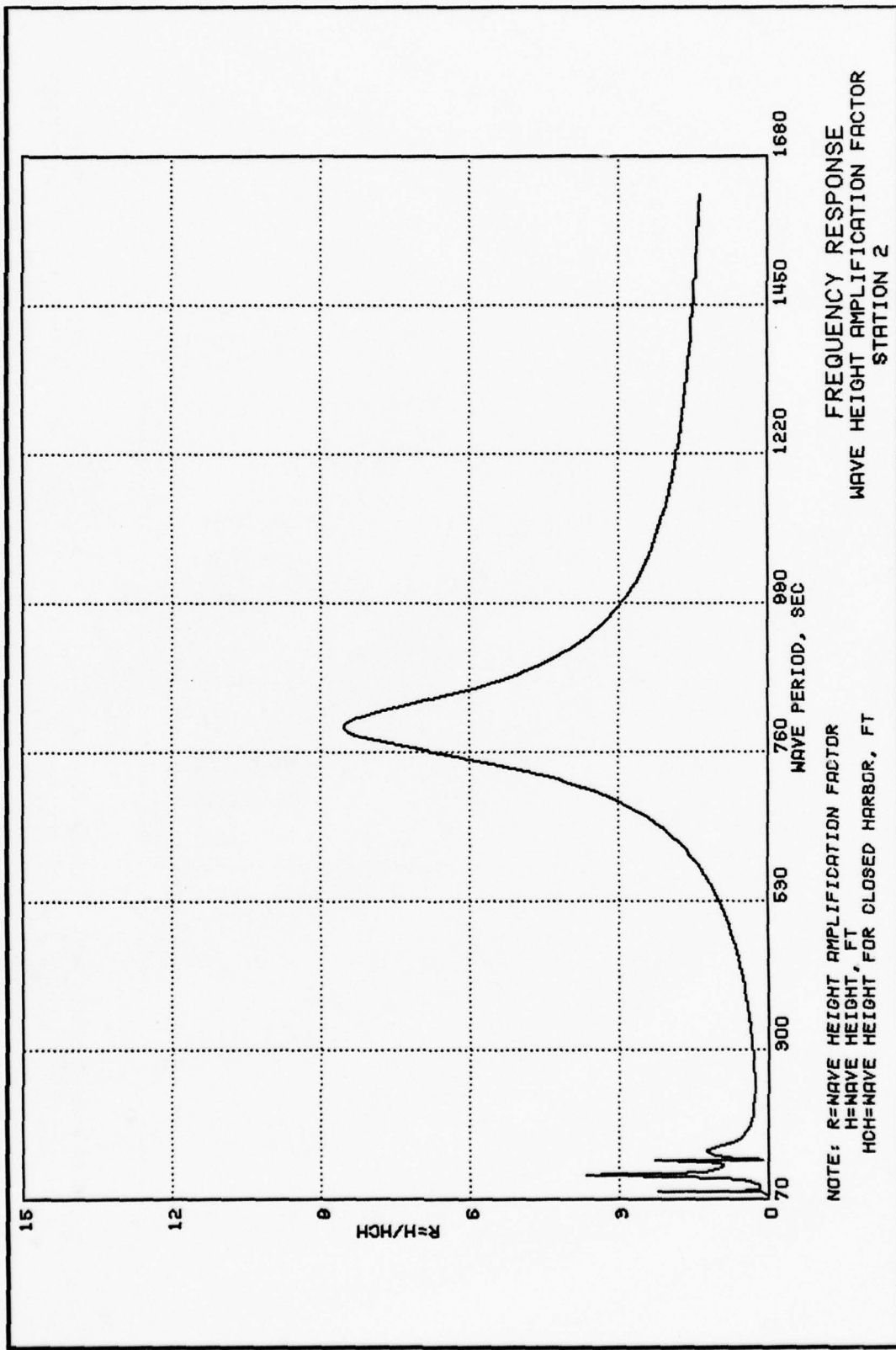


PLATE 6





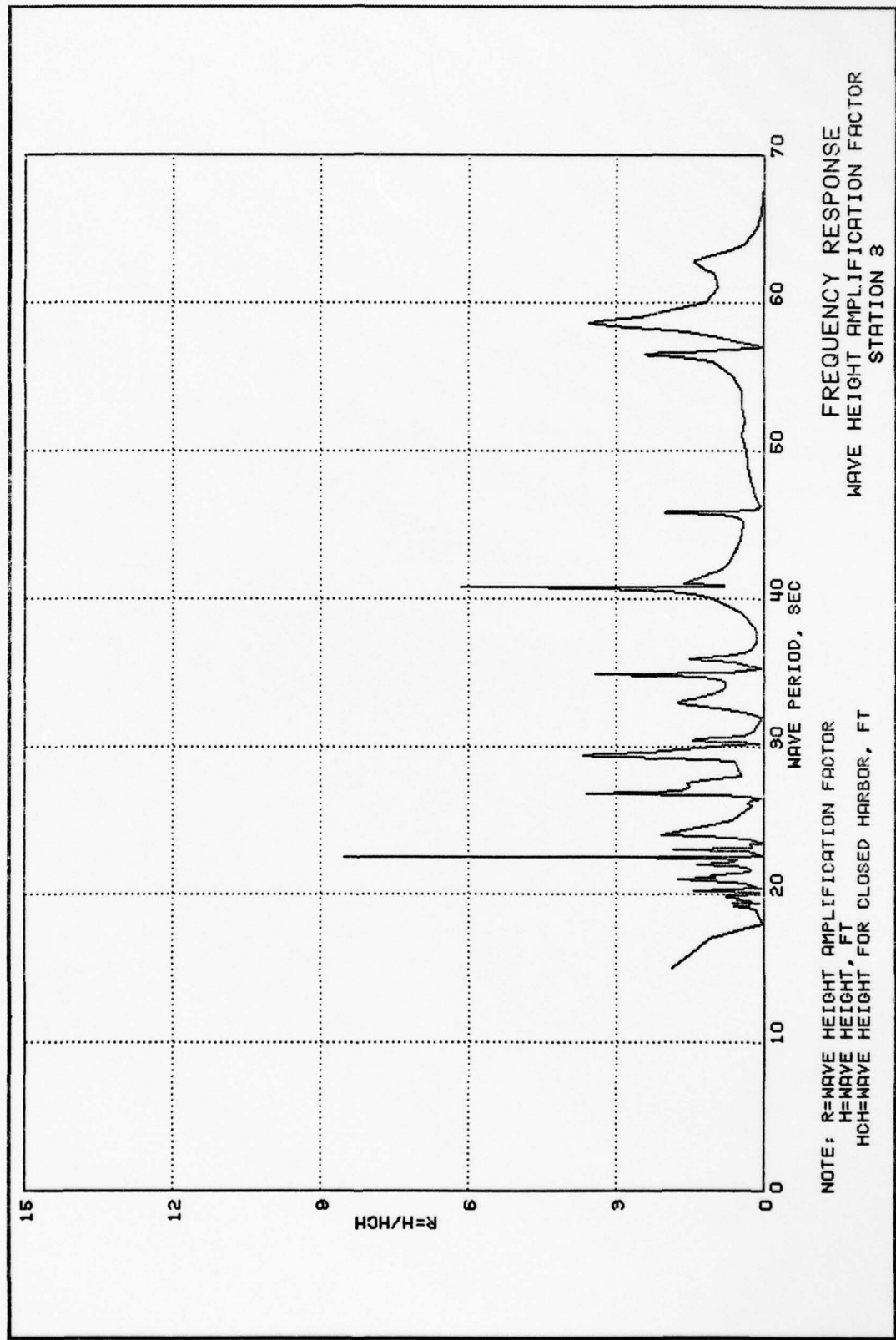
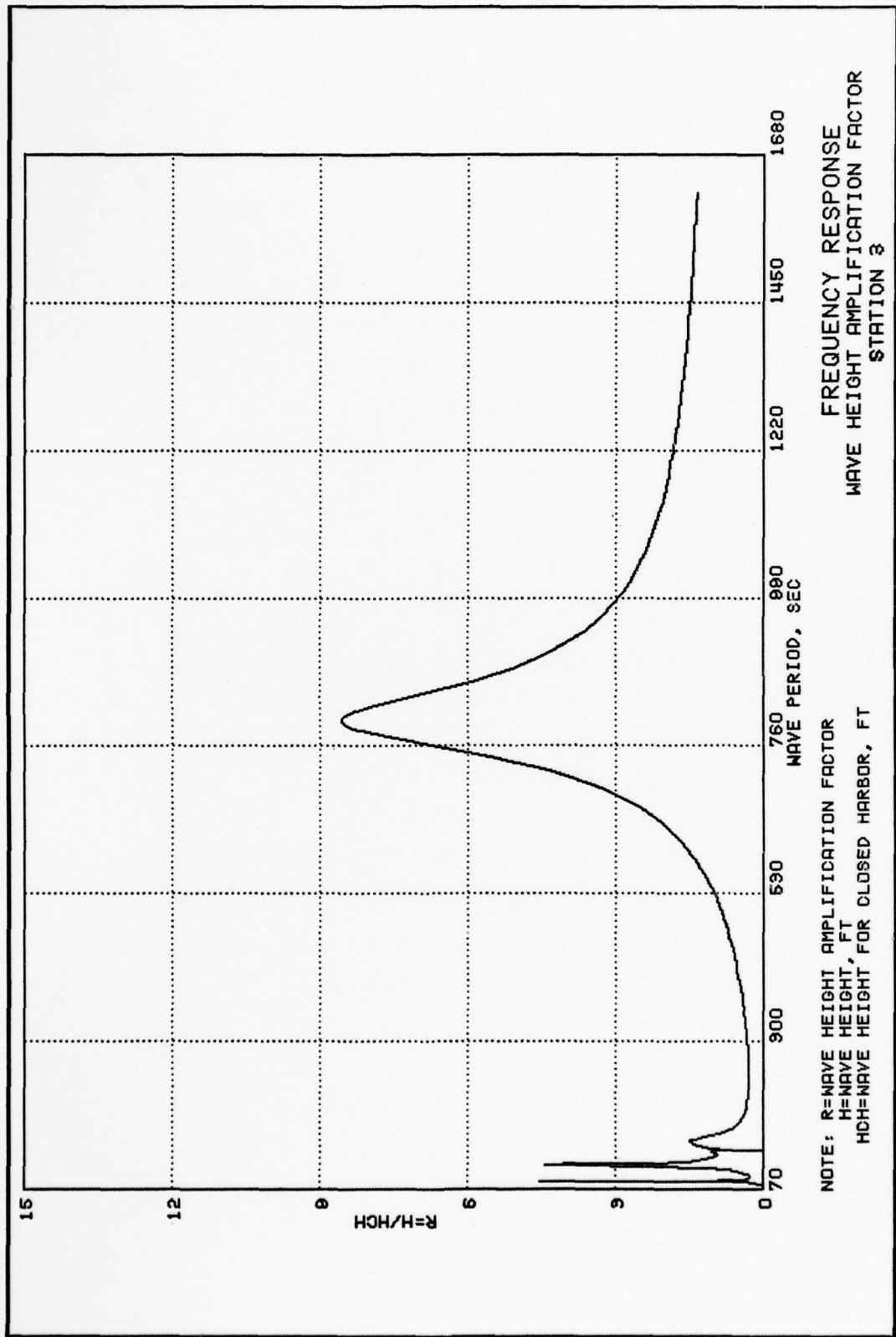


PLATE 8



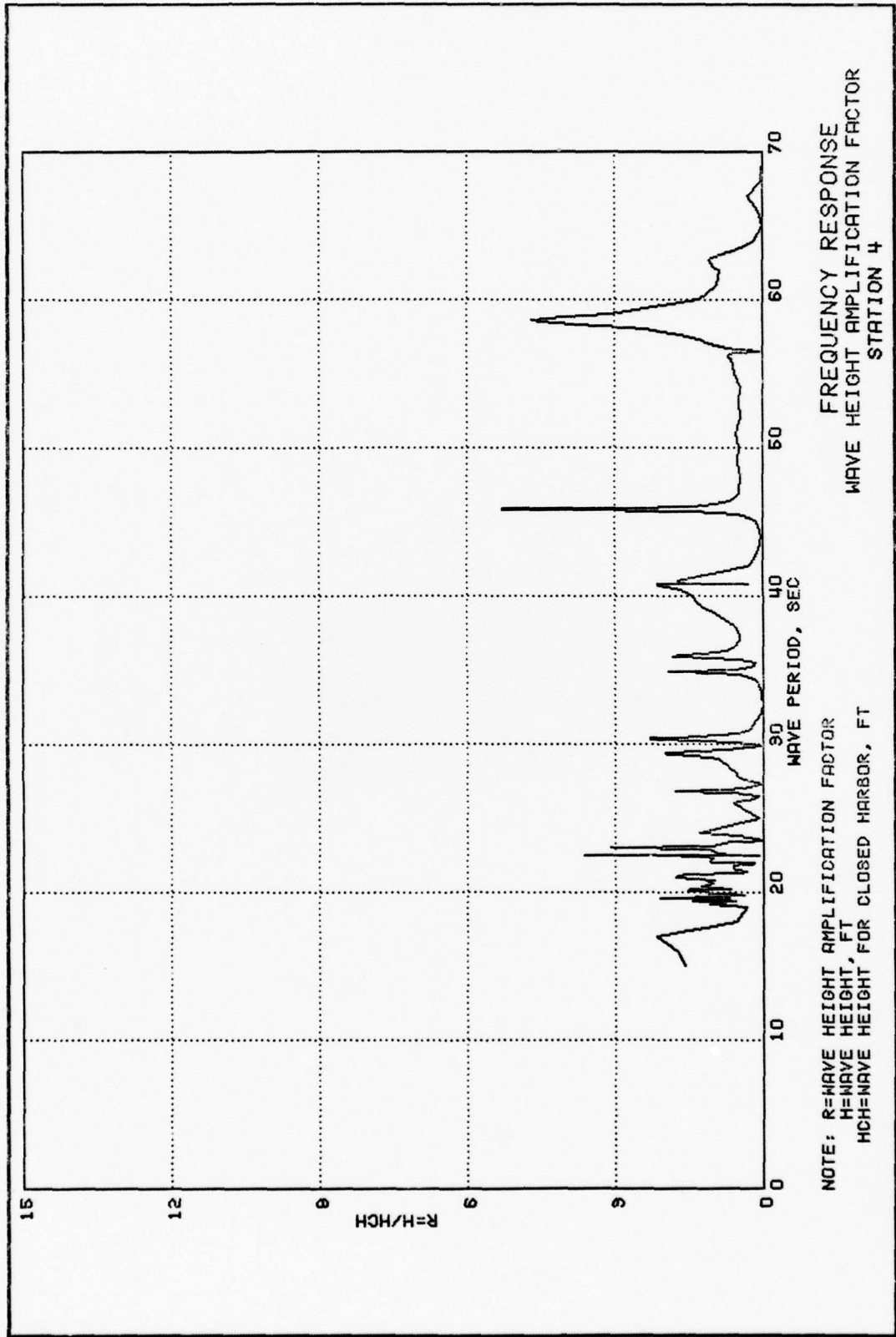


PLATE 10

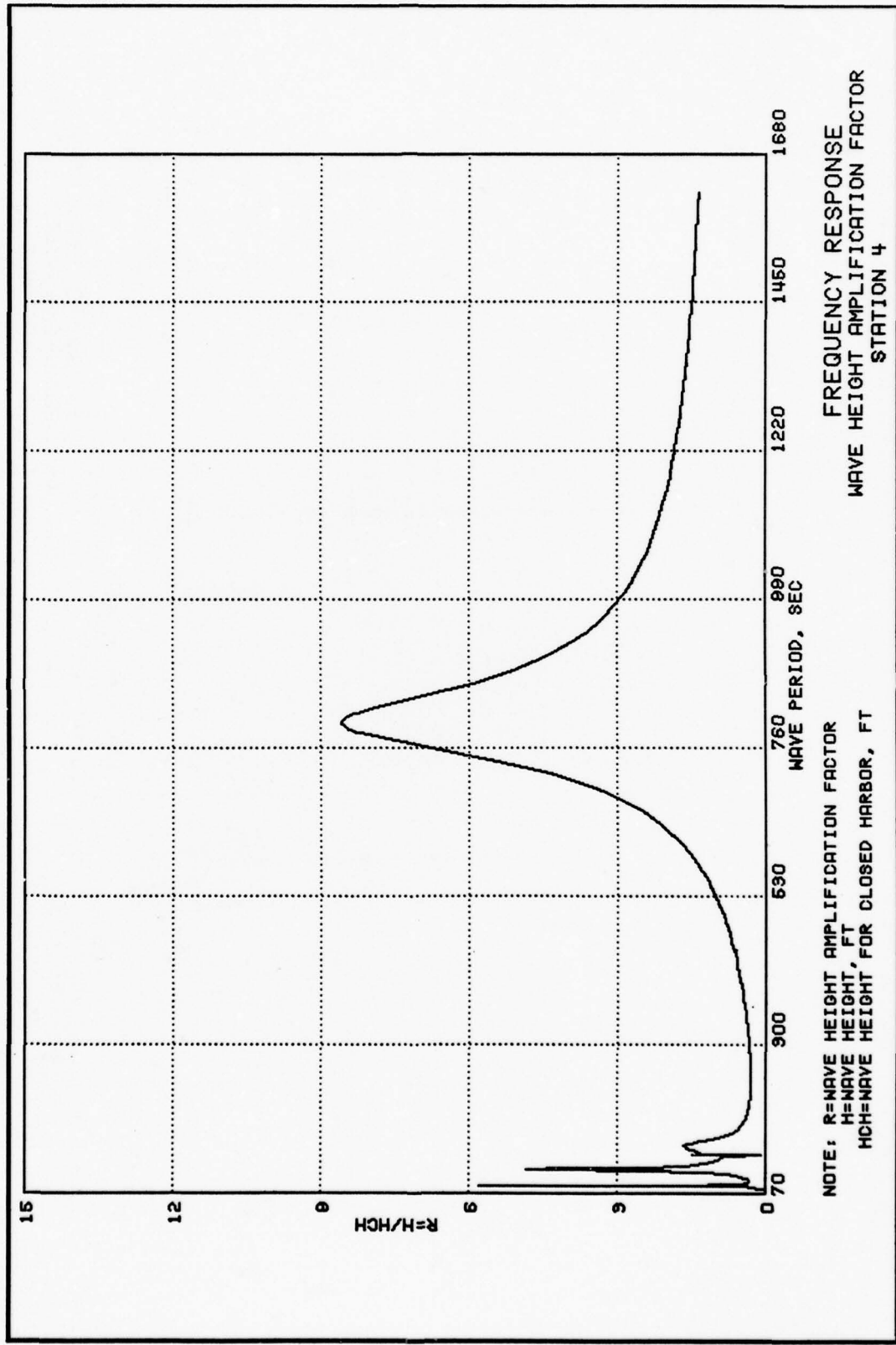


PLATE 11

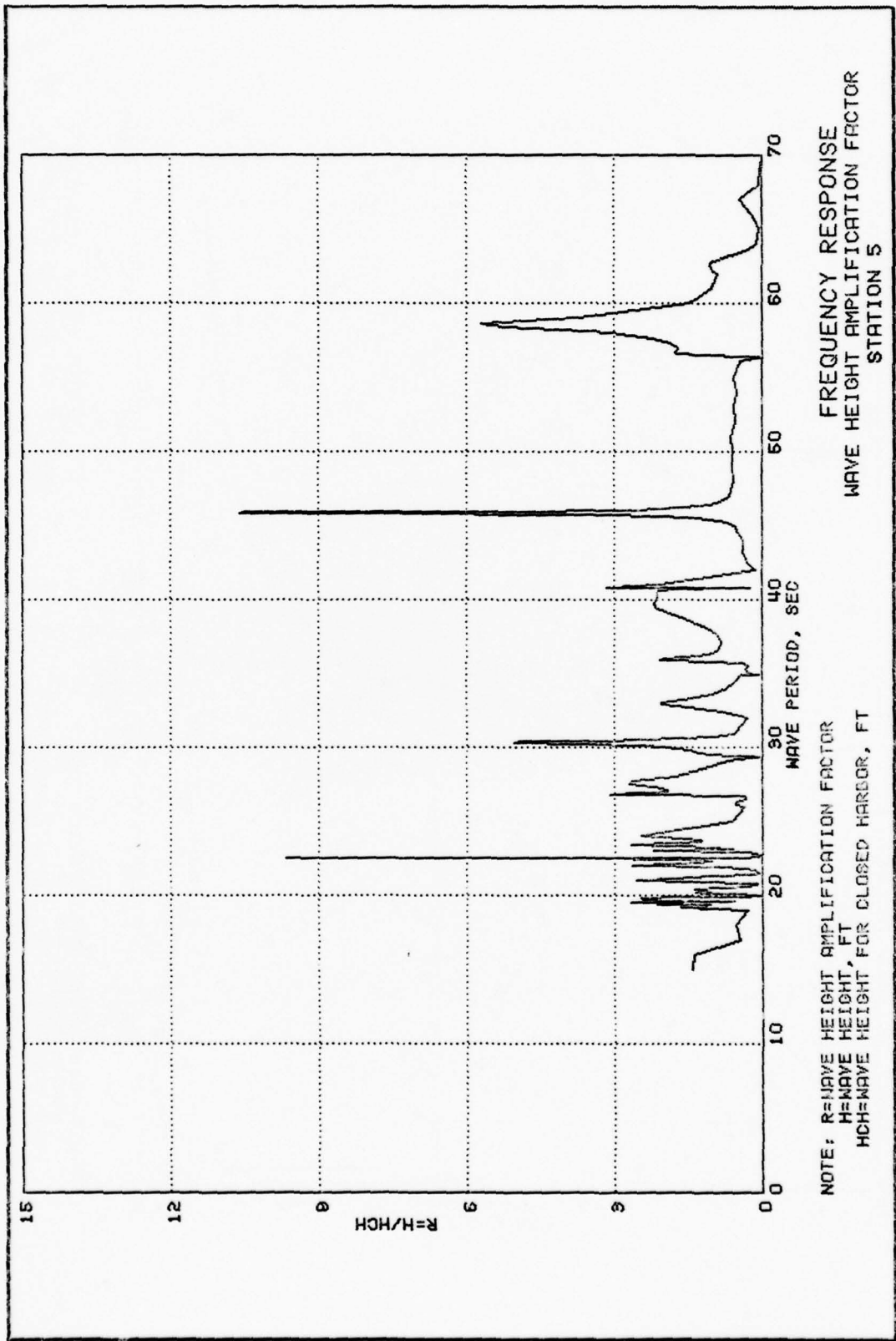
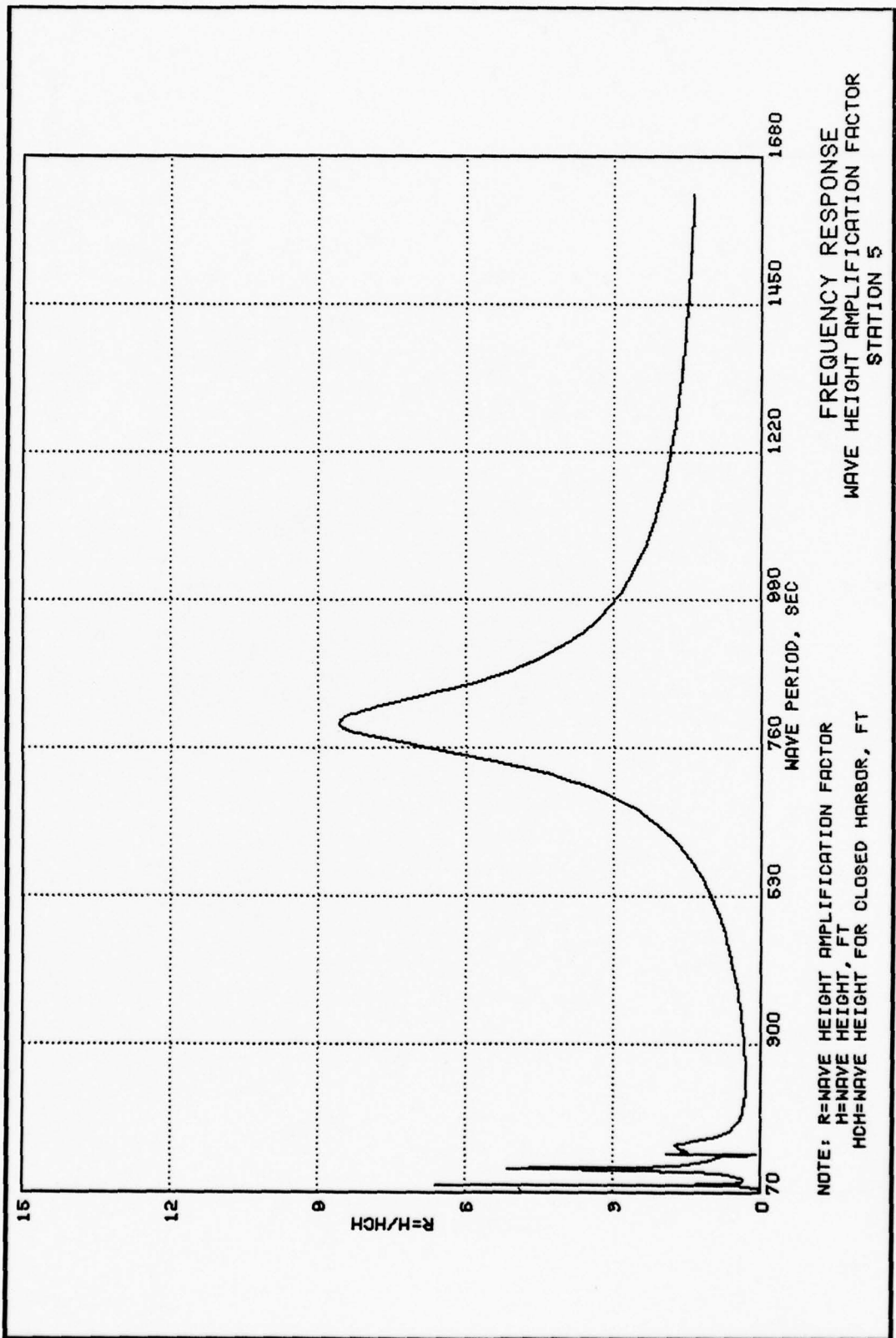


PLATE 12



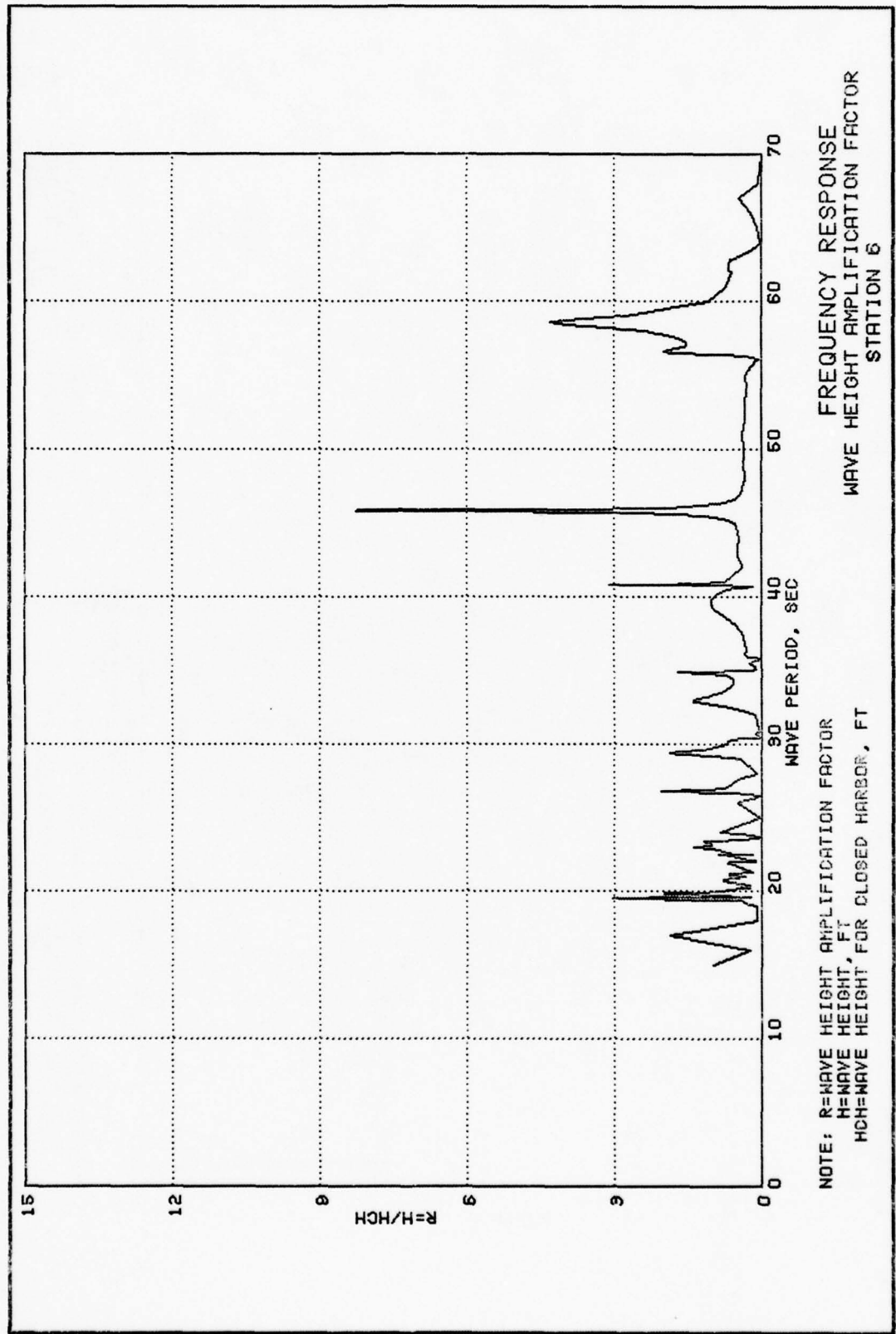


PLATE 14



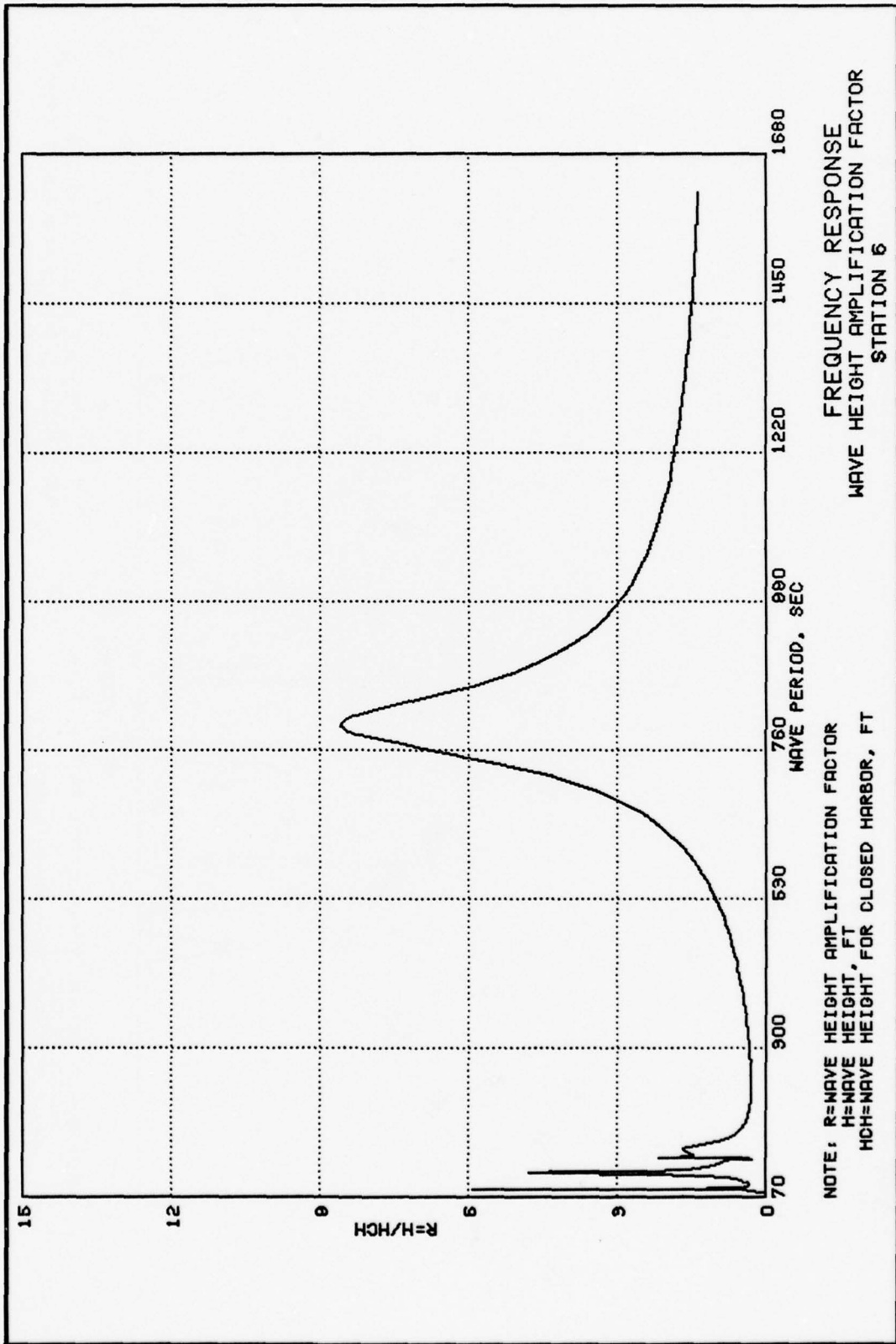


PLATE 15

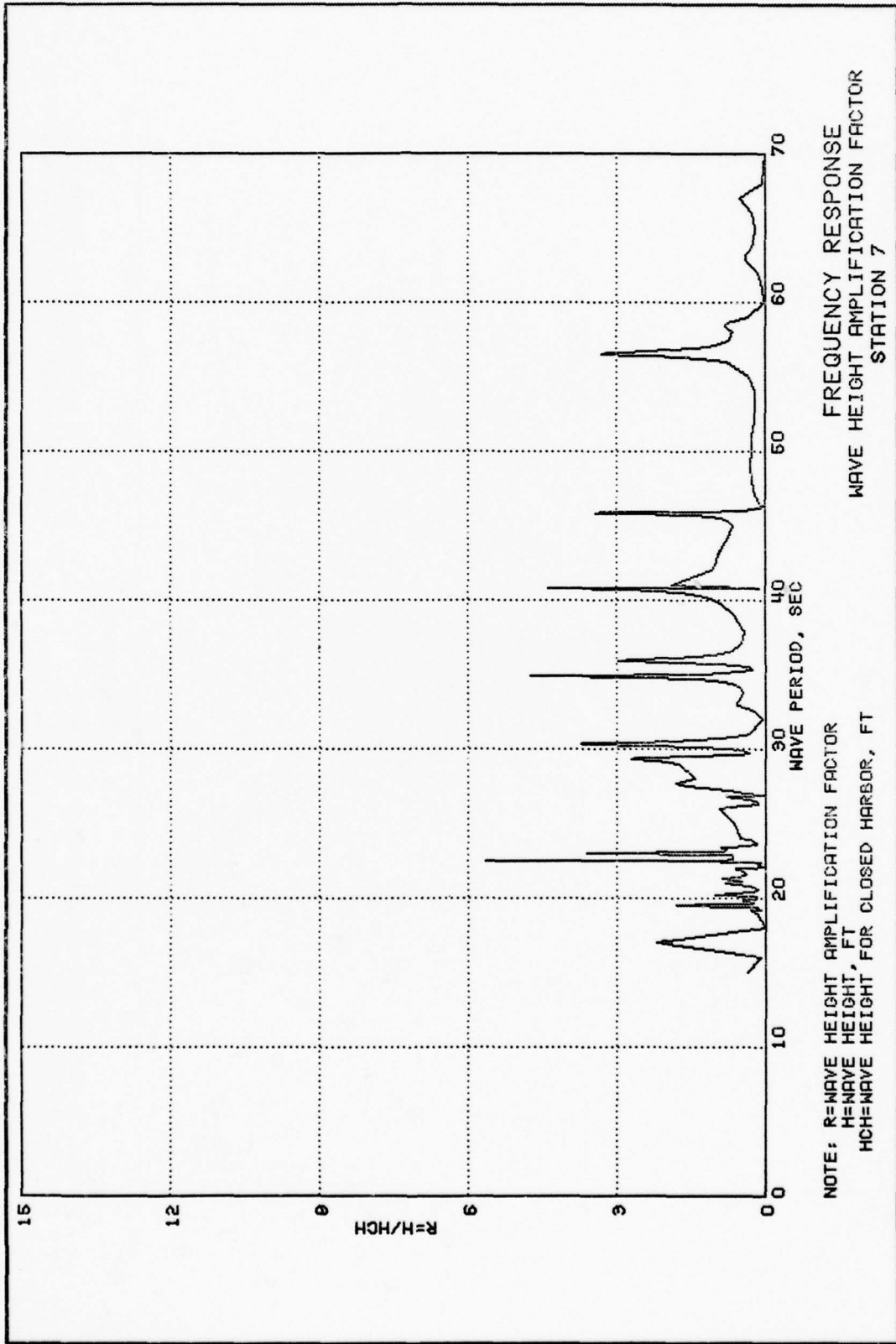
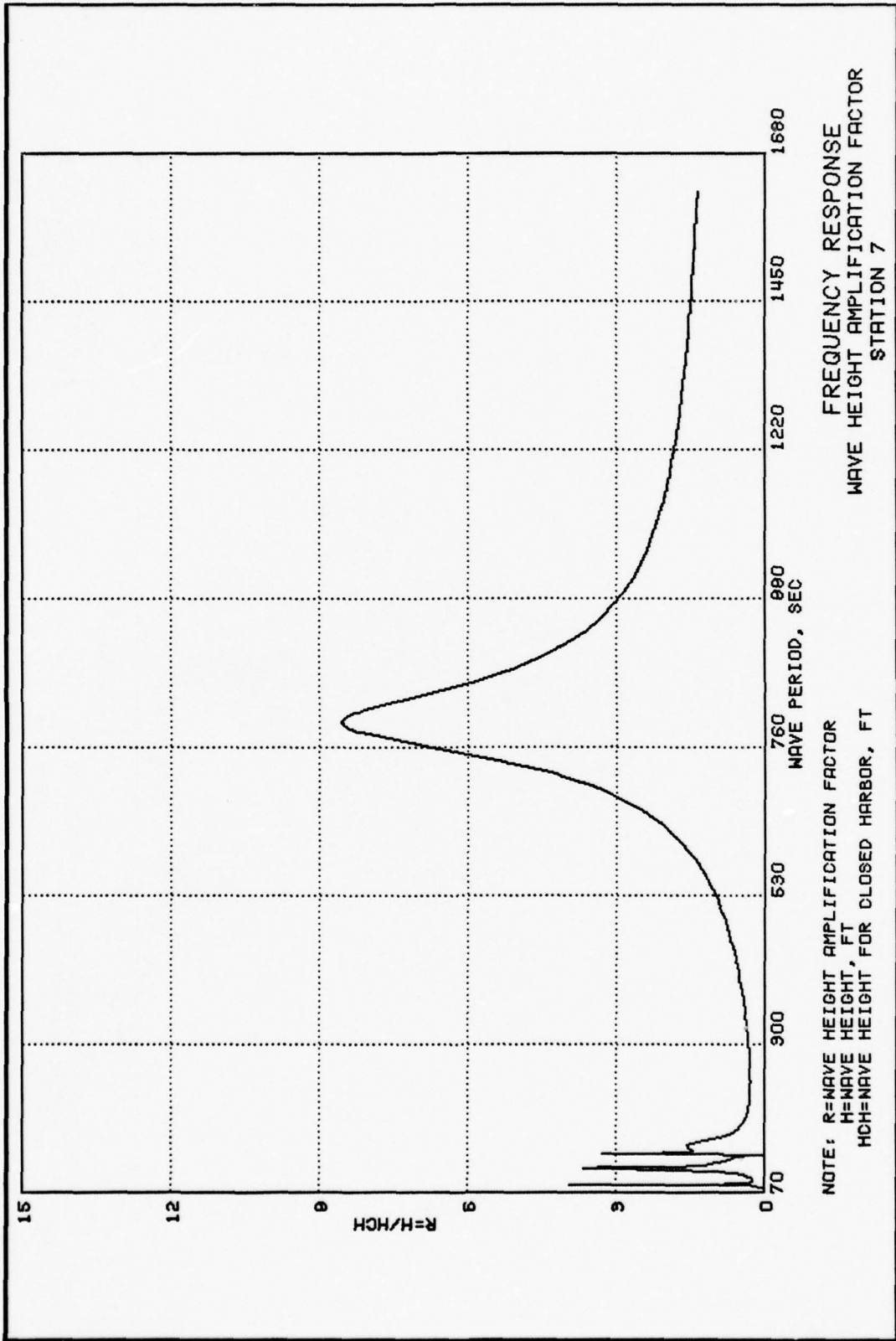


PLATE 16



FREQUENCY RESPONSE  
 WAVE HEIGHT AMPLIFICATION FACTOR  
 STATION 7

NOTE: R=WAVE HEIGHT AMPLIFICATION FACTOR  
 H=WAVE HEIGHT, FT  
 HCH=WAVE HEIGHT FOR CLOSED HARBOR, FT

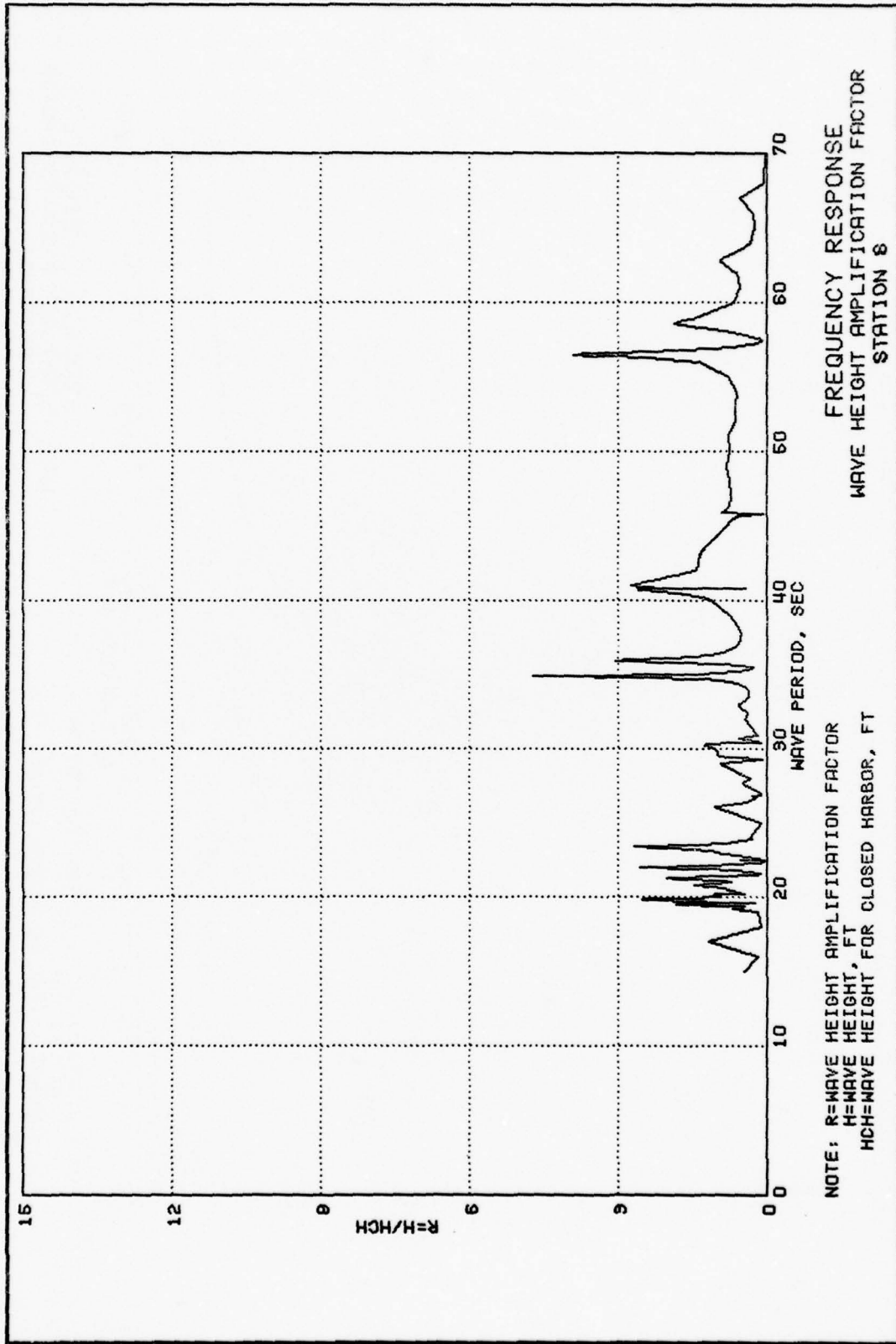
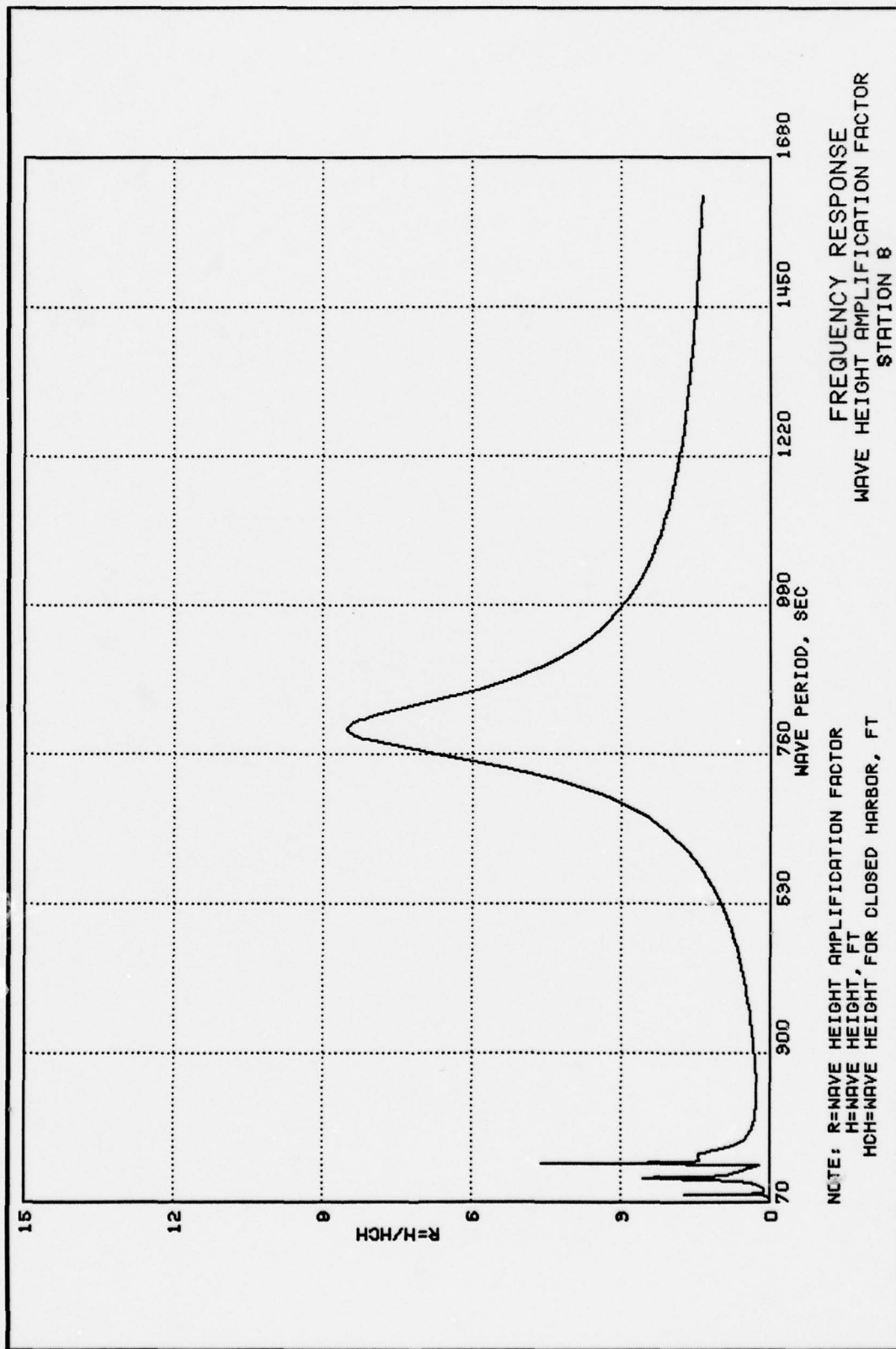


PLATE 18



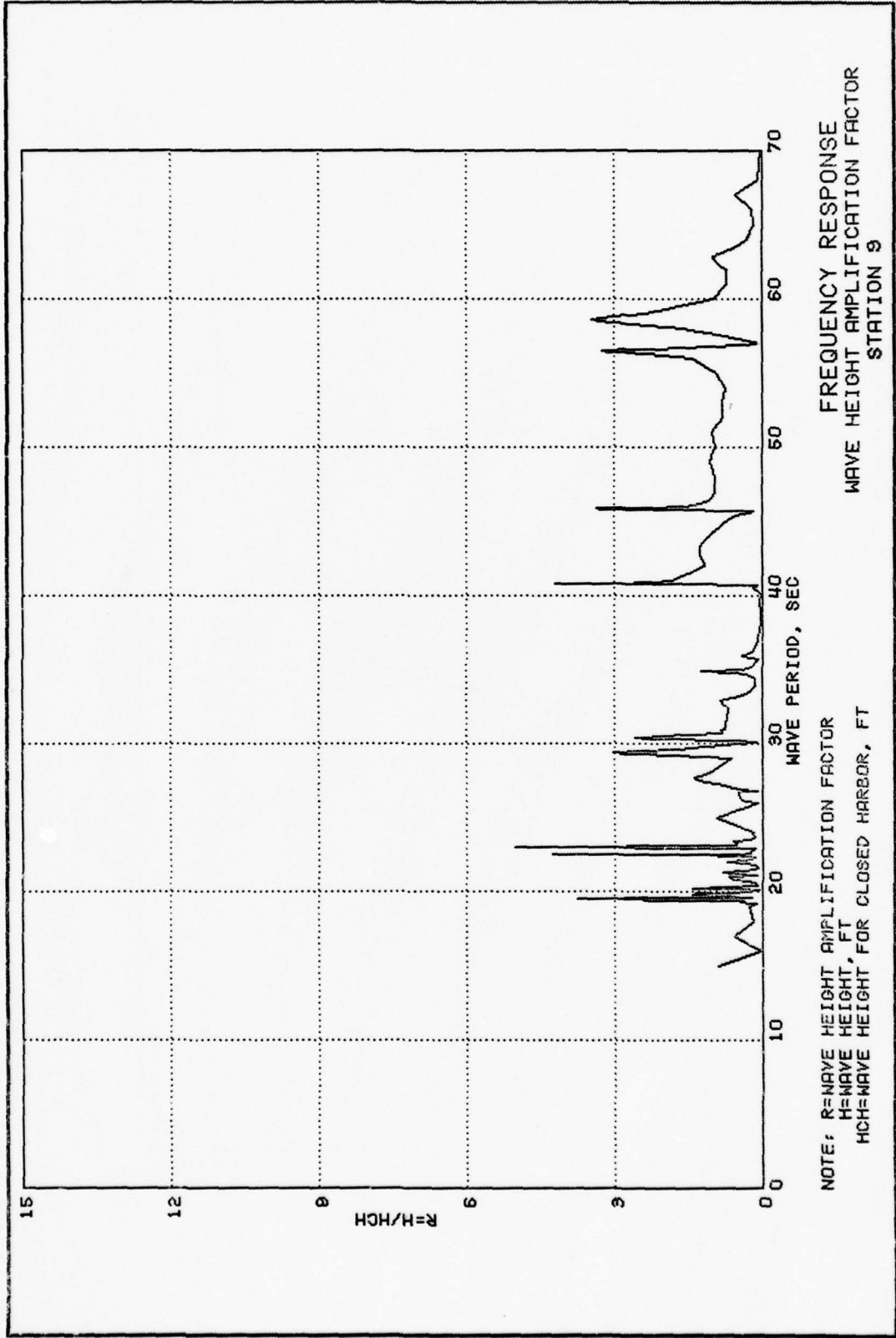
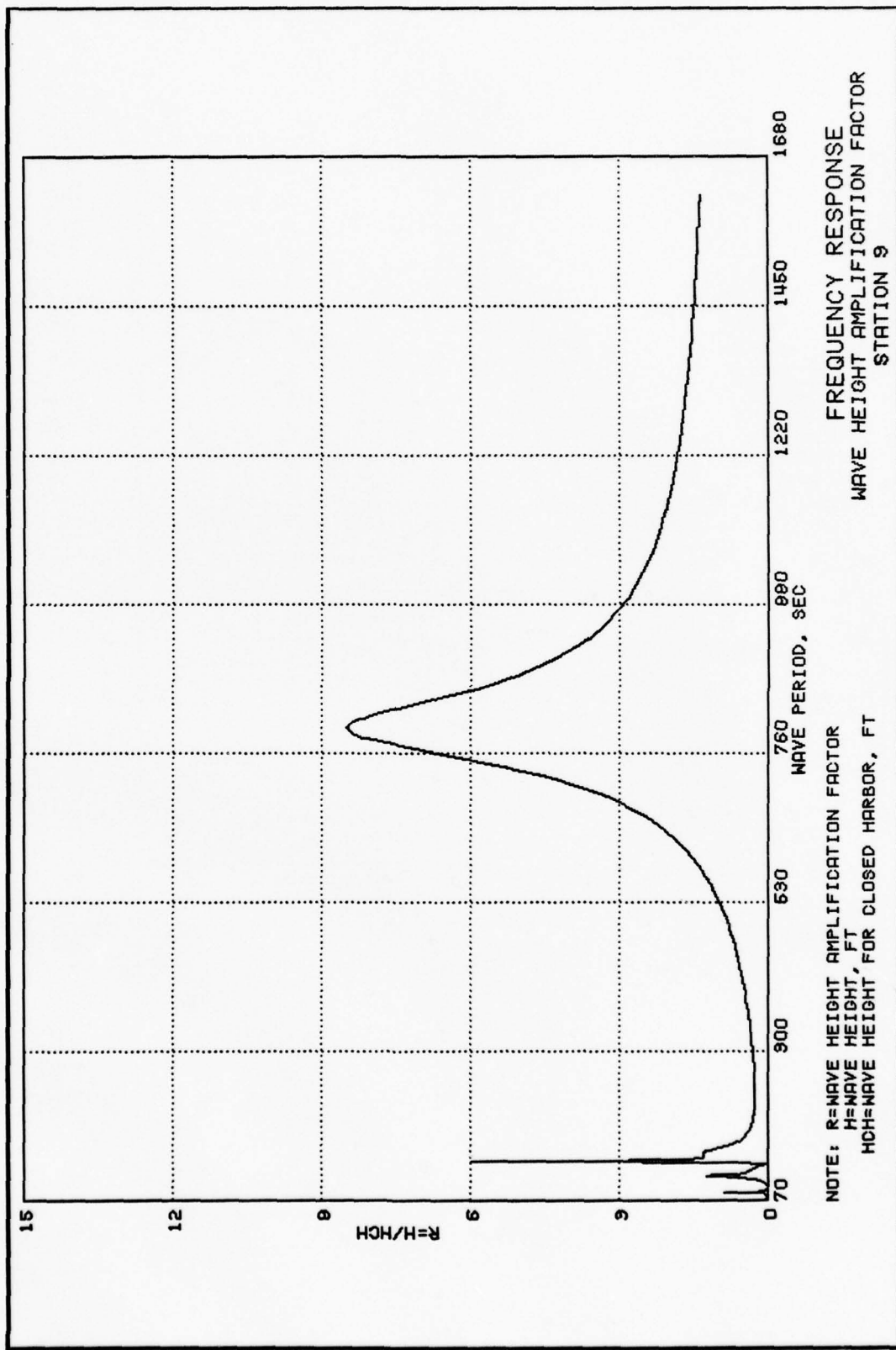


PLATE 20



FREQUENCY RESPONSE  
 WAVE HEIGHT AMPLIFICATION FACTOR  
 STATION 9

NOTE: R=WAVE HEIGHT AMPLIFICATION FACTOR  
 H=WAVE HEIGHT, FT  
 HCH=WAVE HEIGHT FOR CLOSED HARBOR, FT

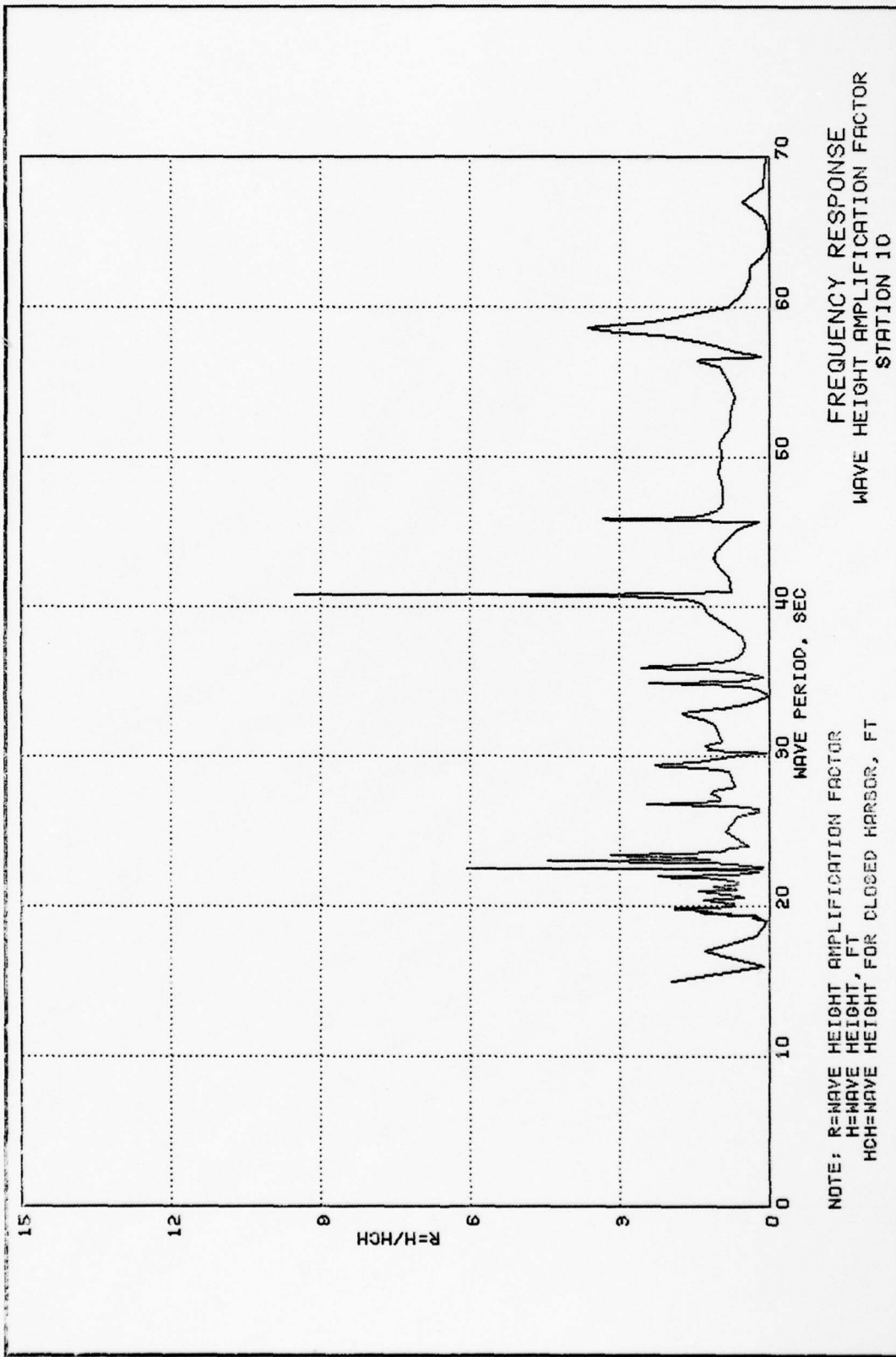
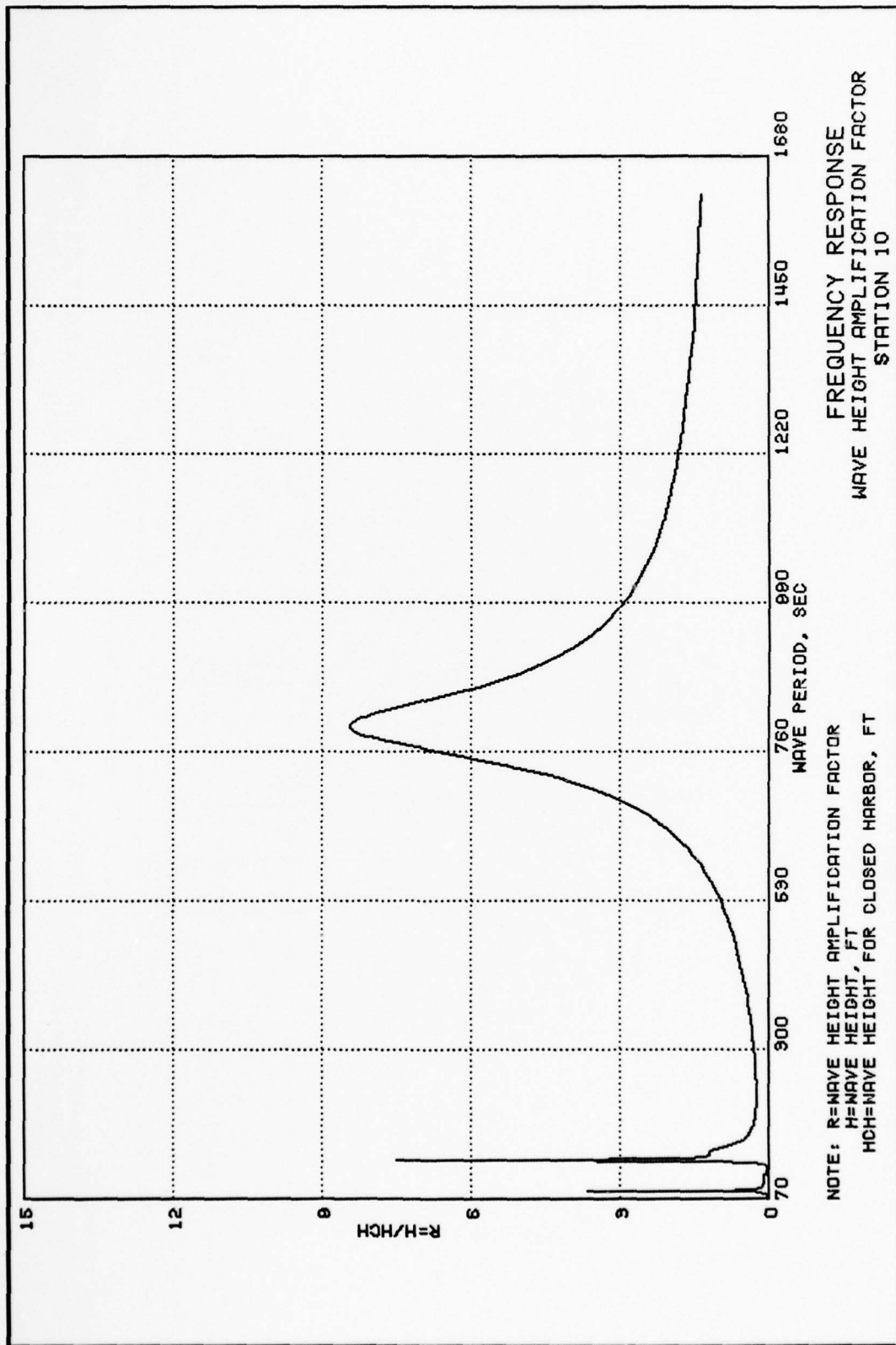


PLATE 22





FREQUENCY RESPONSE  
 WAVE HEIGHT AMPLIFICATION FACTOR  
 STATION 10

NOTE: R=WAVE HEIGHT AMPLIFICATION FACTOR  
 H=WAVE HEIGHT, FT  
 HCH=WAVE HEIGHT FOR CLOSED HARBOR, FT

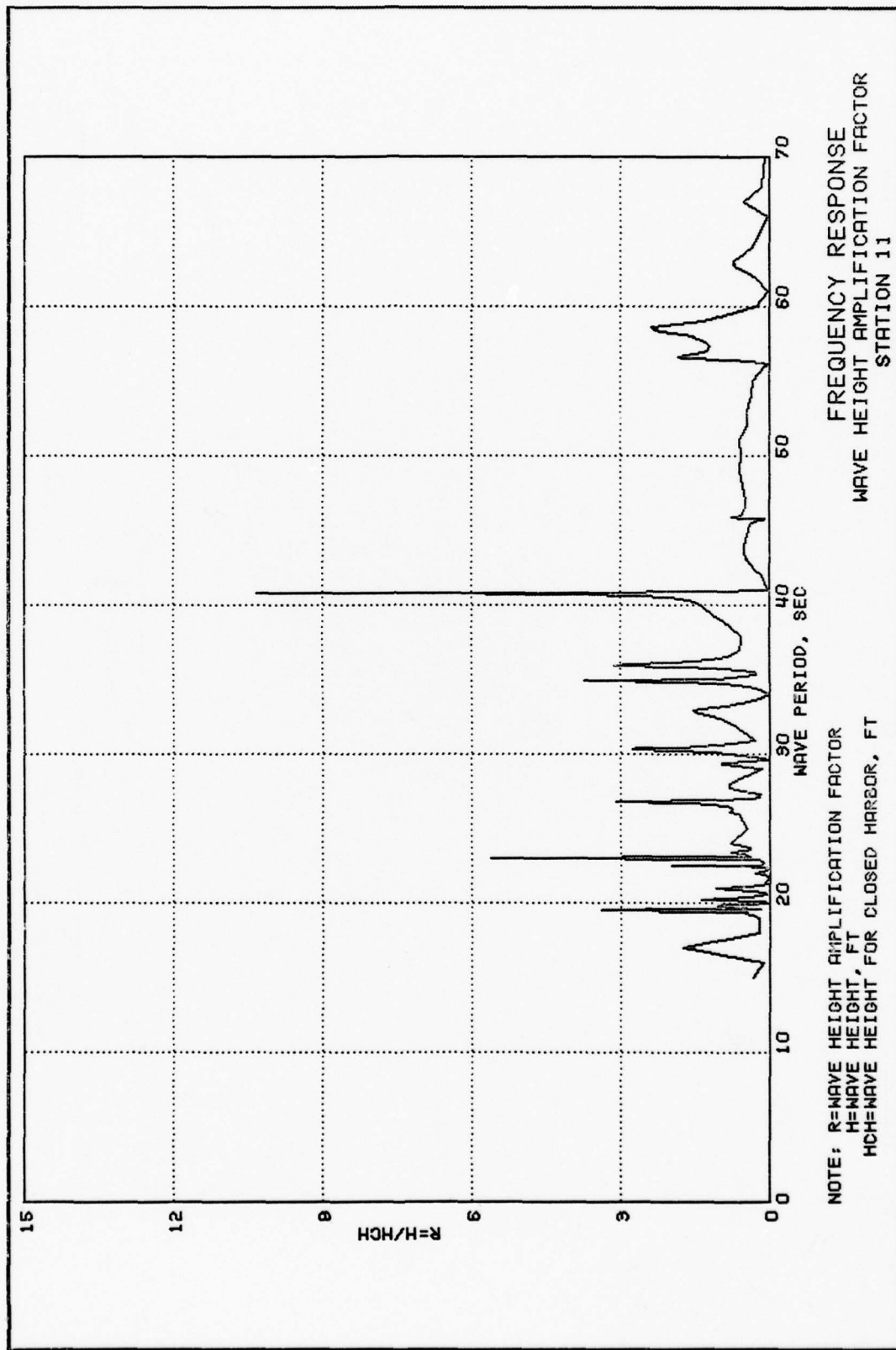
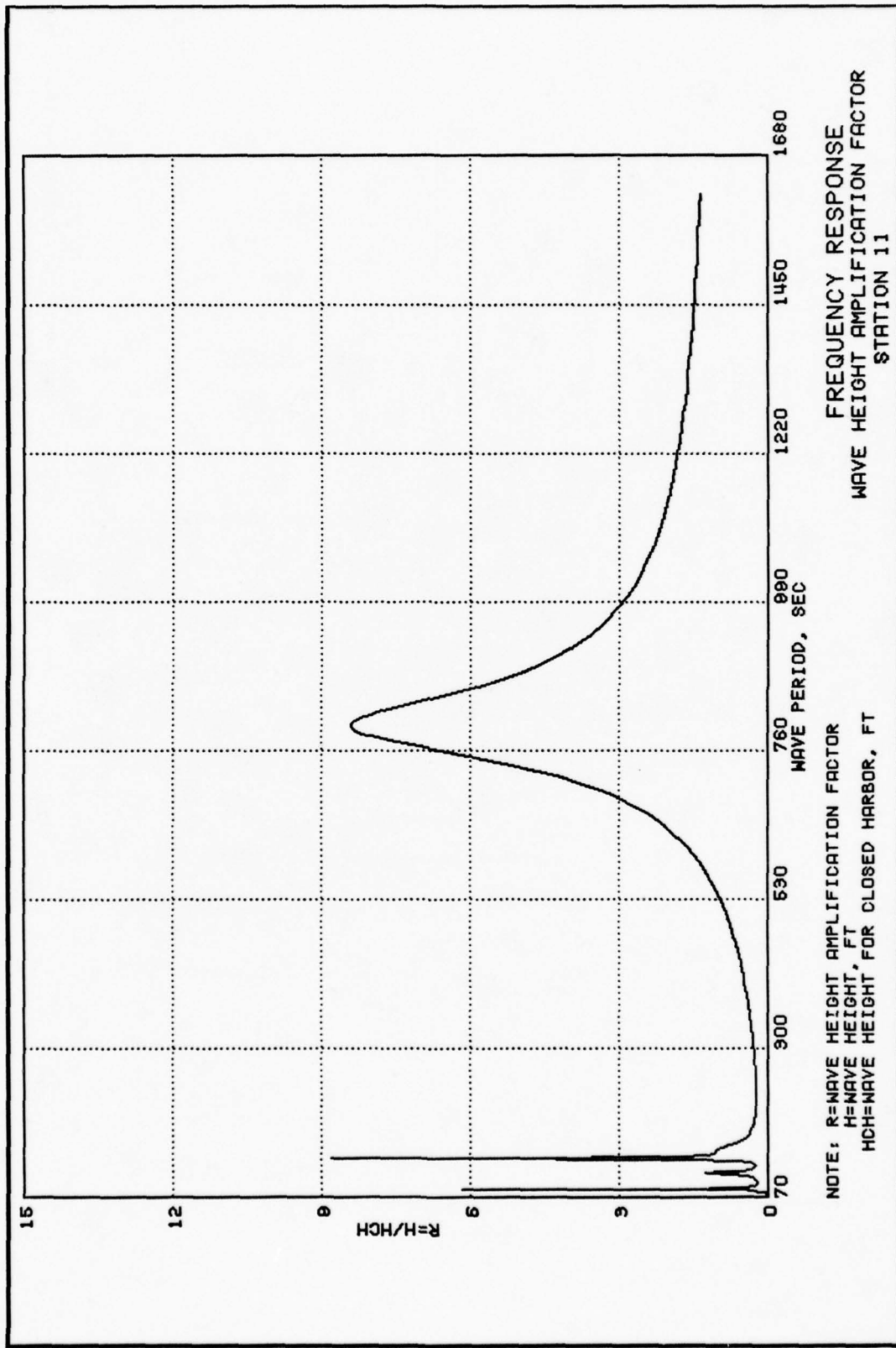


PLATE 24



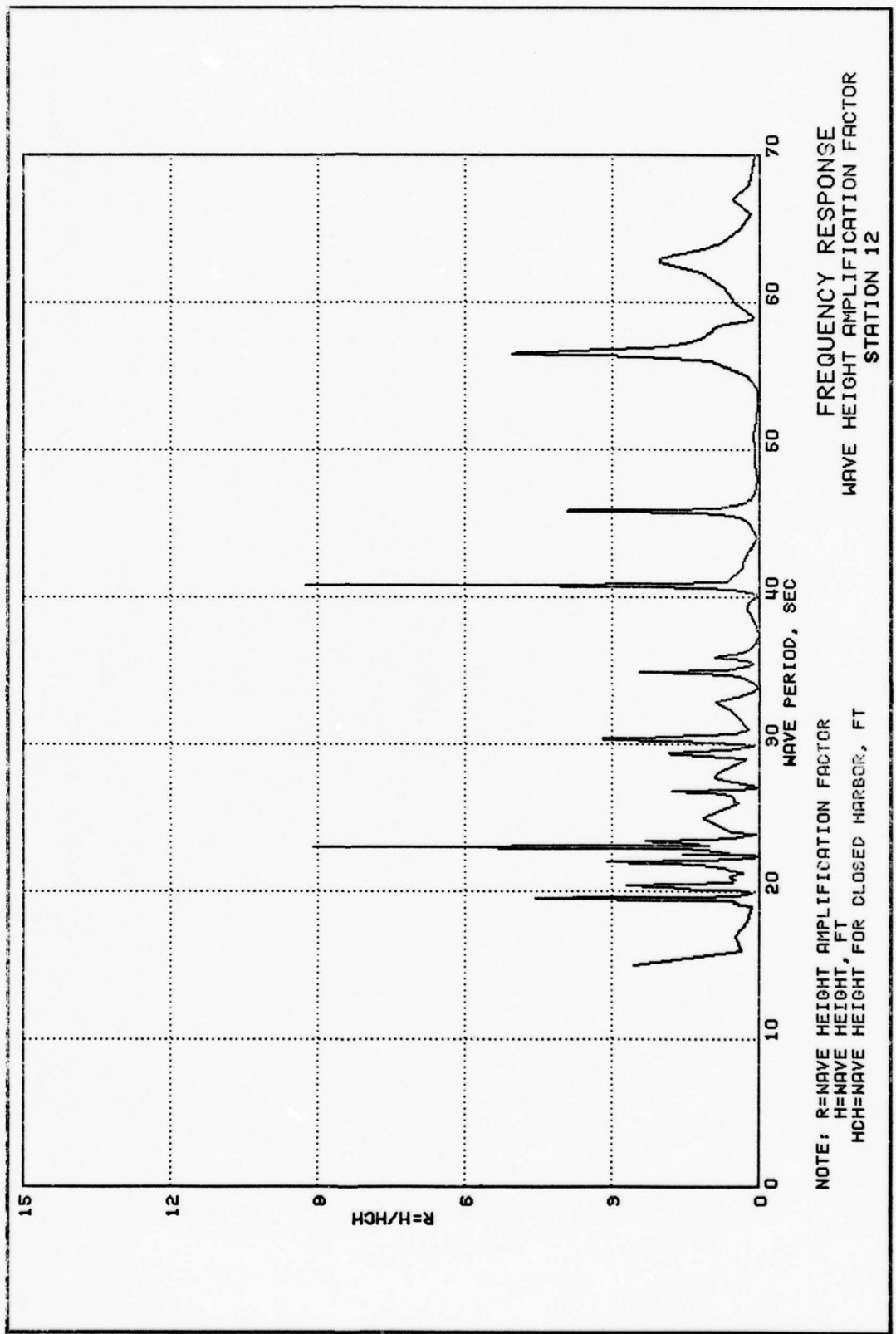
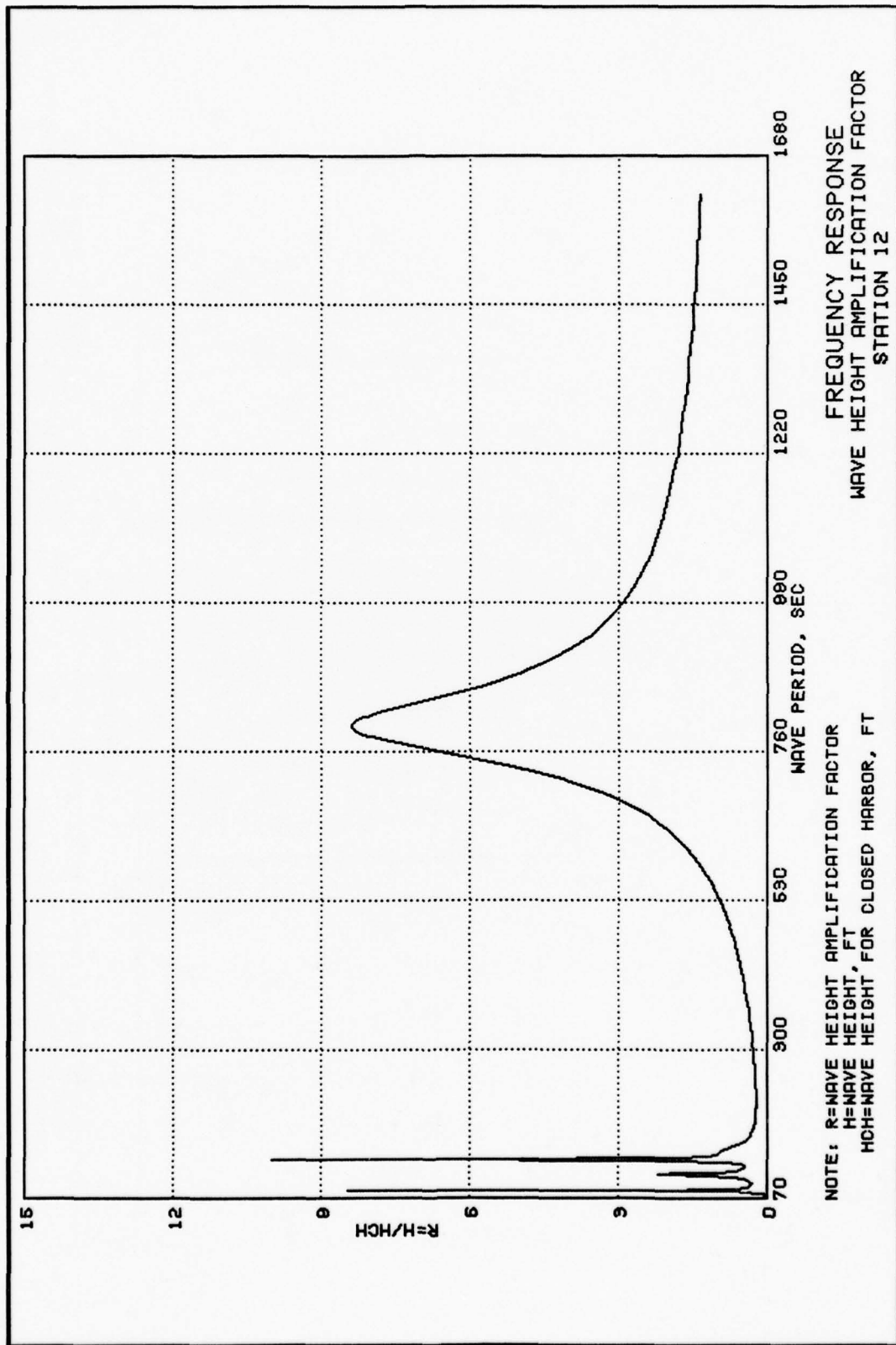
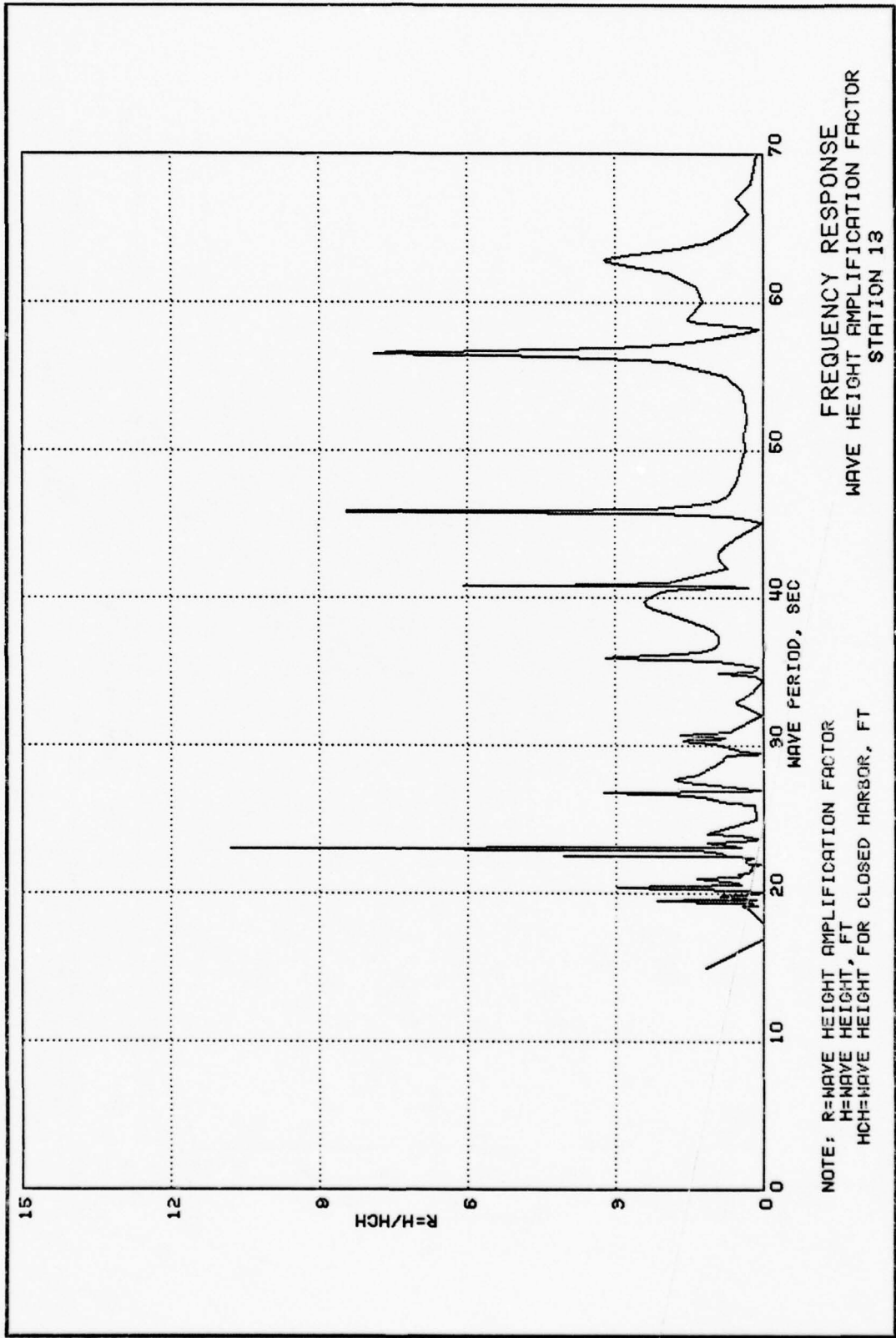


PLATE 26

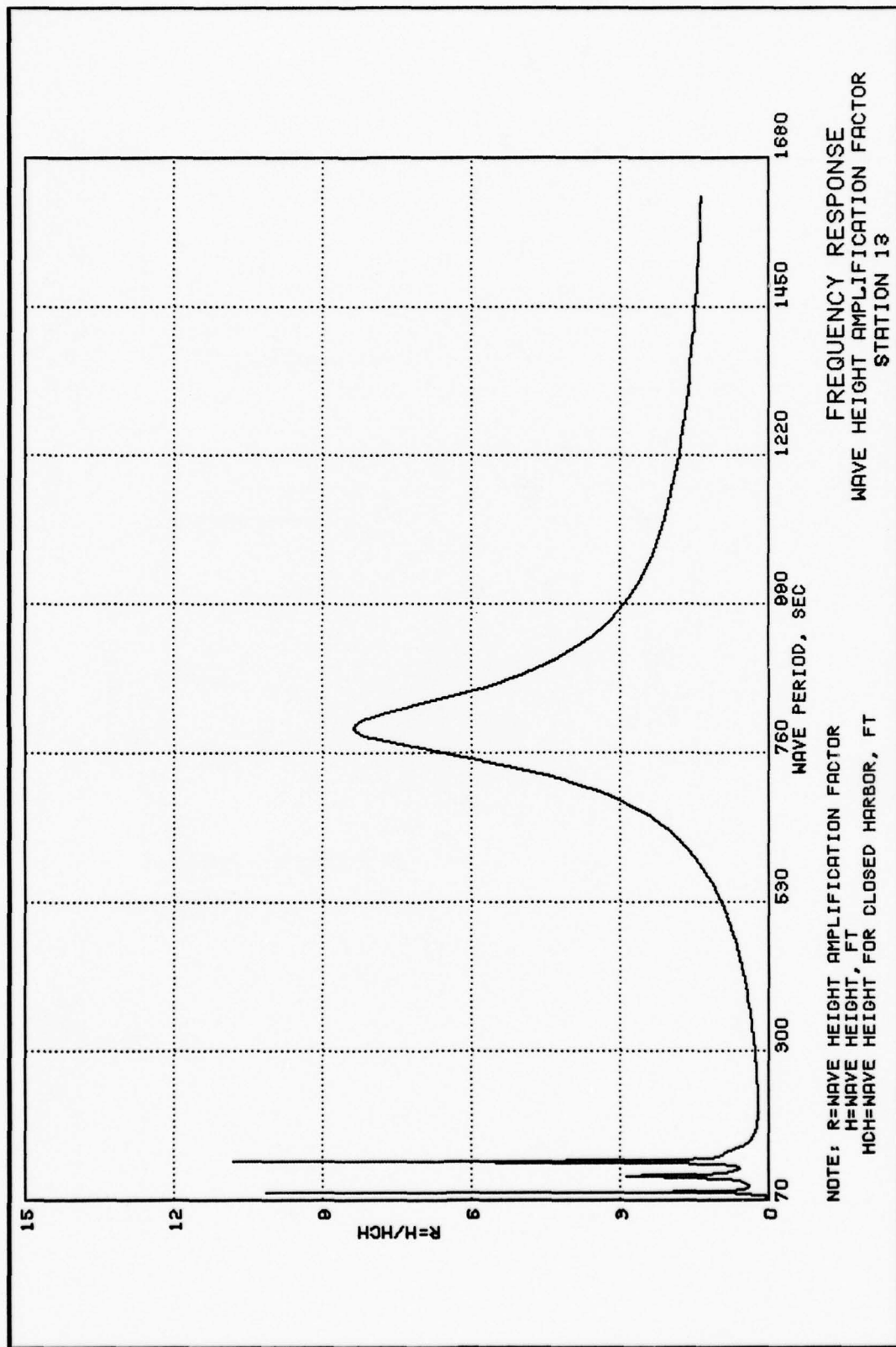




FREQUENCY RESPONSE  
 WAVE HEIGHT AMPLIFICATION FACTOR  
 STATION 13

NOTE: R=HAVE HEIGHT AMPLIFICATION FACTOR  
 H=HAVE HEIGHT, FT  
 HCH=HAVE HEIGHT FOR CLOSED HARBOR, FT

PLATE 28



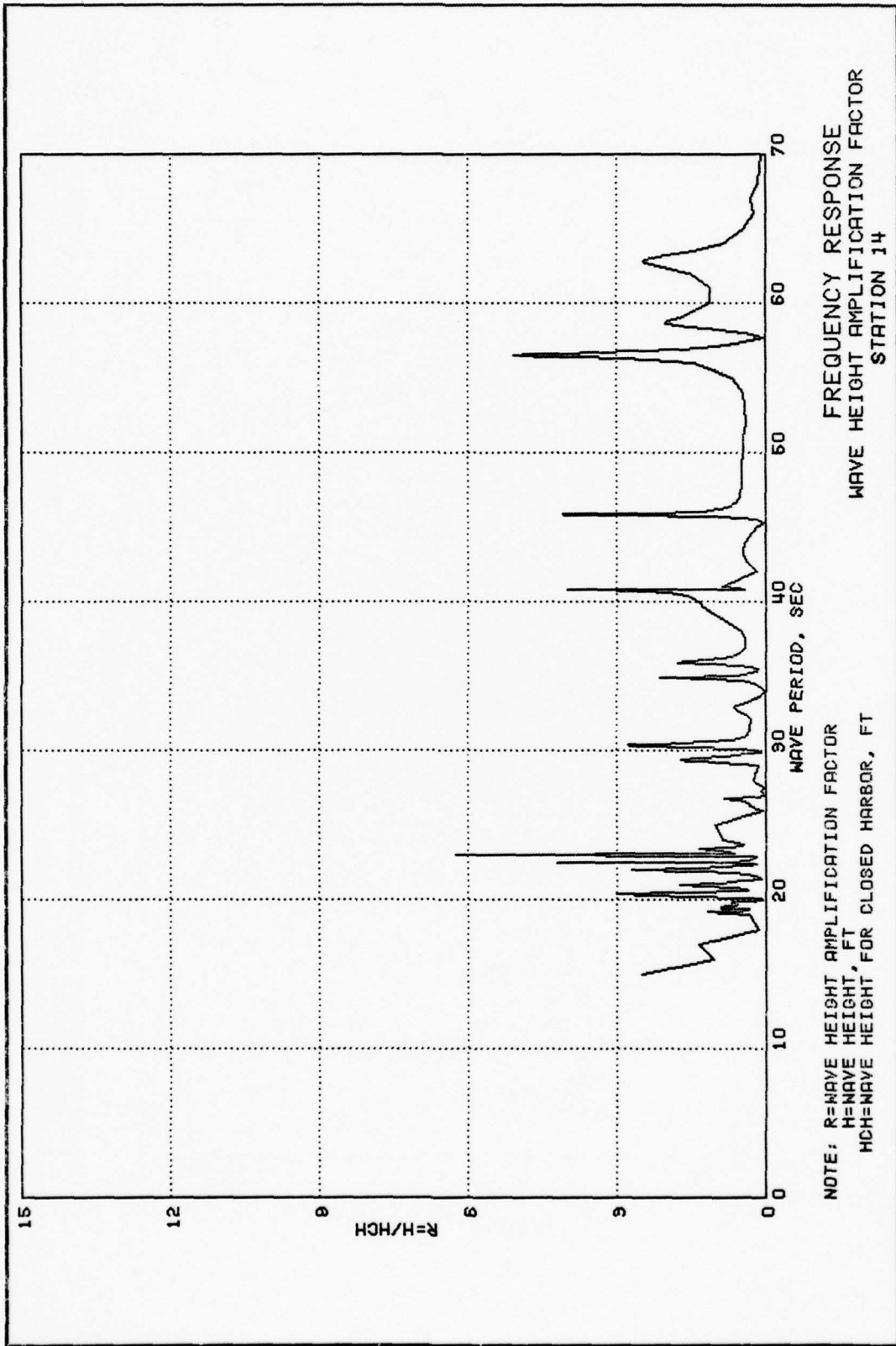
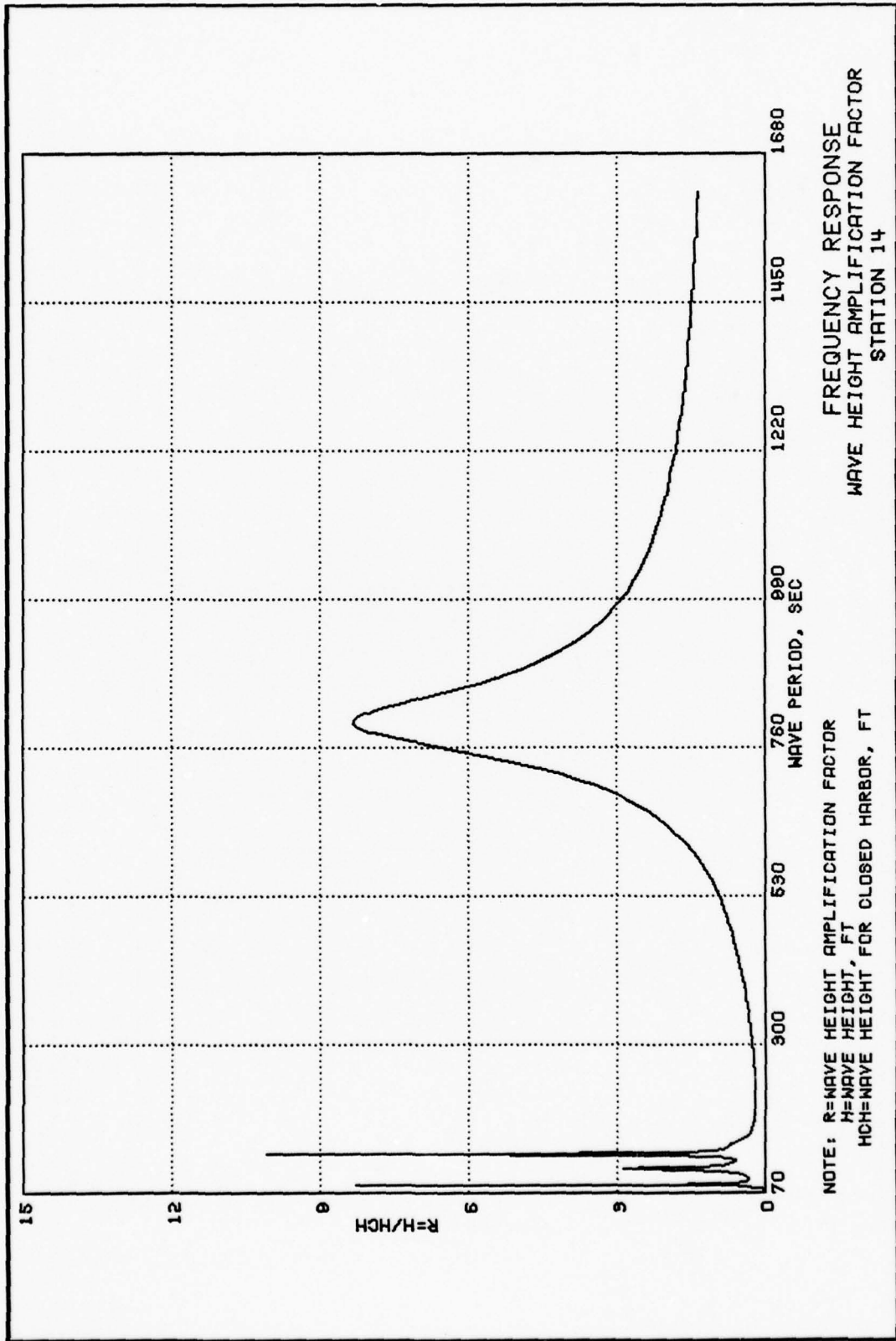


PLATE 30





FREQUENCY RESPONSE  
 WAVE HEIGHT AMPLIFICATION FACTOR  
 STATION 14

NOTE: R=WAVE HEIGHT AMPLIFICATION FACTOR  
 H=WAVE HEIGHT, FT  
 HCH=WAVE HEIGHT FOR CLOSED HARBOR, FT

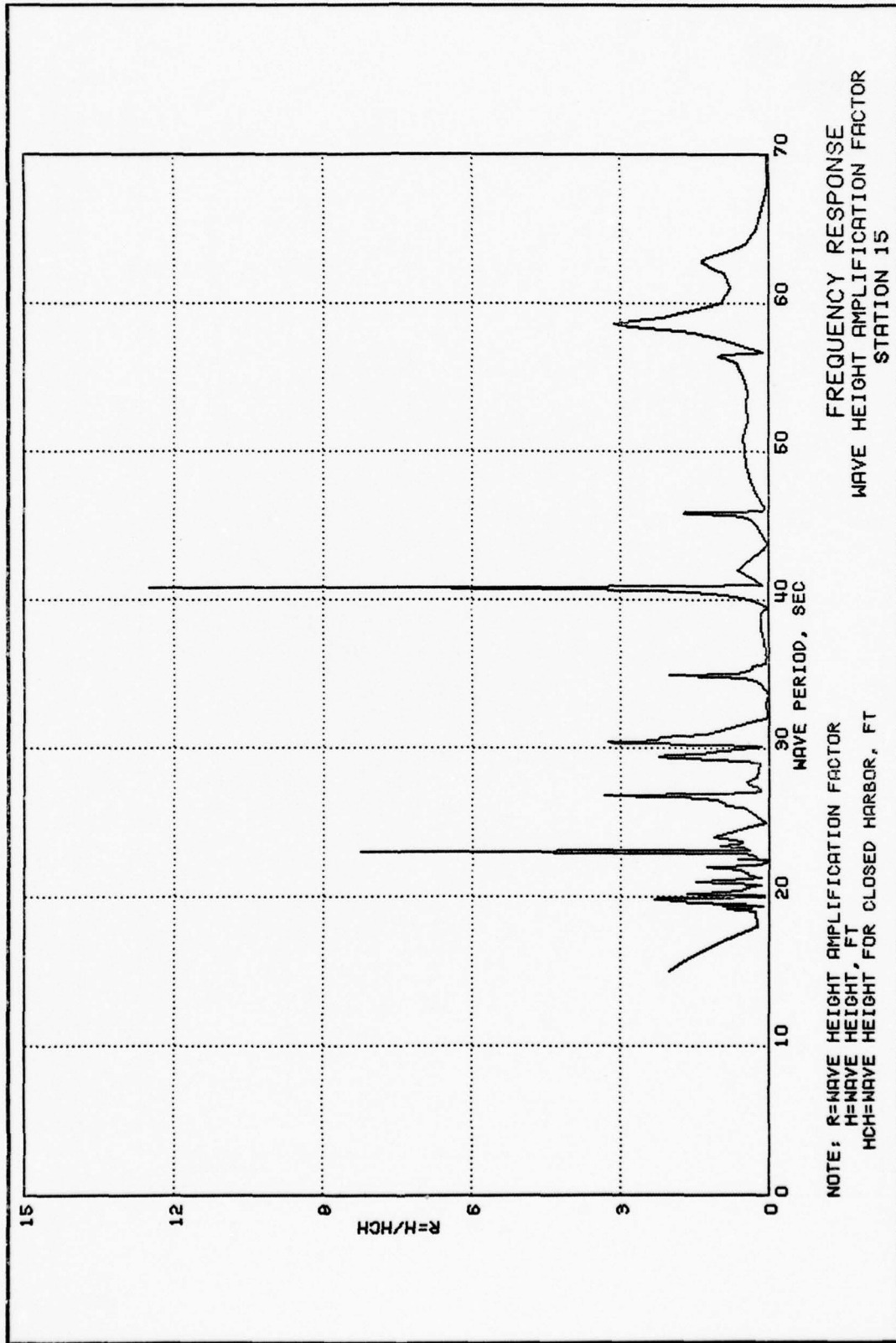
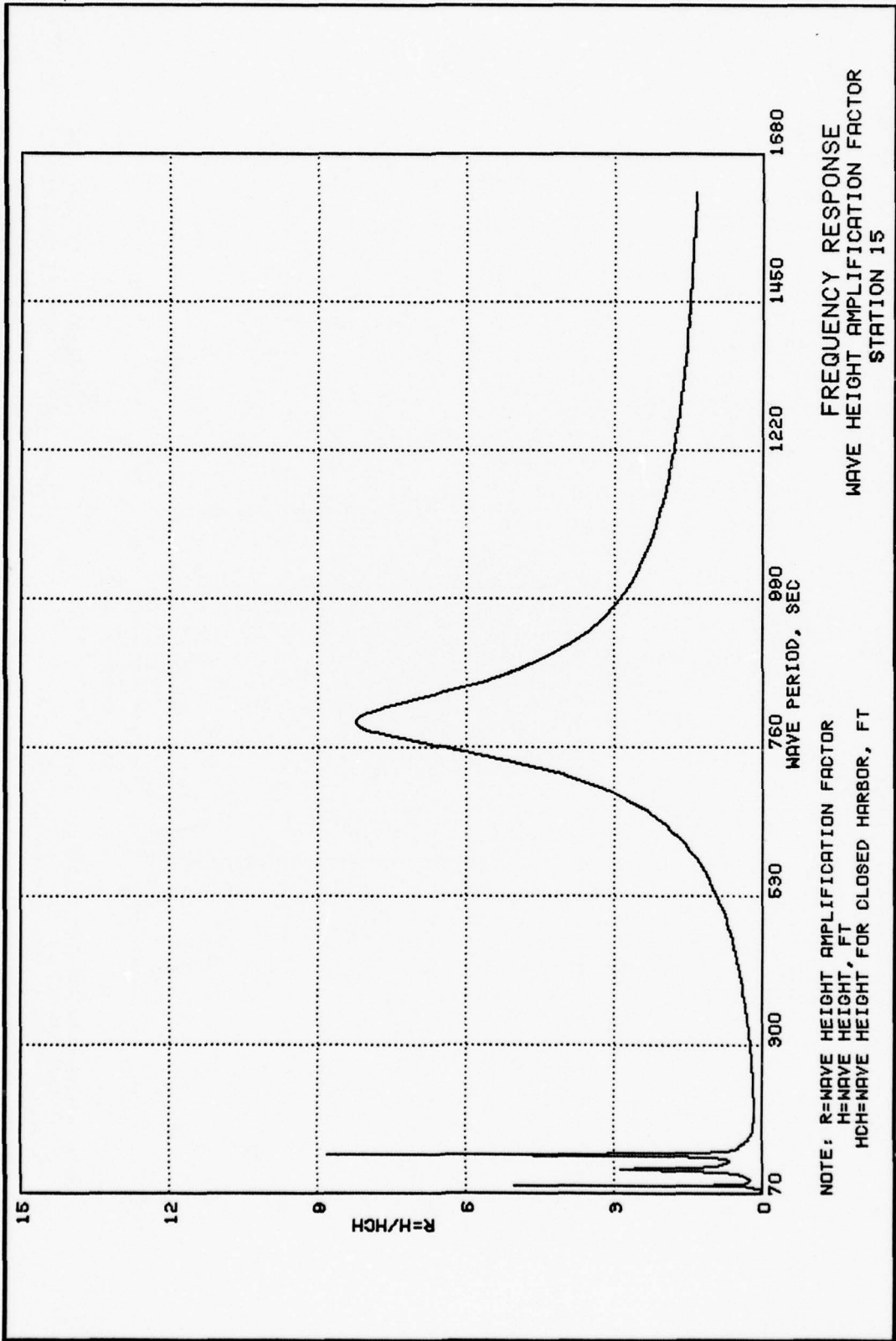


PLATE 32



FREQUENCY RESPONSE  
 WAVE HEIGHT AMPLIFICATION FACTOR  
 STATION 15

NOTE: R=WAVE HEIGHT AMPLIFICATION FACTOR  
 H=WAVE HEIGHT, FT  
 HCH=WAVE HEIGHT FOR CLOSED HARBOR, FT

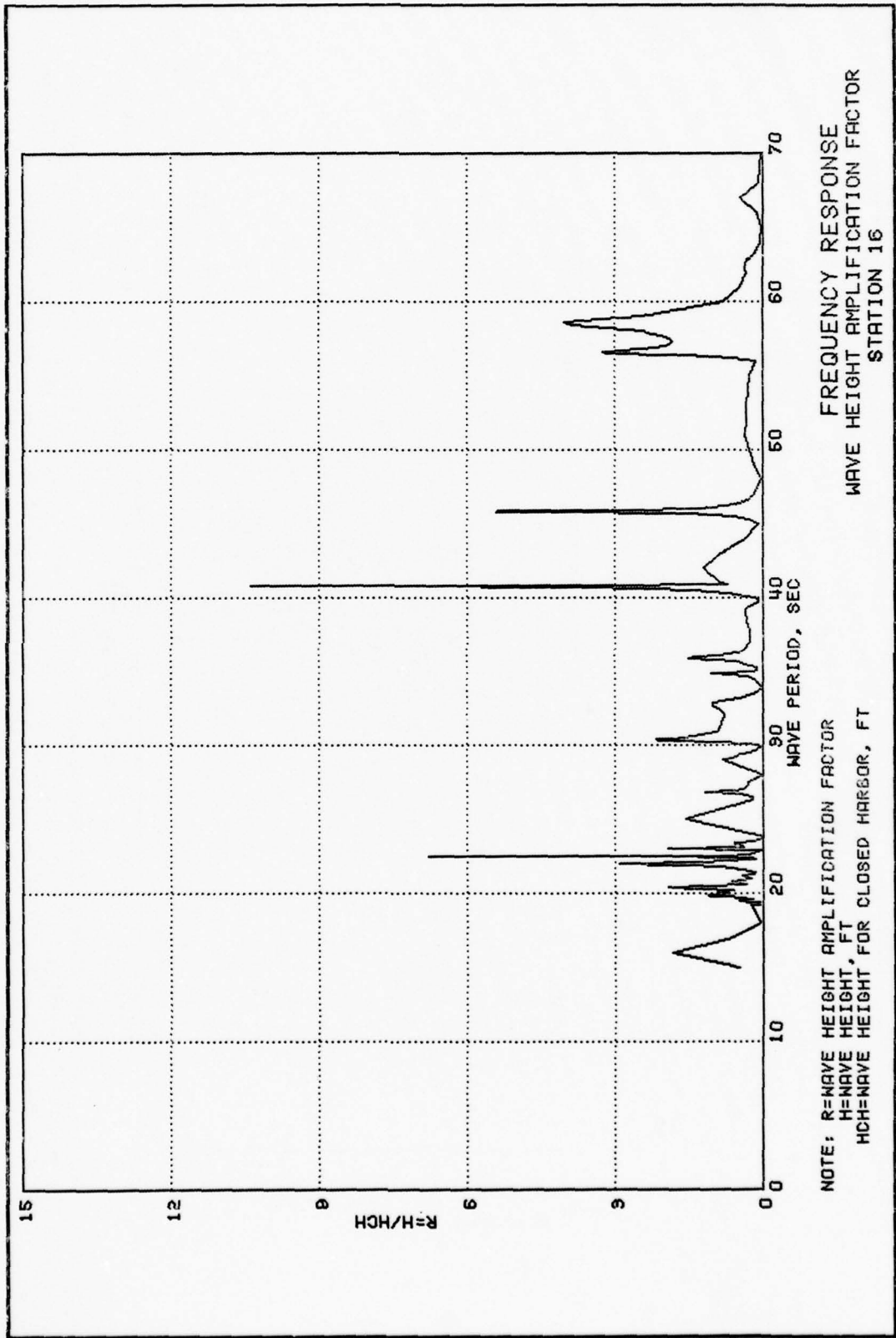
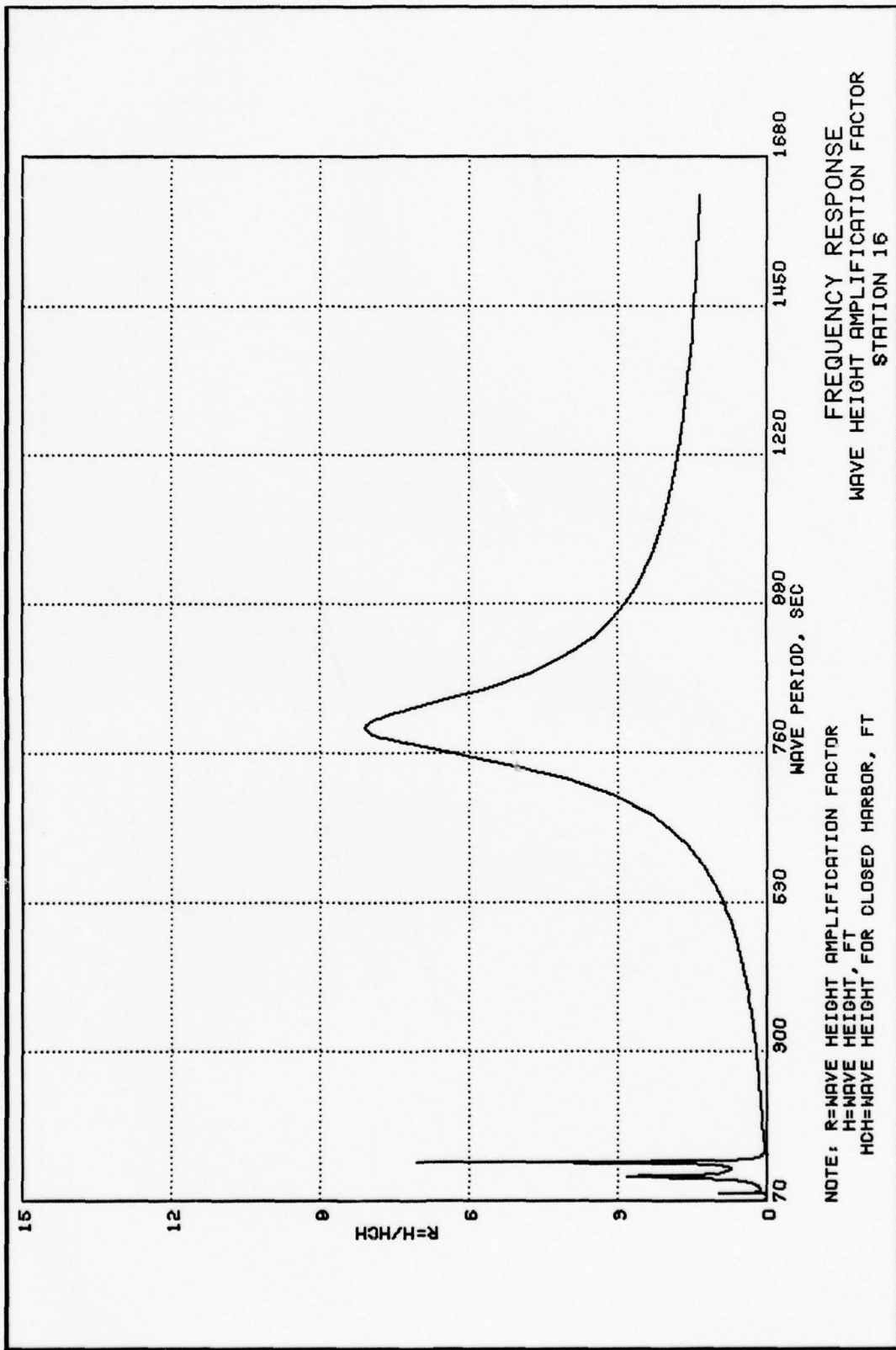


PLATE 34



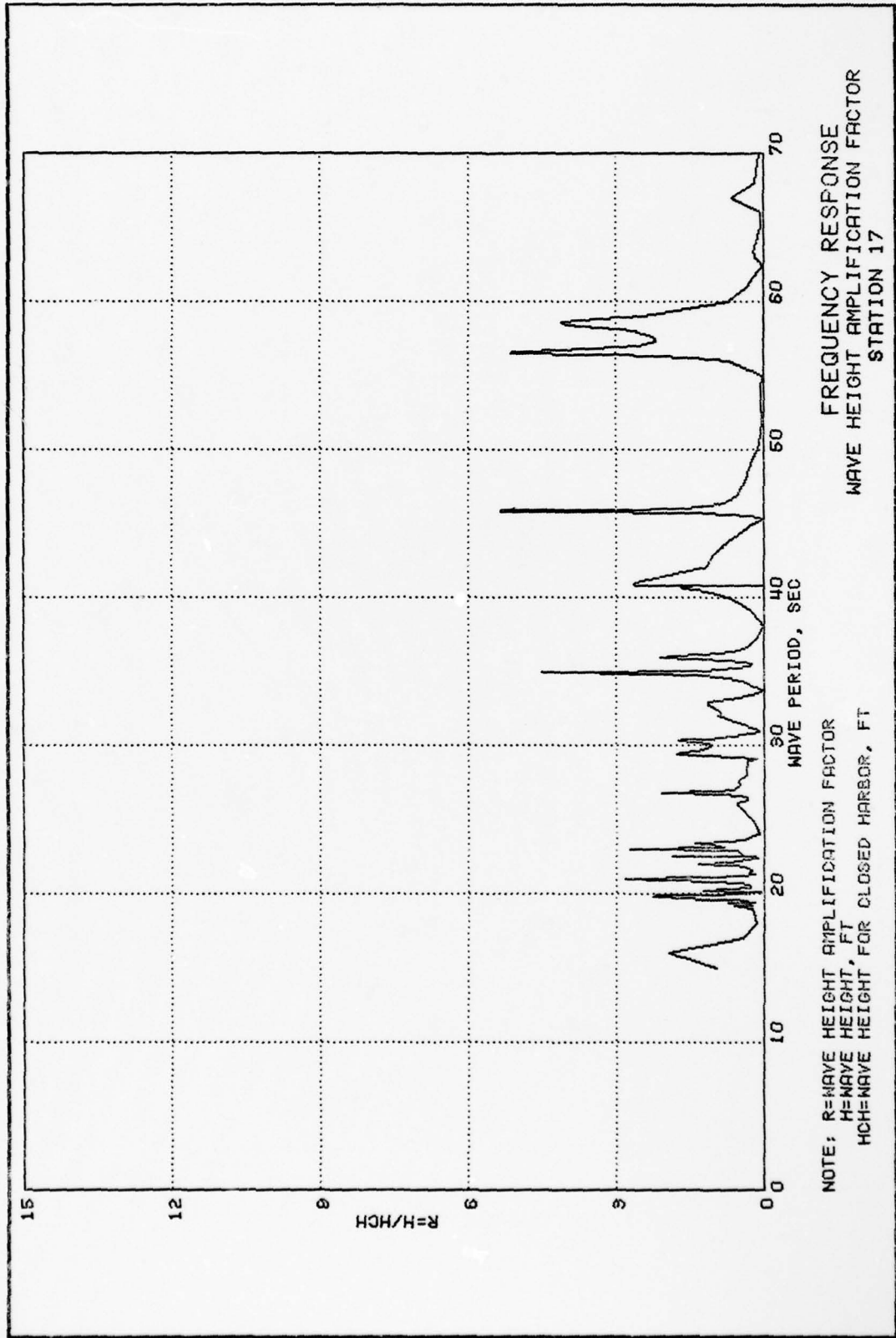
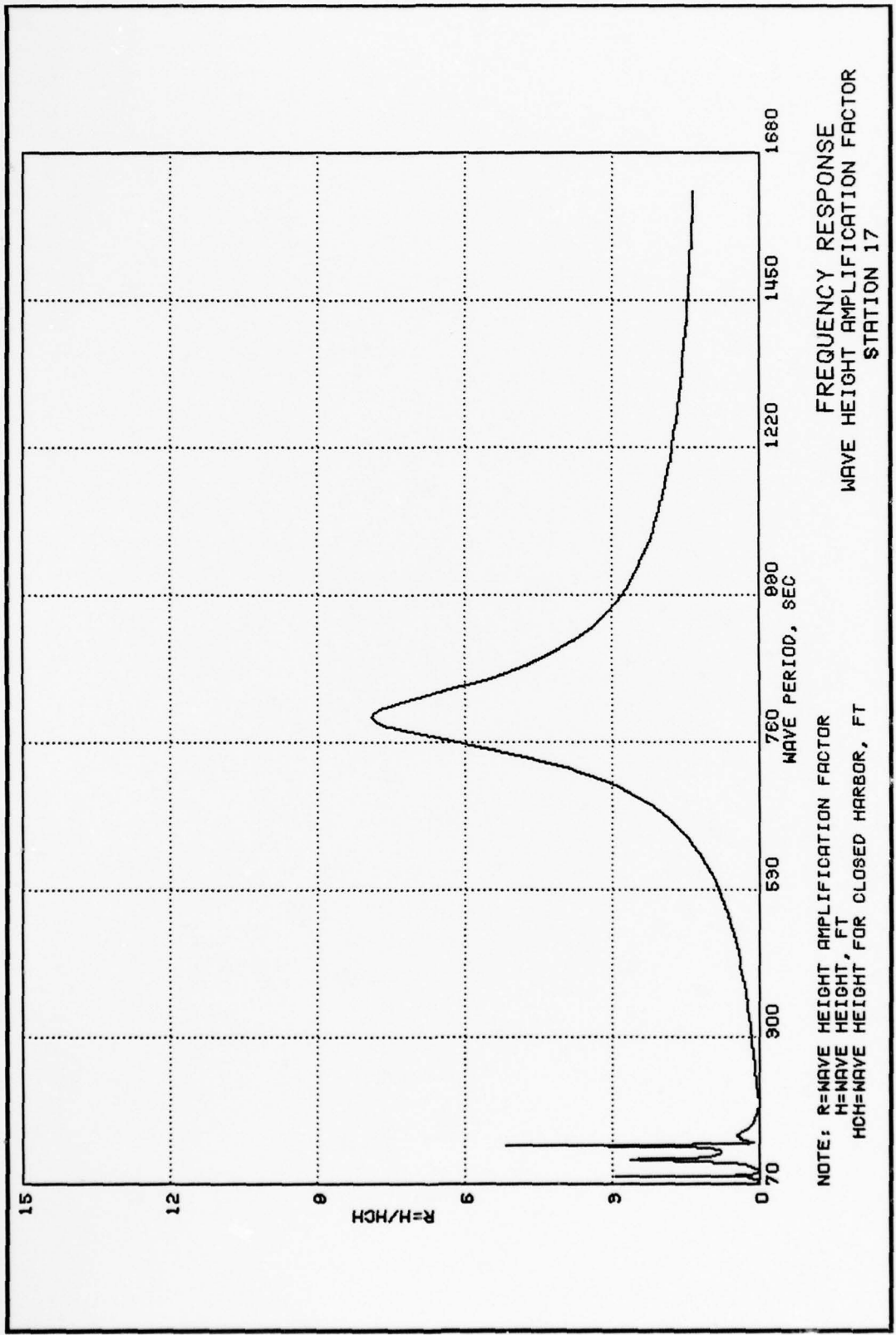


PLATE 36



FREQUENCY RESPONSE  
 WAVE HEIGHT AMPLIFICATION FACTOR  
 STATION 17

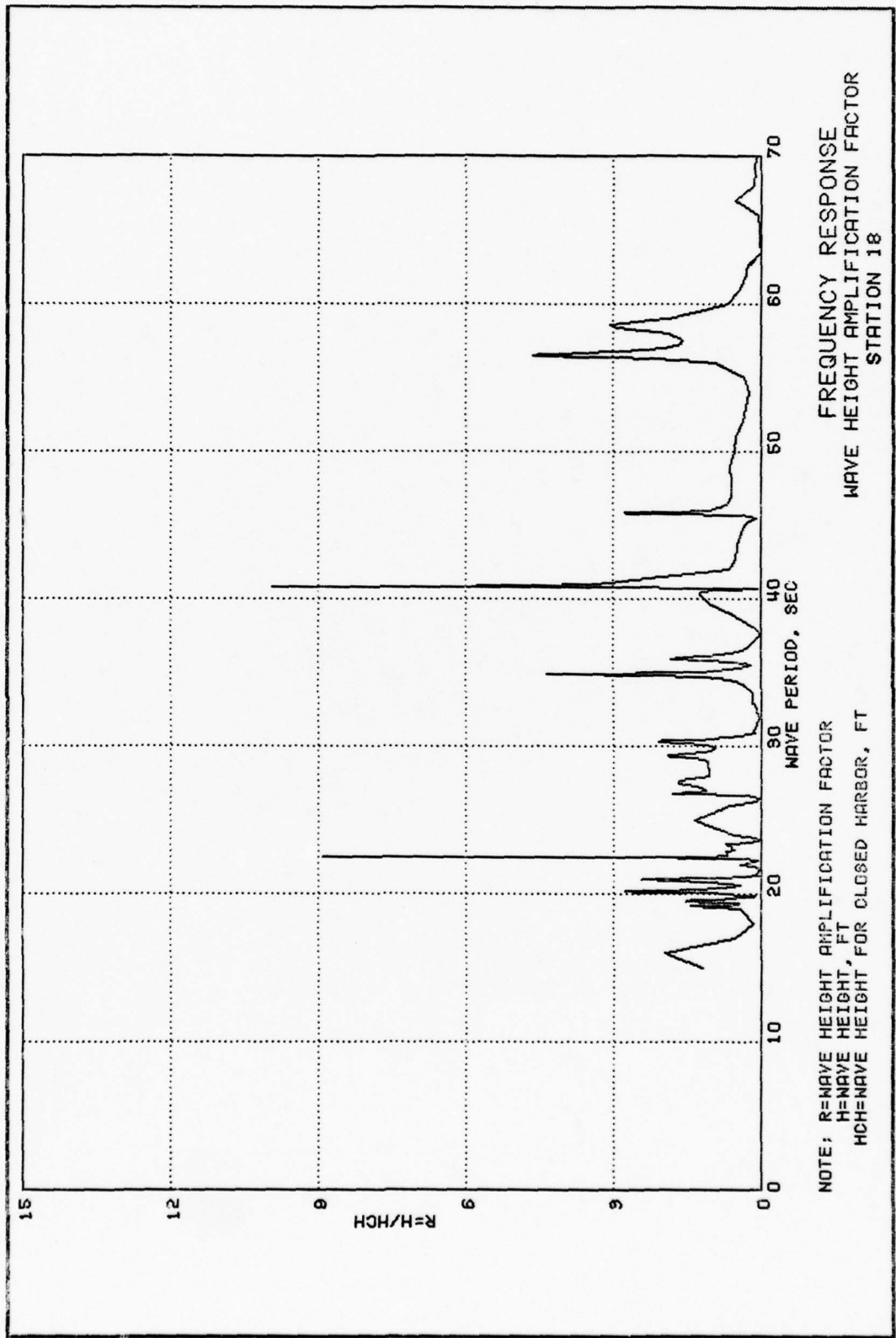
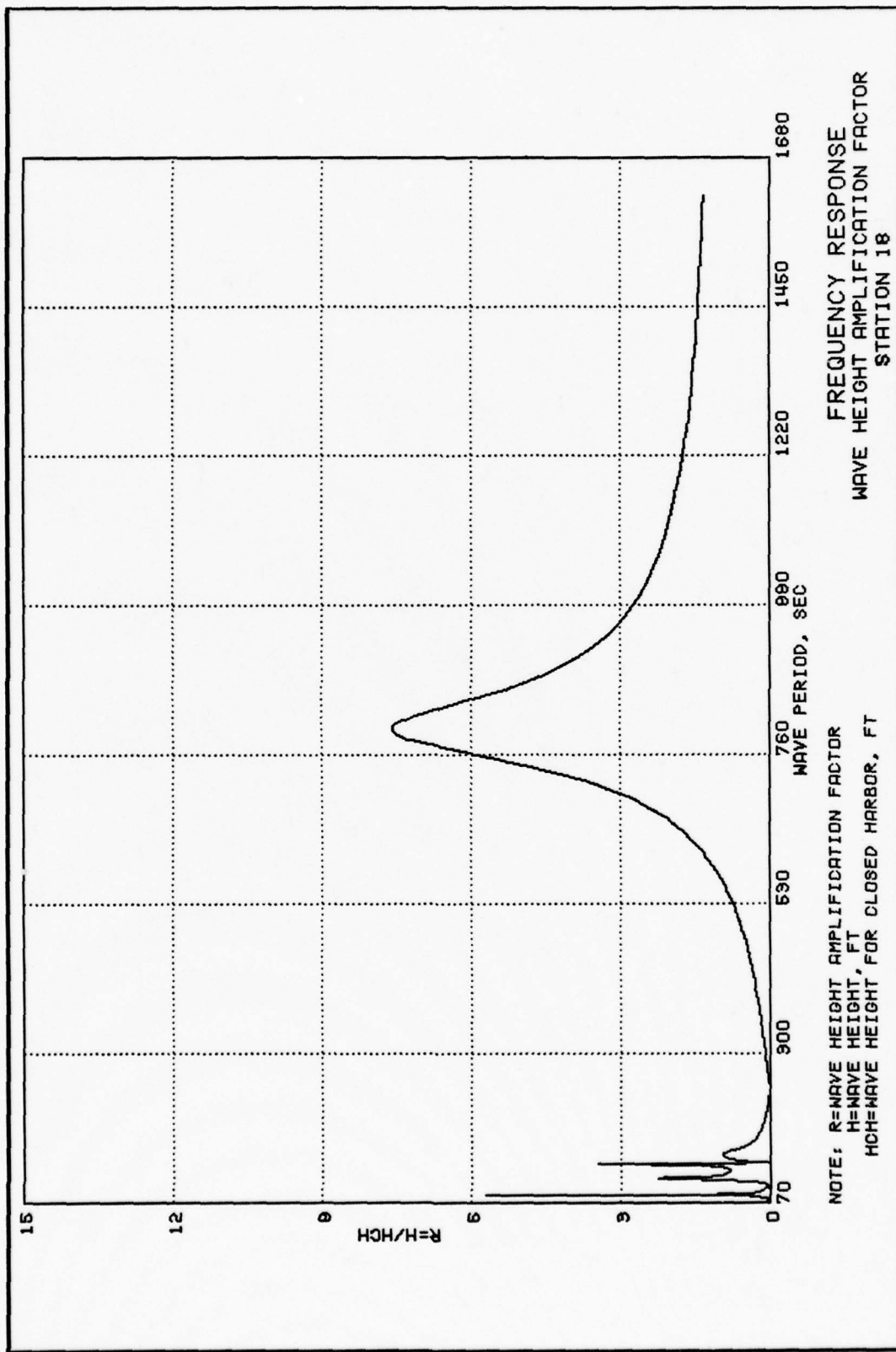


PLATE 38





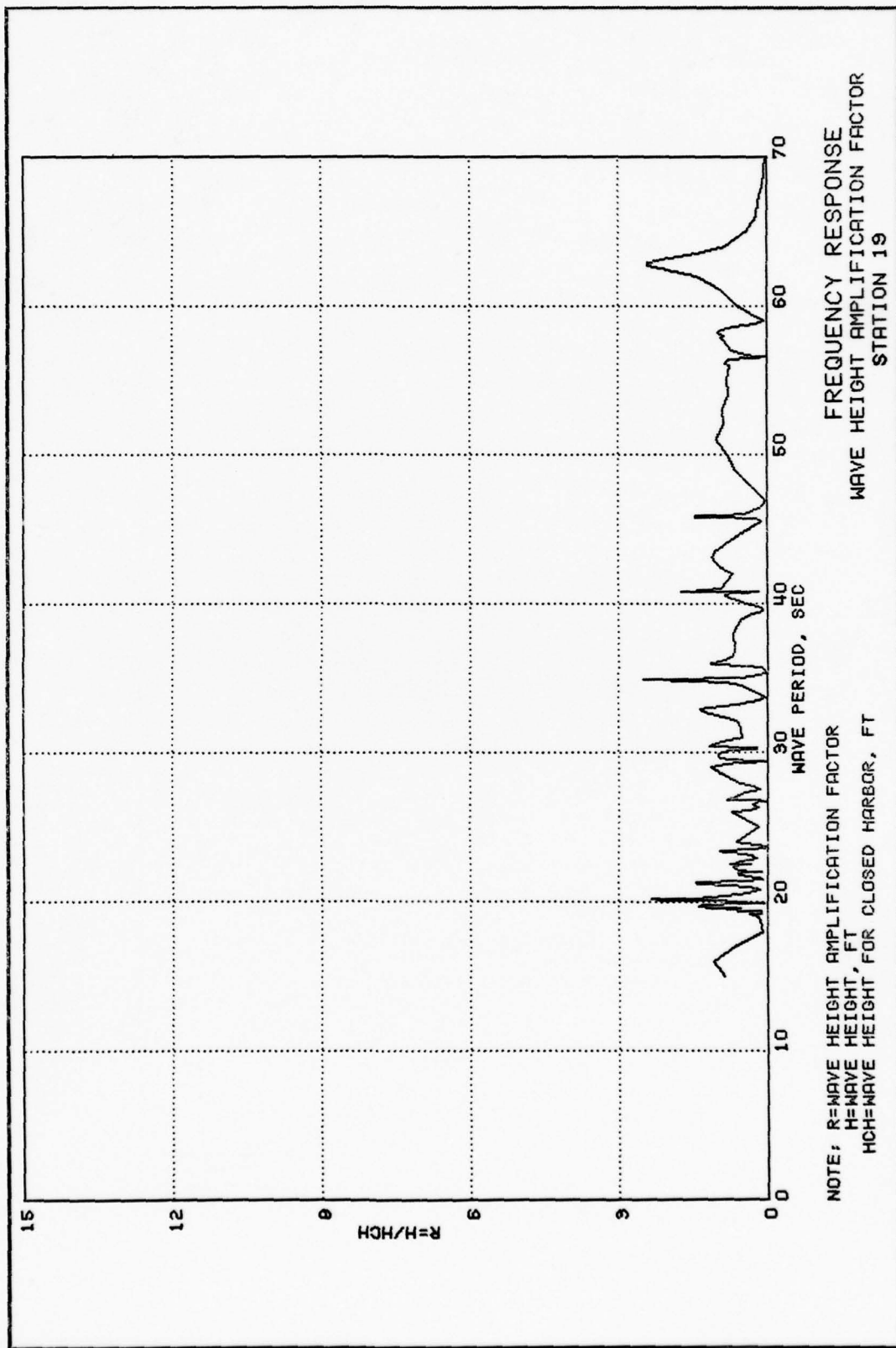
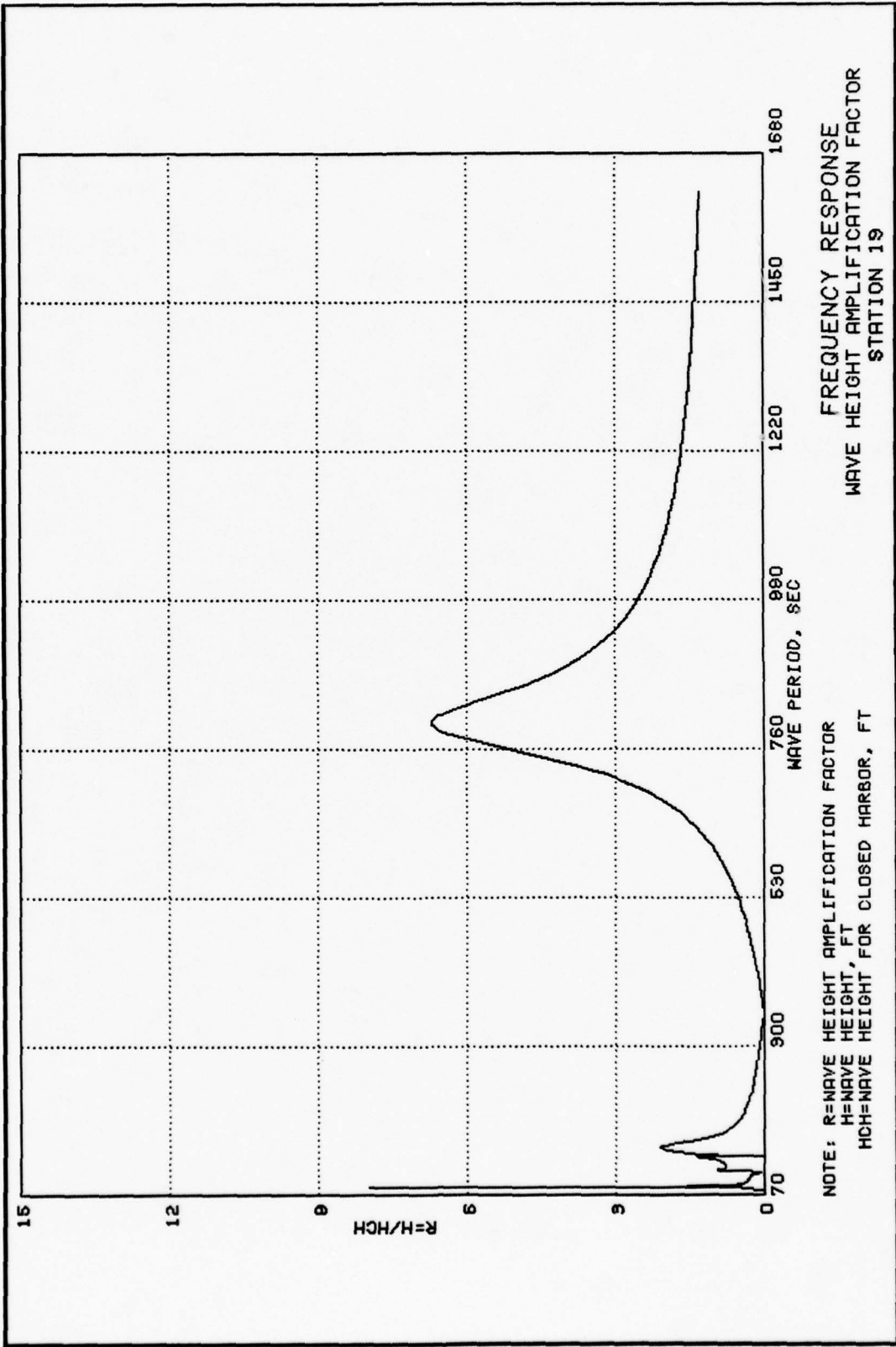
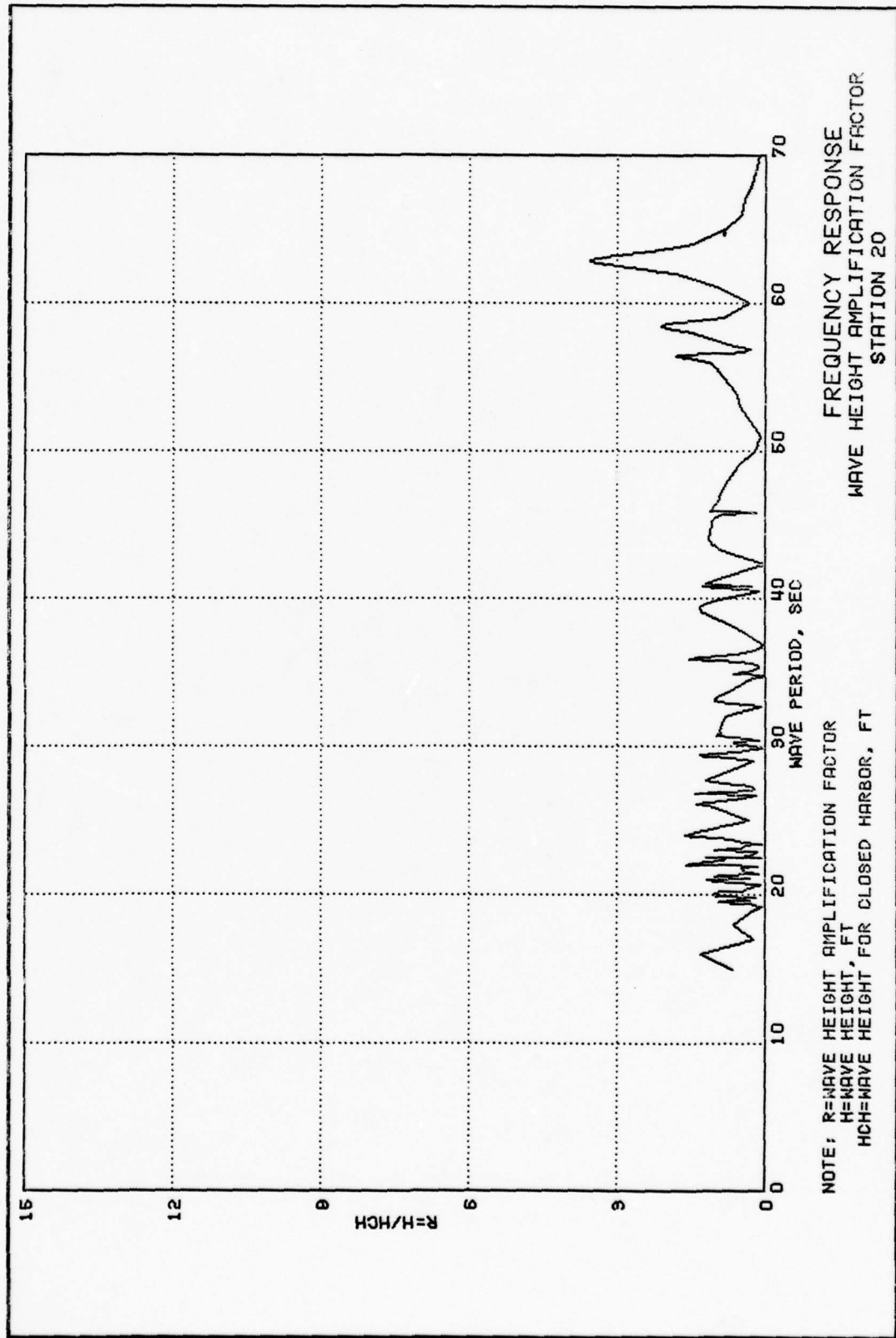


PLATE 40

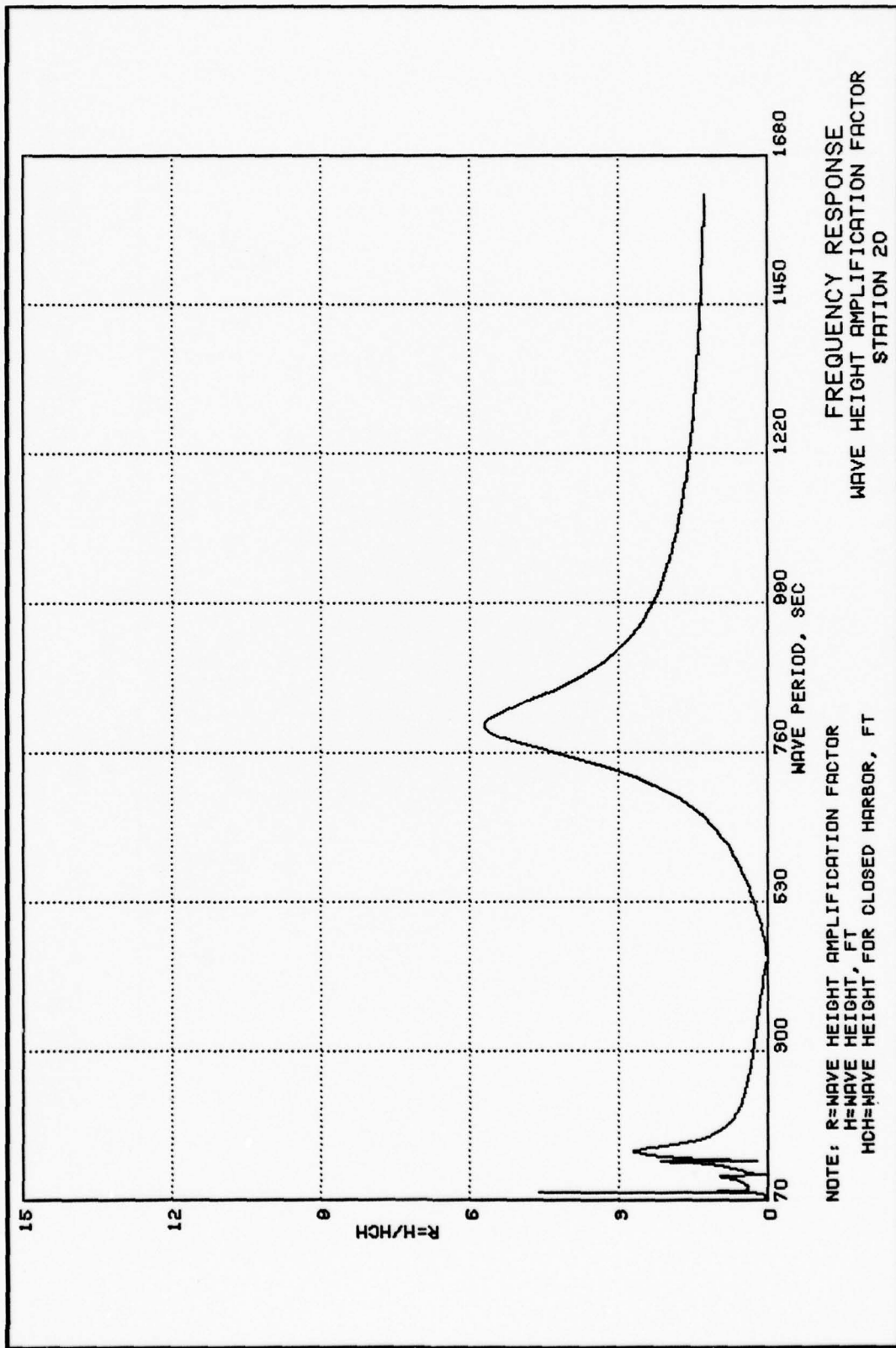




FREQUENCY RESPONSE  
 WAVE HEIGHT AMPLIFICATION FACTOR  
 STATION 20

NOTE: R=WAVE HEIGHT AMPLIFICATION FACTOR  
 H=WAVE HEIGHT, FT  
 HCH=WAVE HEIGHT FOR CLOSED HARBOR, FT

PLATE 42



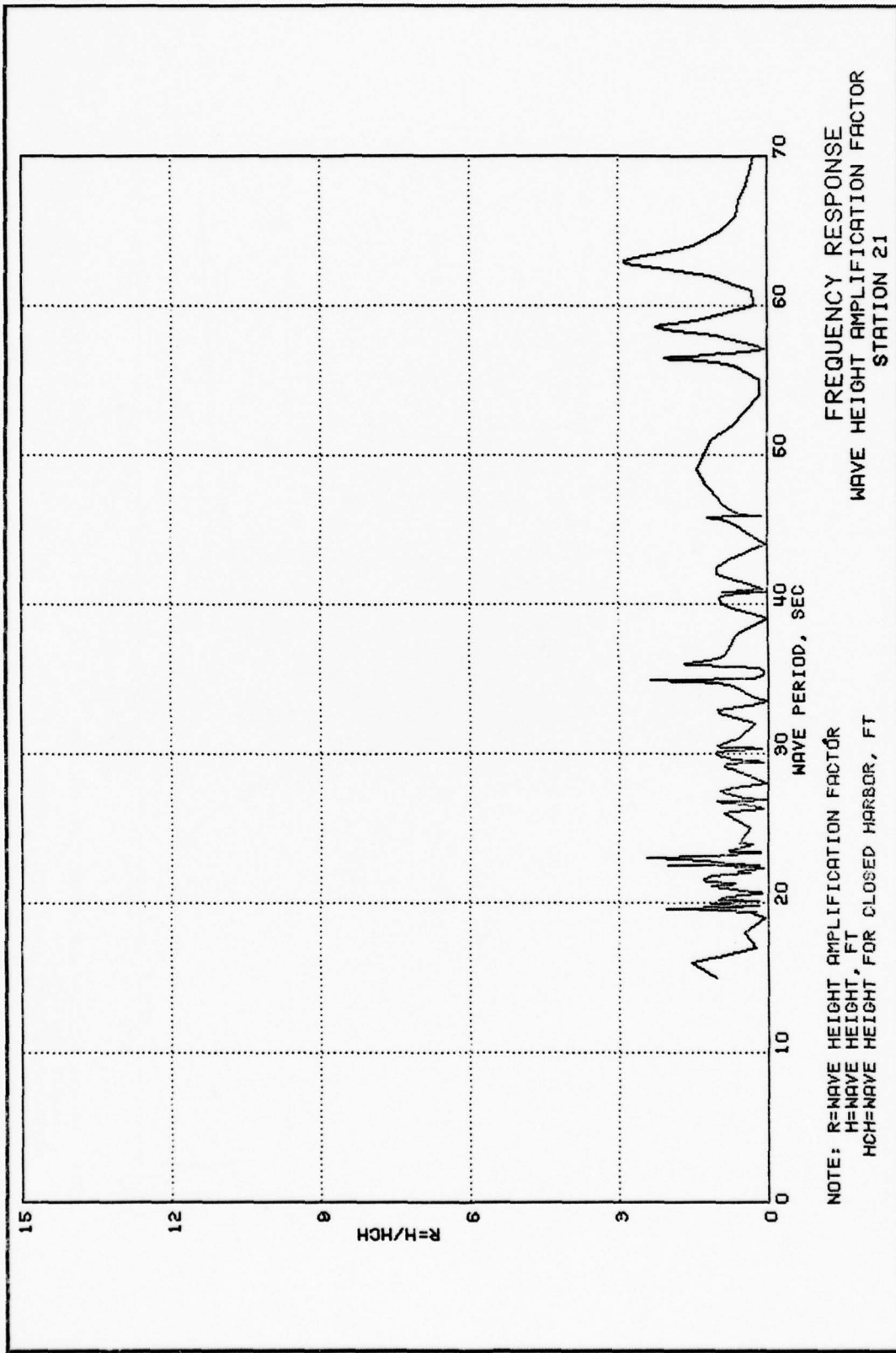
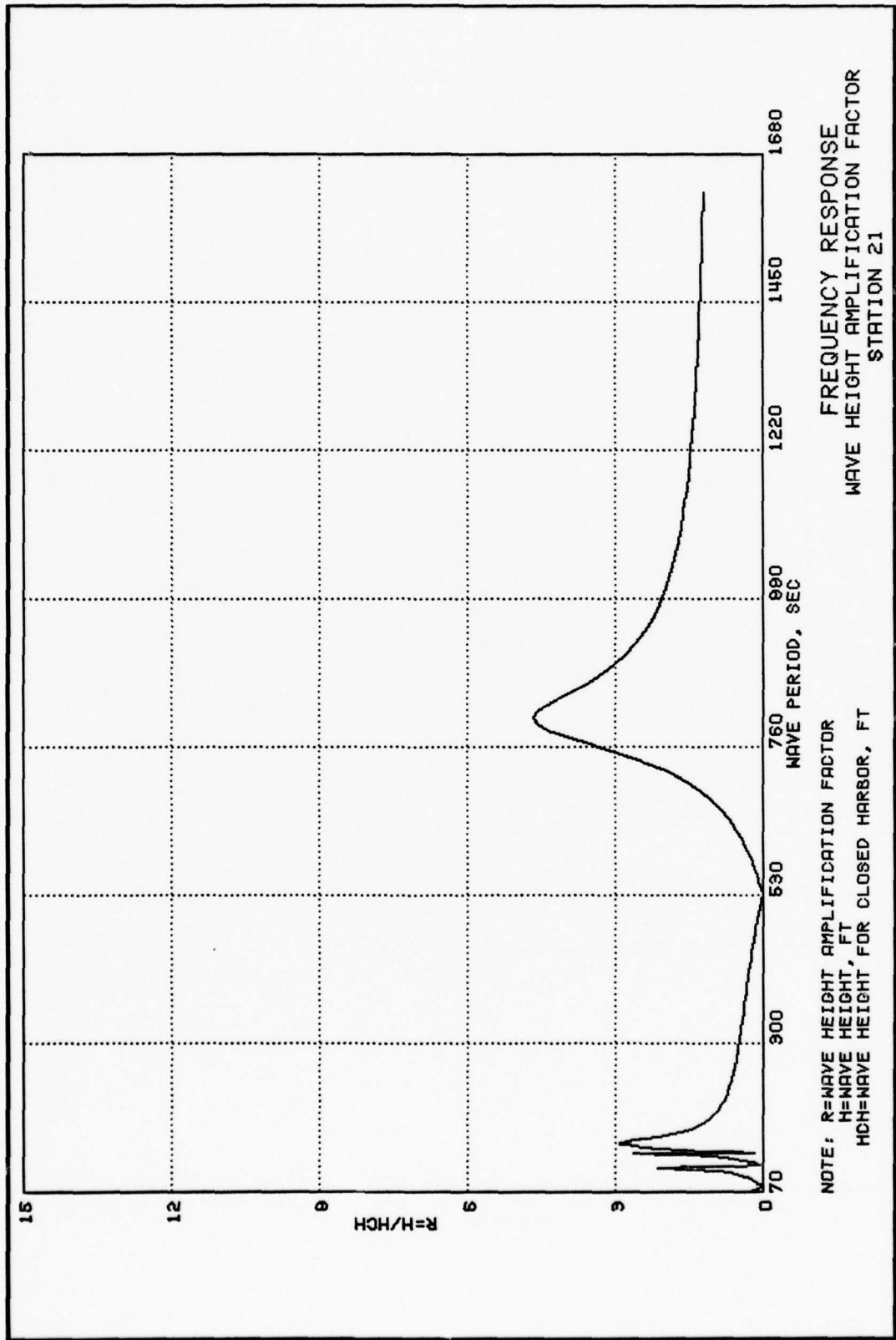


PLATE 44



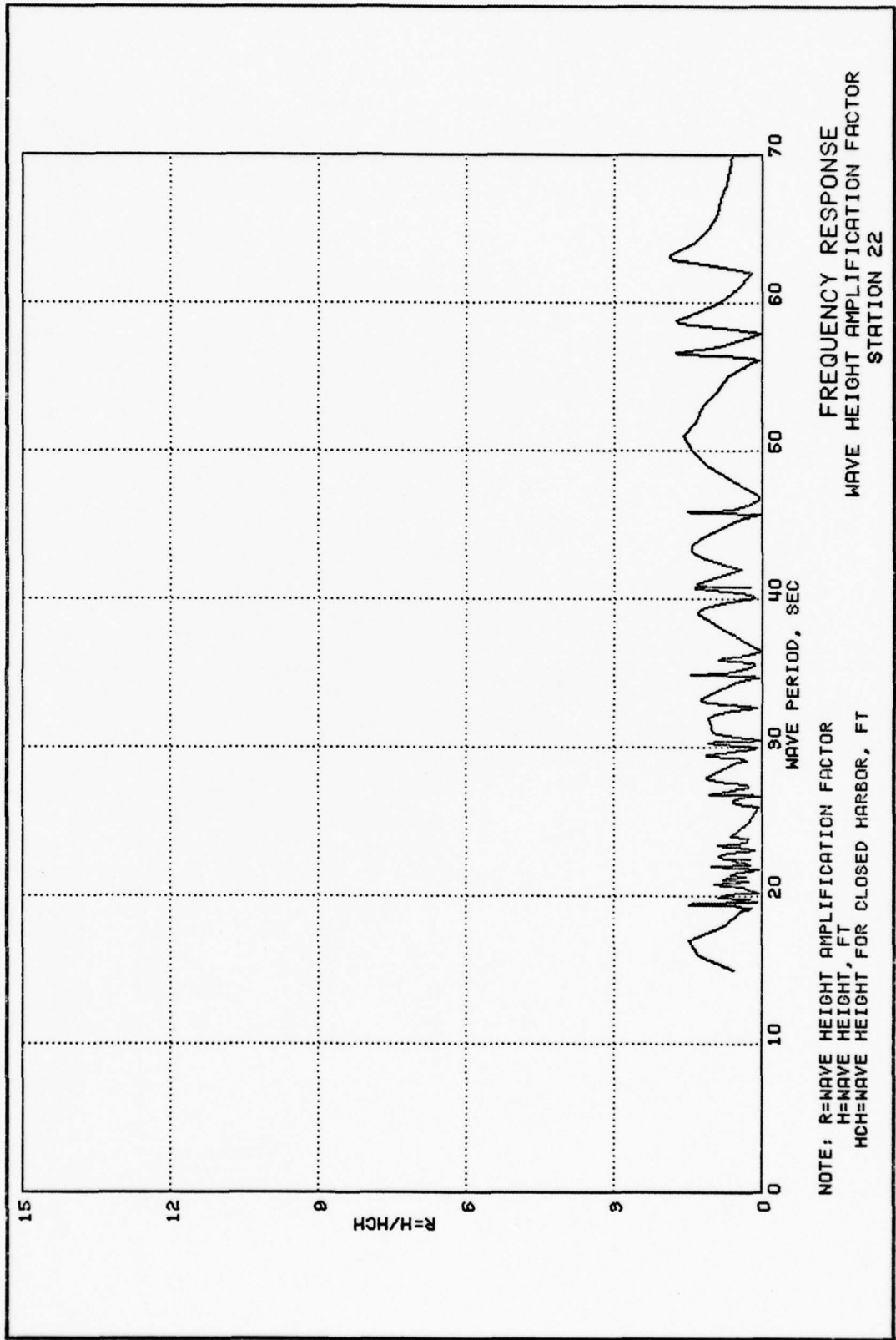
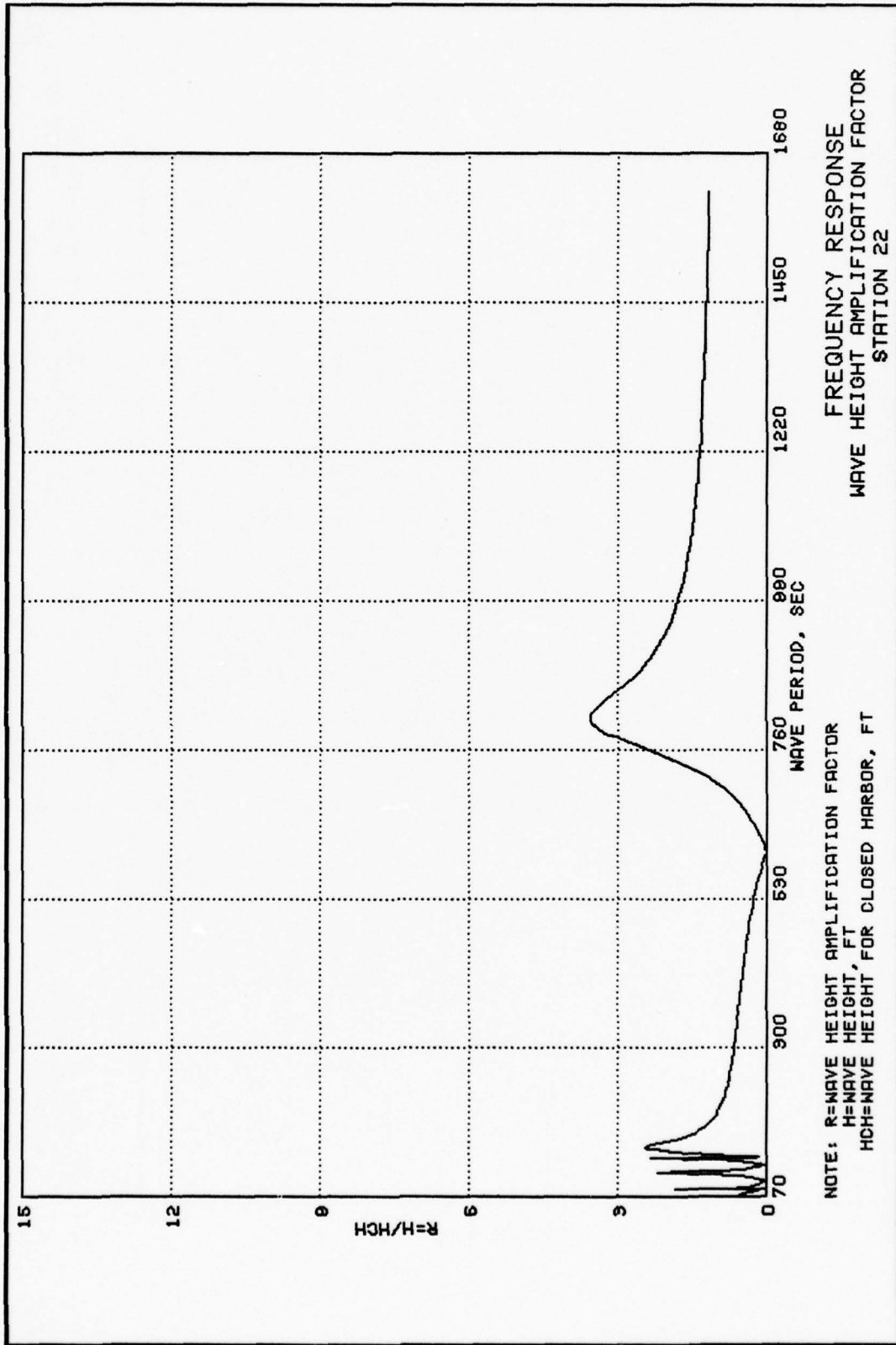


PLATE 46





FREQUENCY RESPONSE  
 WAVE HEIGHT AMPLIFICATION FACTOR  
 STATION 22

NOTE: R=WAVE HEIGHT AMPLIFICATION FACTOR  
 H=WAVE HEIGHT, FT  
 HCH=WAVE HEIGHT FOR CLOSED HARBOR, FT

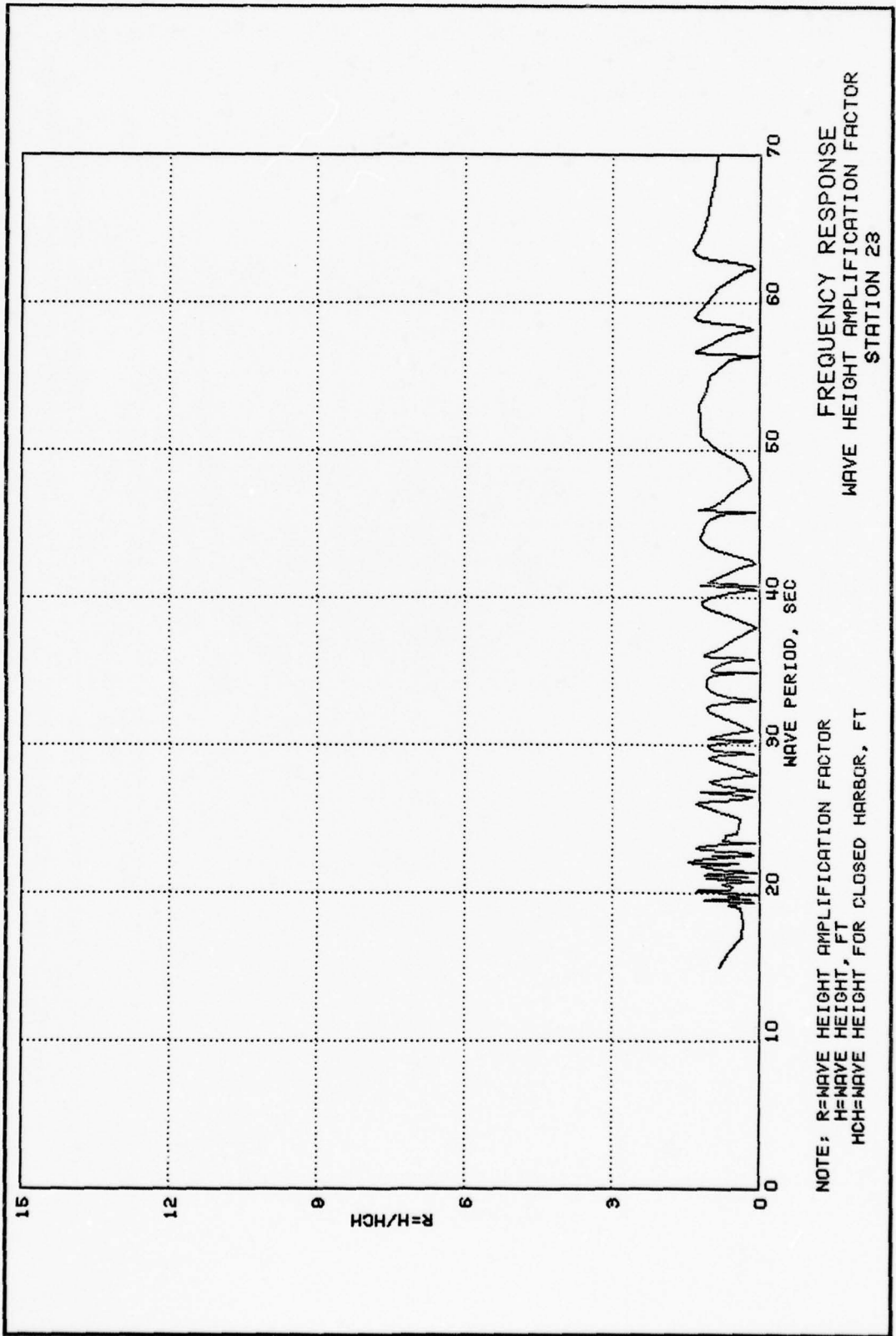
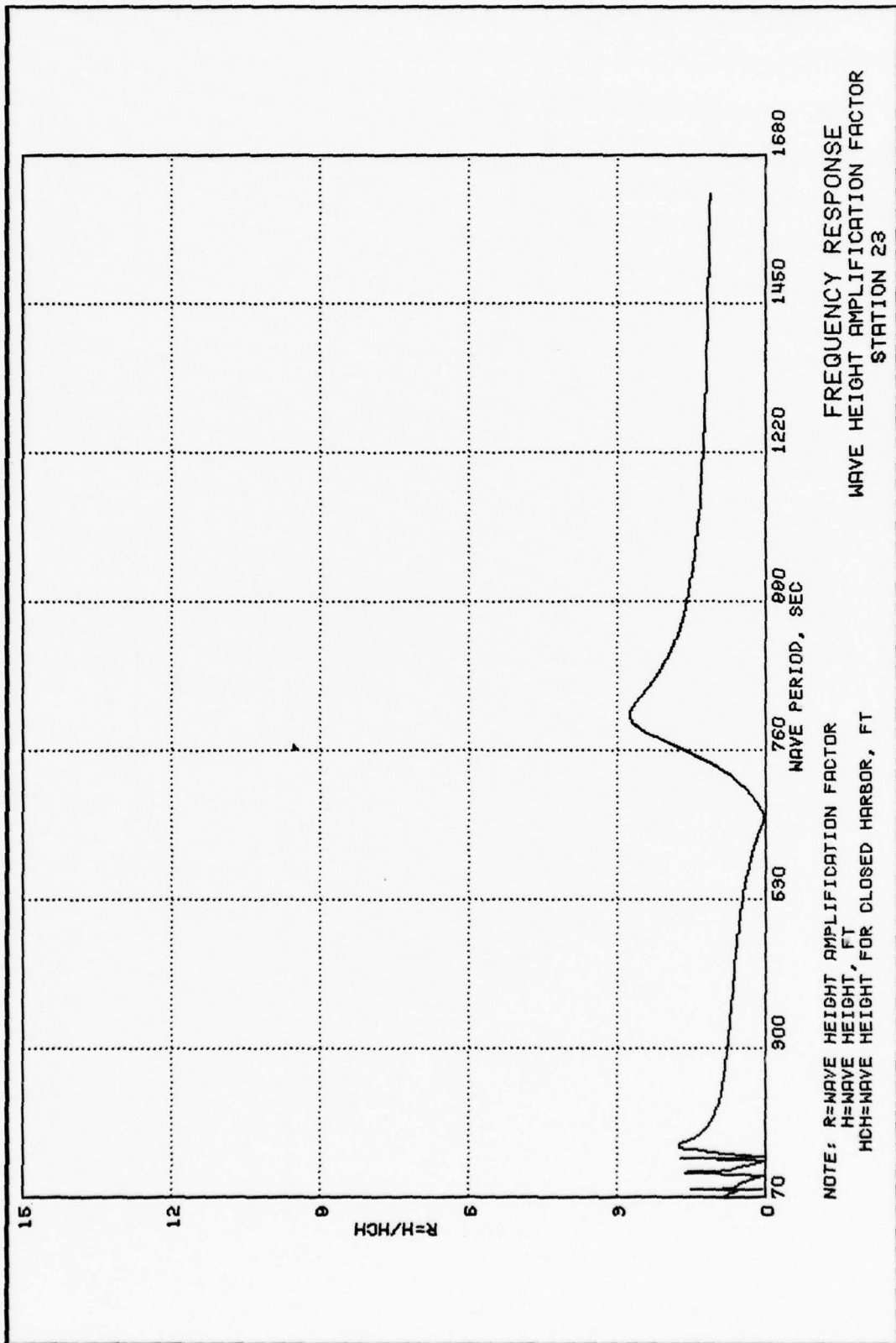
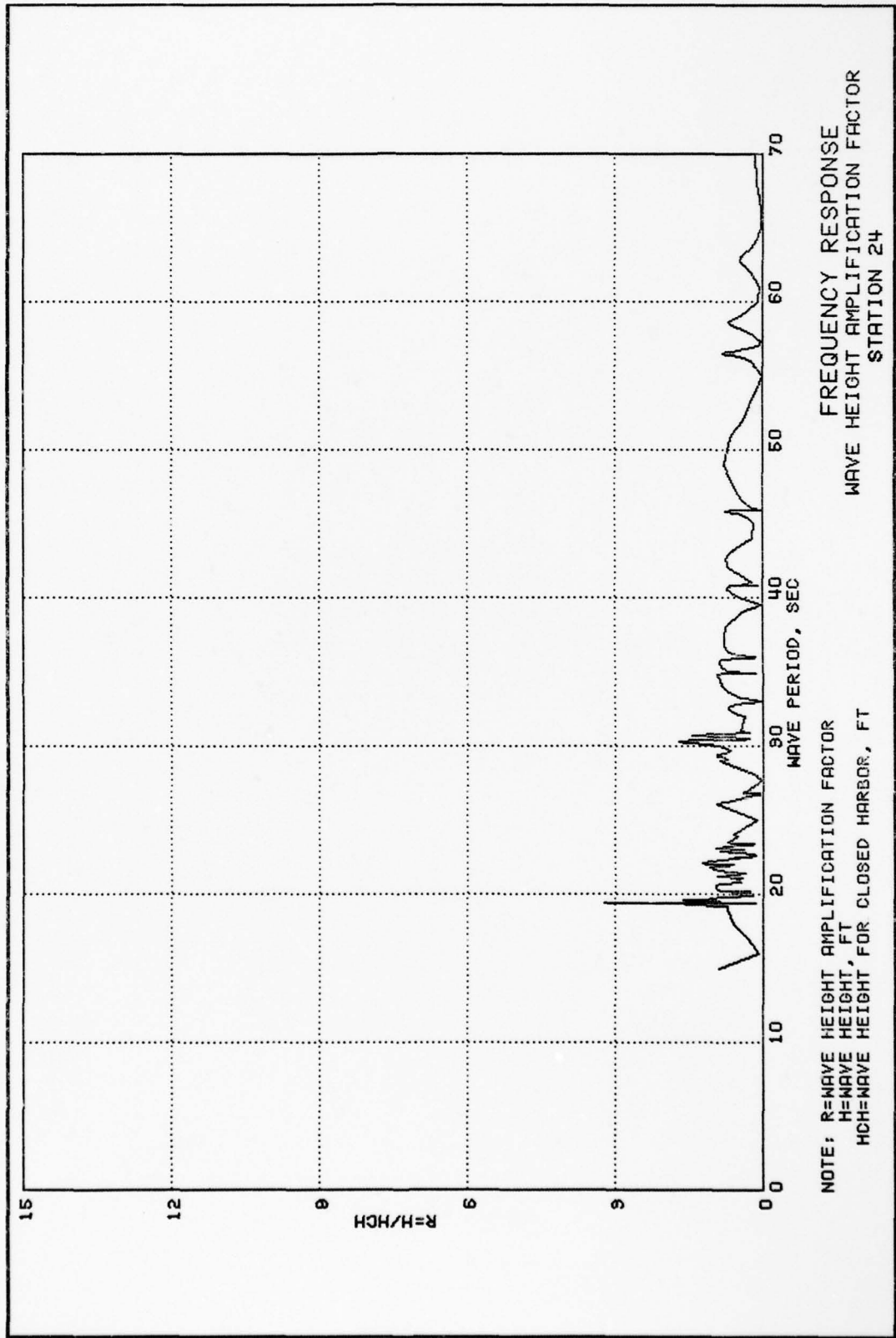


PLATE 48



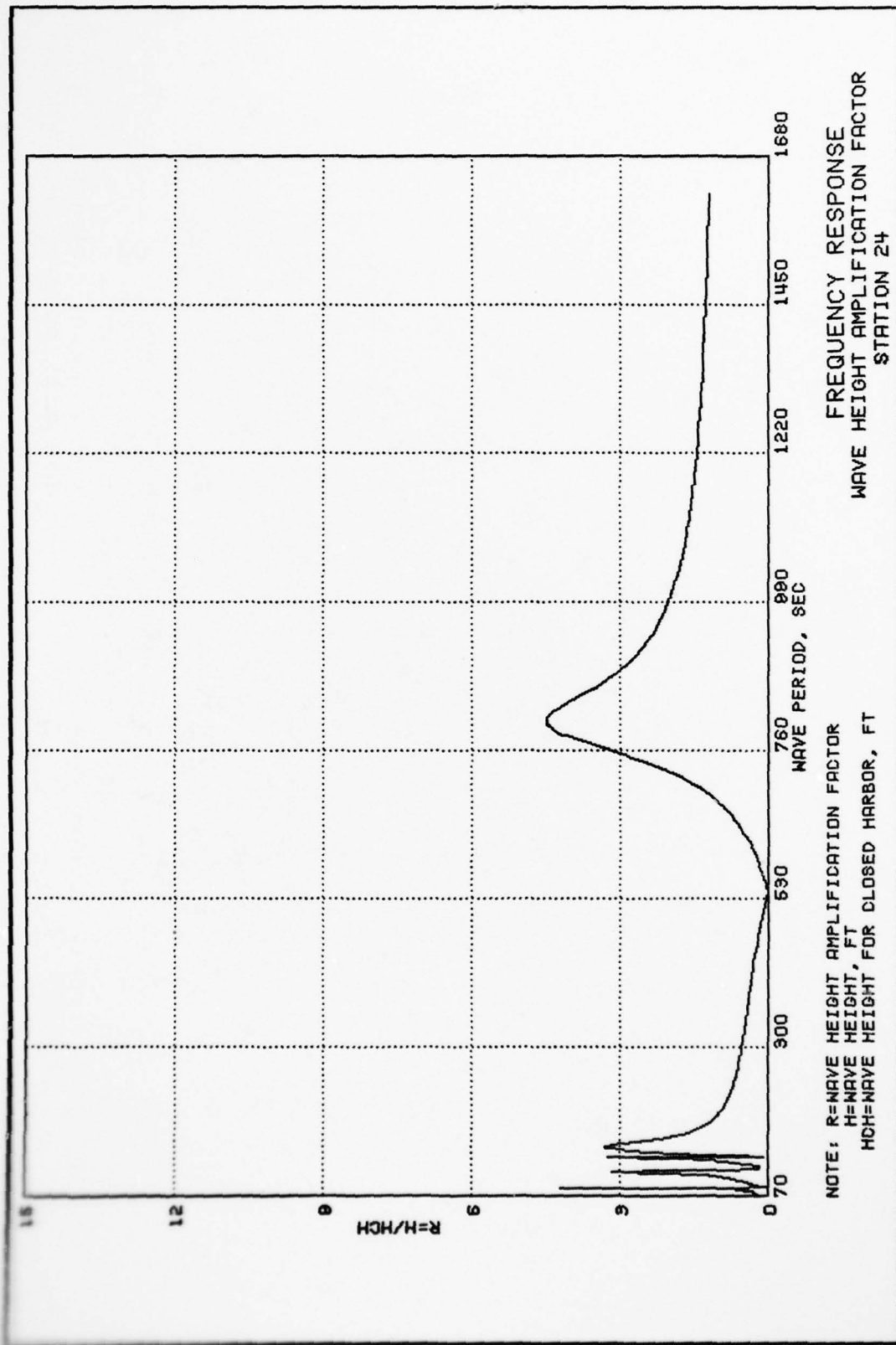
NOTE: R=WAVE HEIGHT AMPLIFICATION FACTOR  
 H=WAVE HEIGHT, FT  
 HCH=WAVE HEIGHT FOR CLOSED HARBOR, FT



FREQUENCY RESPONSE  
 WAVE HEIGHT AMPLIFICATION FACTOR  
 STATION 24

NOTE: R=WAVE HEIGHT AMPLIFICATION FACTOR  
 H=WAVE HEIGHT, FT  
 HCH=WAVE HEIGHT FOR CLOSED HARBOR, FT

PLATE 50



FREQUENCY RESPONSE  
 WAVE HEIGHT AMPLIFICATION FACTOR  
 STATION 24

NOTE: R=WAVE HEIGHT AMPLIFICATION FACTOR  
 H=WAVE HEIGHT, FT  
 HCH=WAVE HEIGHT FOR CLOSED HARBOR, FT

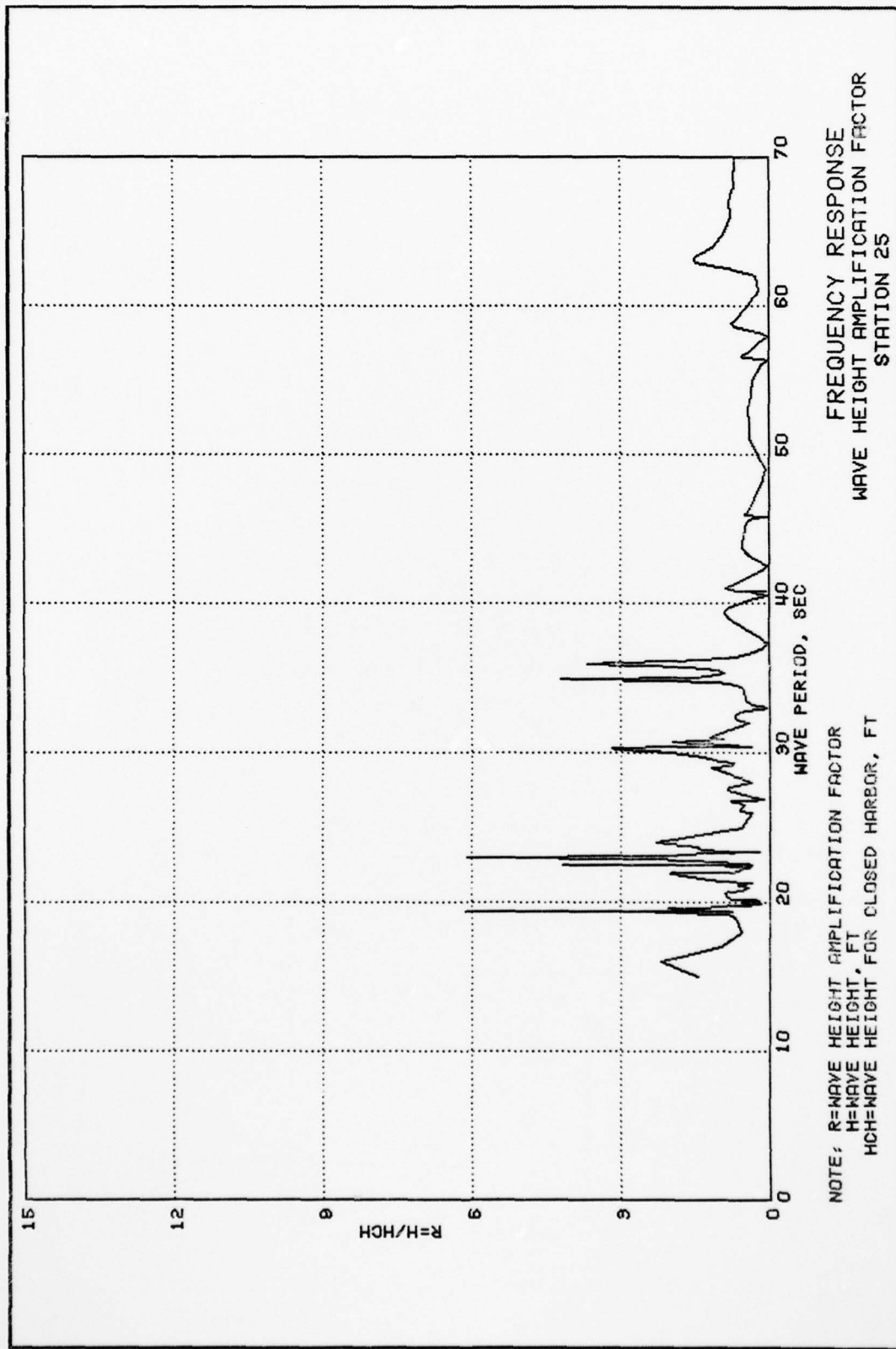
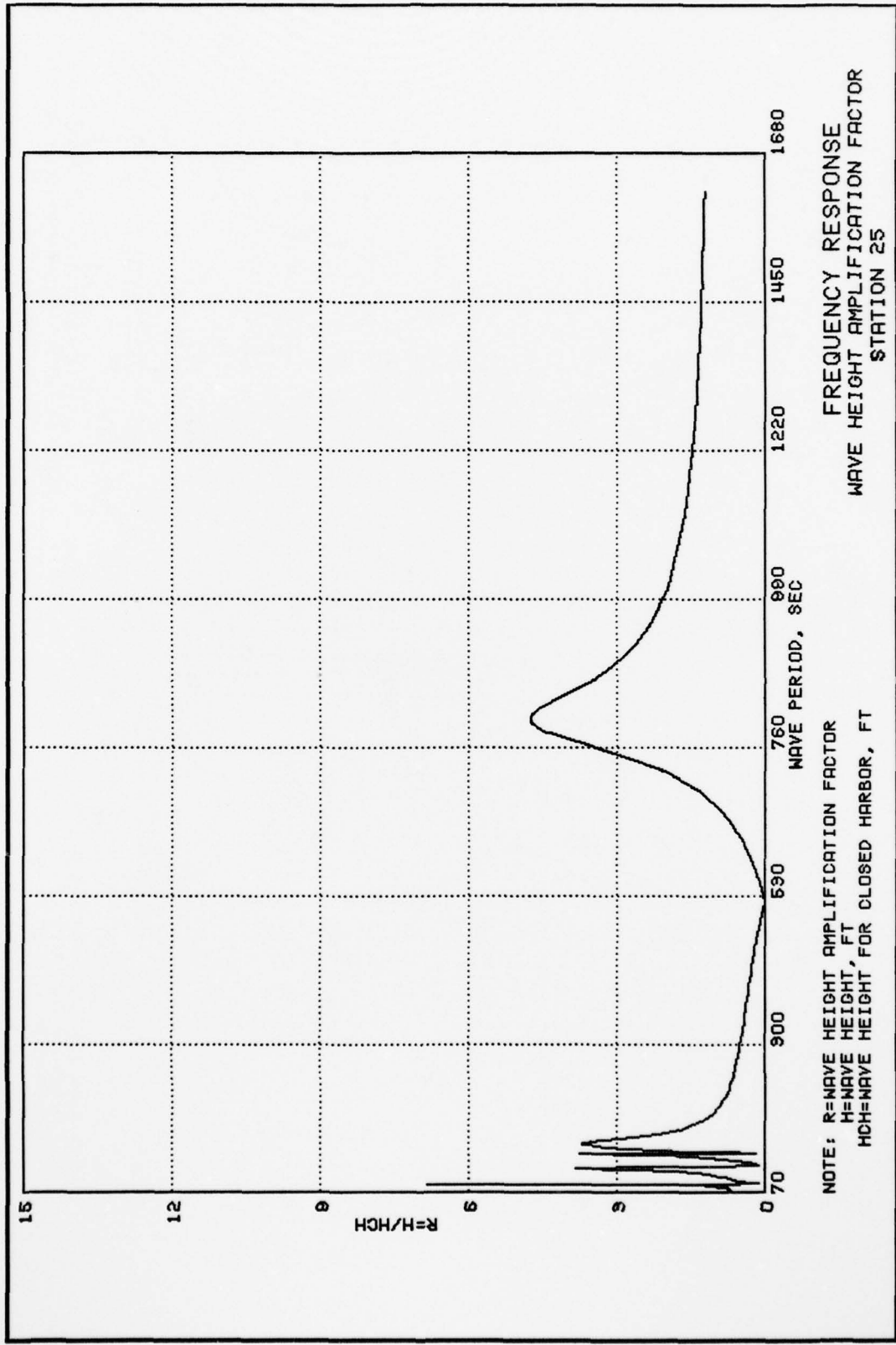


PLATE 52



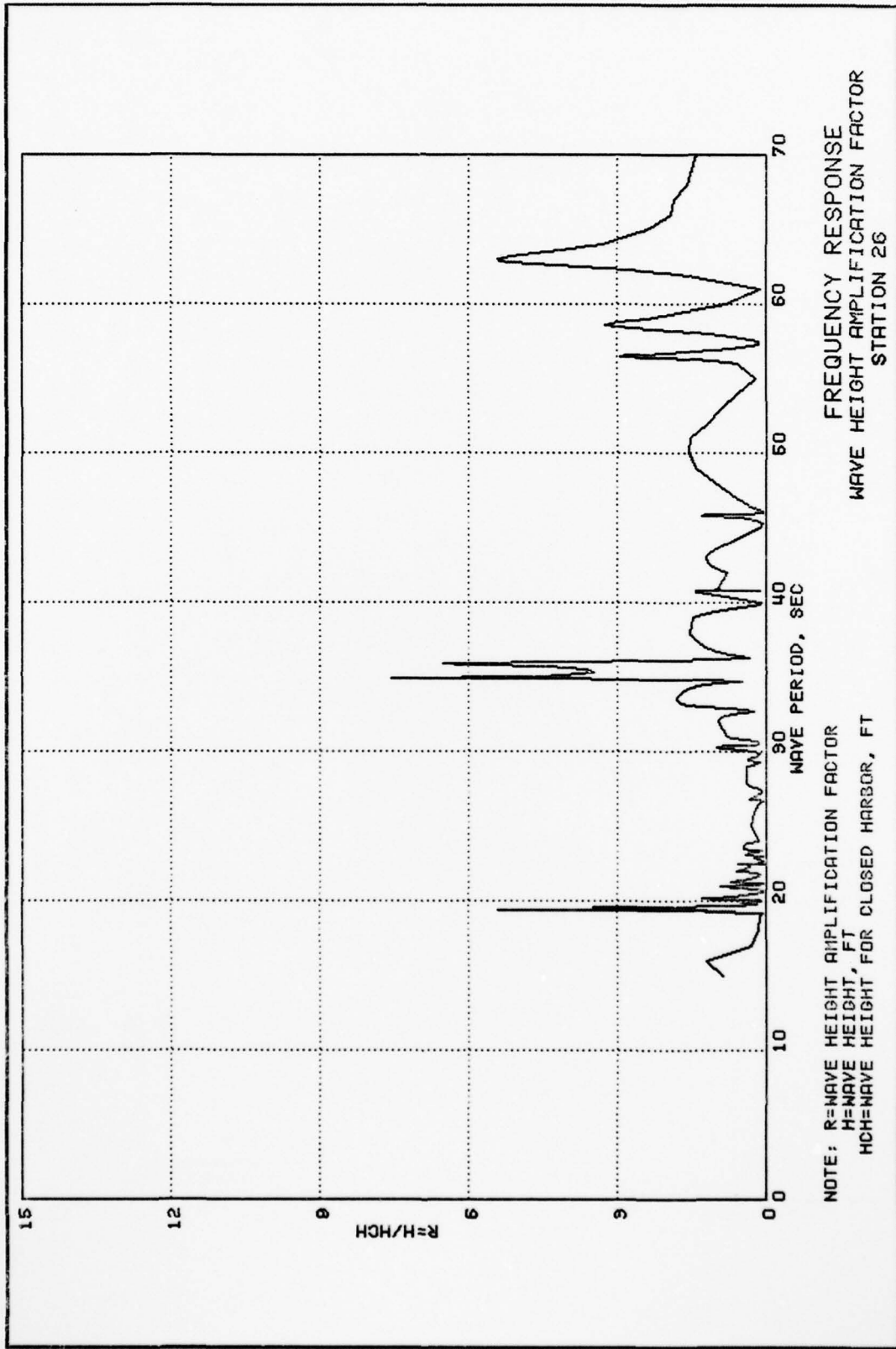
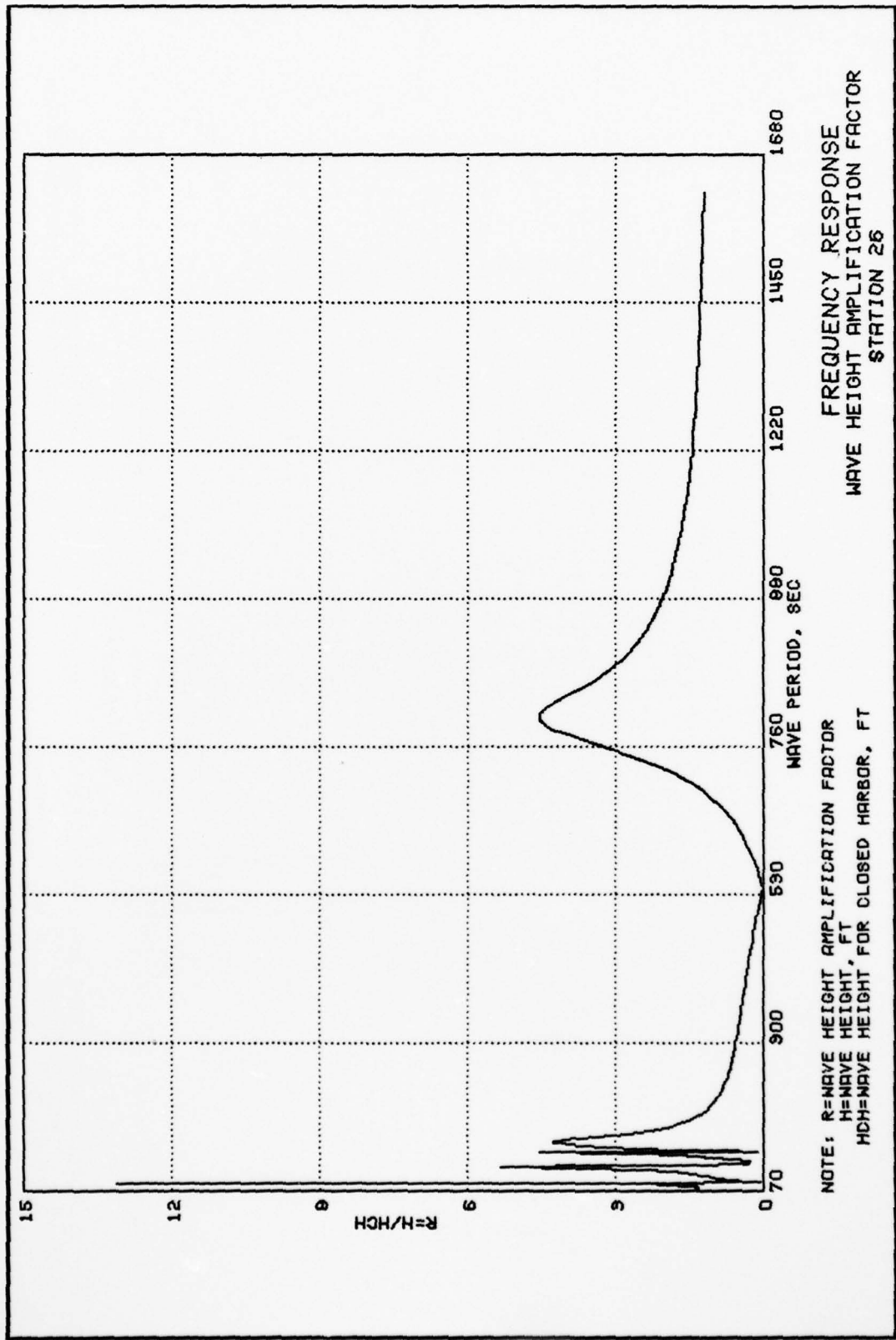


PLATE 54





FREQUENCY RESPONSE  
 WAVE HEIGHT AMPLIFICATION FACTOR  
 STATION 26

NOTE: R=WAVE HEIGHT AMPLIFICATION FACTOR  
 H=WAVE HEIGHT, FT  
 HCH=WAVE HEIGHT FOR CLOSED HARBOR, FT

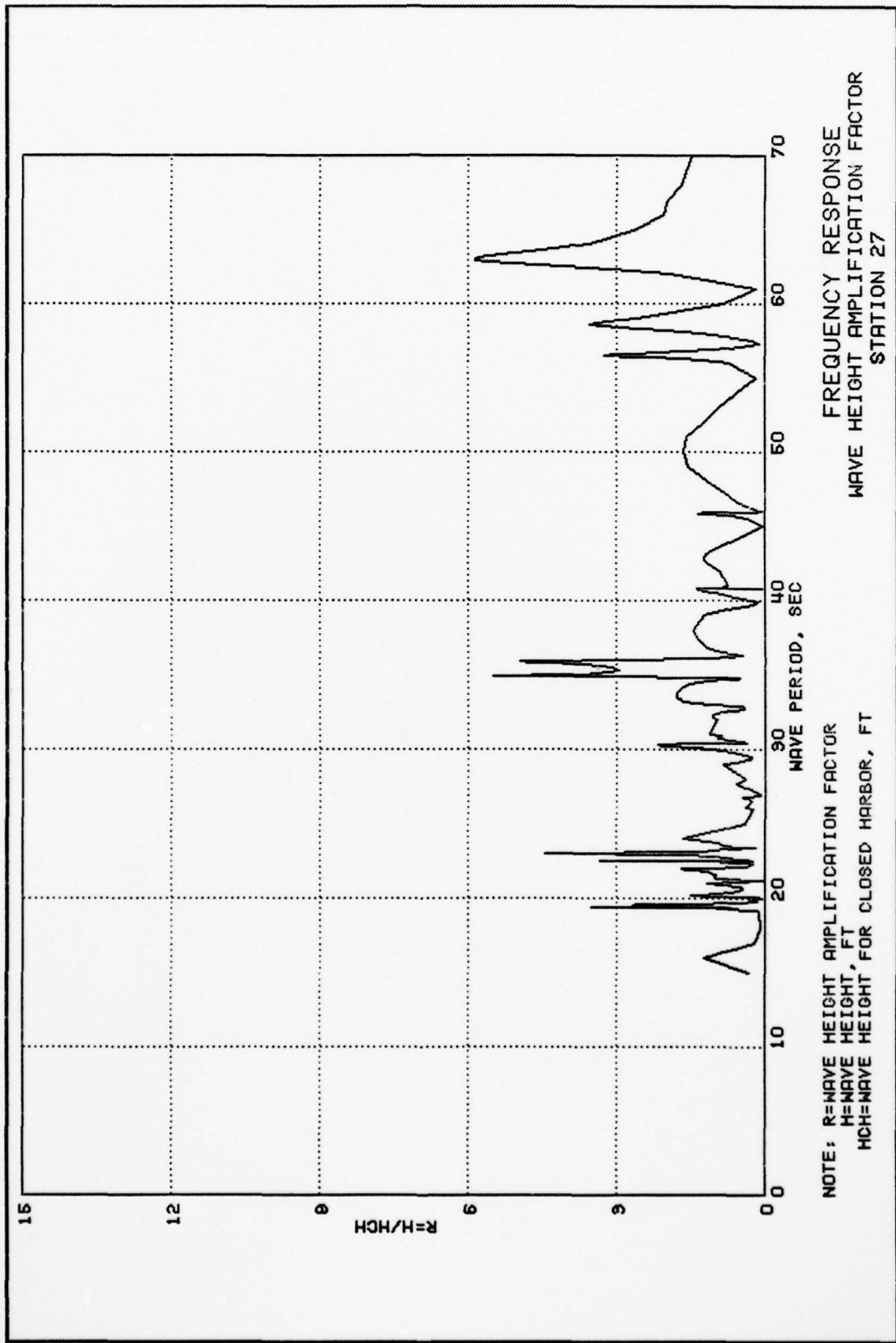
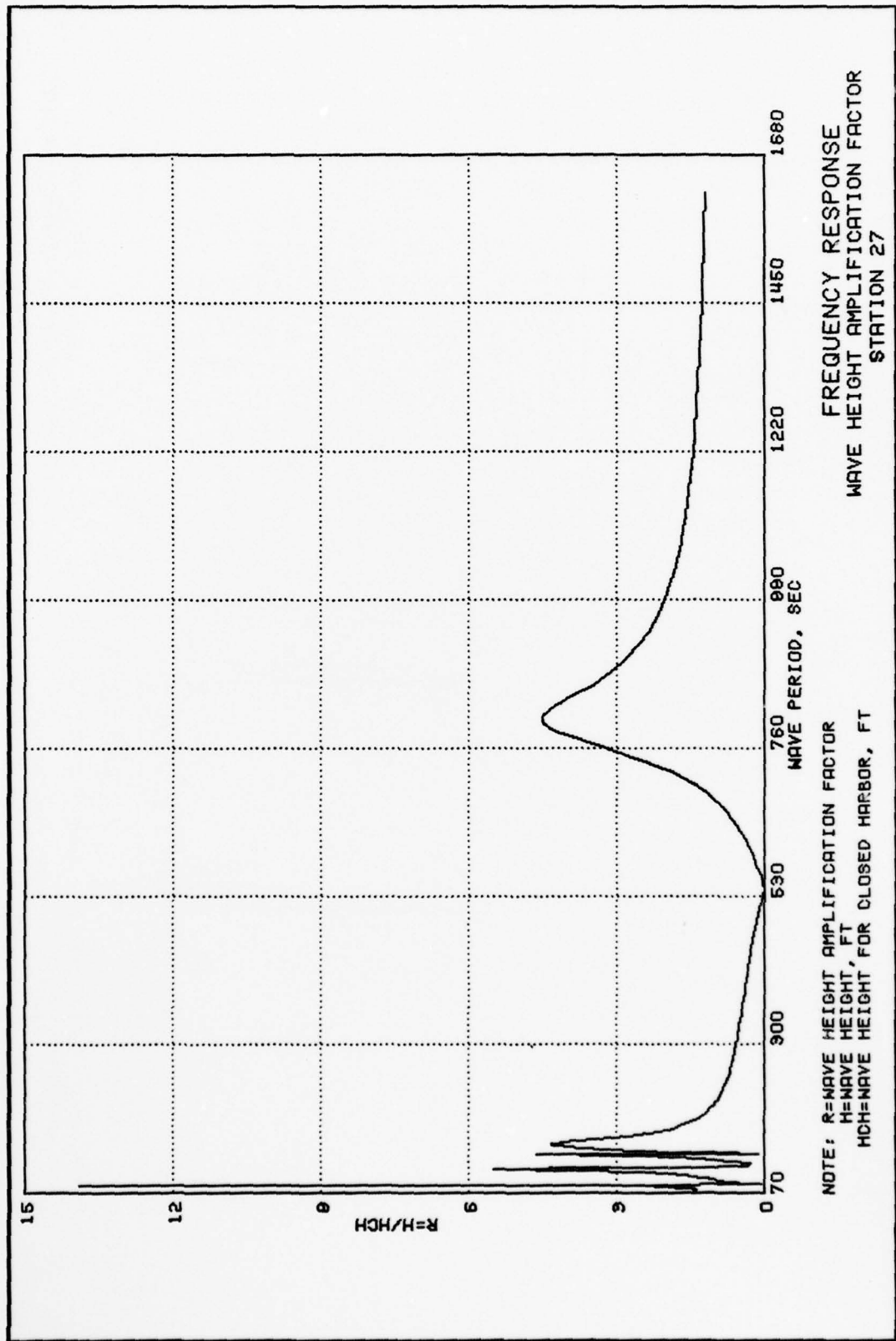
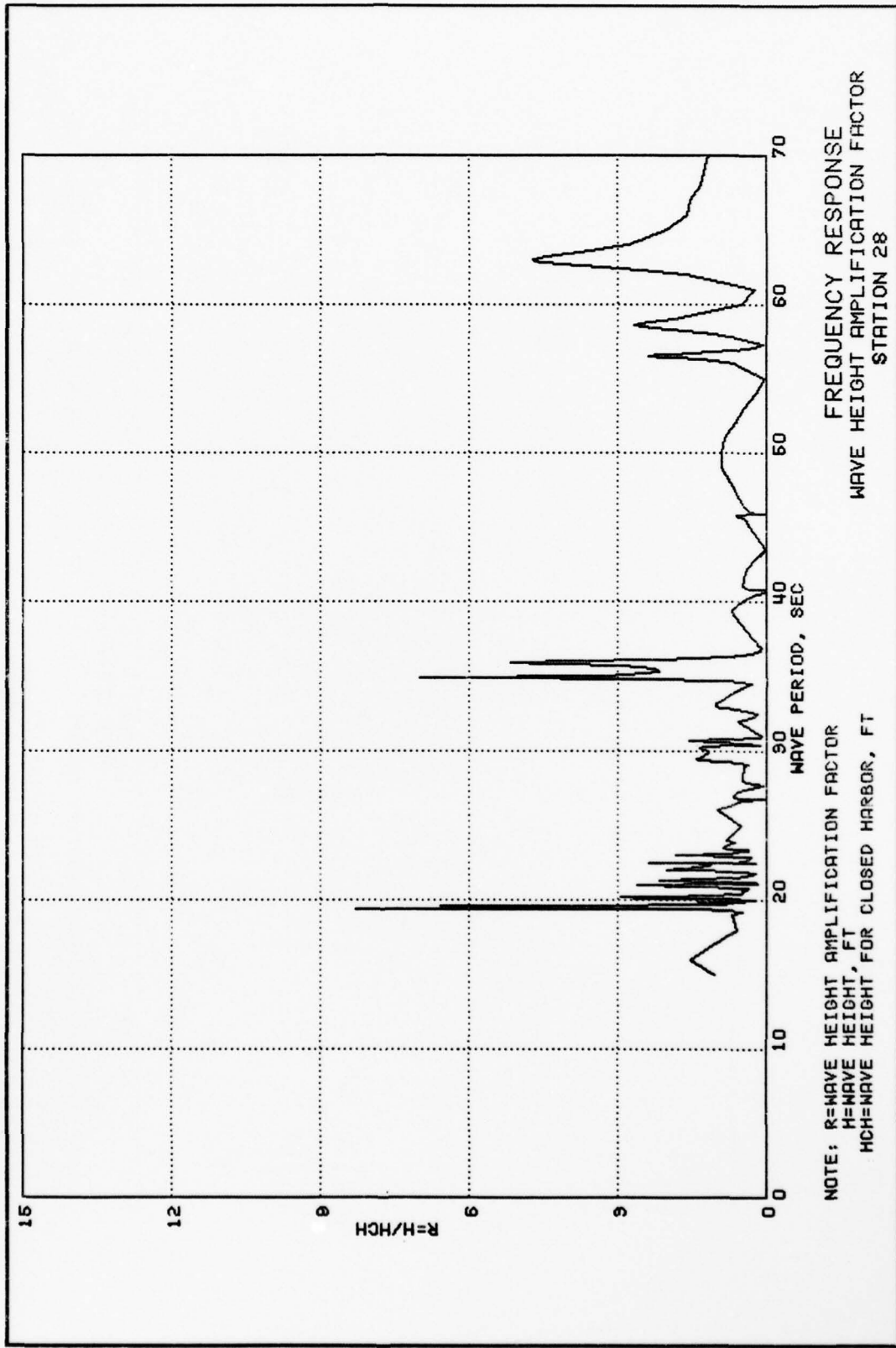


PLATE 56

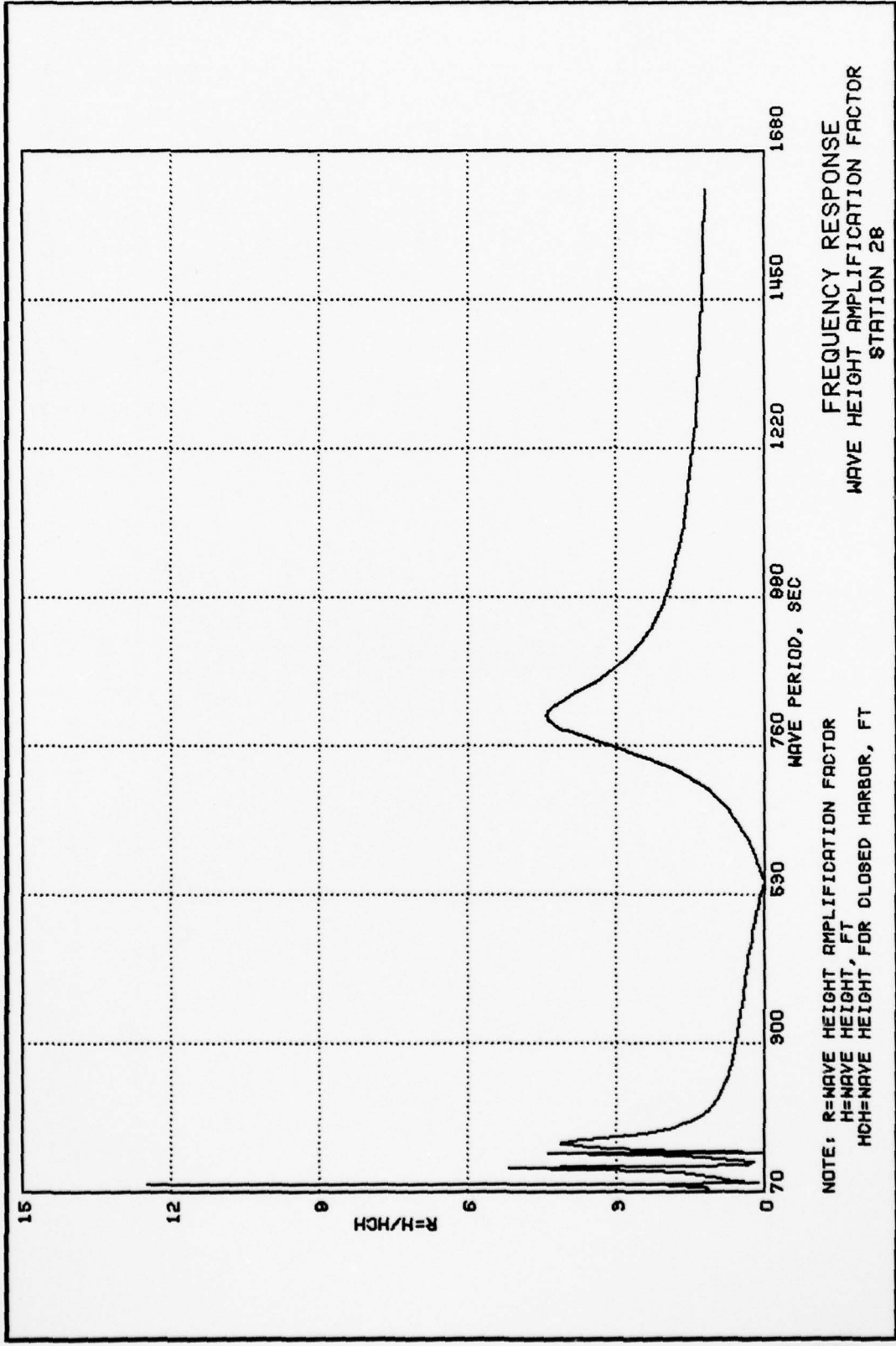




NOTE: R=WAVE HEIGHT AMPLIFICATION FACTOR  
 H=WAVE HEIGHT, FT  
 HCH=WAVE HEIGHT FOR CLOSED HARBOR, FT

FREQUENCY RESPONSE  
 WAVE HEIGHT AMPLIFICATION FACTOR  
 STATION 28

PLATE 58



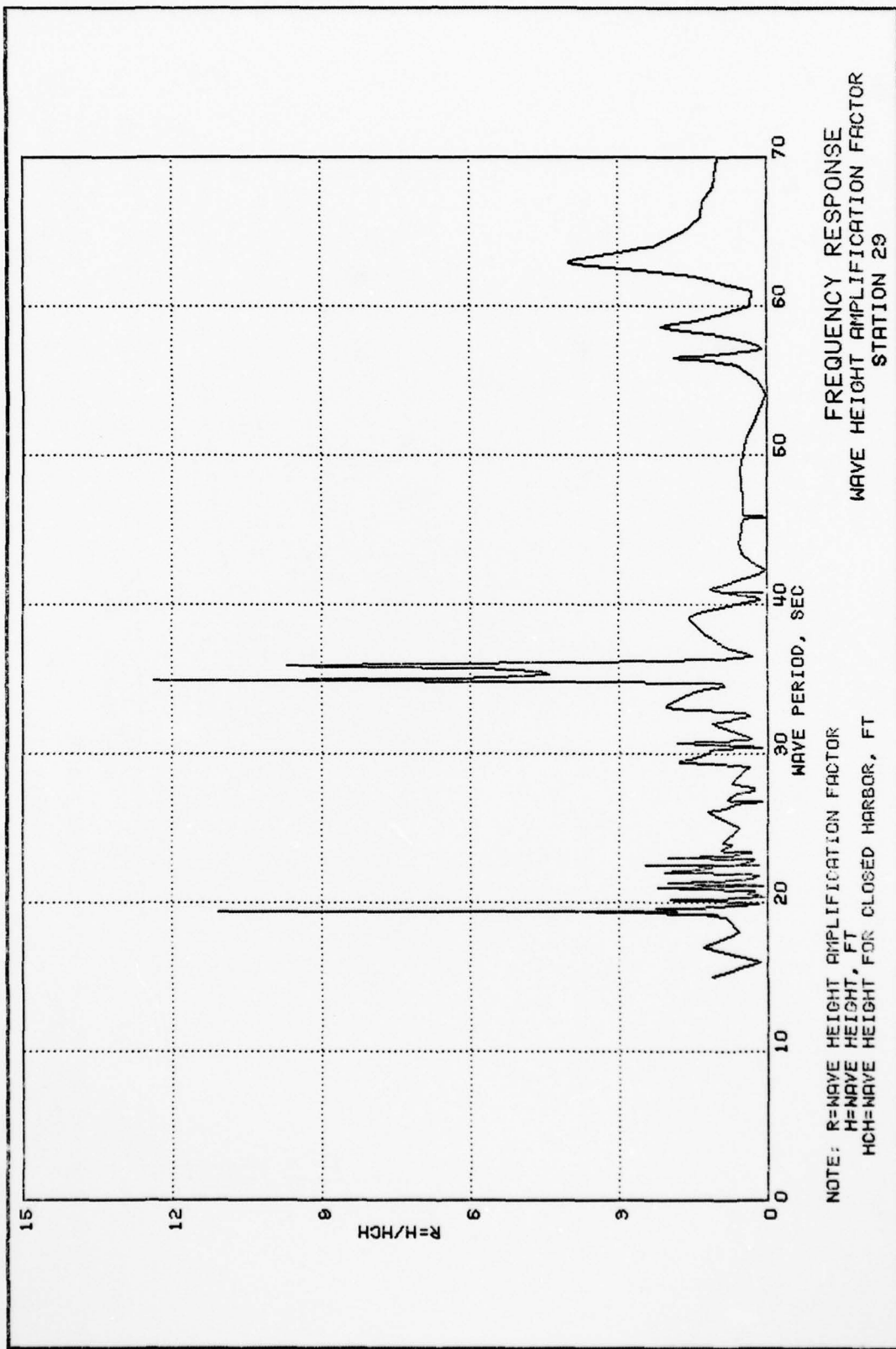
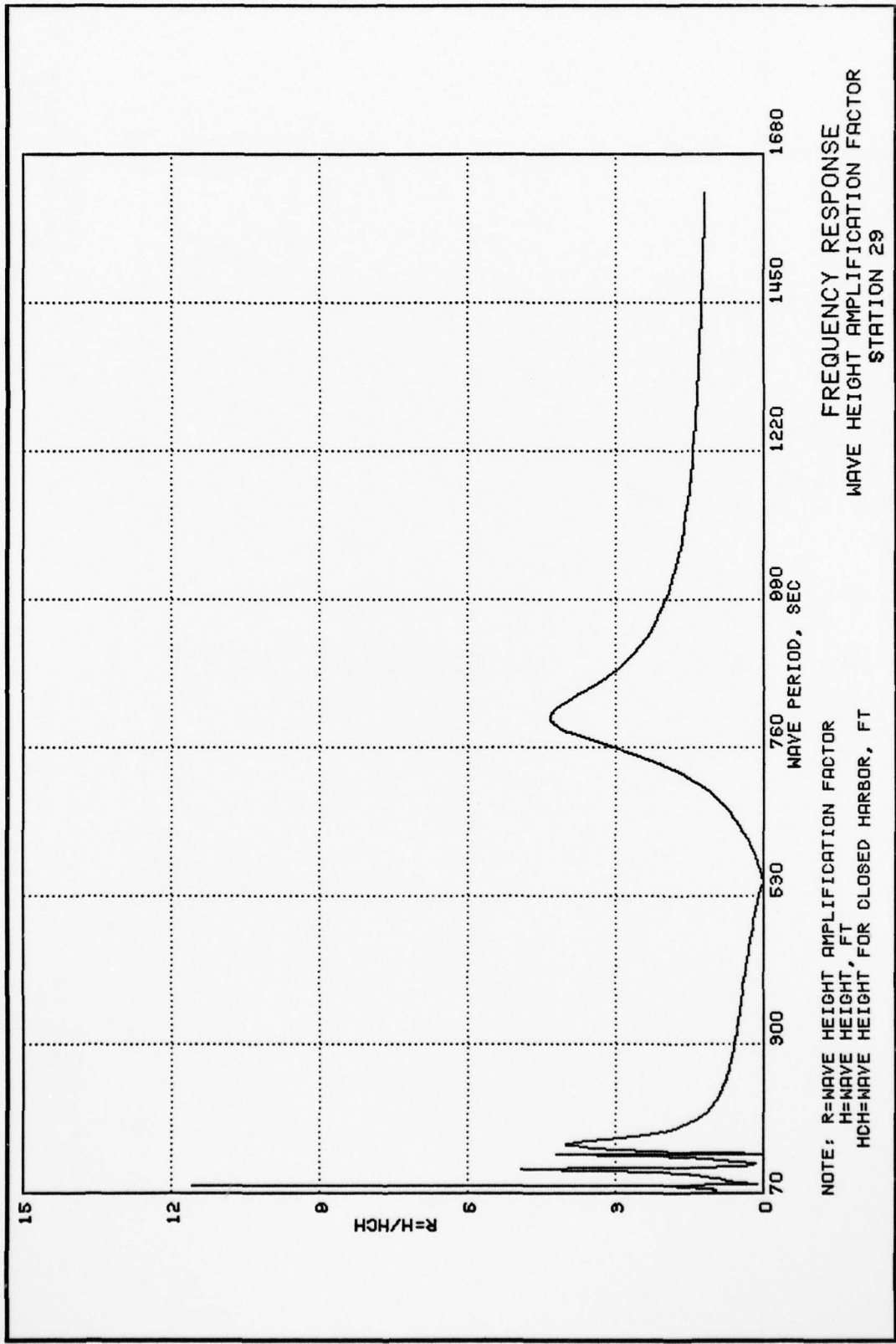


PLATE 60



FREQUENCY RESPONSE  
 WAVE HEIGHT AMPLIFICATION FACTOR  
 STATION 29

NOTE: R=WAVE HEIGHT AMPLIFICATION FACTOR  
 H=WAVE HEIGHT, FT  
 HCH=WAVE HEIGHT FOR CLOSED HARBOR, FT

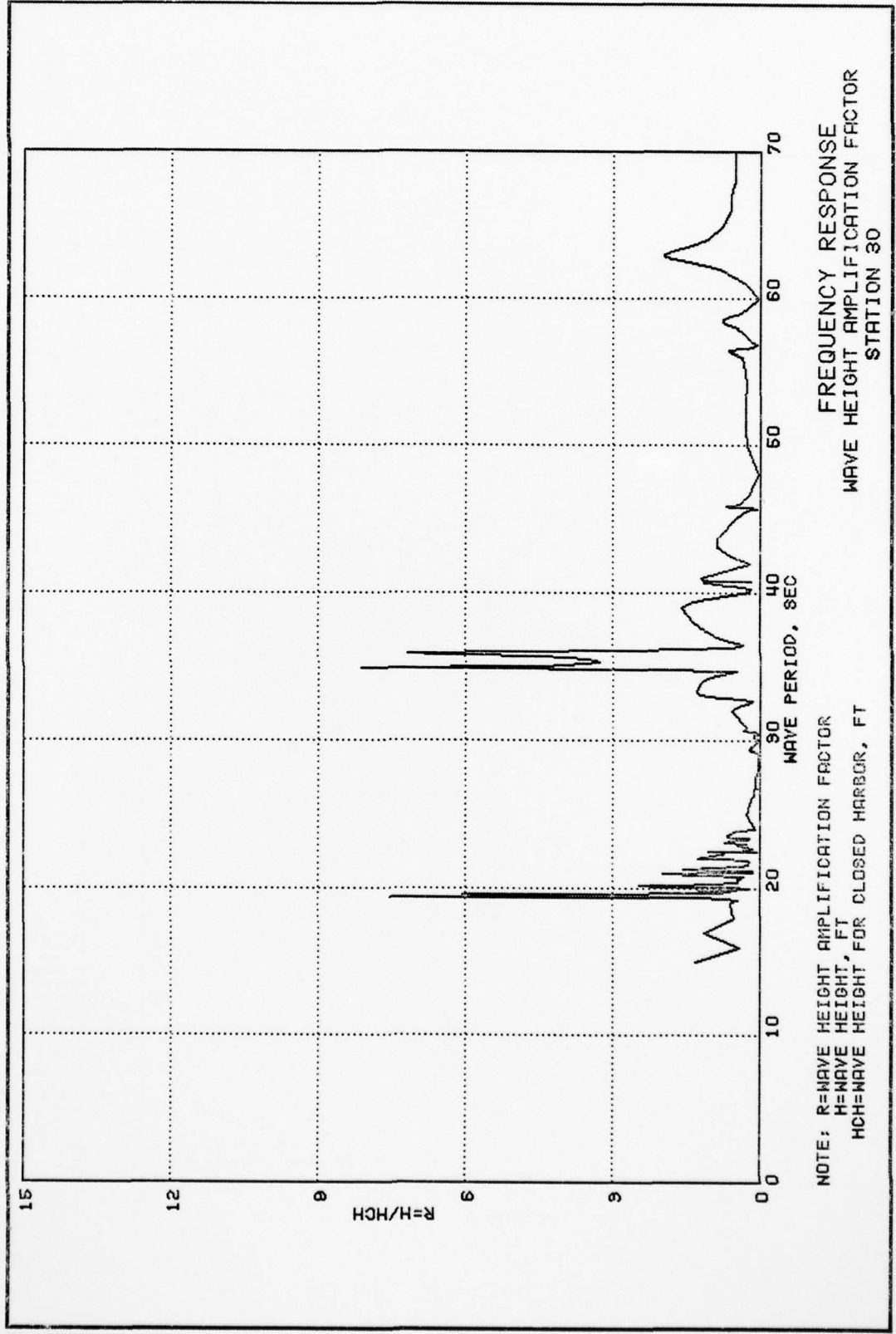
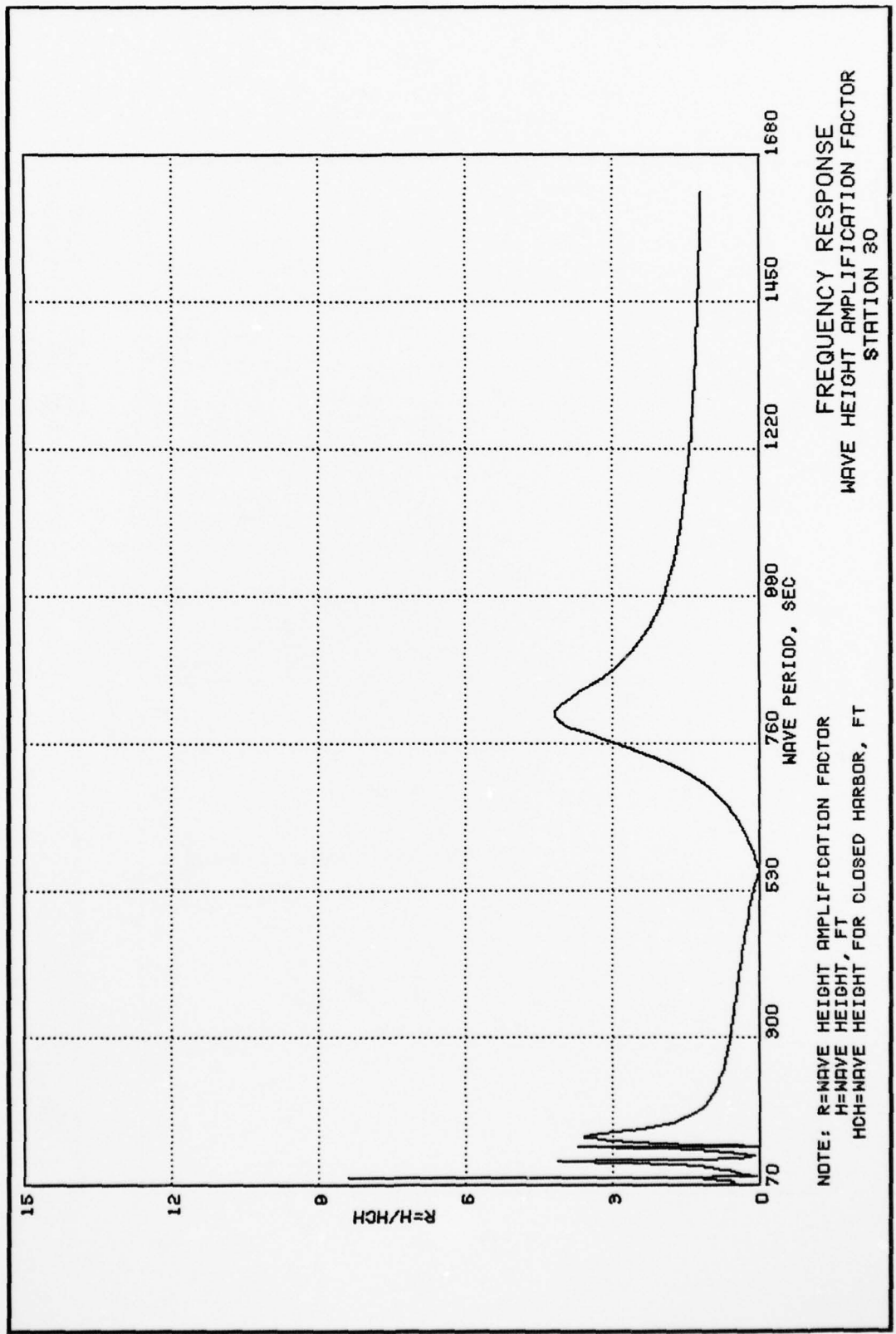


PLATE 62





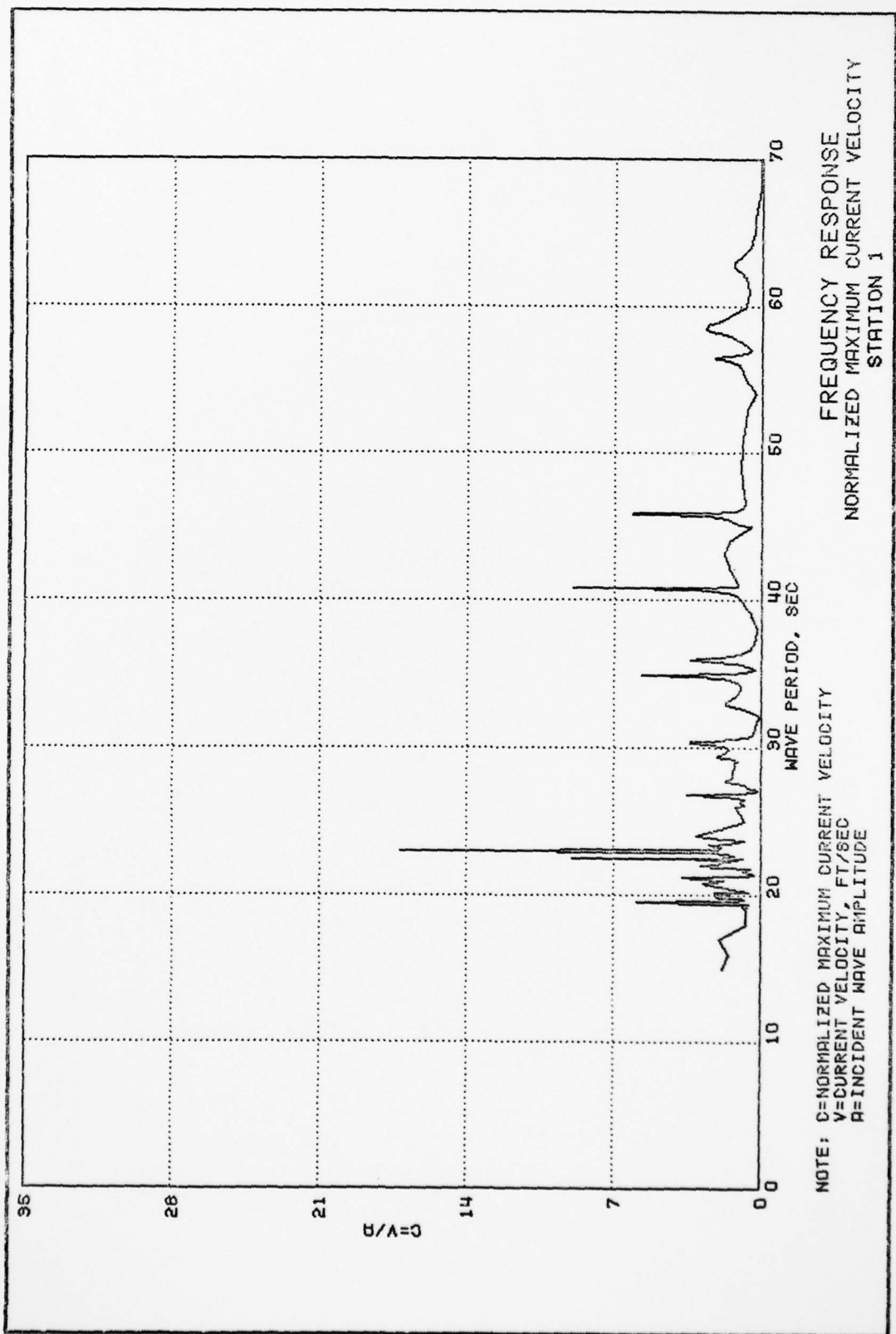
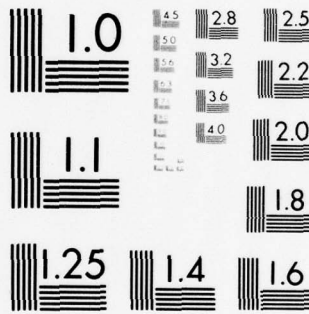
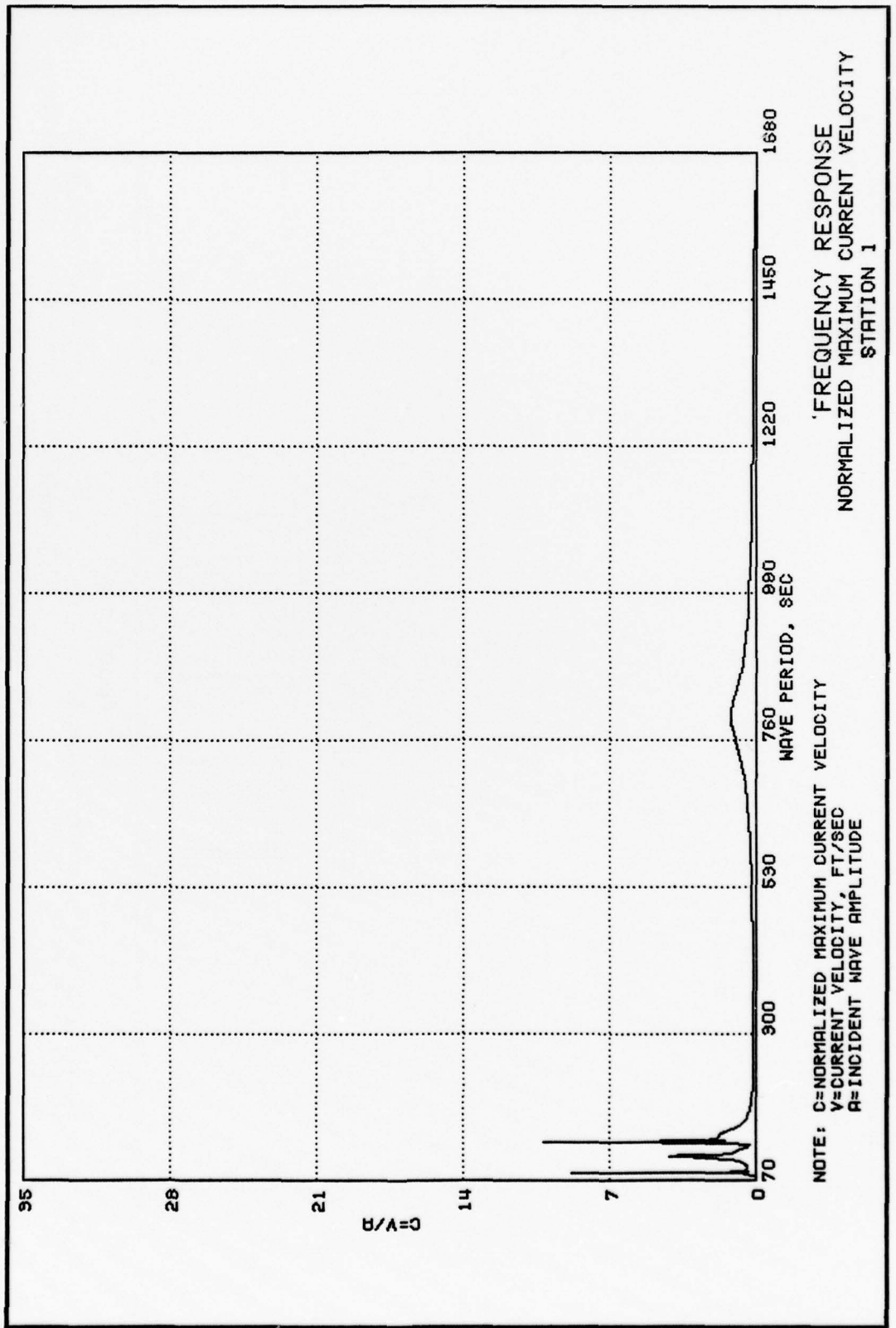


PLATE 64





MICROCOPY RESOLUTION TEST CHART  
NATIONAL BUREAU OF STANDARDS-1963-A



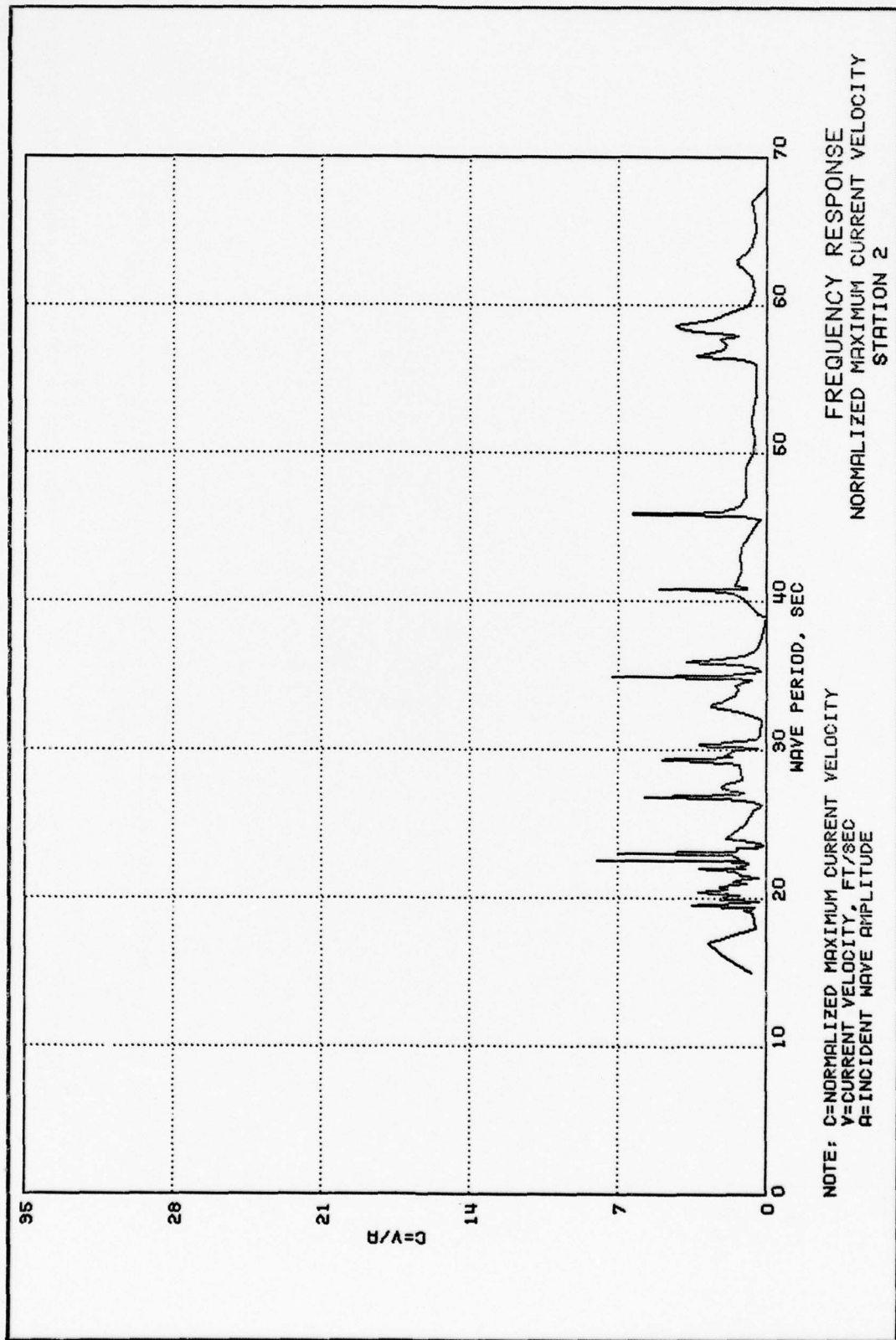
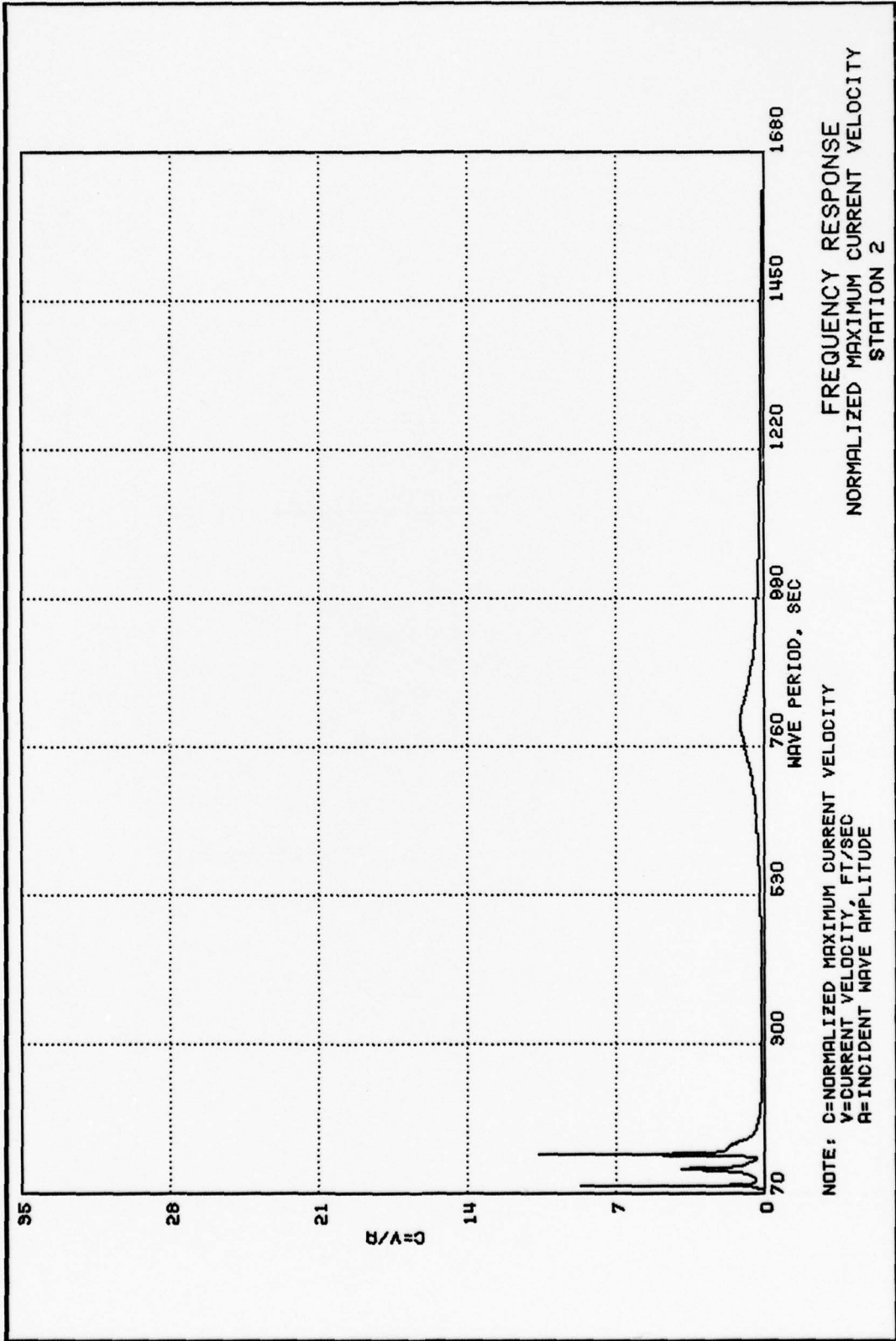
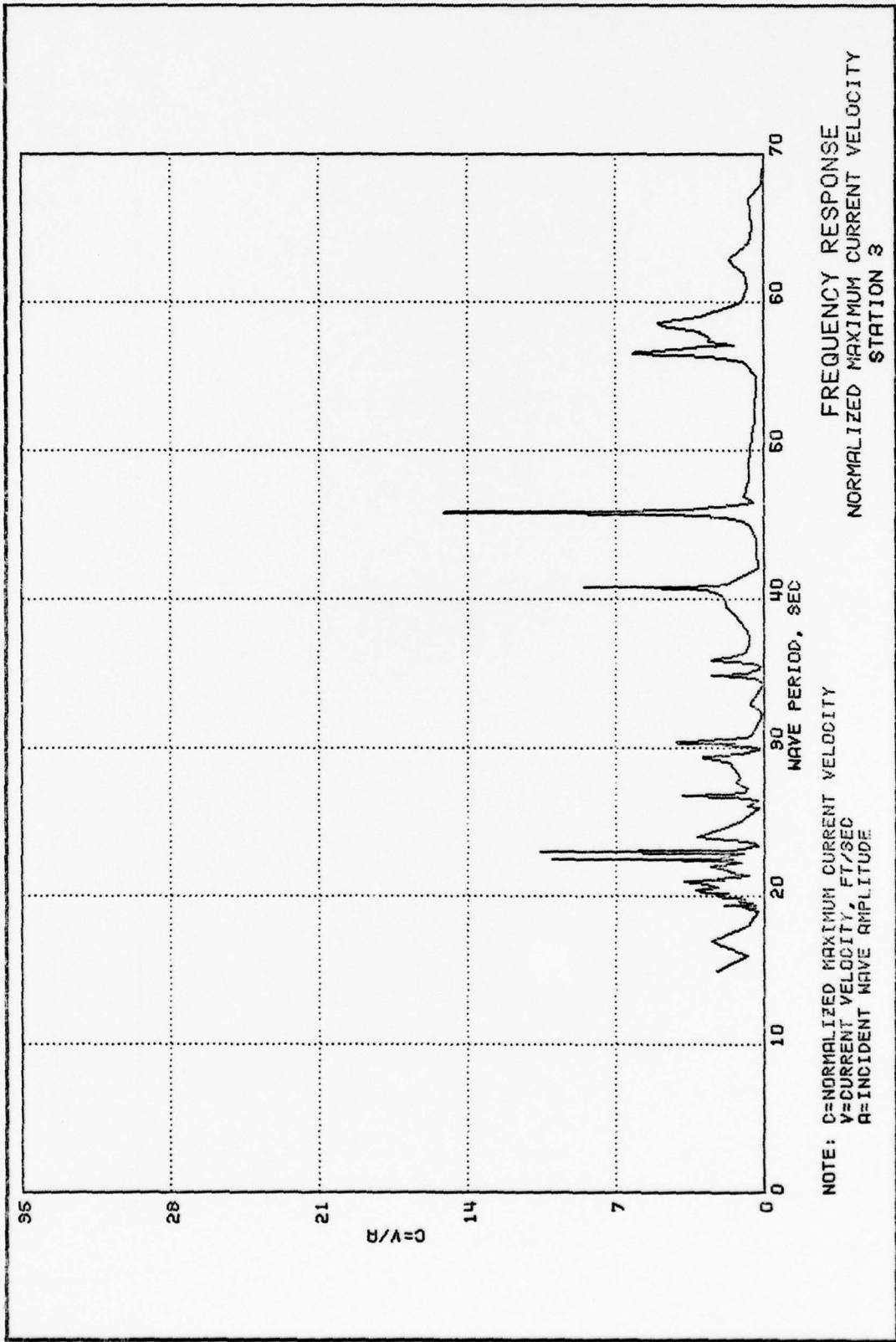


PLATE 66



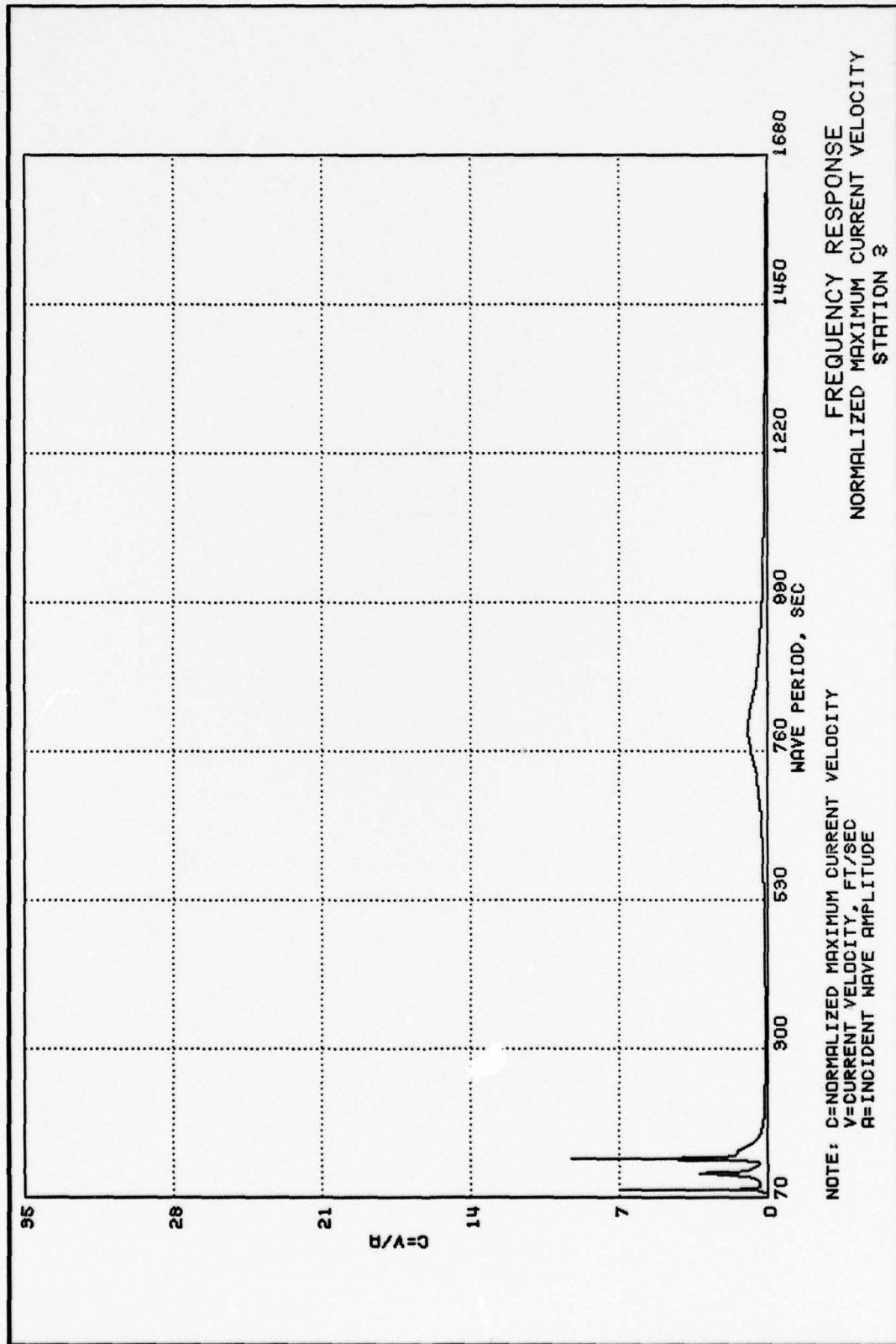


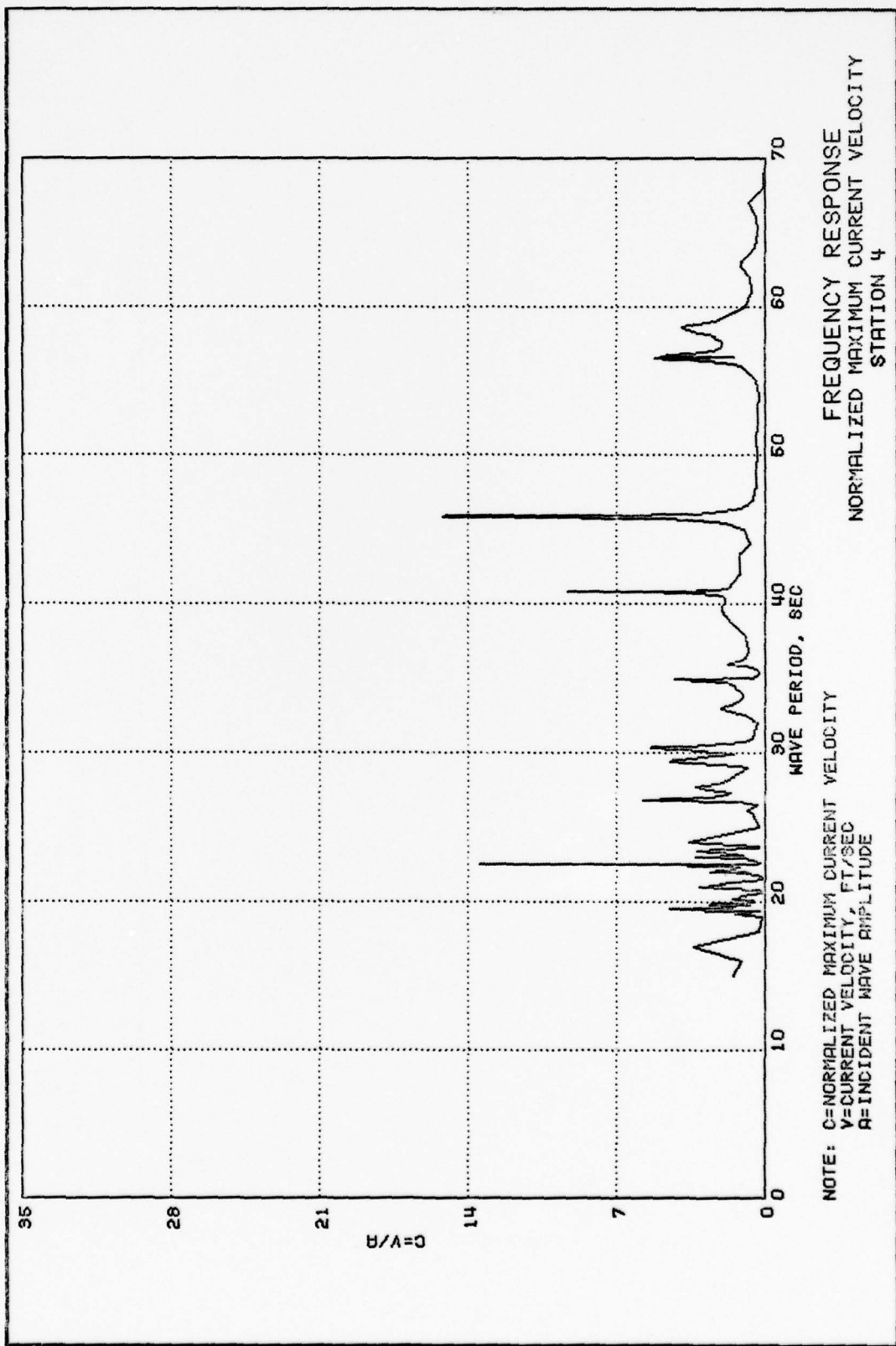
FREQUENCY RESPONSE  
 NORMALIZED MAXIMUM CURRENT VELOCITY  
 STATION 3

NOTE: C=NORMALIZED MAXIMUM CURRENT VELOCITY  
 V=CURRENT VELOCITY, FT/SEC  
 A=INCIDENT WAVE AMPLITUDE

PLATE 68



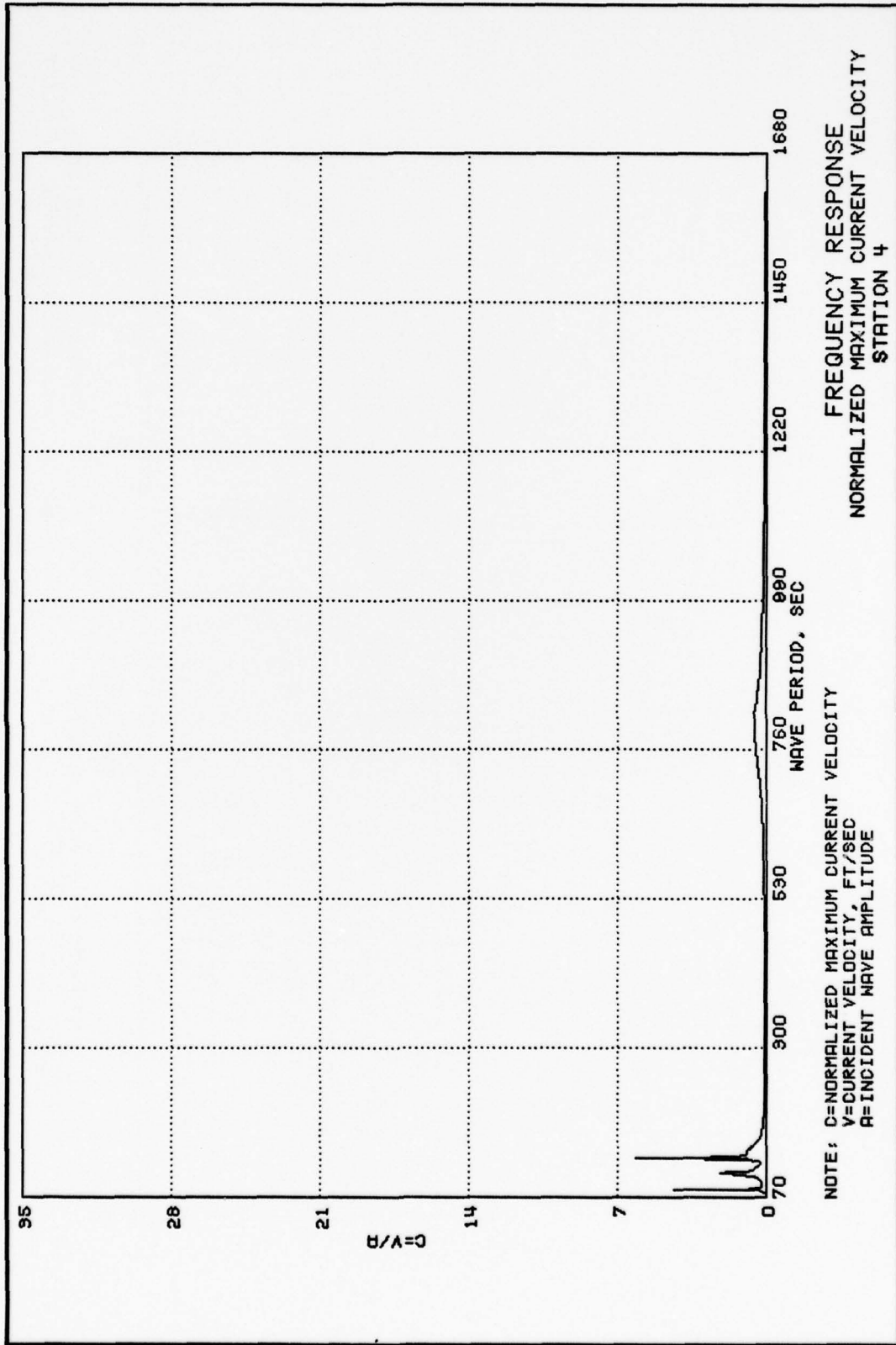


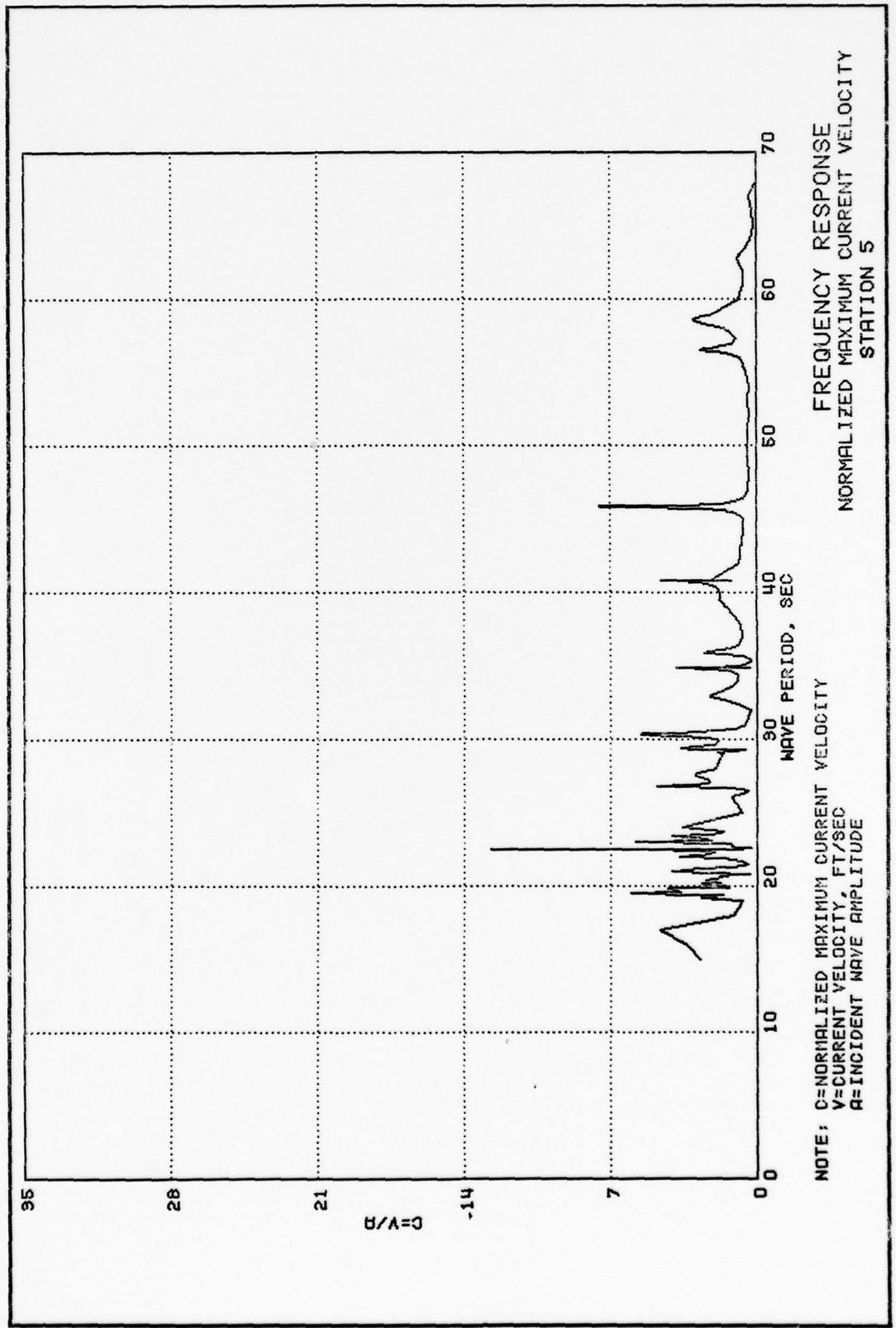


FREQUENCY RESPONSE  
 NORMALIZED MAXIMUM CURRENT VELOCITY  
 STATION 4

NOTE: C=NORMALIZED MAXIMUM CURRENT VELOCITY  
 V=CURRENT VELOCITY, FT/SEC  
 A=INCIDENT WAVE AMPLITUDE

PLATE 70

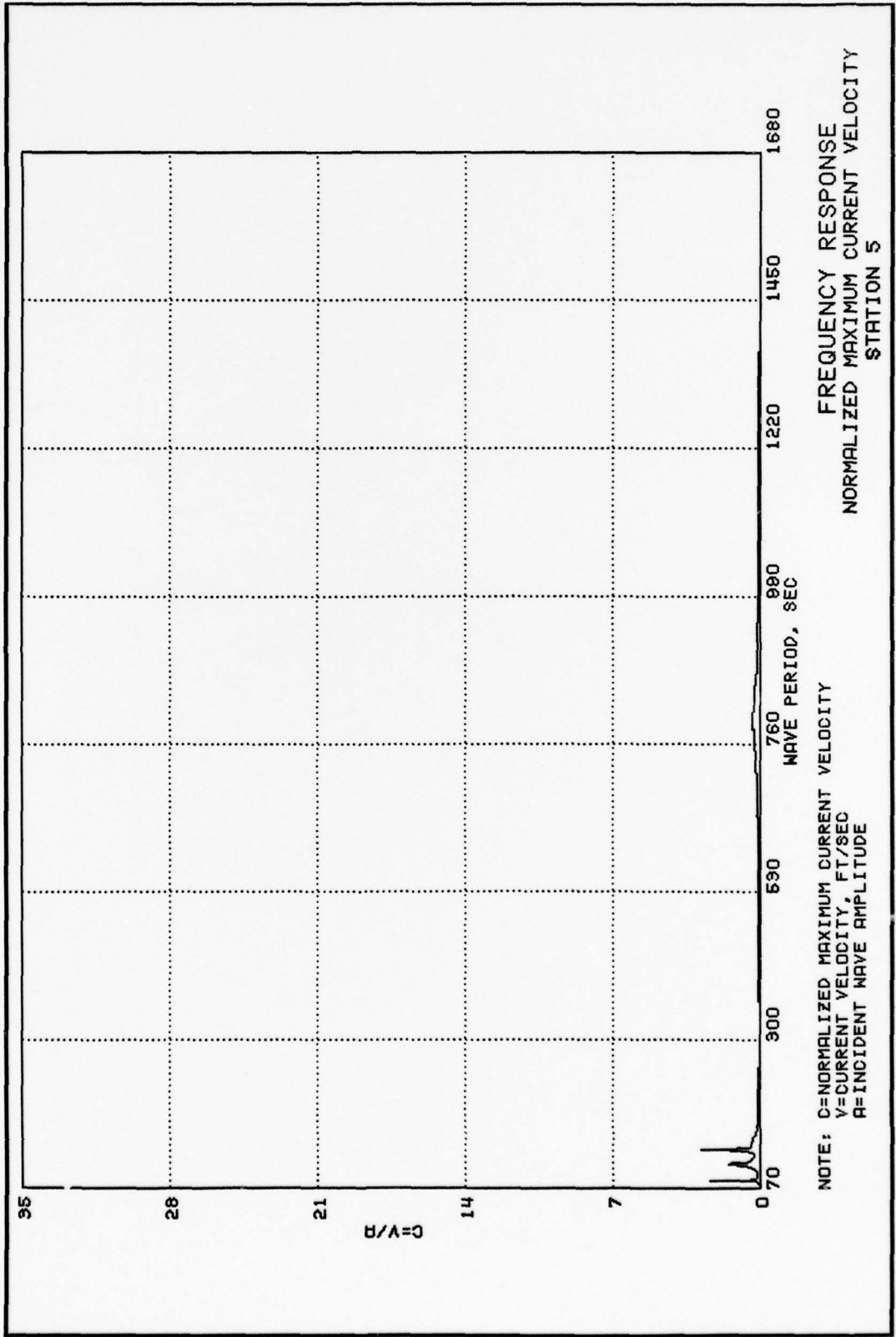


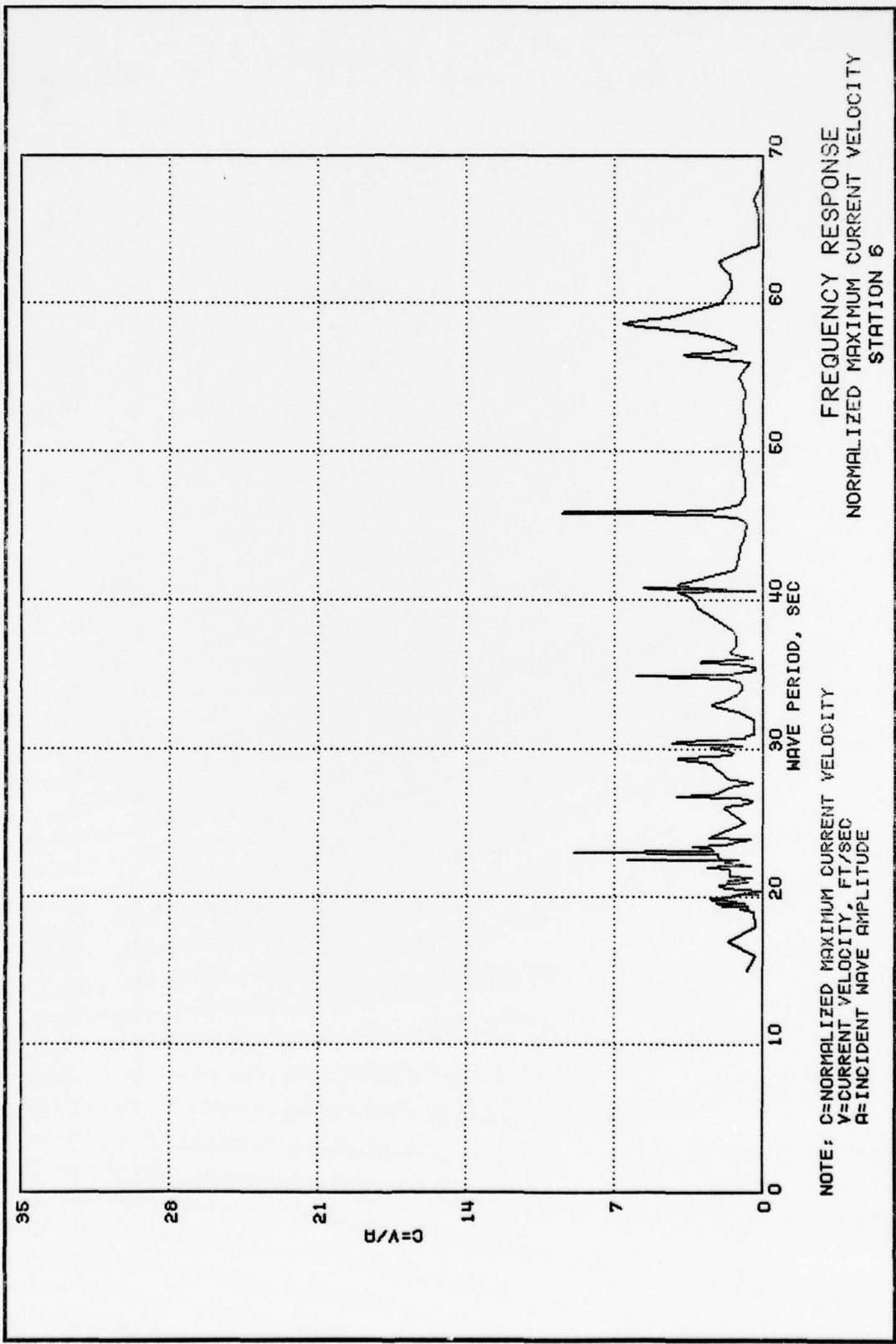


FREQUENCY RESPONSE  
 NORMALIZED MAXIMUM CURRENT VELOCITY  
 STATION 5

NOTE: C=NORMALIZED MAXIMUM CURRENT VELOCITY  
 V=CURRENT VELOCITY, FT/SEC  
 A=INCIDENT WAVE AMPLITUDE

PLATE 72

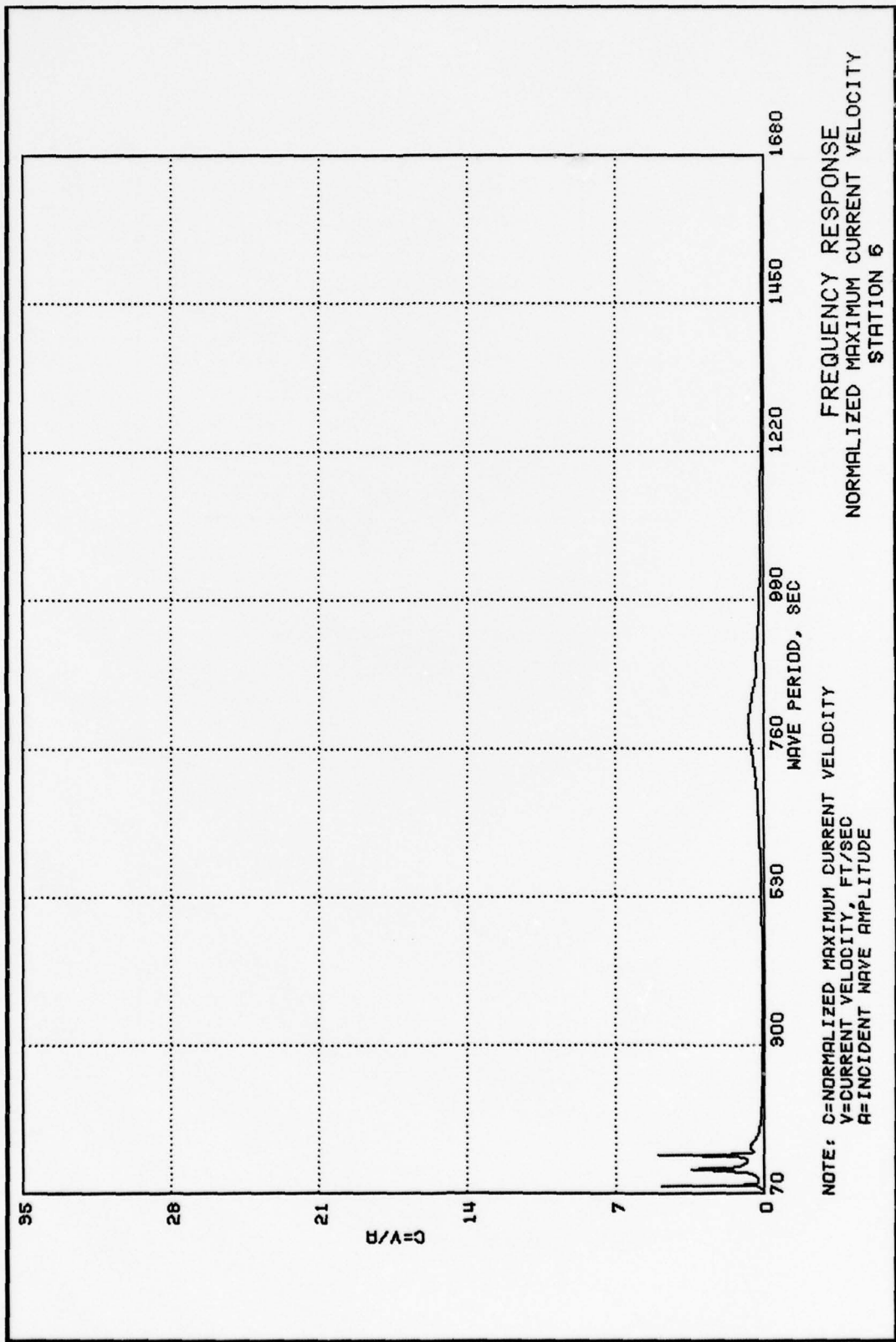




FREQUENCY RESPONSE  
 NORMALIZED MAXIMUM CURRENT VELOCITY  
 STATION 6

NOTE: C=NORMALIZED MAXIMUM CURRENT VELOCITY  
 V=CURRENT VELOCITY, FT/SEC  
 A=INCIDENT WAVE AMPLITUDE

PLATE 74



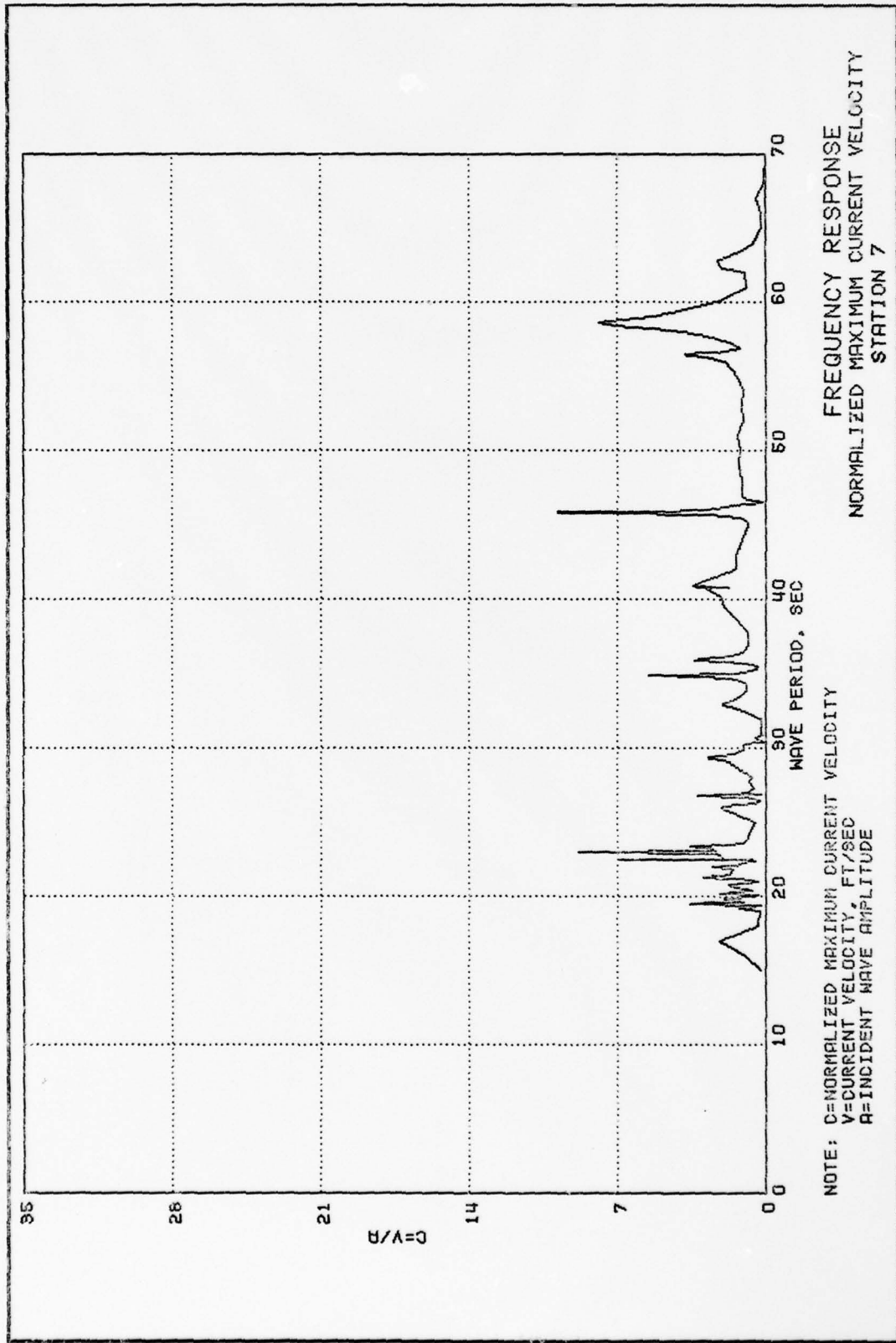
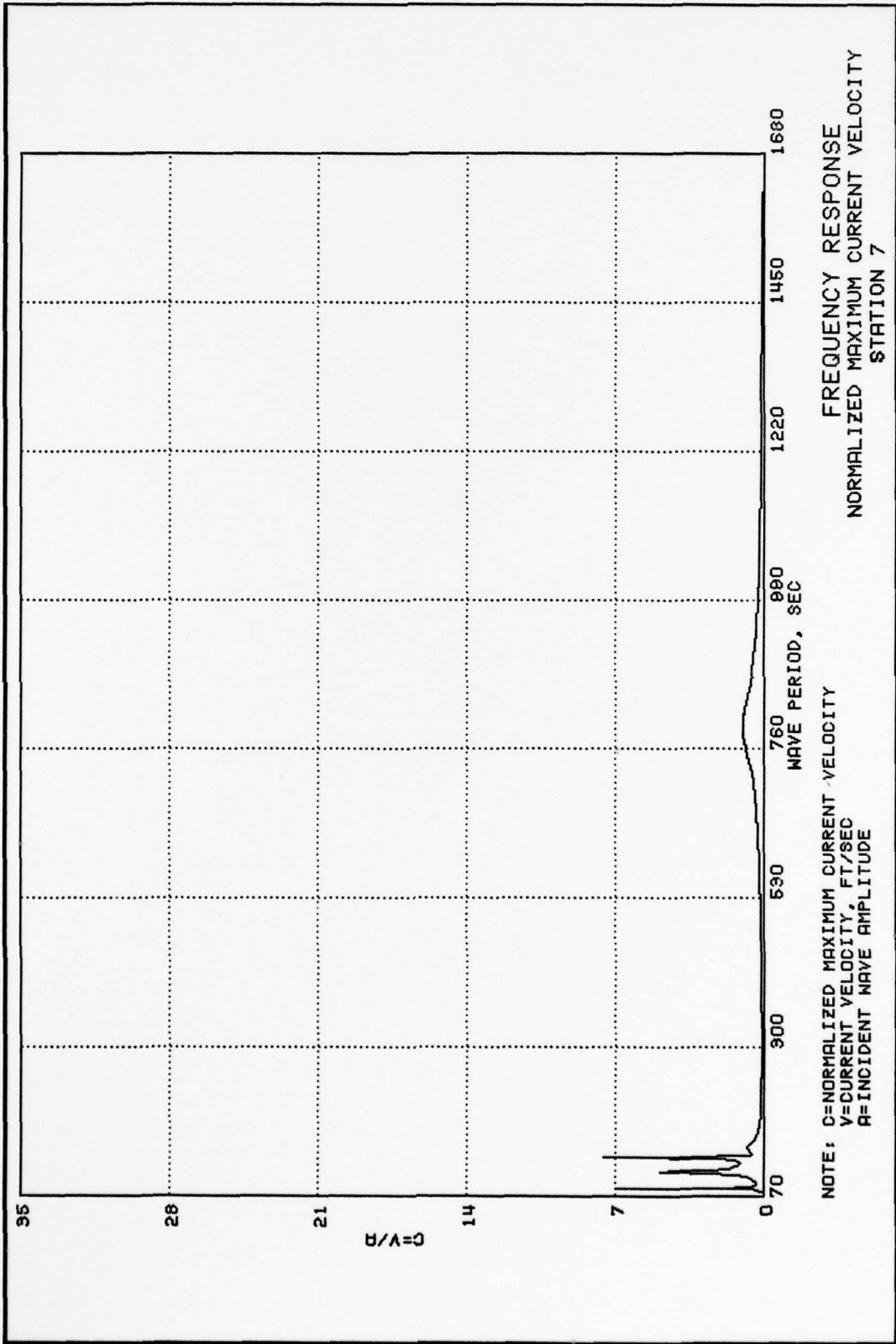


PLATE 76





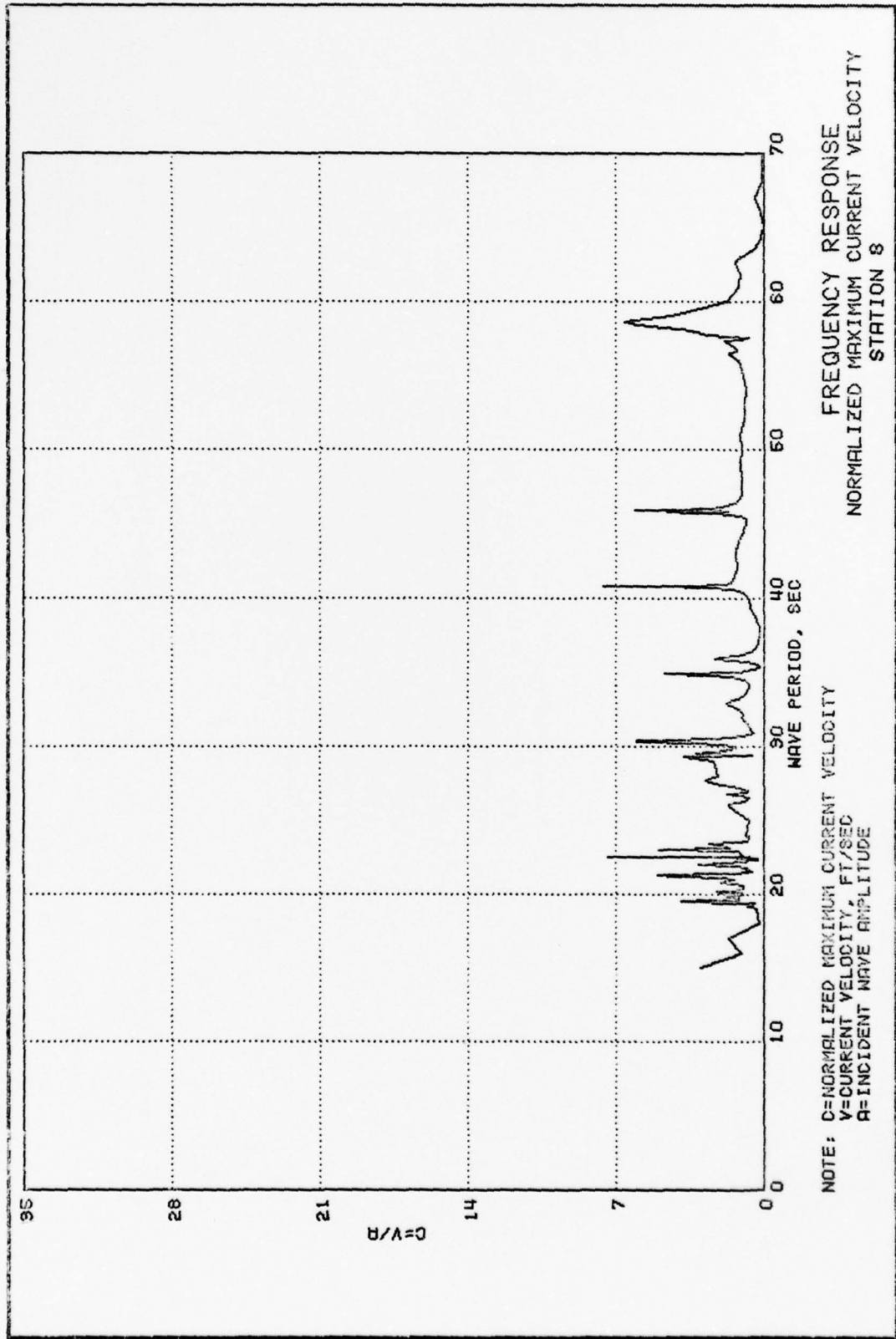
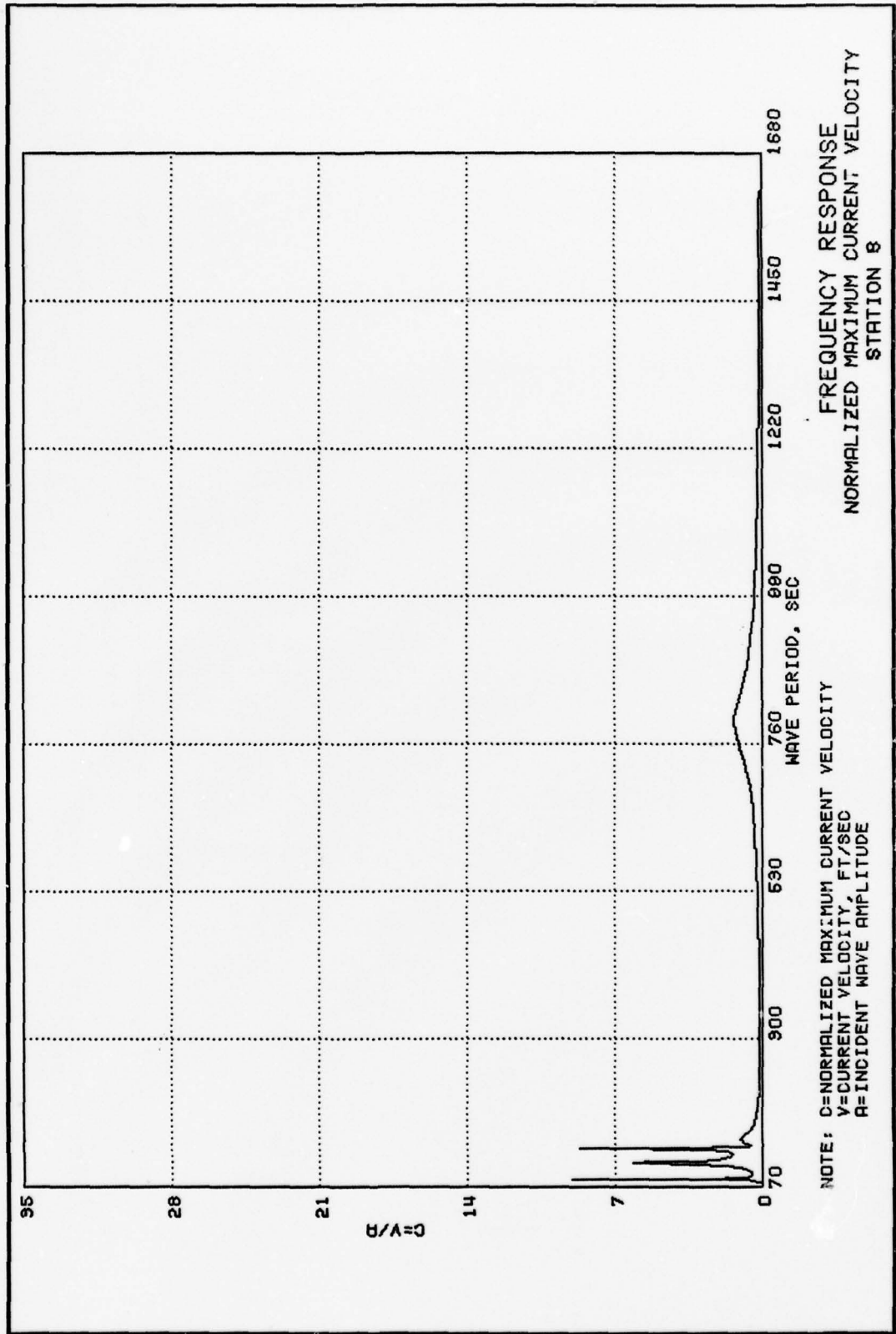
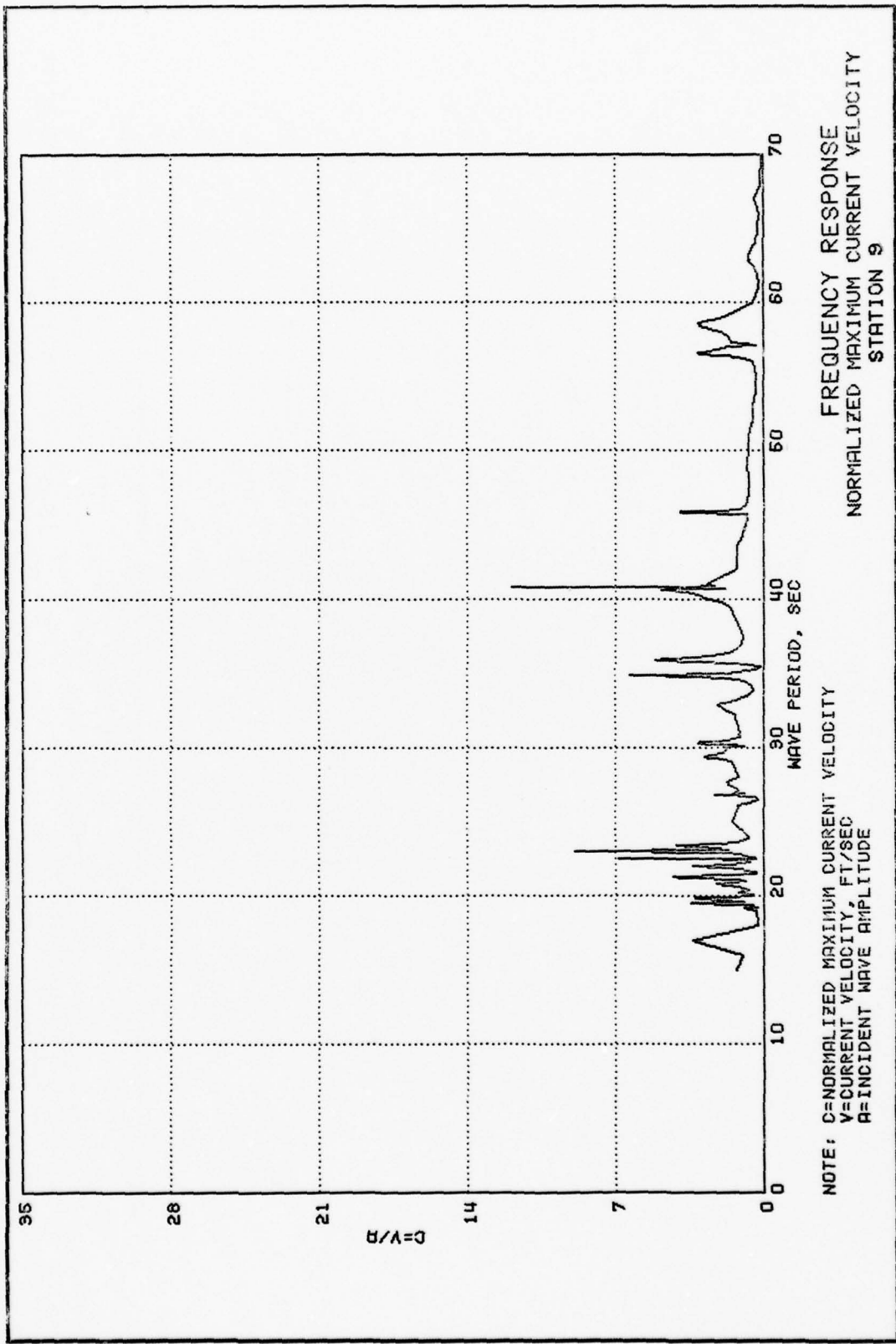


PLATE 78

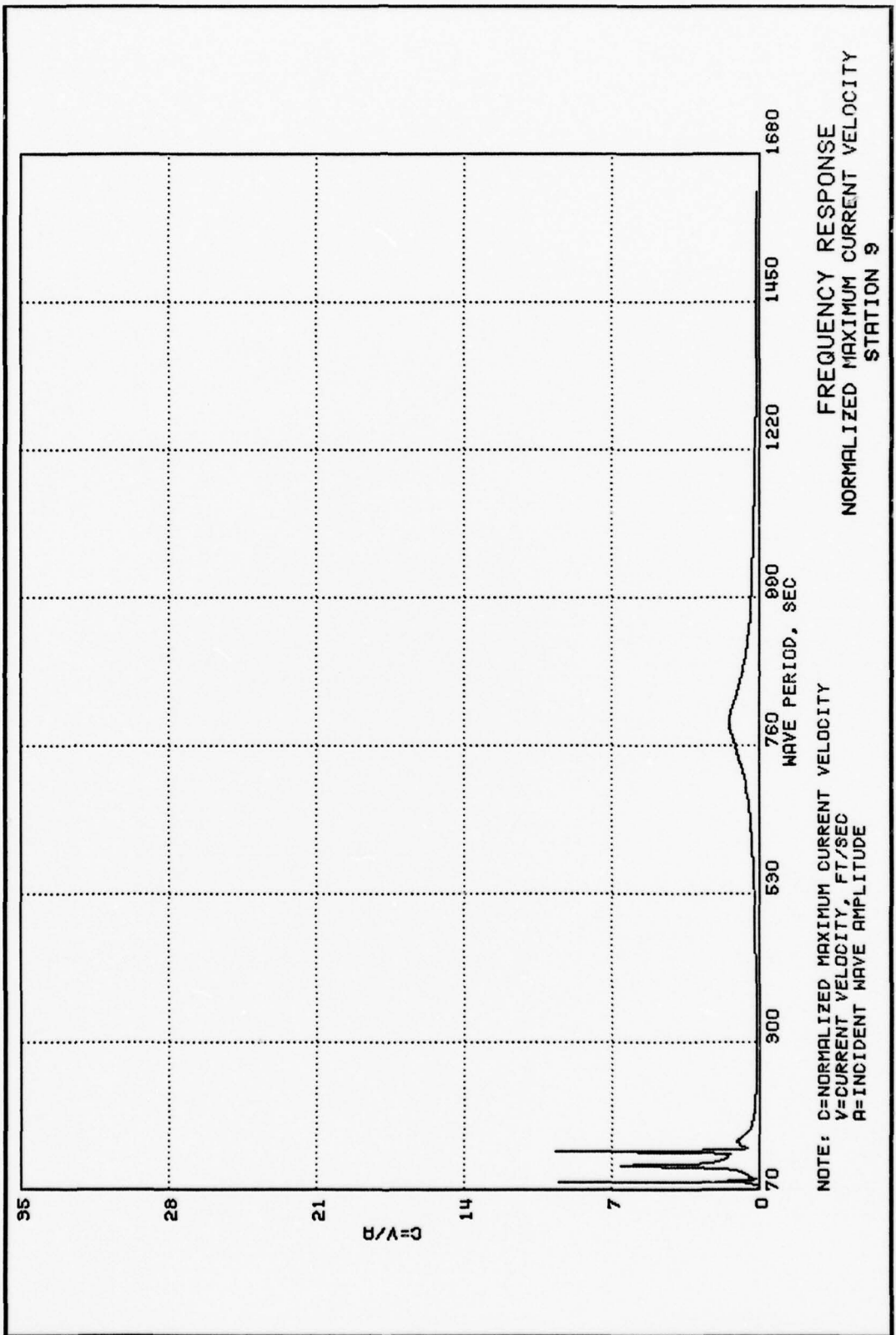




FREQUENCY RESPONSE  
 NORMALIZED MAXIMUM CURRENT VELOCITY  
 STATION 9

NOTE: C=NORMALIZED MAXIMUM CURRENT VELOCITY  
 V=CURRENT VELOCITY, FT/SEC  
 R=INCIDENT WAVE AMPLITUDE

PLATE 80



FREQUENCY RESPONSE  
 NORMALIZED MAXIMUM CURRENT VELOCITY  
 STATION 9

NOTE: C=NORMALIZED MAXIMUM CURRENT VELOCITY  
 V=CURRENT VELOCITY, FT/SEC  
 A=INCIDENT WAVE AMPLITUDE

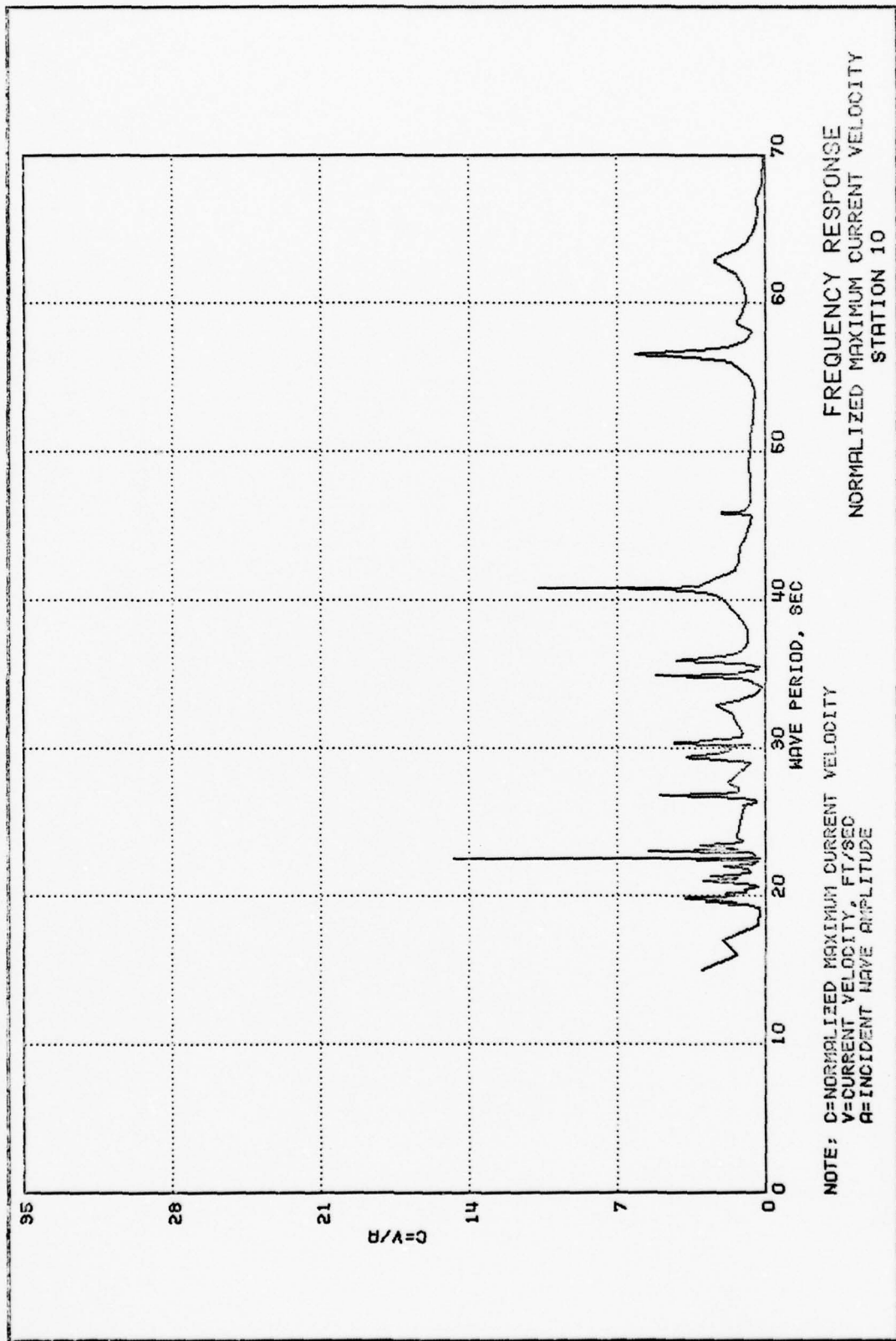
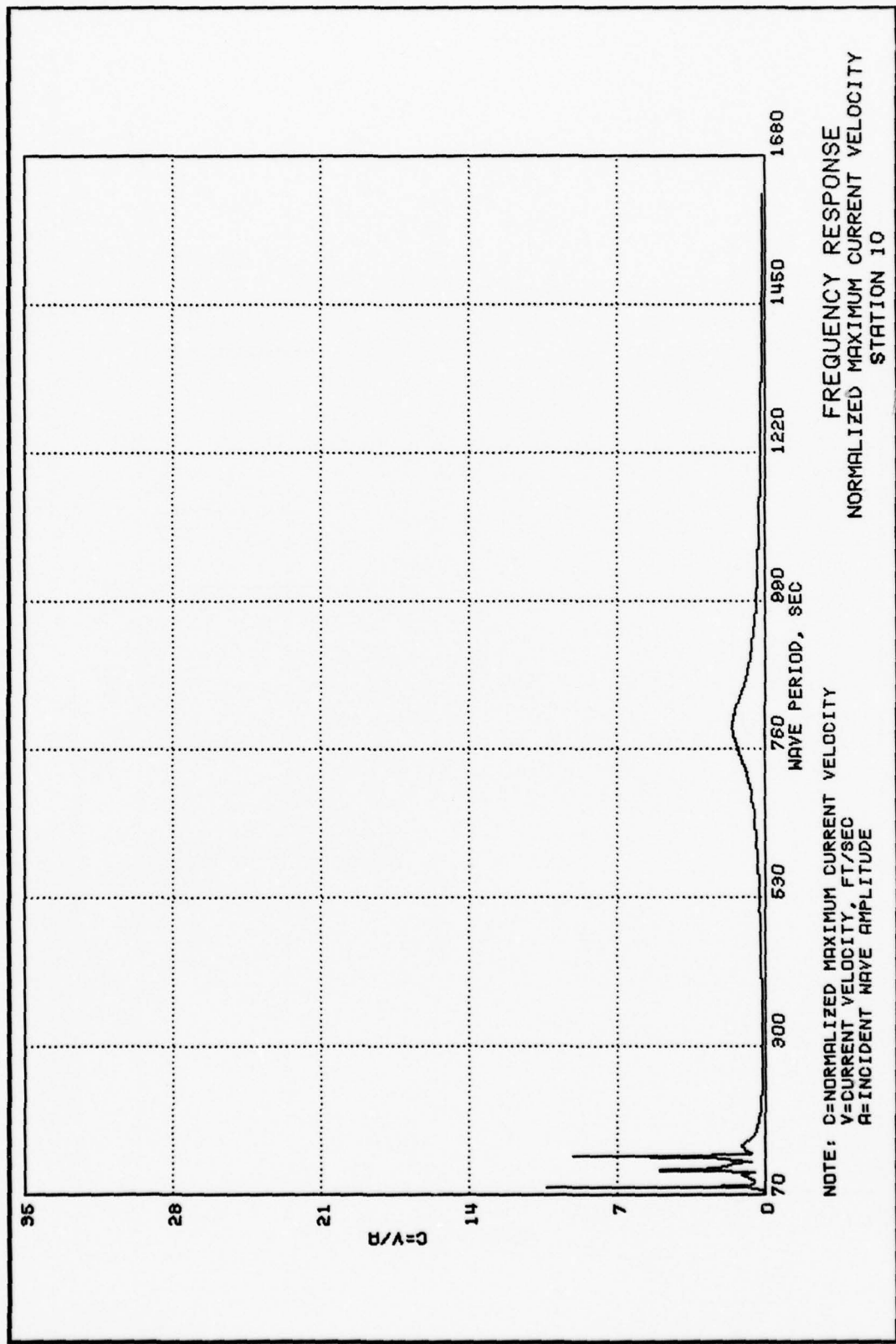
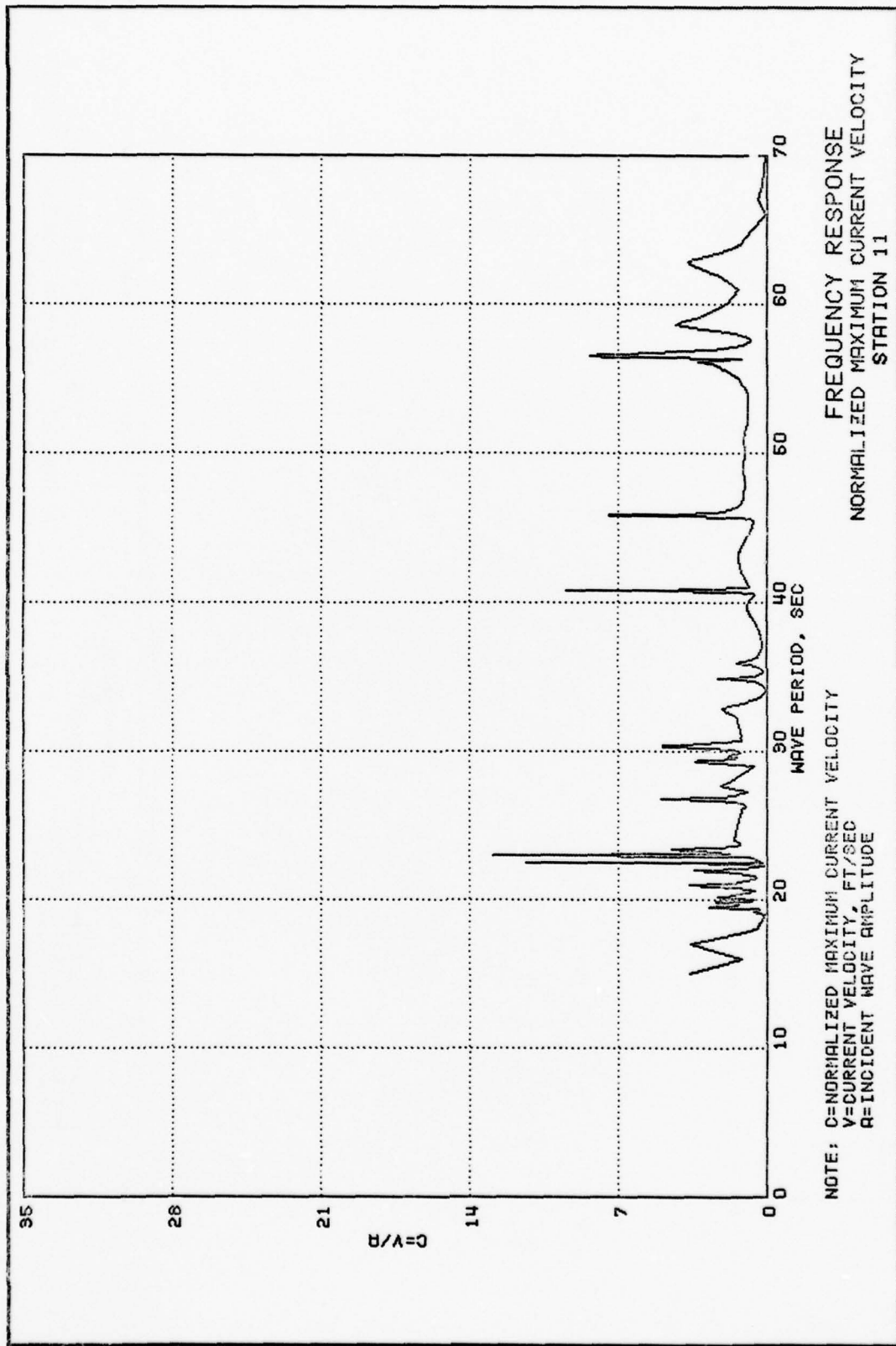


PLATE 82



FREQUENCY RESPONSE  
 NORMALIZED MAXIMUM CURRENT VELOCITY  
 STATION 10

NOTE: C=NORMALIZED MAXIMUM CURRENT VELOCITY  
 V=CURRENT VELOCITY, FT/SEC  
 A=INCIDENT WAVE AMPLITUDE

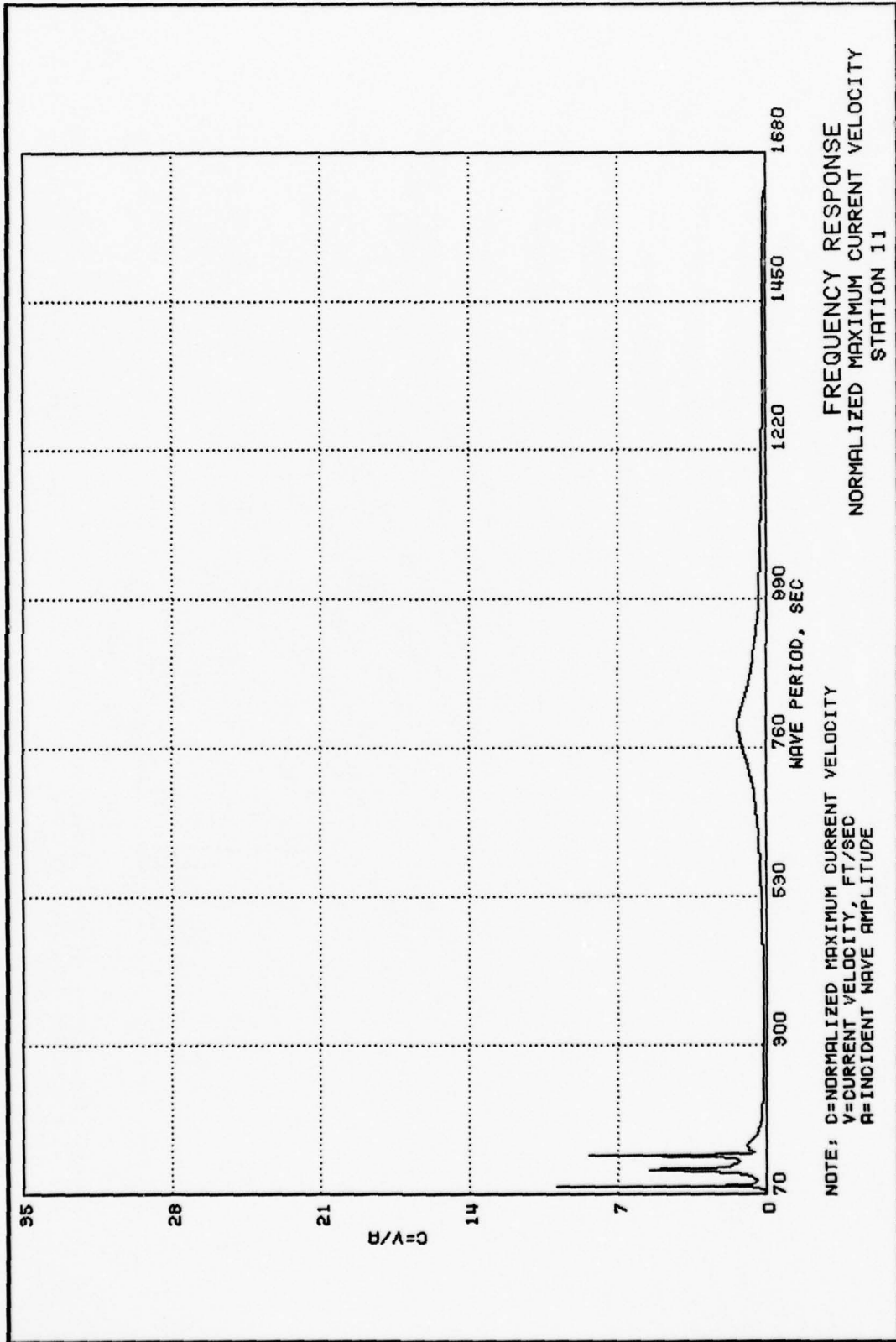


FREQUENCY RESPONSE  
 NORMALIZED MAXIMUM CURRENT VELOCITY  
 STATION 11

NOTE: C=NORMALIZED MAXIMUM CURRENT VELOCITY  
 V=CURRENT VELOCITY, FT/SEC  
 R=INCIDENT WAVE AMPLITUDE

PLATE 84





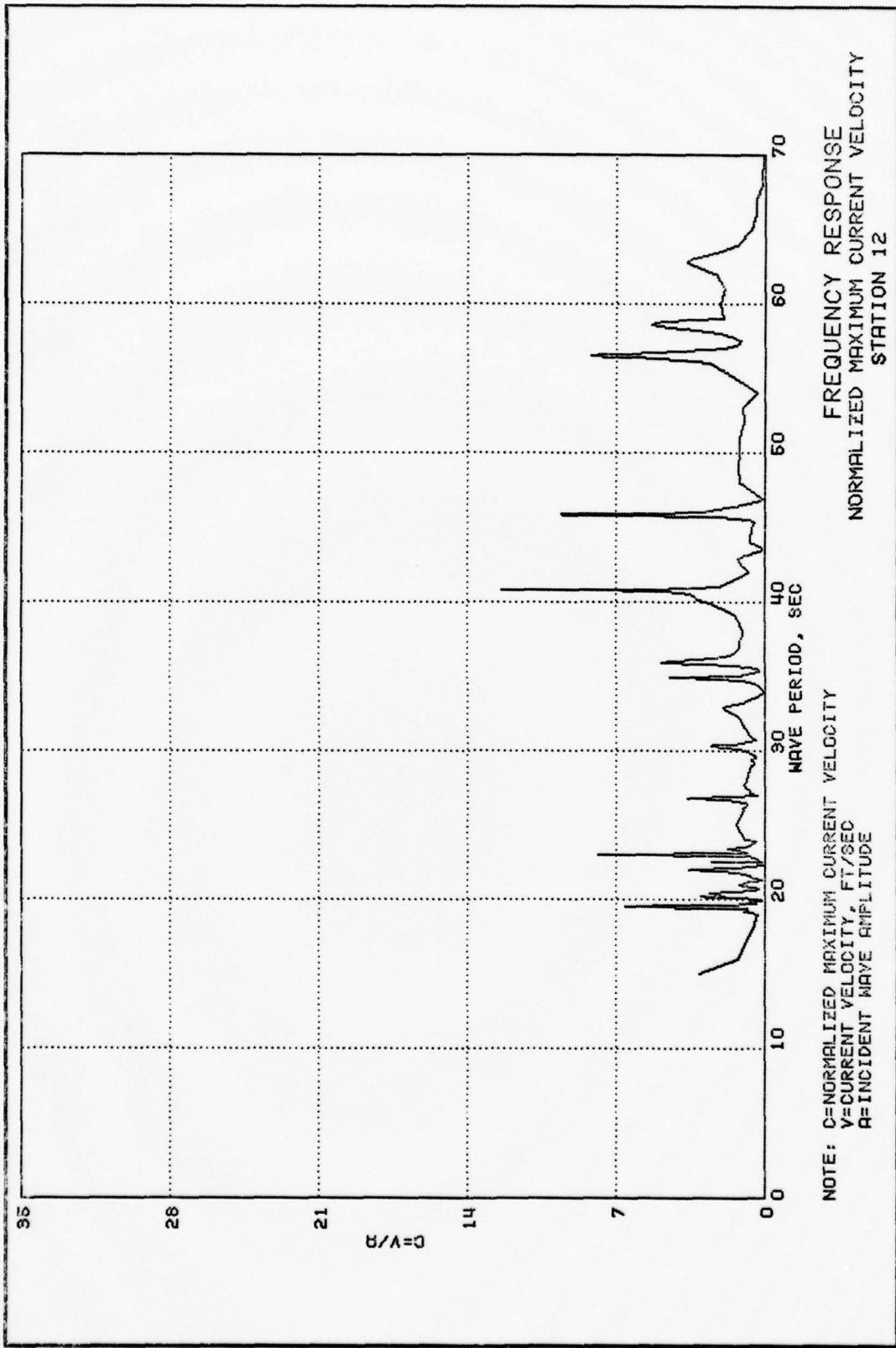
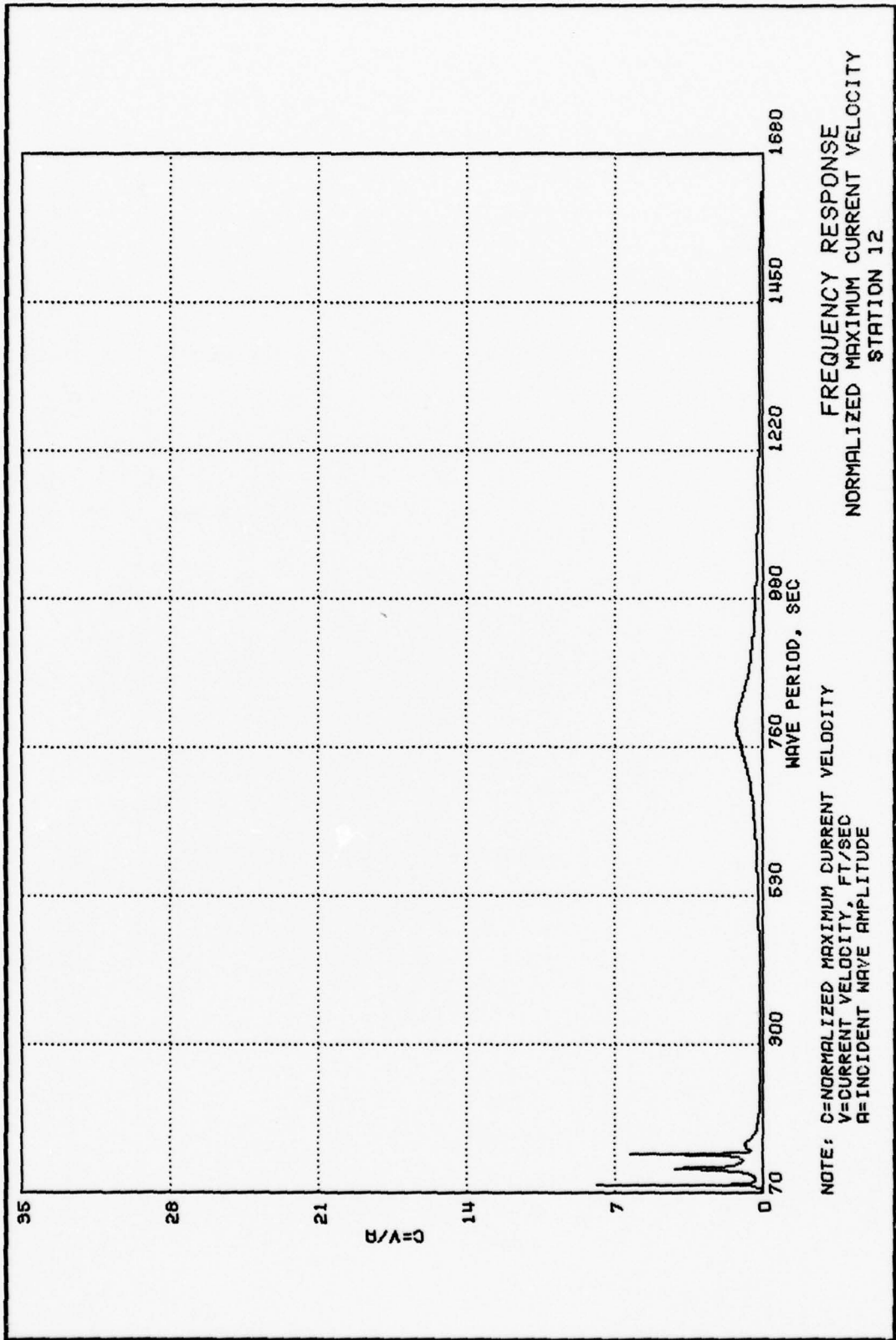


PLATE 86



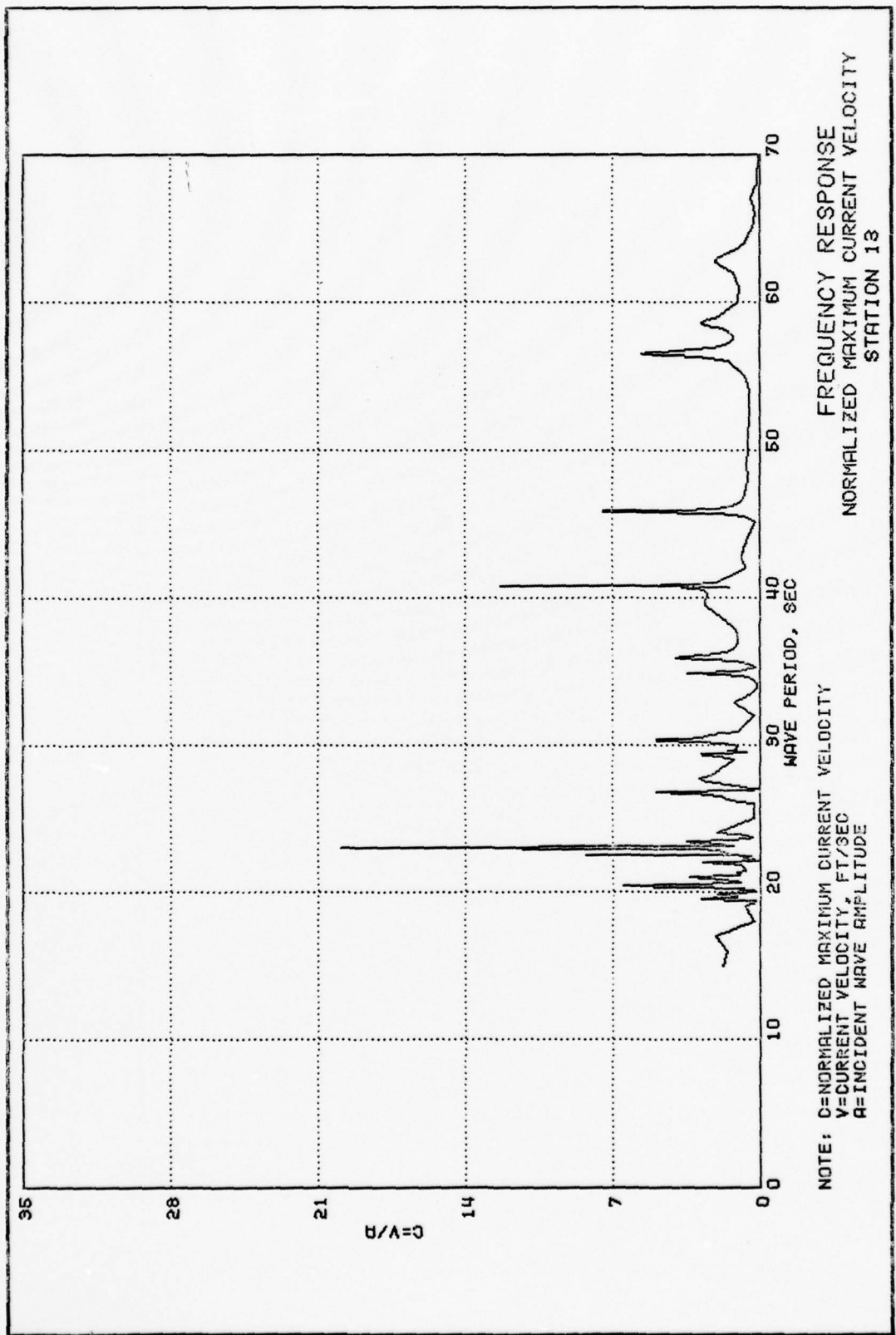
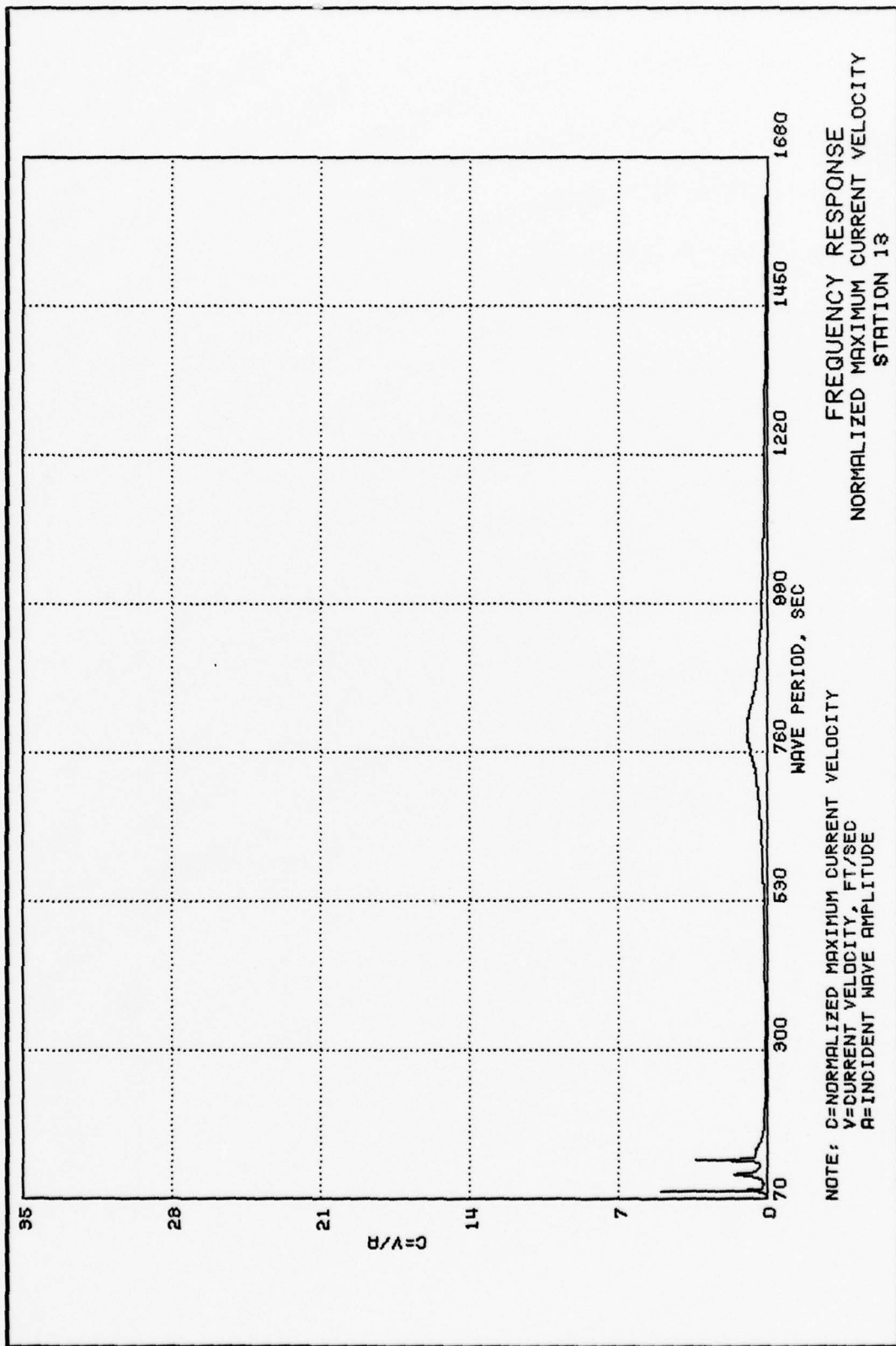
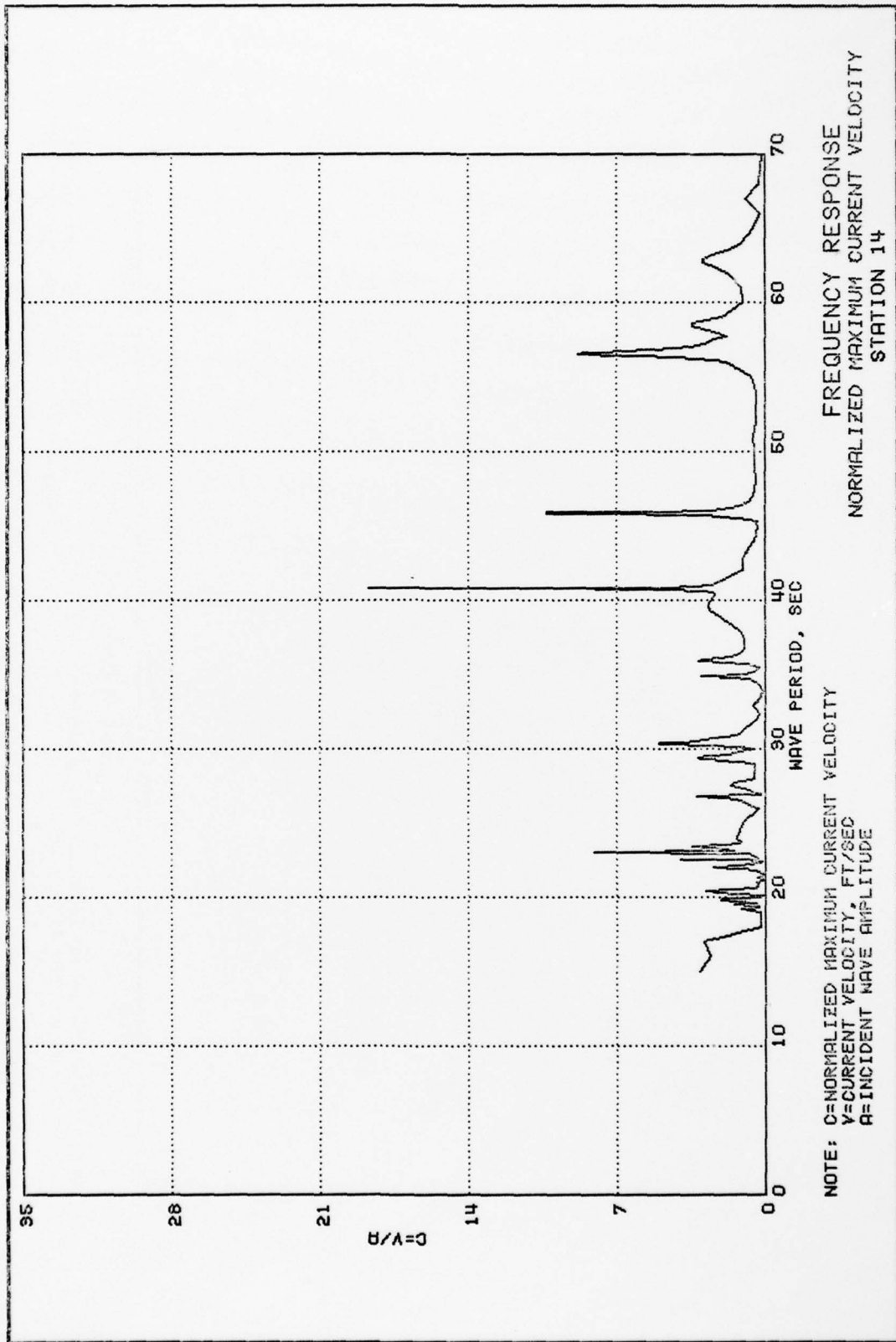


PLATE 88



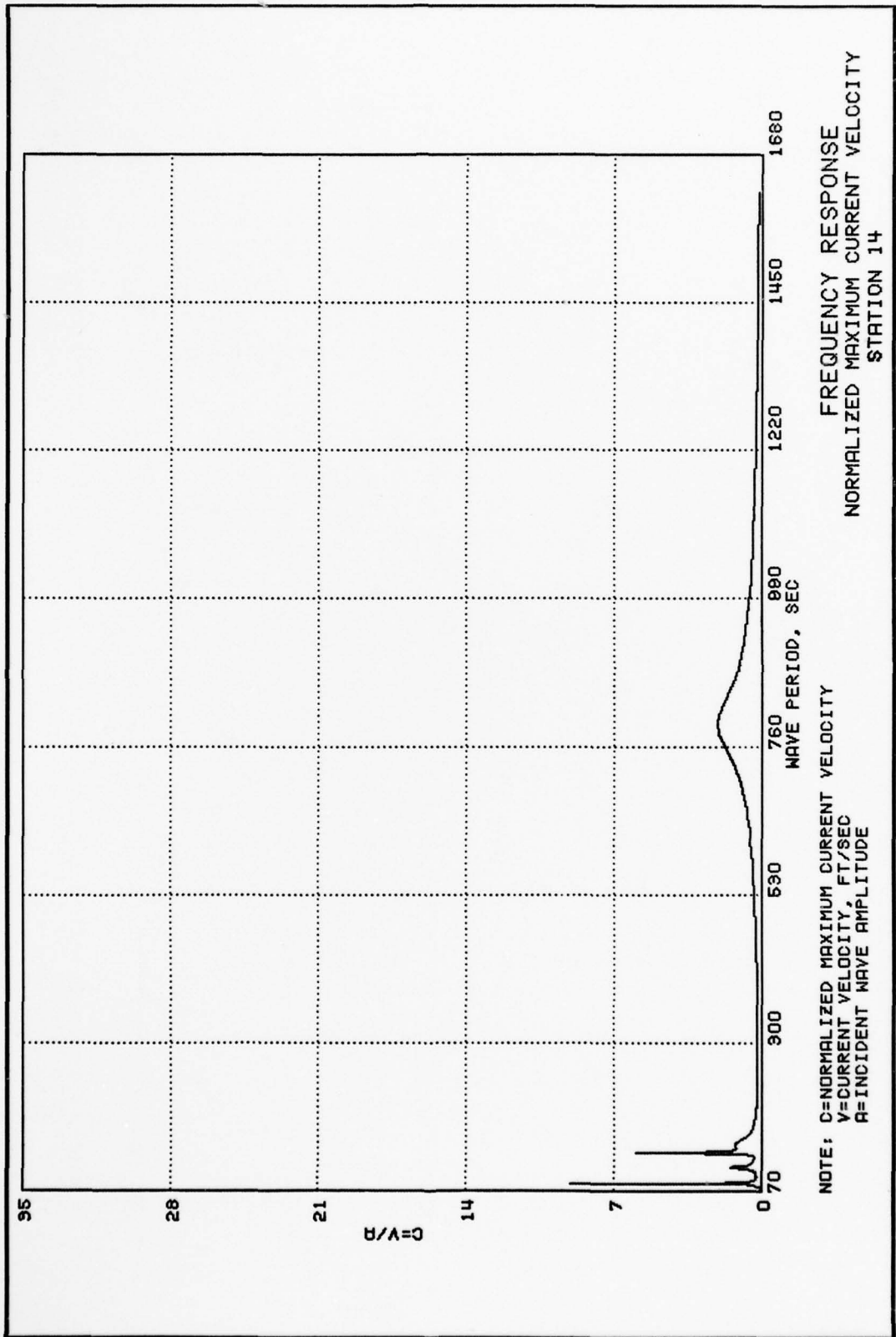
NOTE: C=NORMALIZED MAXIMUM CURRENT VELOCITY  
 V=CURRENT VELOCITY, FT/SEC  
 A=INCIDENT WAVE AMPLITUDE



FREQUENCY RESPONSE  
 NORMALIZED MAXIMUM CURRENT VELOCITY  
 STATION 14

NOTE: C=NORMALIZED MAXIMUM CURRENT VELOCITY  
 V=CURRENT VELOCITY, FT/SEC  
 A=INCIDENT WAVE AMPLITUDE

PLATE 90



FREQUENCY RESPONSE  
 NORMALIZED MAXIMUM CURRENT VELOCITY  
 STATION 14

NOTE: C=NORMALIZED MAXIMUM CURRENT VELOCITY  
 V=CURRENT VELOCITY, FT/SEC  
 R=INCIDENT WAVE AMPLITUDE

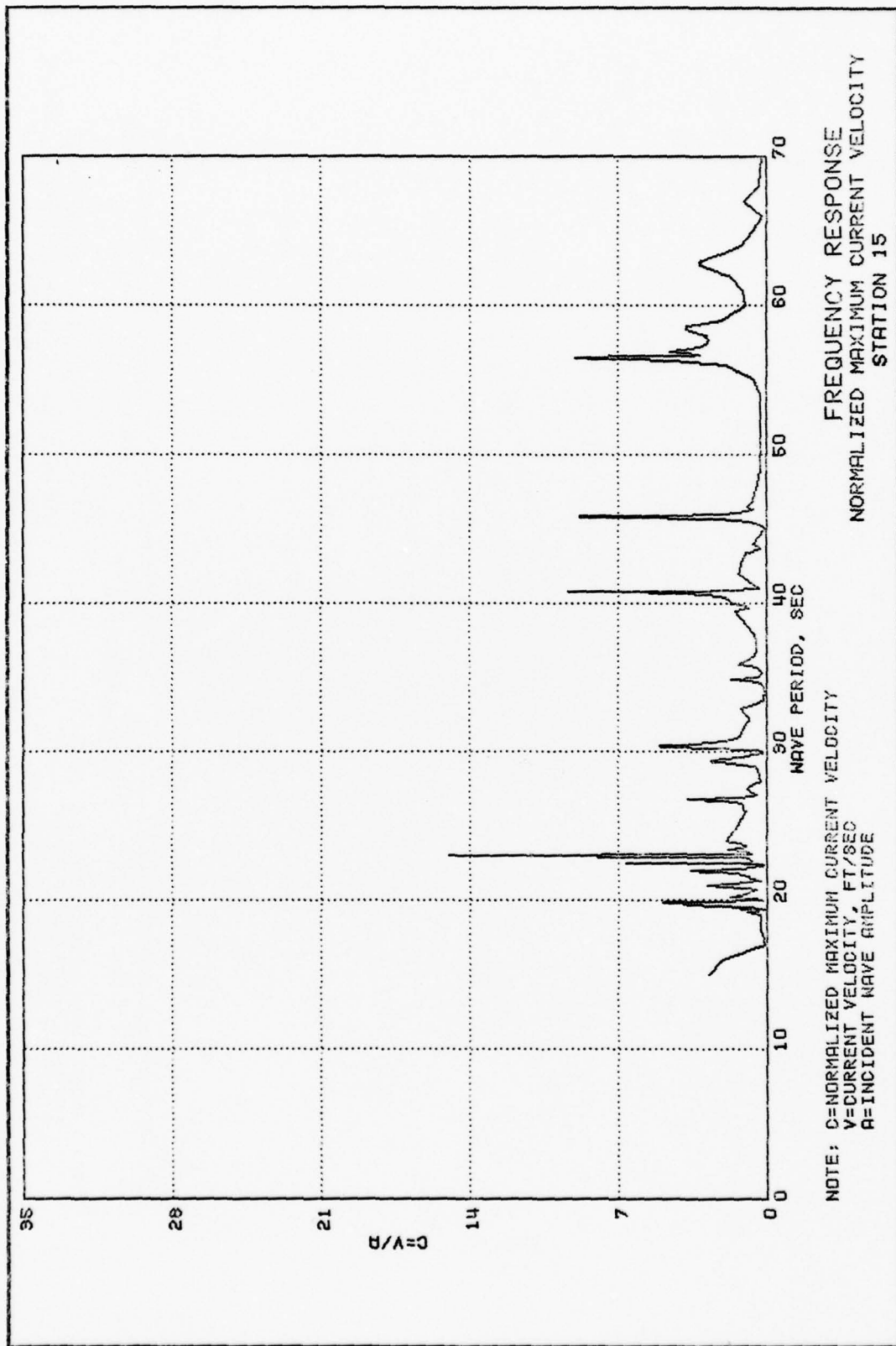
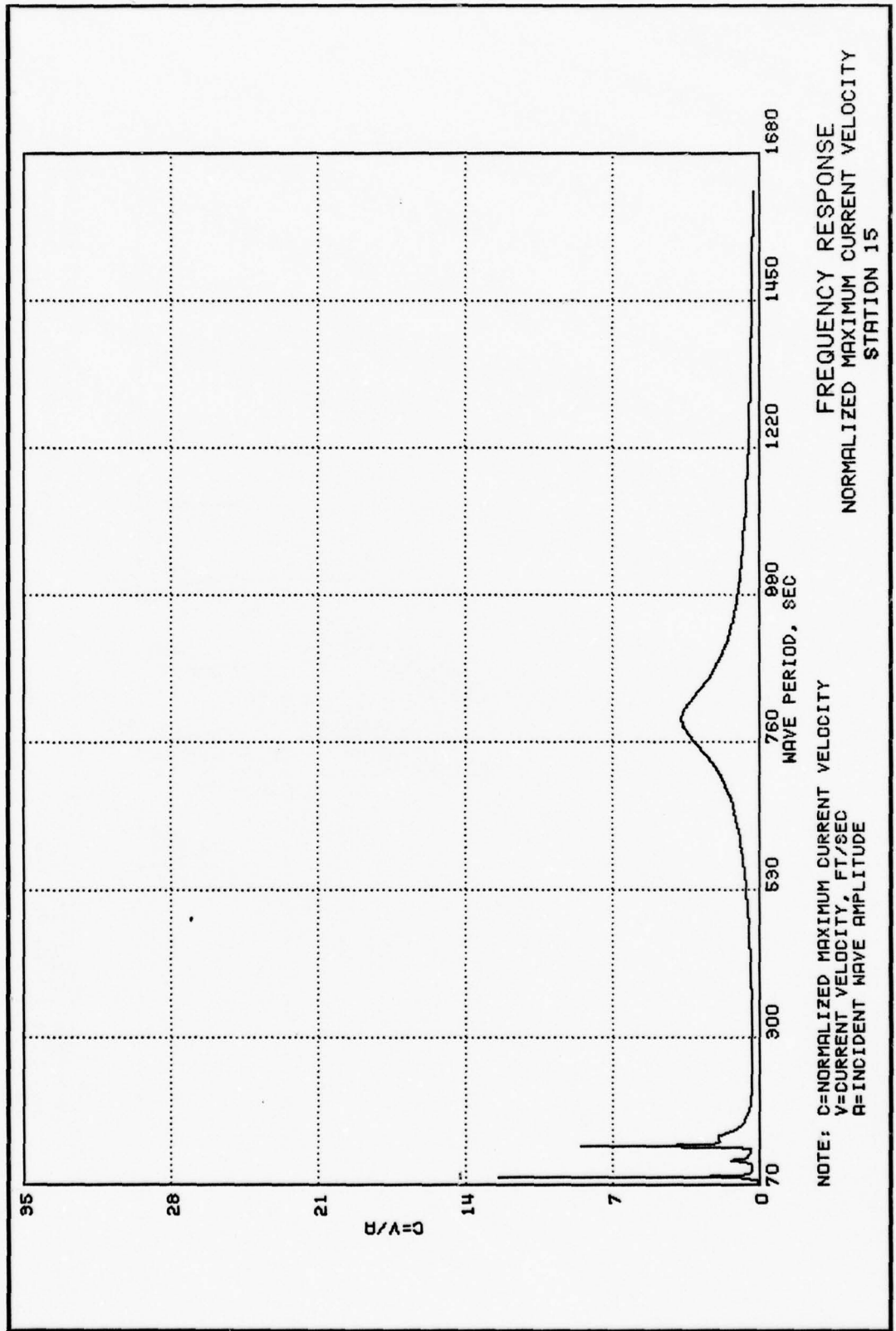


PLATE 92





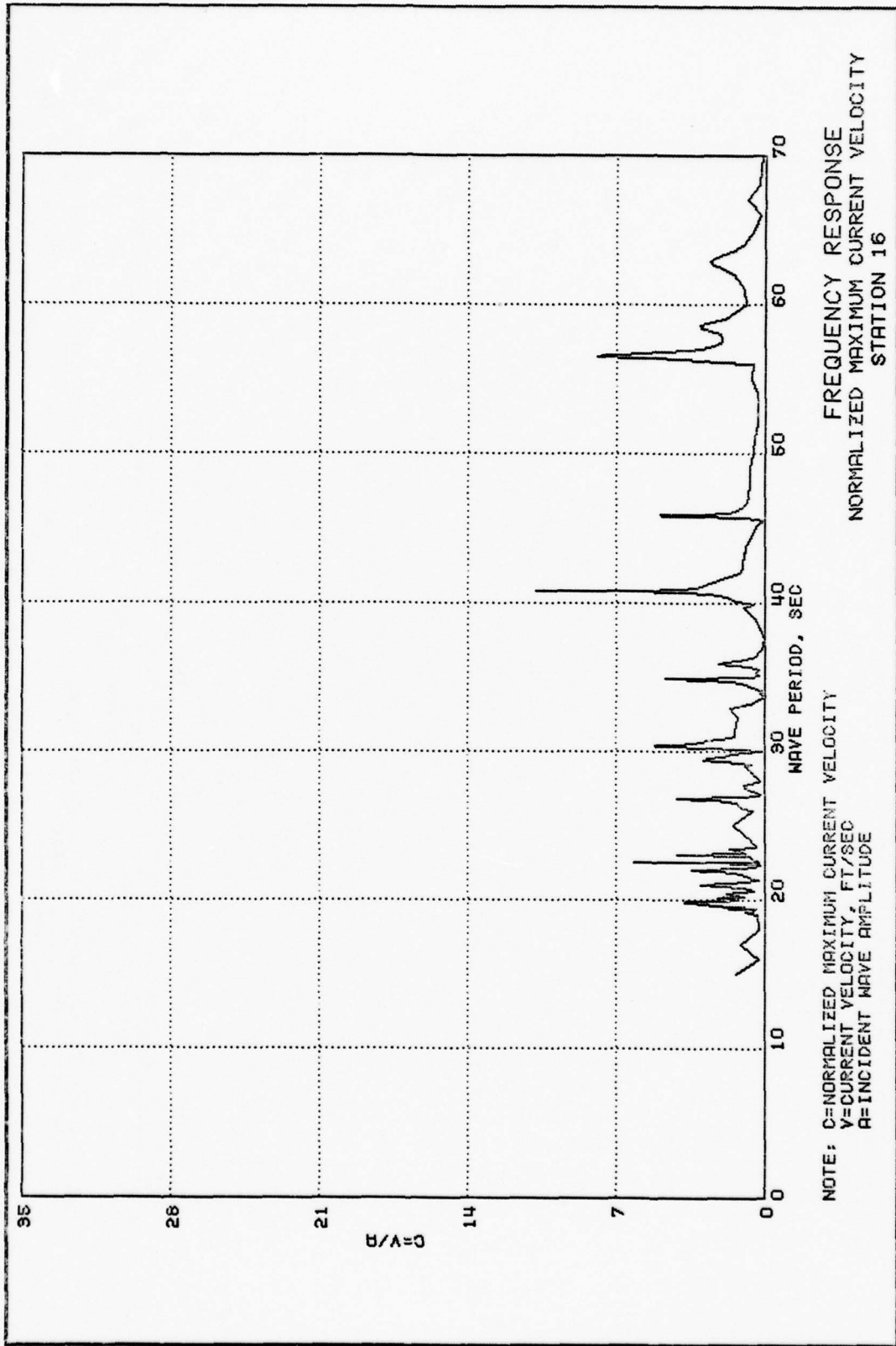
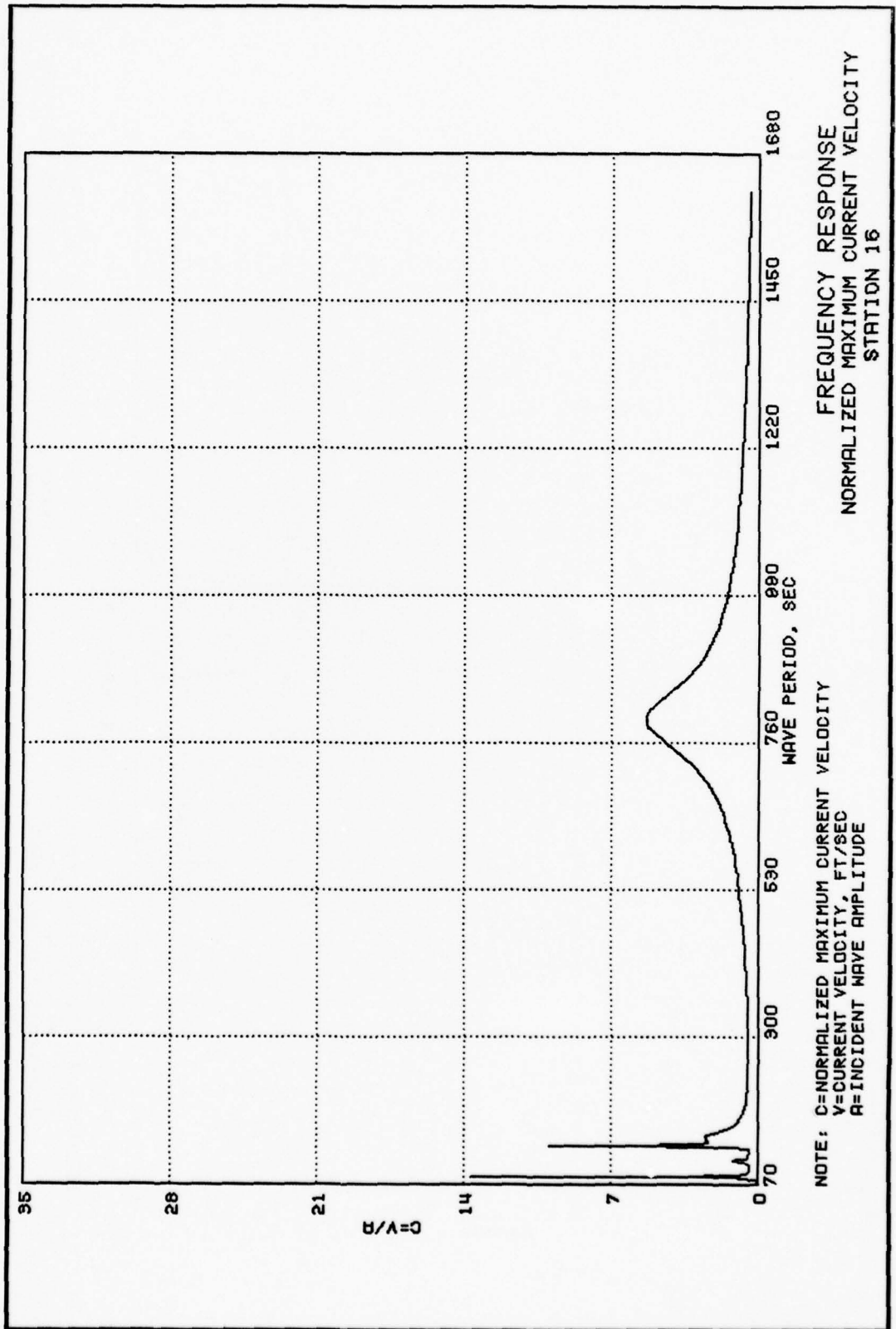
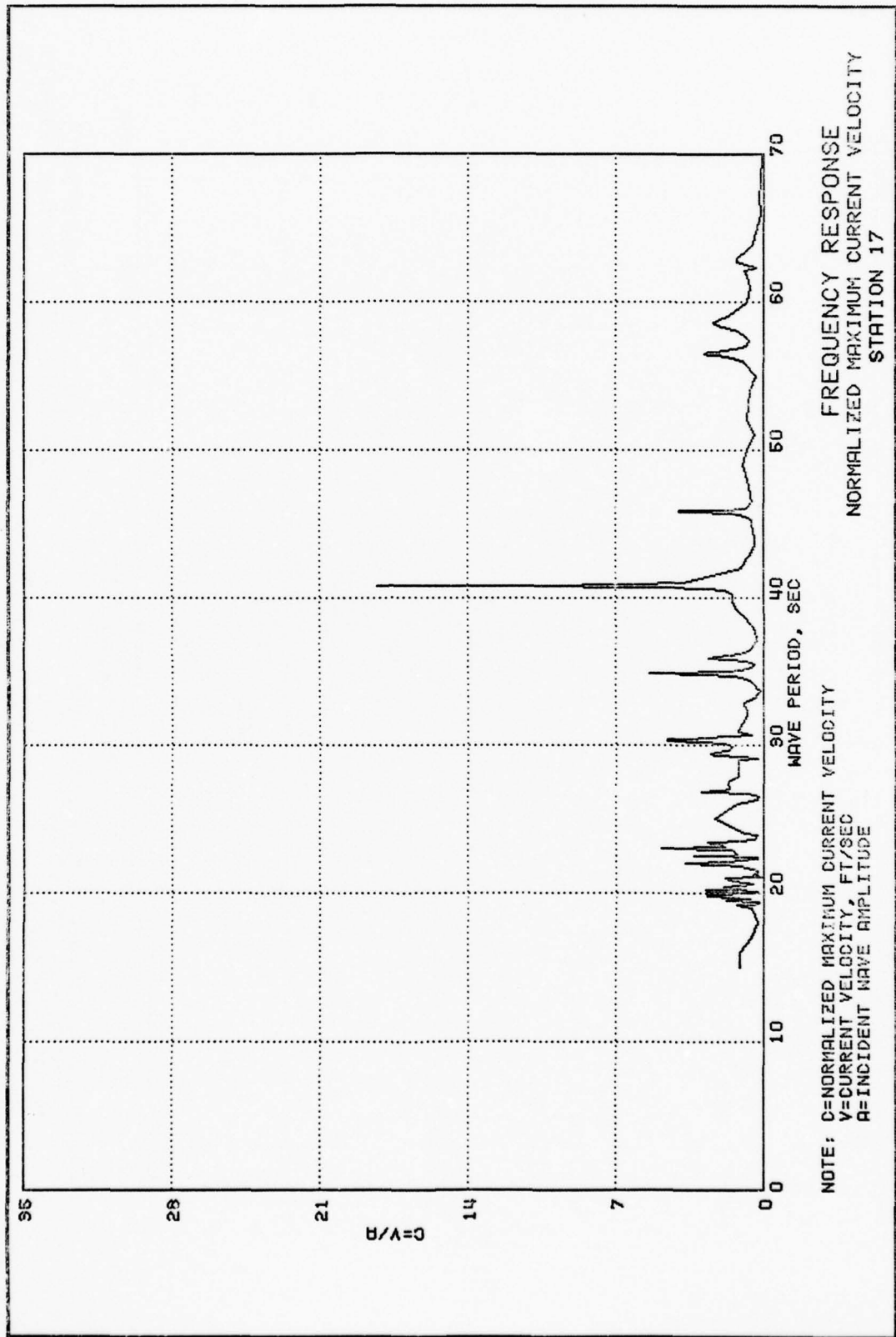


PLATE 94



FREQUENCY RESPONSE  
 NORMALIZED MAXIMUM CURRENT VELOCITY  
 STATION 16

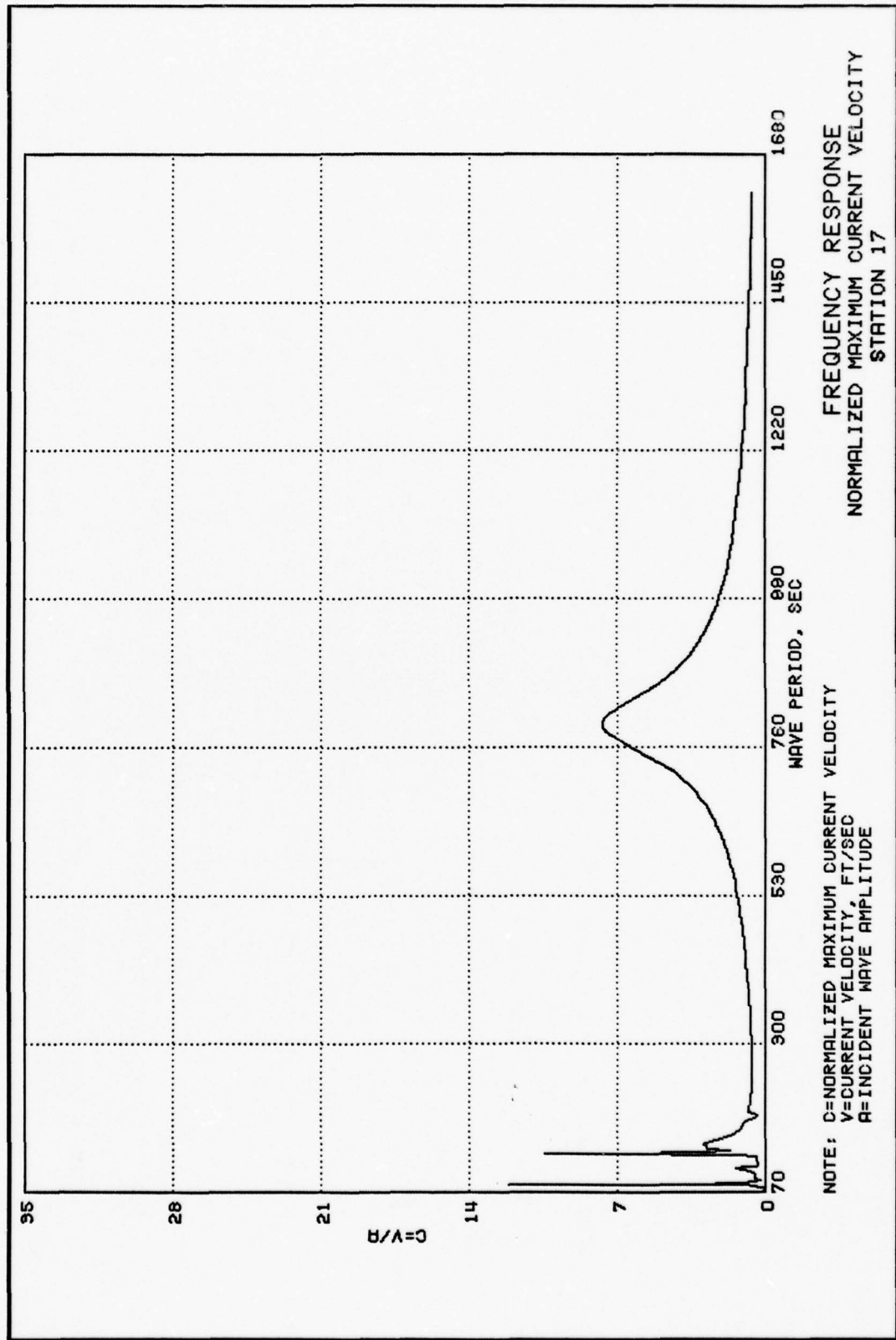
NOTE: C=NORMALIZED MAXIMUM CURRENT VELOCITY  
 V=CURRENT VELOCITY, FT/SEC  
 A=INCIDENT WAVE AMPLITUDE



FREQUENCY RESPONSE  
 NORMALIZED MAXIMUM CURRENT VELOCITY  
 STATION 17

NOTE: C=NORMALIZED MAXIMUM CURRENT VELOCITY  
 V=CURRENT VELOCITY, FT/SEC  
 A=INCIDENT WAVE AMPLITUDE

PLATE 96



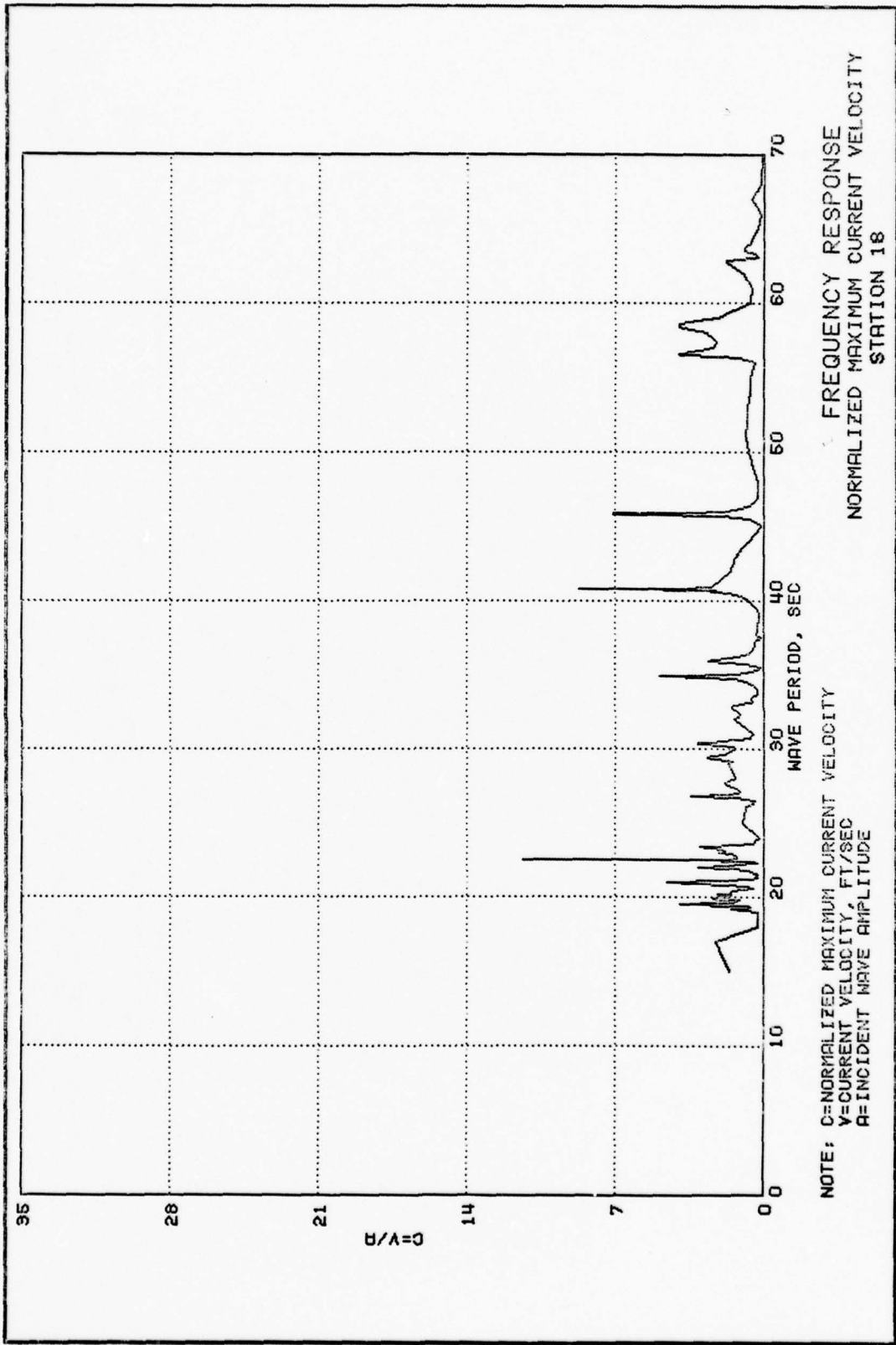
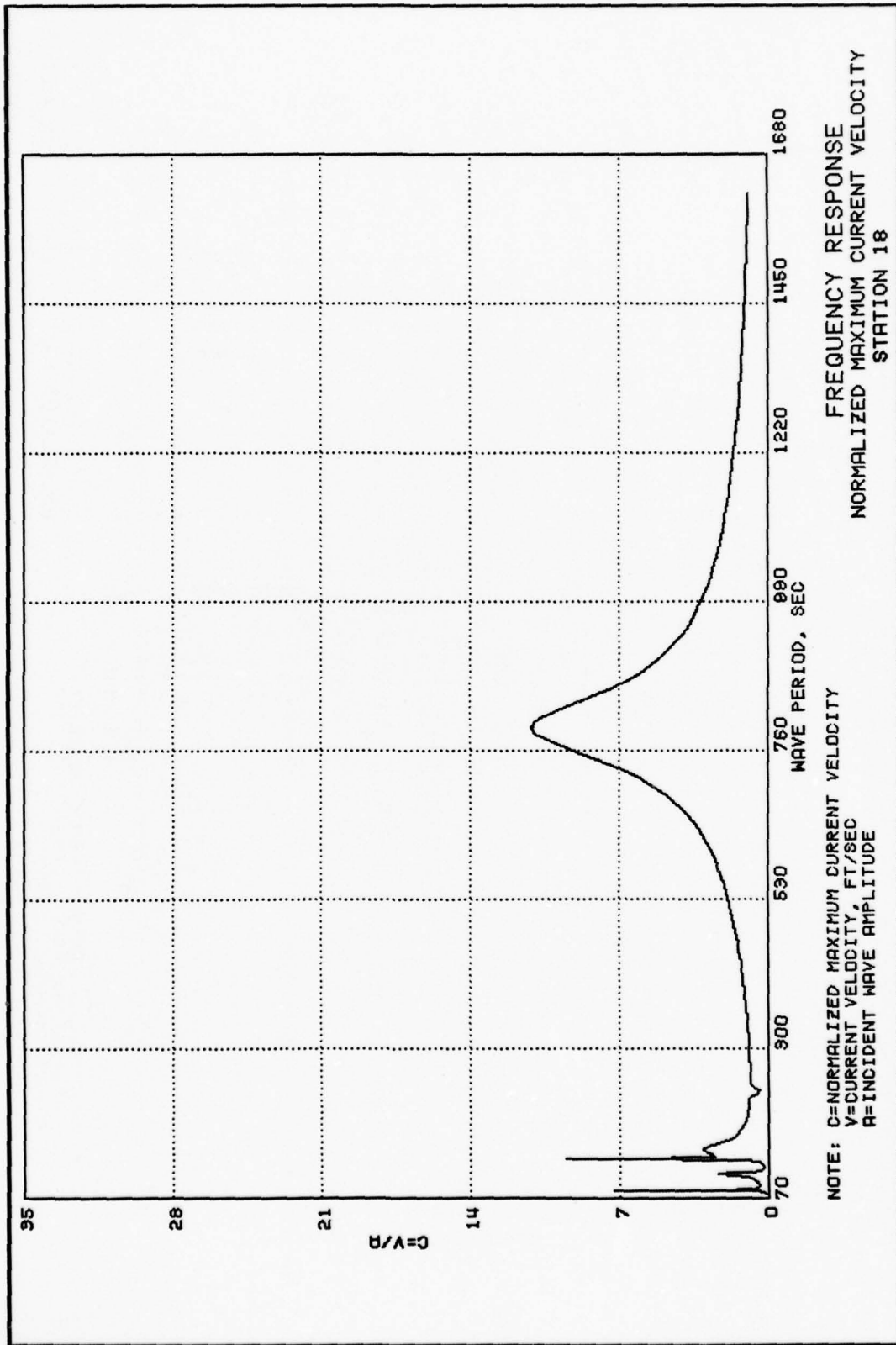
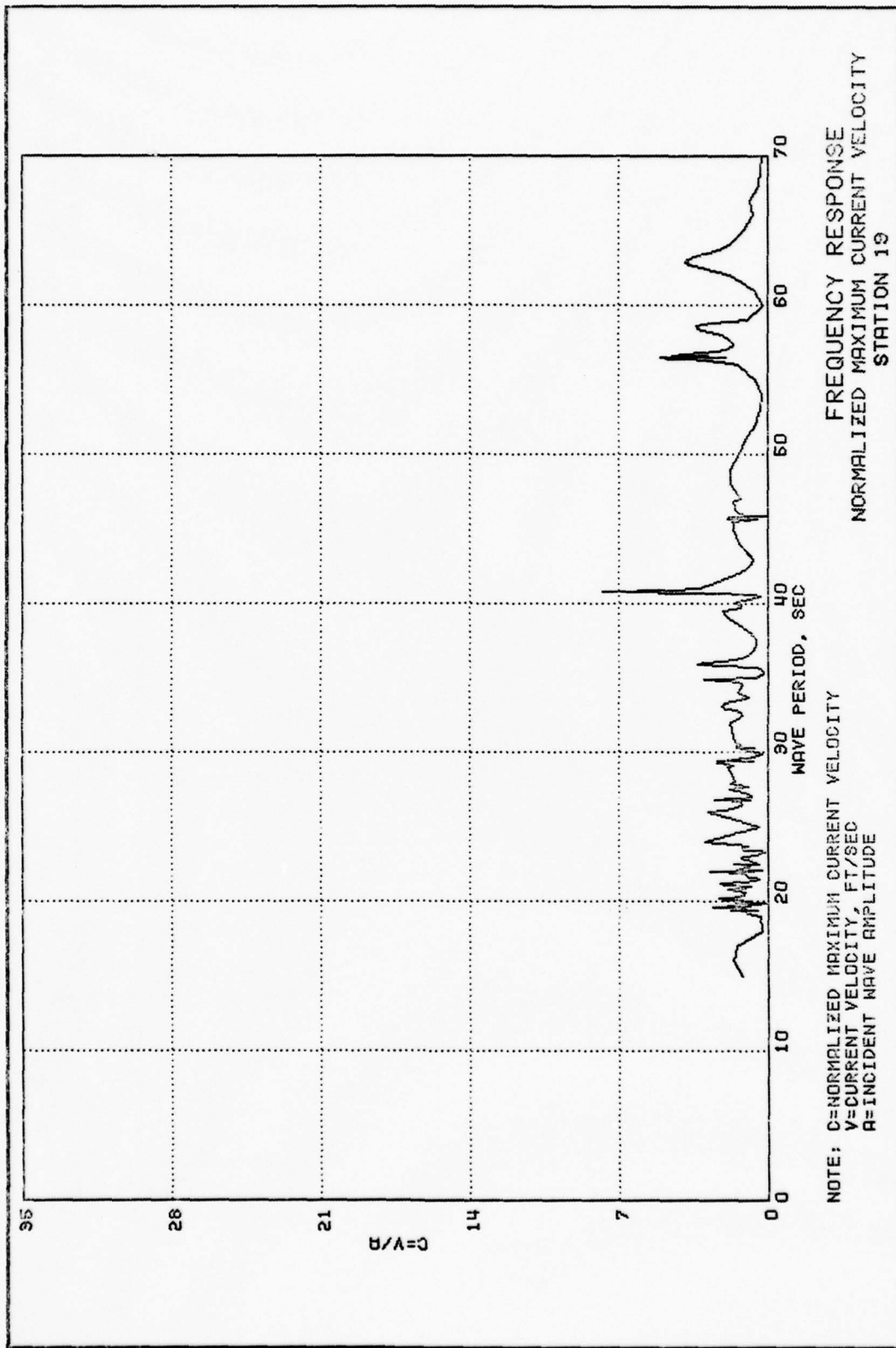


PLATE 98



FREQUENCY RESPONSE  
 NORMALIZED MAXIMUM CURRENT VELOCITY  
 STATION 18

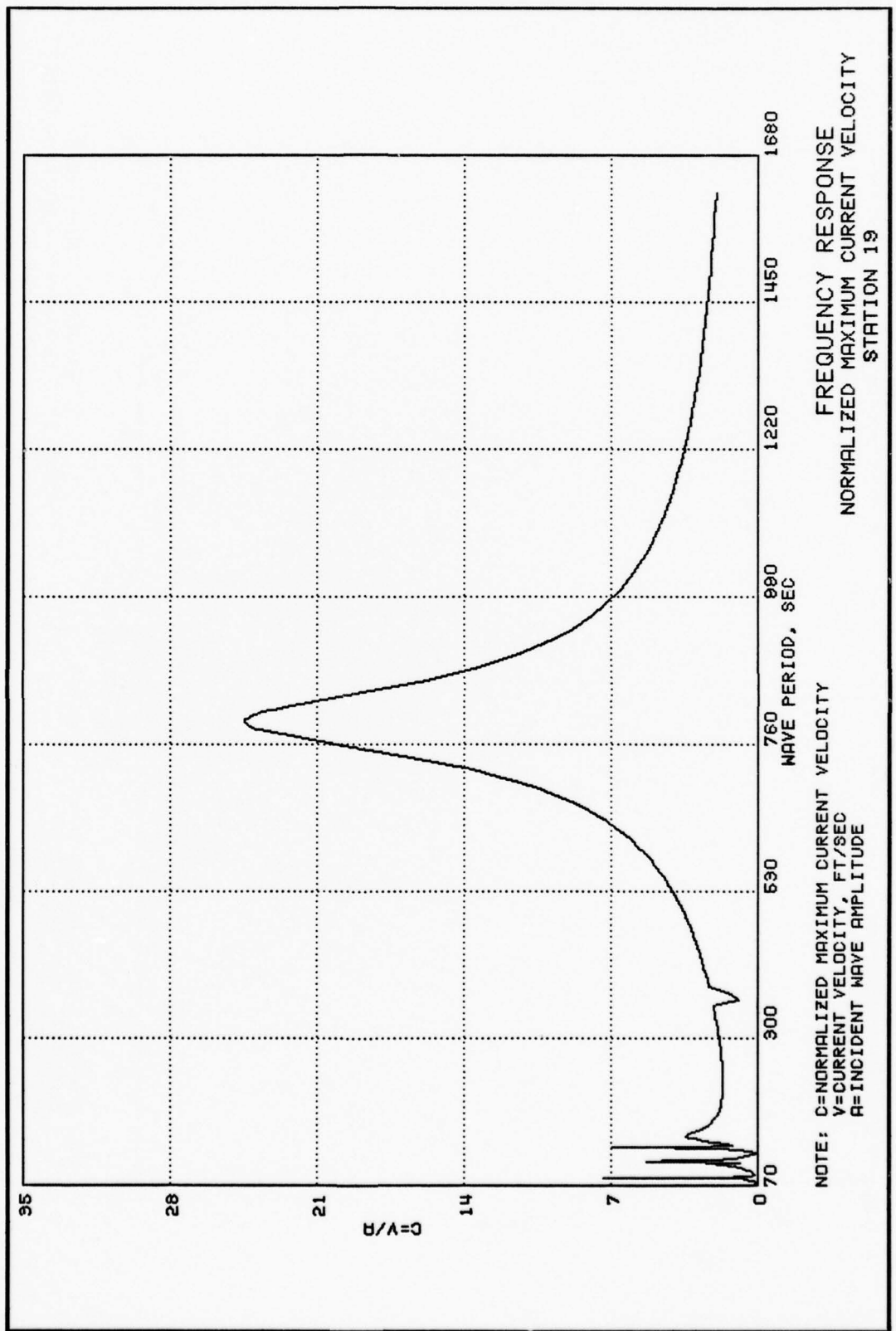
NOTE: C=NORMALIZED MAXIMUM CURRENT VELOCITY  
 V=CURRENT VELOCITY, FT./SEC  
 A=INCIDENT WAVE AMPLITUDE

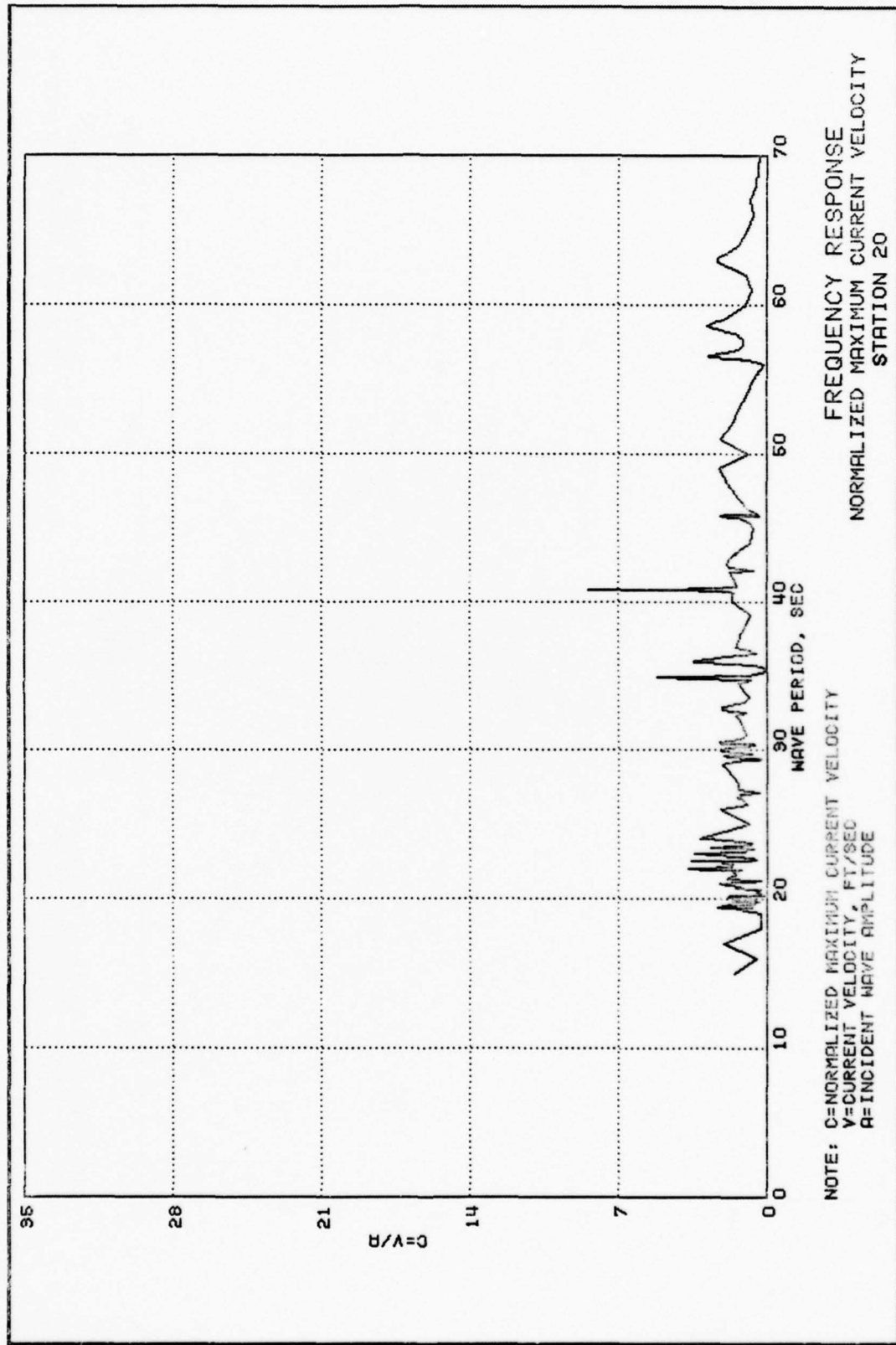


FREQUENCY RESPONSE  
 NORMALIZED MAXIMUM CURRENT VELOCITY  
 STATION 19

NOTE: C=NORMALIZED MAXIMUM CURRENT VELOCITY  
 V=CURRENT VELOCITY, FT/SEC  
 A=INCIDENT WAVE AMPLITUDE







FREQUENCY RESPONSE  
 NORMALIZED MAXIMUM CURRENT VELOCITY  
 STATION 20

NOTE: C=NORMALIZED MAXIMUM CURRENT VELOCITY  
 V=CURRENT VELOCITY, FT/SEC  
 R=INCIDENT WAVE AMPLITUDE

PLATE 102



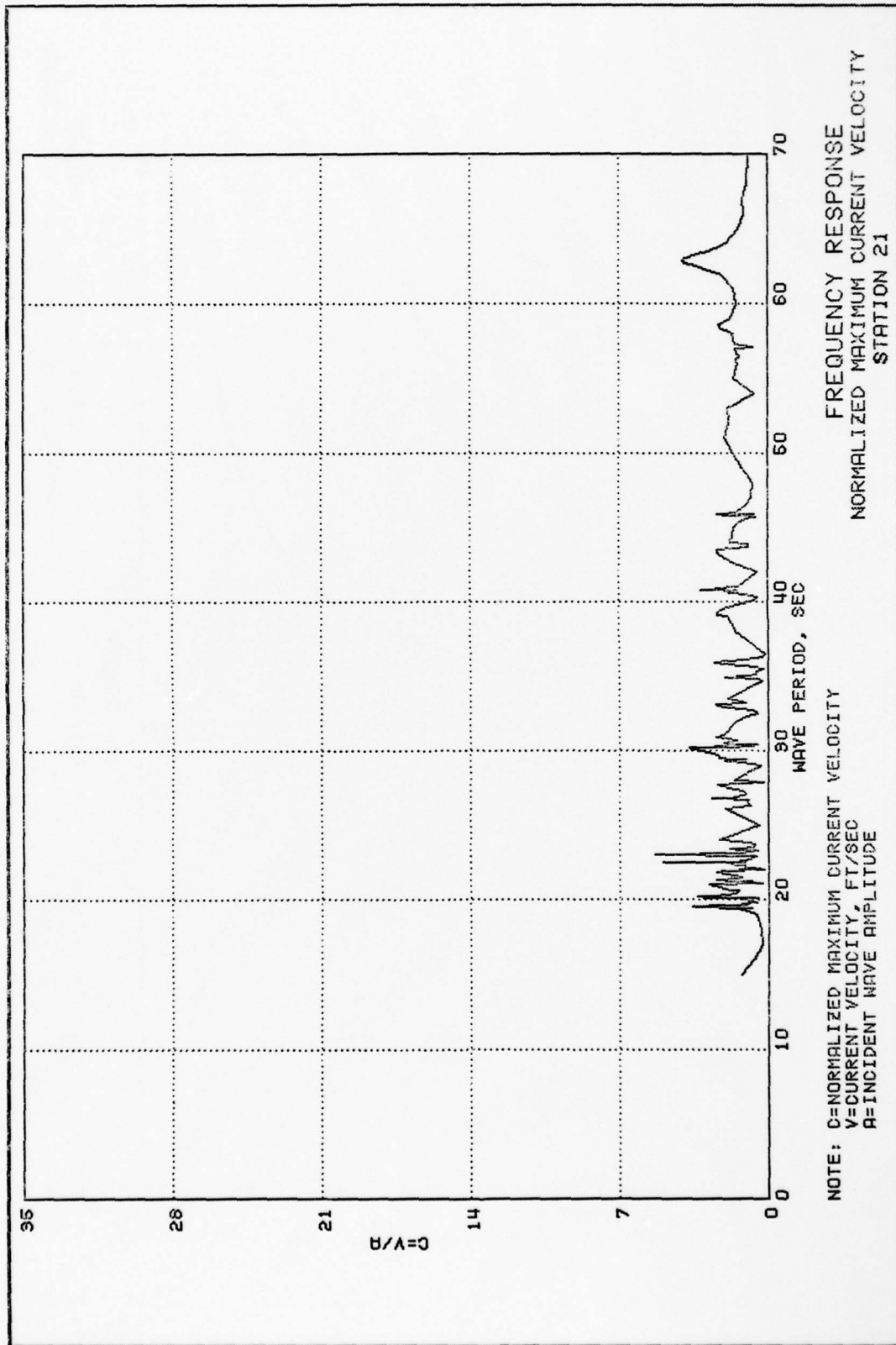
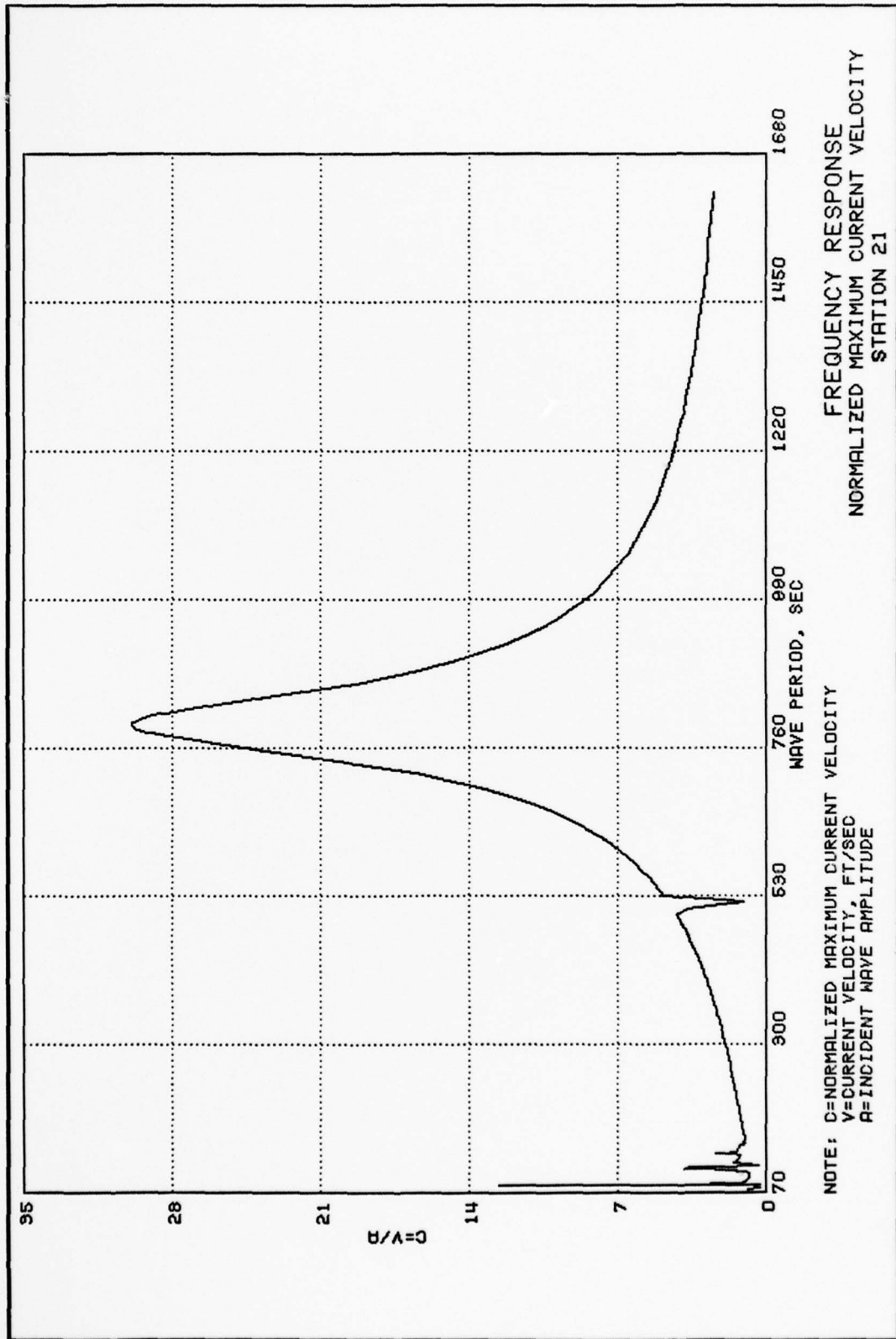
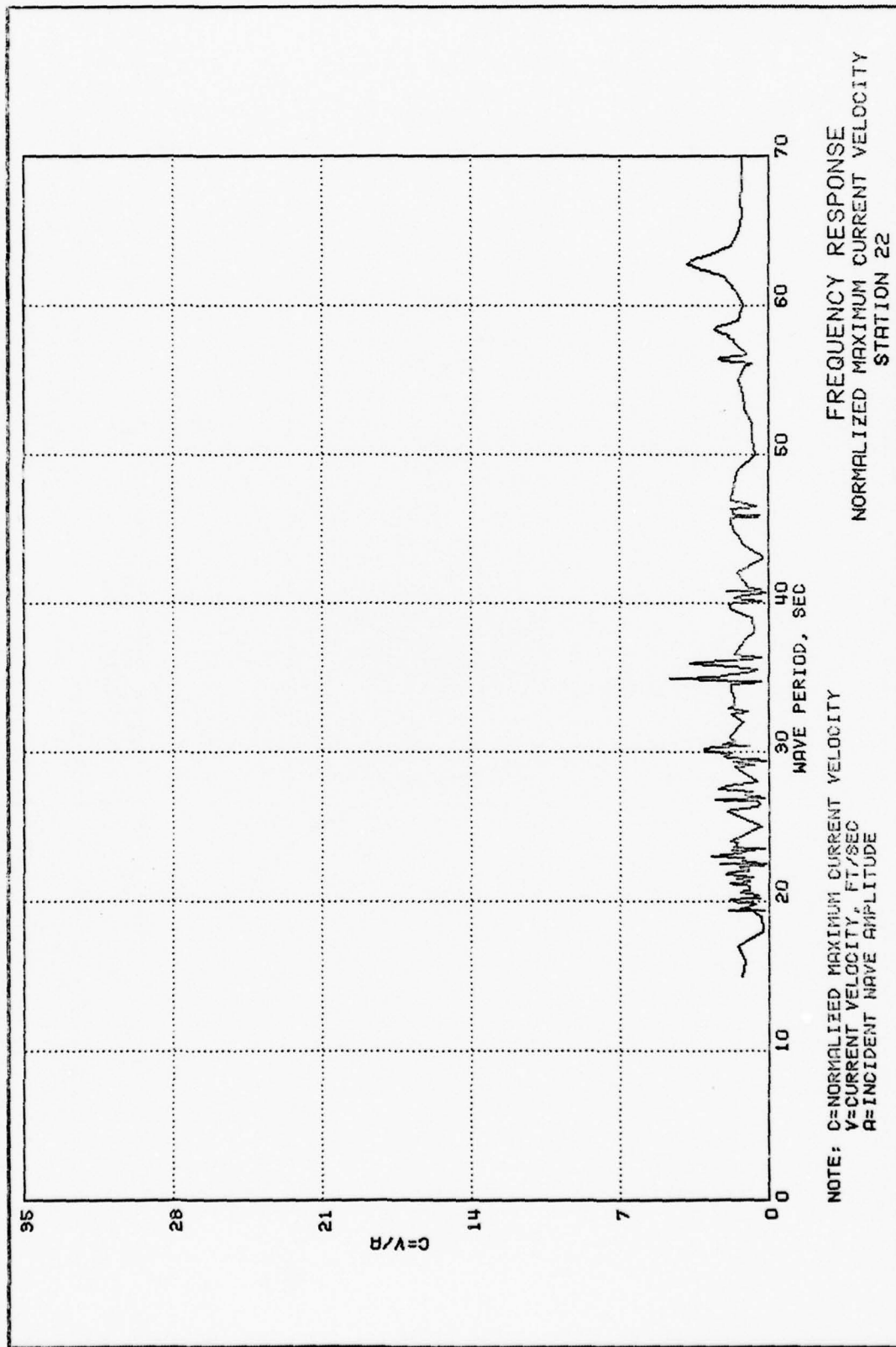


PLATE 104



FREQUENCY RESPONSE  
 NORMALIZED MAXIMUM CURRENT VELOCITY  
 STATION 21

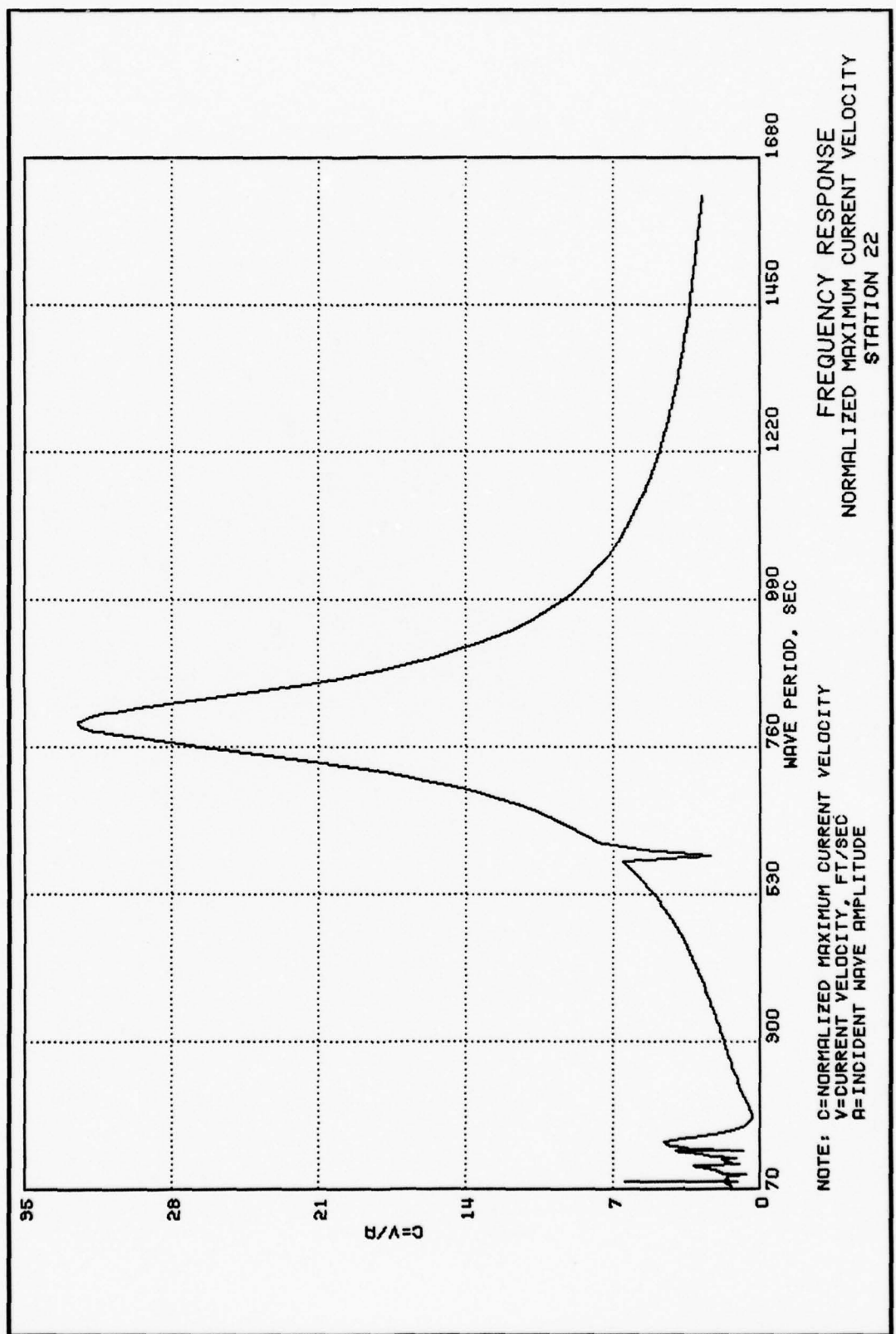
NOTE: C=NORMALIZED MAXIMUM CURRENT VELOCITY  
 V=CURRENT VELOCITY, FT/SEC  
 A=INCIDENT WAVE AMPLITUDE



FREQUENCY RESPONSE  
 NORMALIZED MAXIMUM CURRENT VELOCITY  
 STATION 22

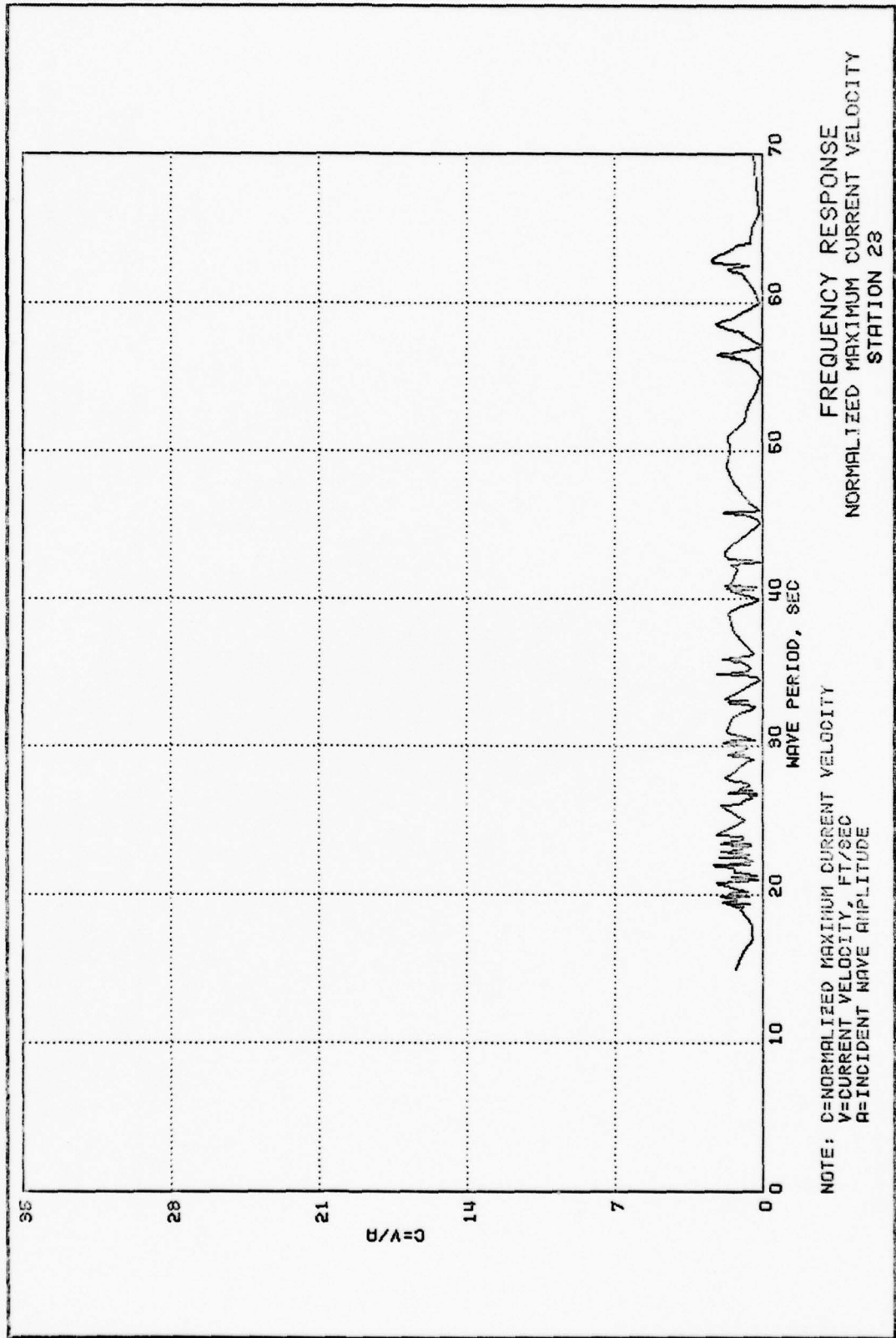
NOTE: C=NORMALIZED MAXIMUM CURRENT VELOCITY  
 V=CURRENT VELOCITY, FT/SEC  
 A=INCIDENT WAVE AMPLITUDE

PLATE 106

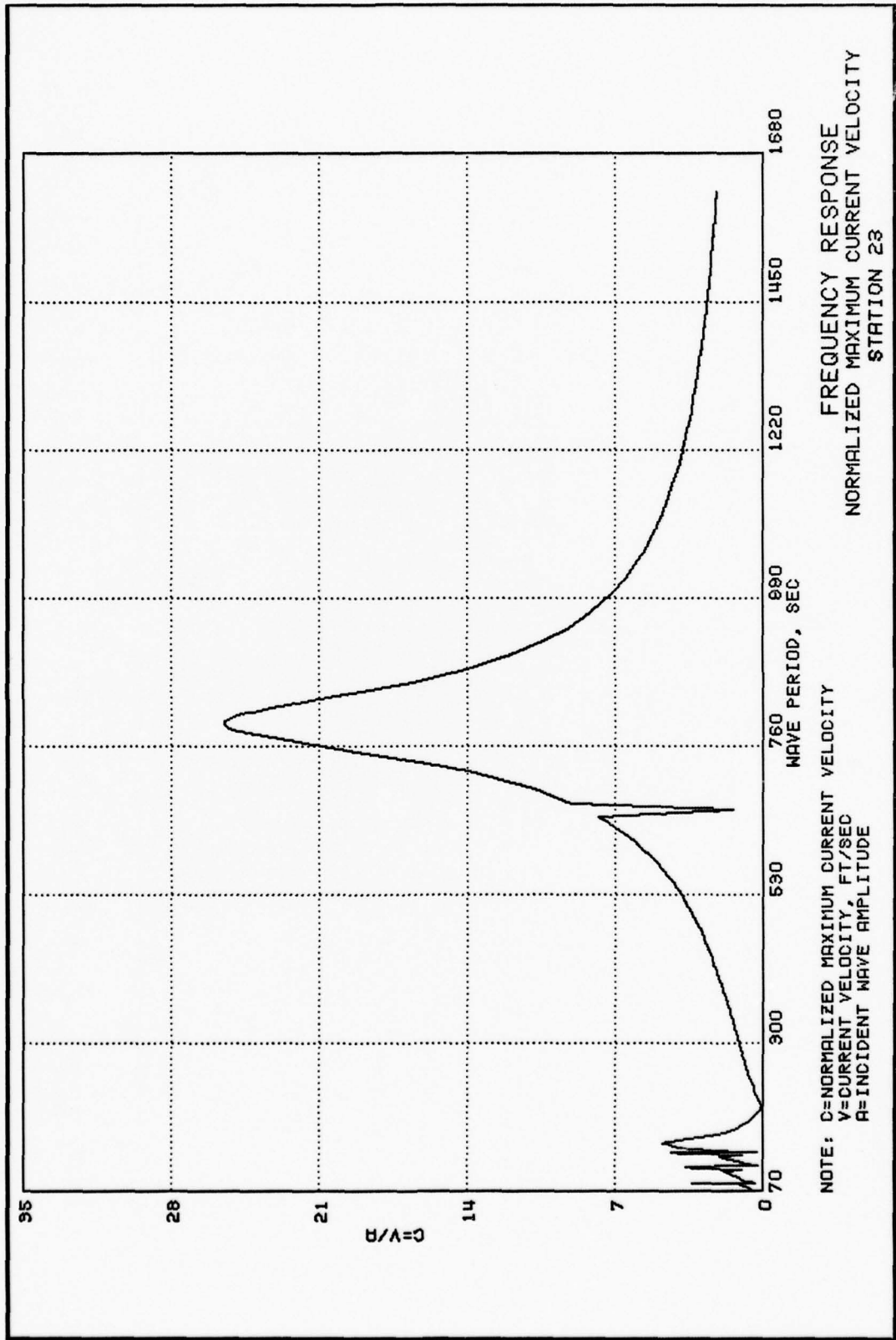


FREQUENCY RESPONSE  
 NORMALIZED MAXIMUM CURRENT VELOCITY  
 STATION 22

NOTE: C=NORMALIZED MAXIMUM CURRENT VELOCITY  
 V=CURRENT VELOCITY, FT/SEC  
 A=INCIDENT WAVE AMPLITUDE







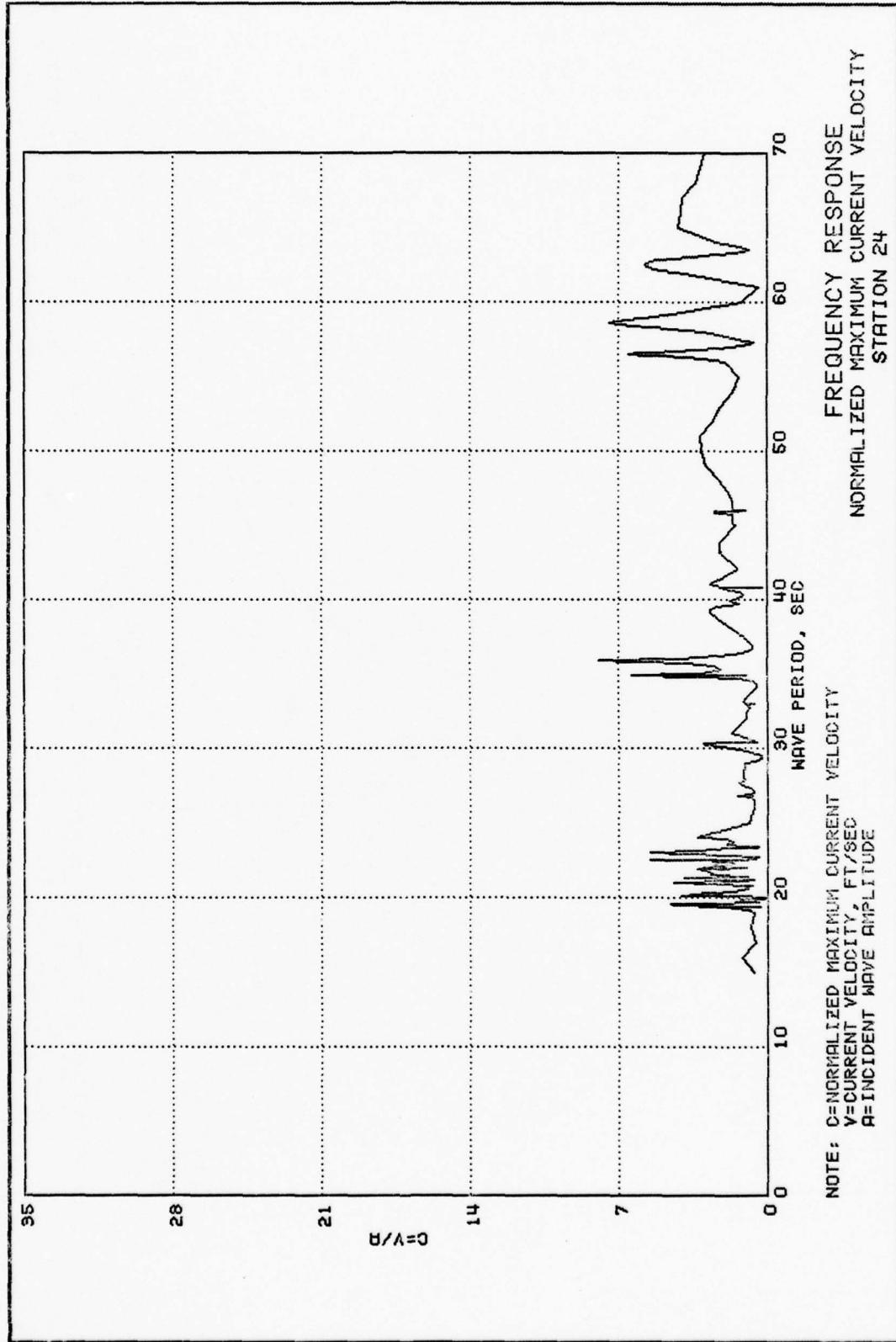
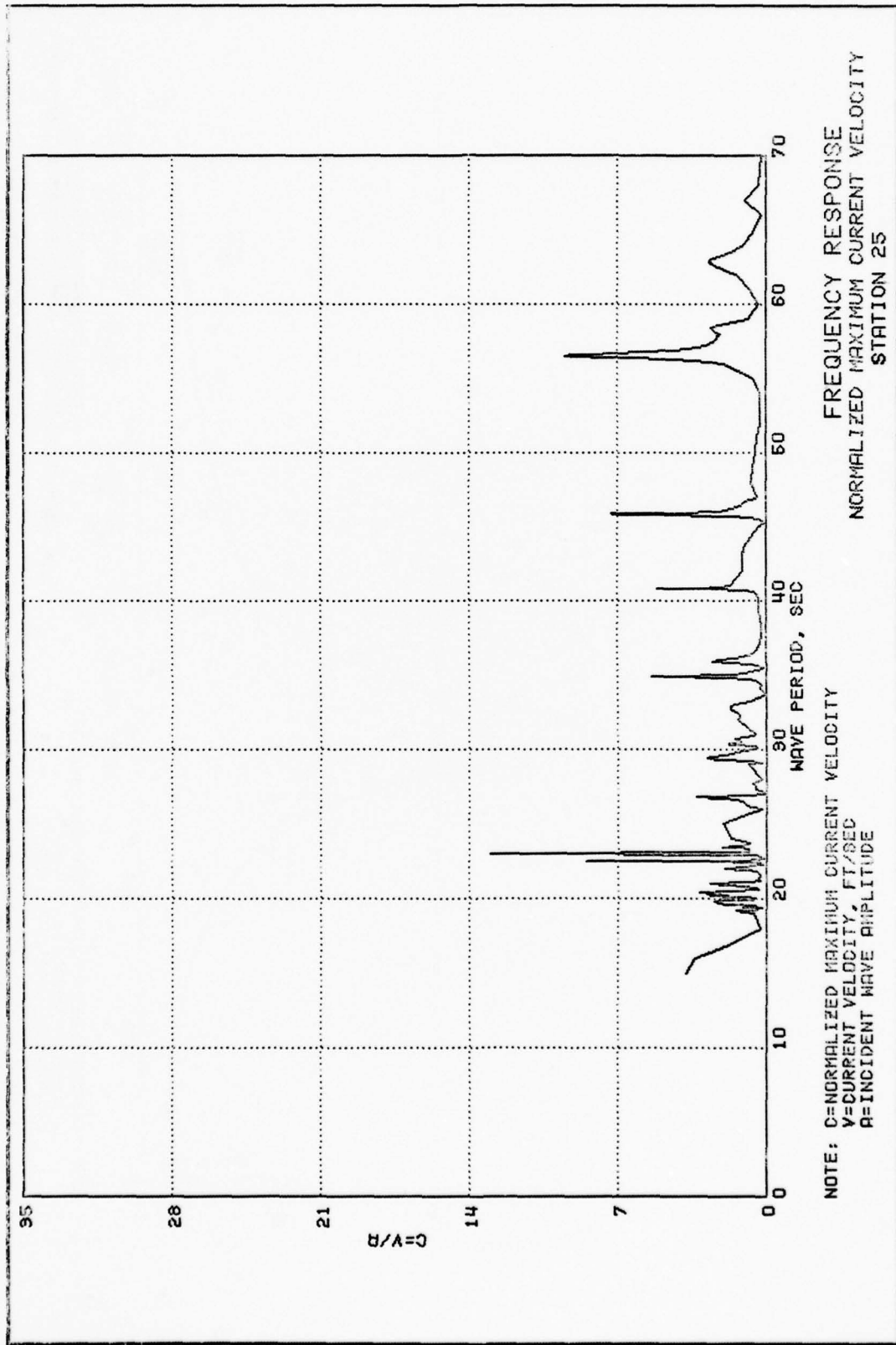


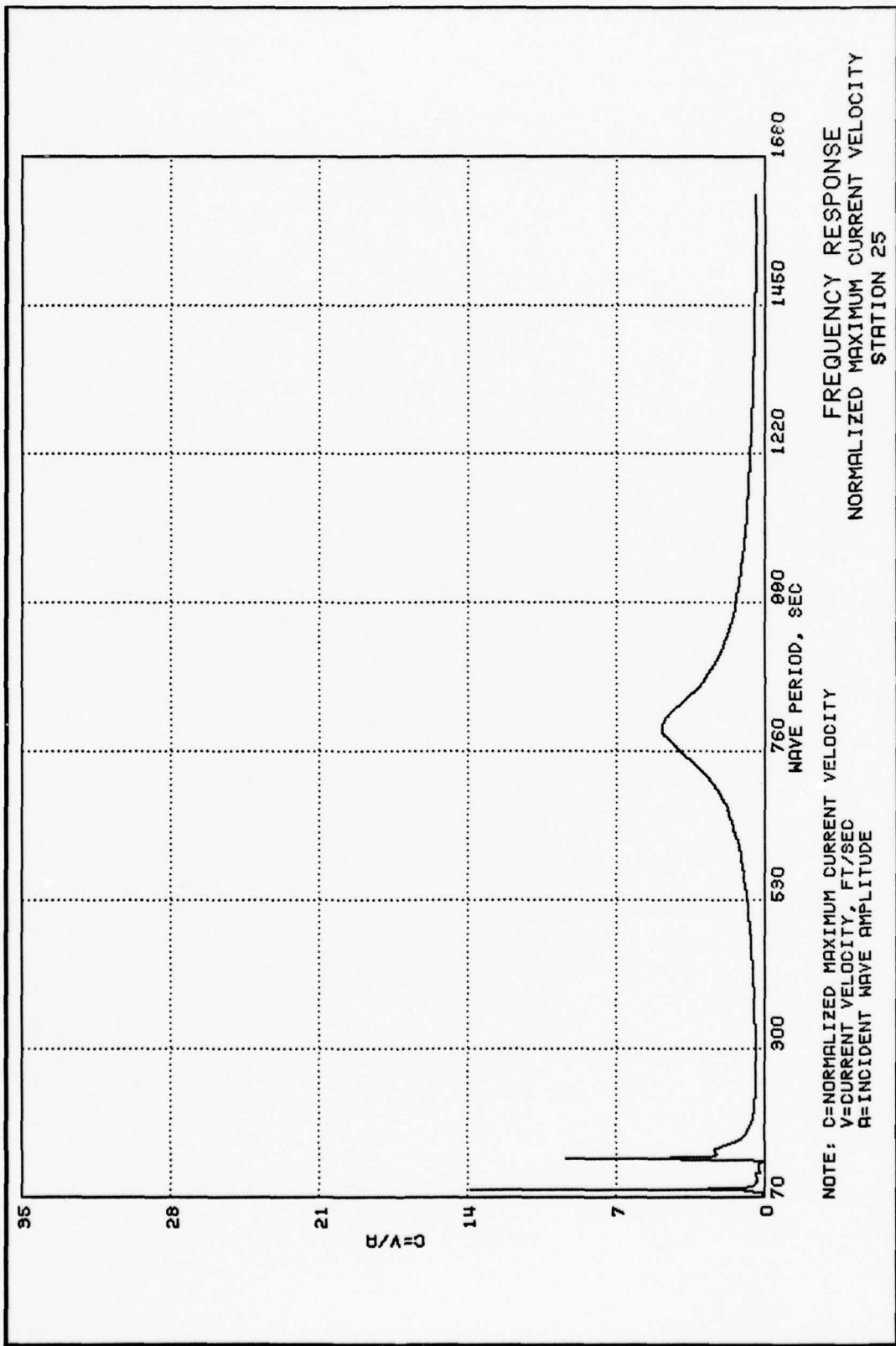
PLATE 110





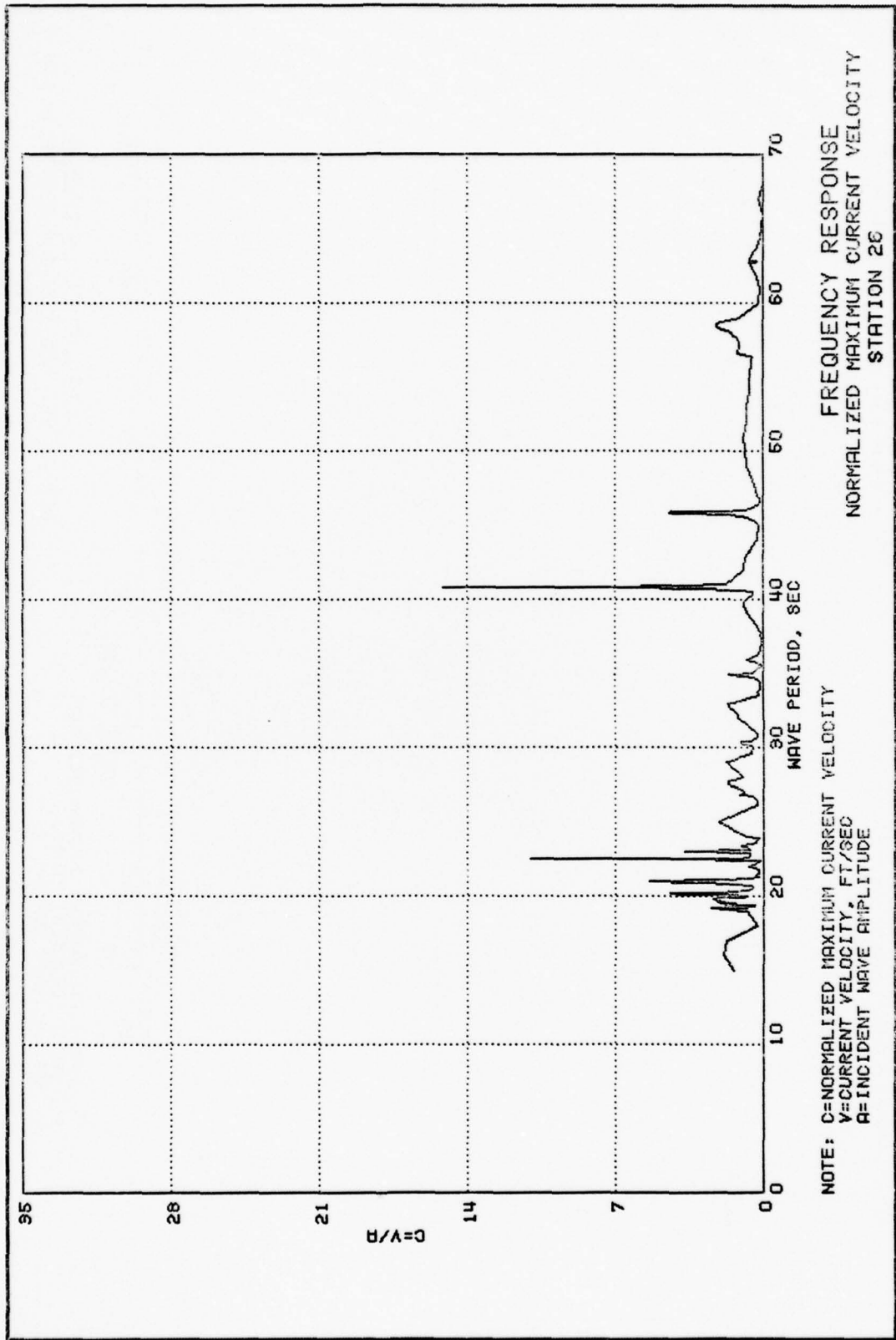
FREQUENCY RESPONSE  
 NORMALIZED MAXIMUM CURRENT VELOCITY  
 STATION 25

NOTE: C=NORMALIZED MAXIMUM CURRENT VELOCITY  
 V=CURRENT VELOCITY, FT/SEC  
 R=INCIDENT WAVE AMPLITUDE



FREQUENCY RESPONSE  
 NORMALIZED MAXIMUM CURRENT VELOCITY  
 STATION 25

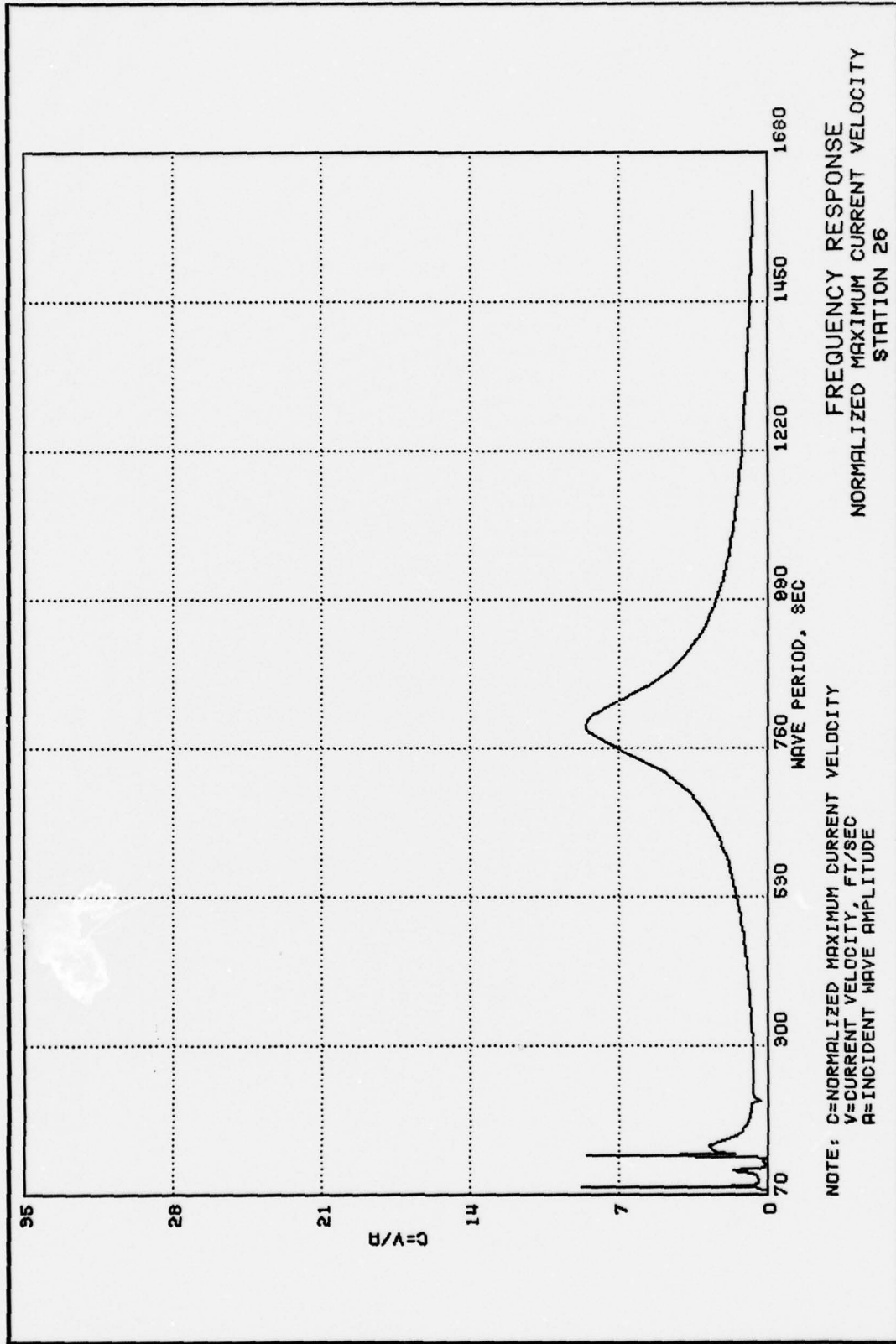
NOTE: C=NORMALIZED MAXIMUM CURRENT VELOCITY  
 V=CURRENT VELOCITY, FT/SEC  
 A=INCIDENT WAVE AMPLITUDE



FREQUENCY RESPONSE  
 NORMALIZED MAXIMUM CURRENT VELOCITY  
 STATION 26

NOTE: C=NORMALIZED MAXIMUM CURRENT VELOCITY  
 V=CURRENT VELOCITY, FT/SEC  
 A=INCIDENT WAVE AMPLITUDE

PLATE 114



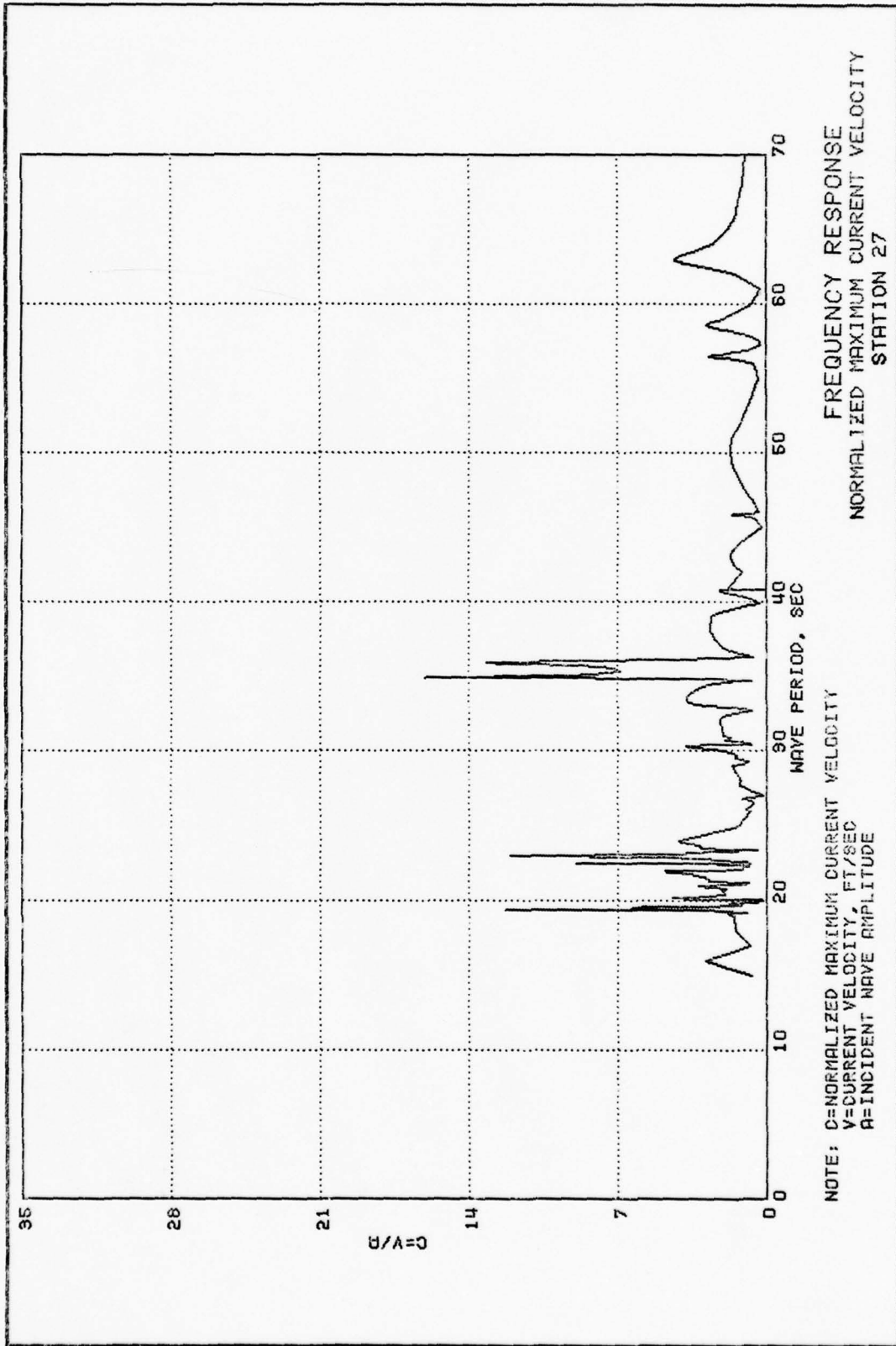
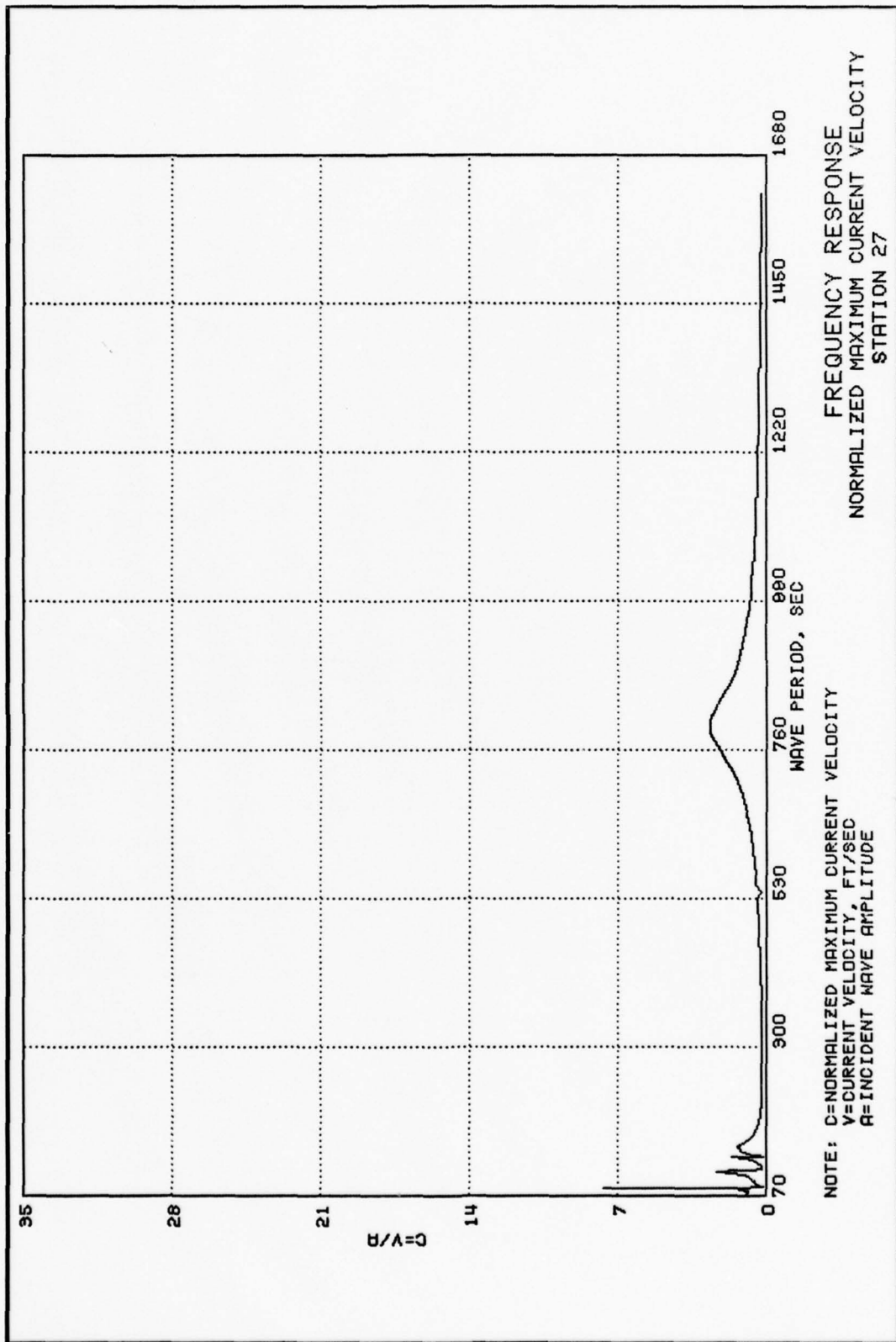


PLATE 116





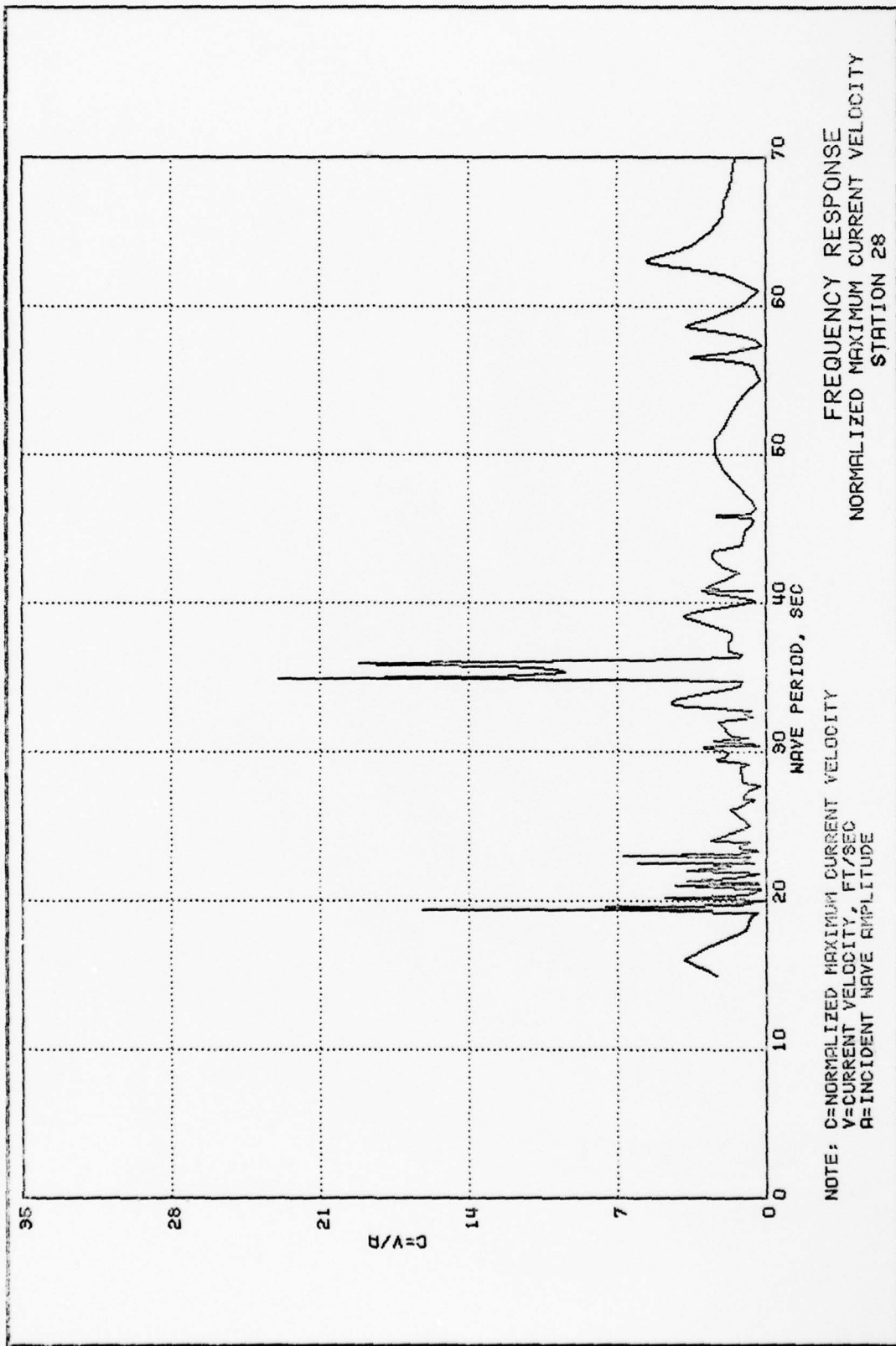
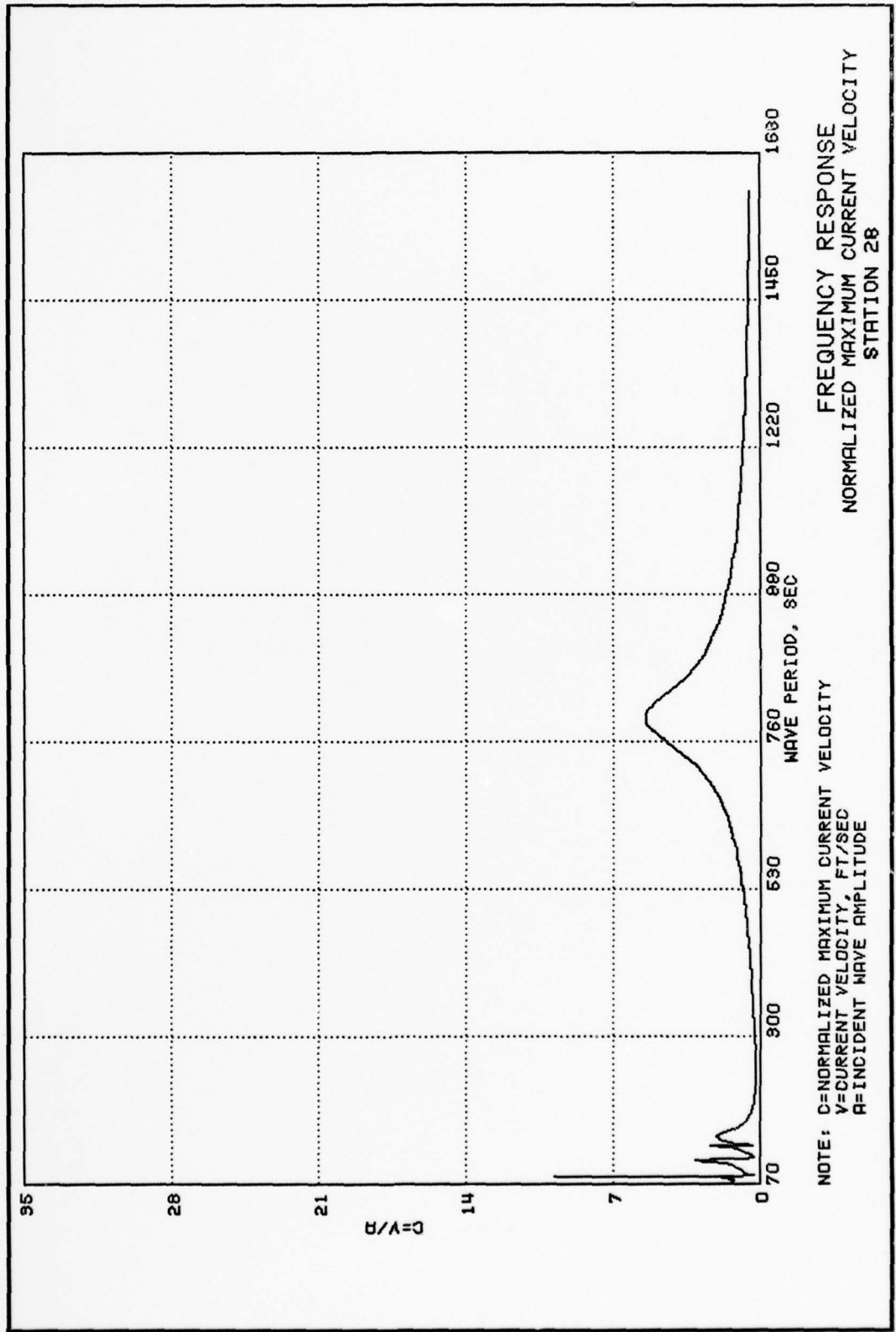
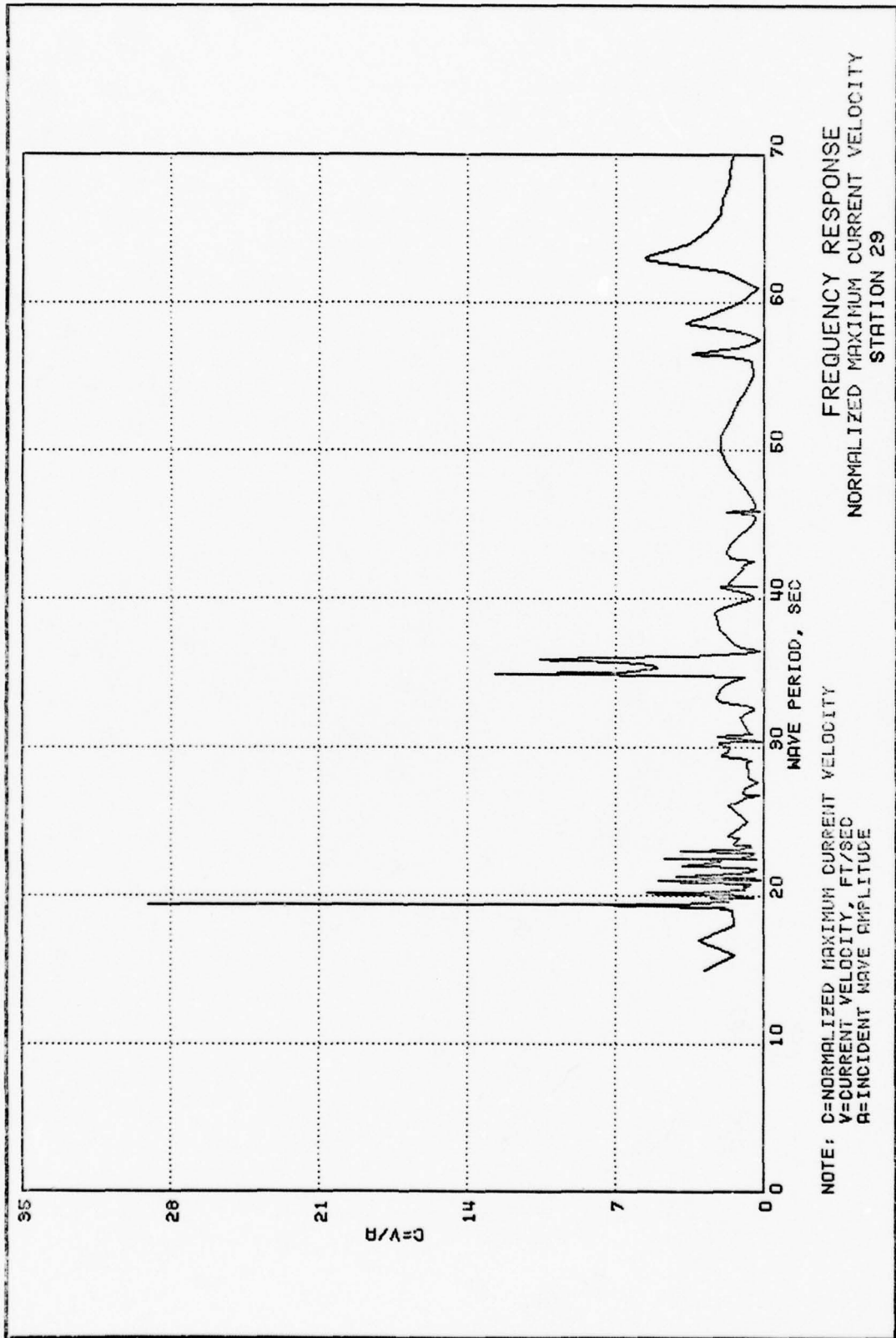


PLATE 118



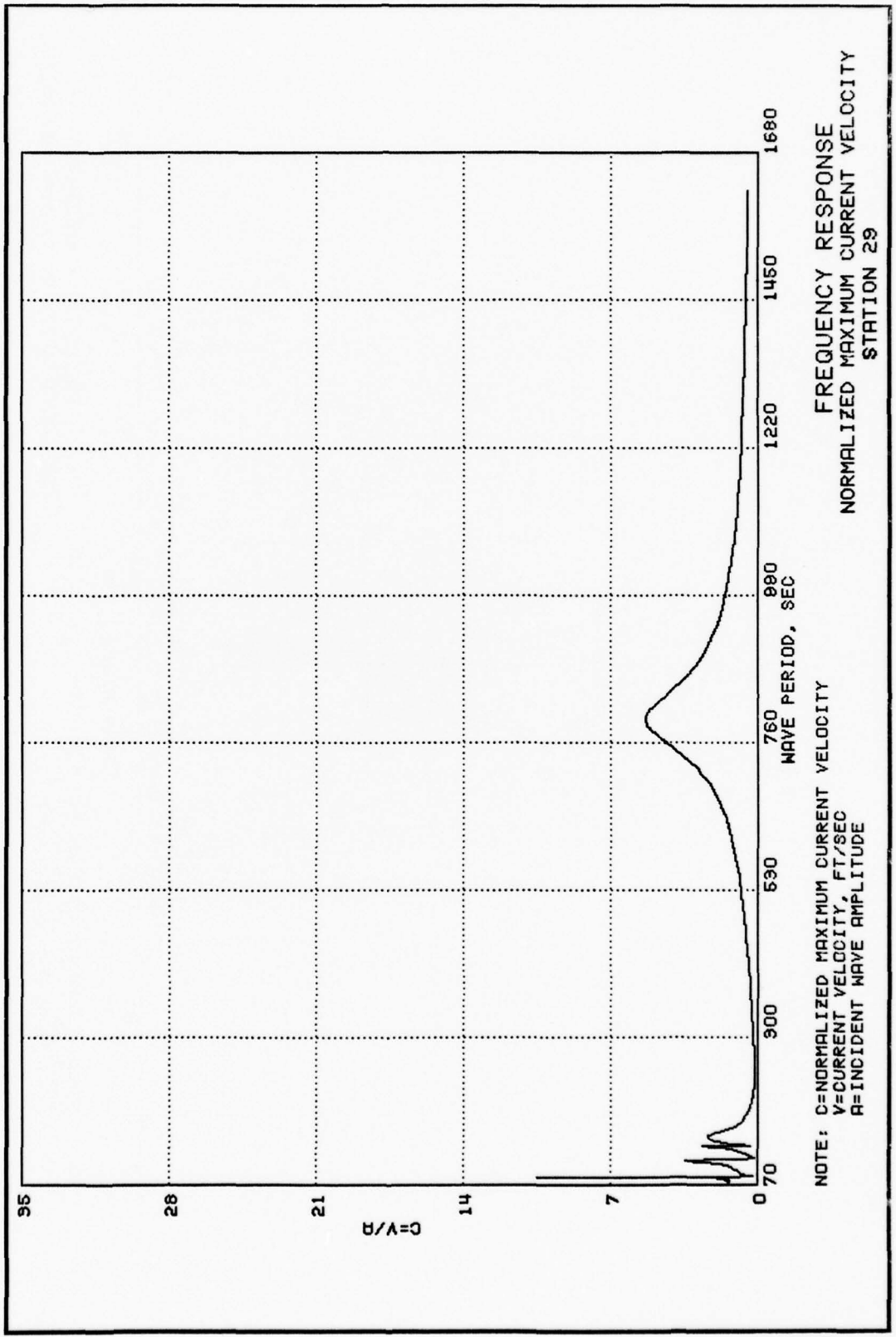
FREQUENCY RESPONSE  
 NORMALIZED MAXIMUM CURRENT VELOCITY  
 STATION 28

NOTE: C=NORMALIZED MAXIMUM CURRENT VELOCITY  
 V=CURRENT VELOCITY, FT/SEC  
 A=INCIDENT WAVE AMPLITUDE



FREQUENCY RESPONSE  
 NORMALIZED MAXIMUM CURRENT VELOCITY  
 STATION 29

NOTE: C=NORMALIZED MAXIMUM CURRENT VELOCITY  
 V=CURRENT VELOCITY, FT/SEC  
 A=INCIDENT WAVE AMPLITUDE



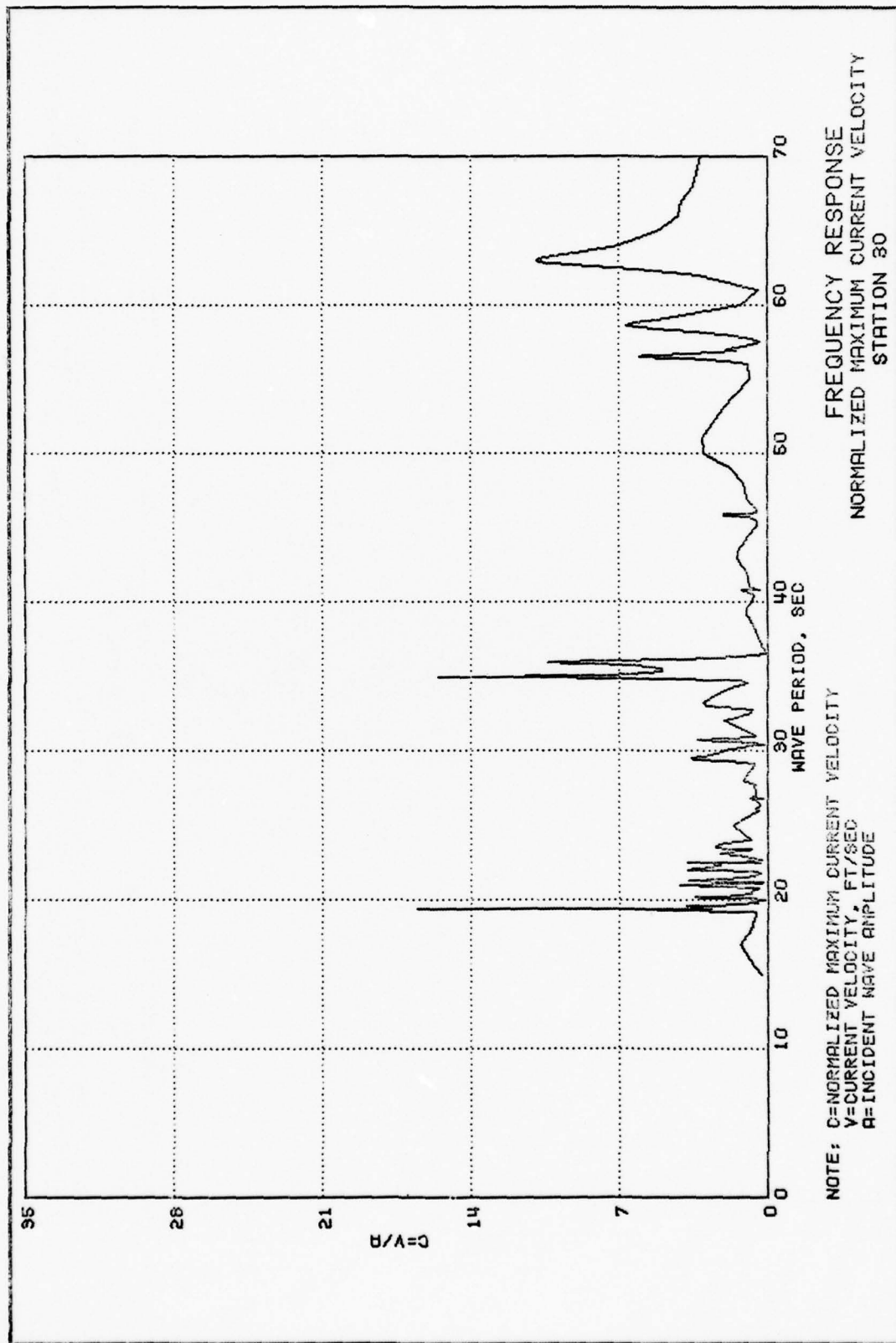
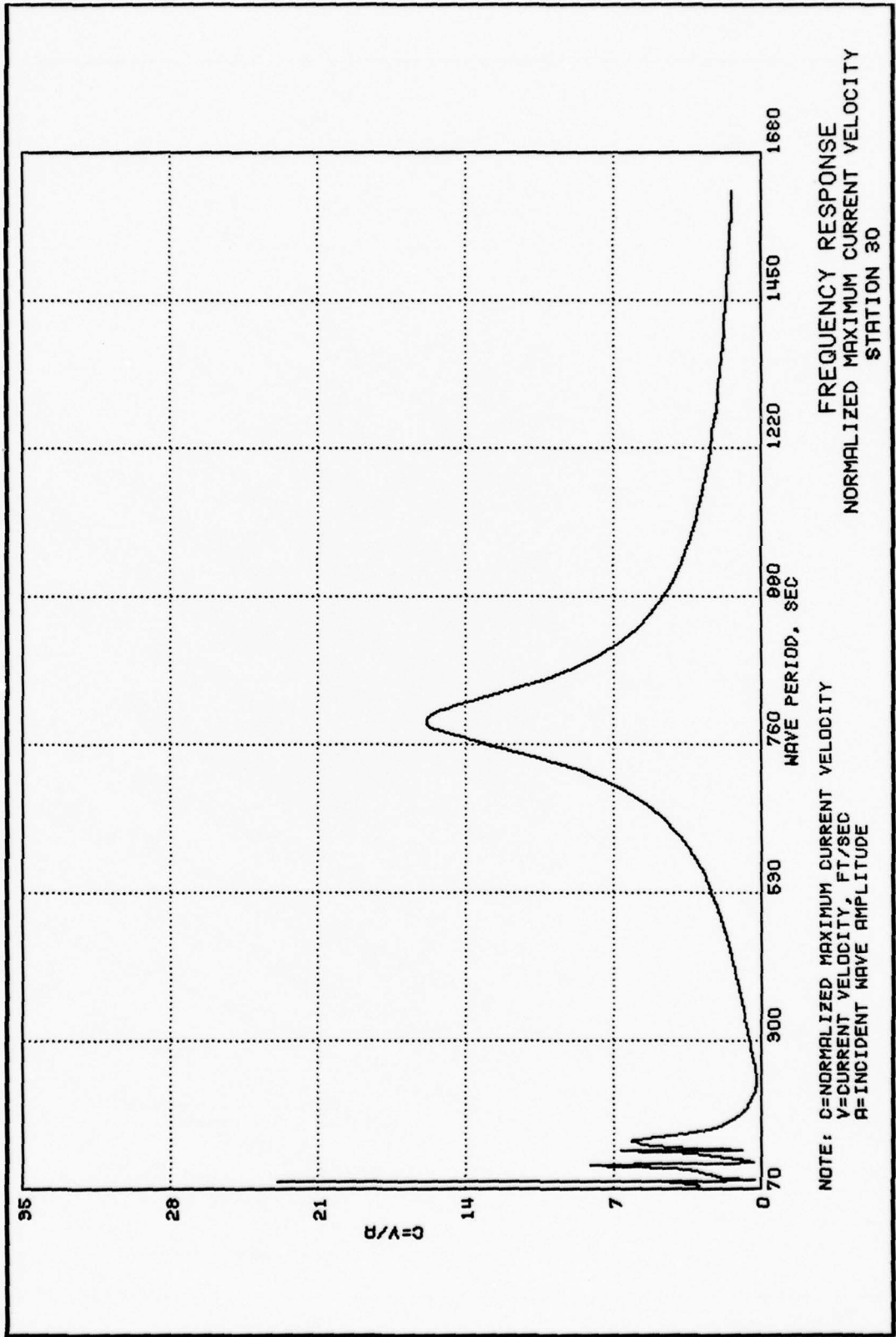


PLATE 122



FREQUENCY RESPONSE  
 NORMALIZED MAXIMUM CURRENT VELOCITY  
 STATION 30

NOTE: C=NORMALIZED MAXIMUM CURRENT VELOCITY  
 V=CURRENT VELOCITY, FT/SEC  
 A=INCIDENT WAVE AMPLITUDE

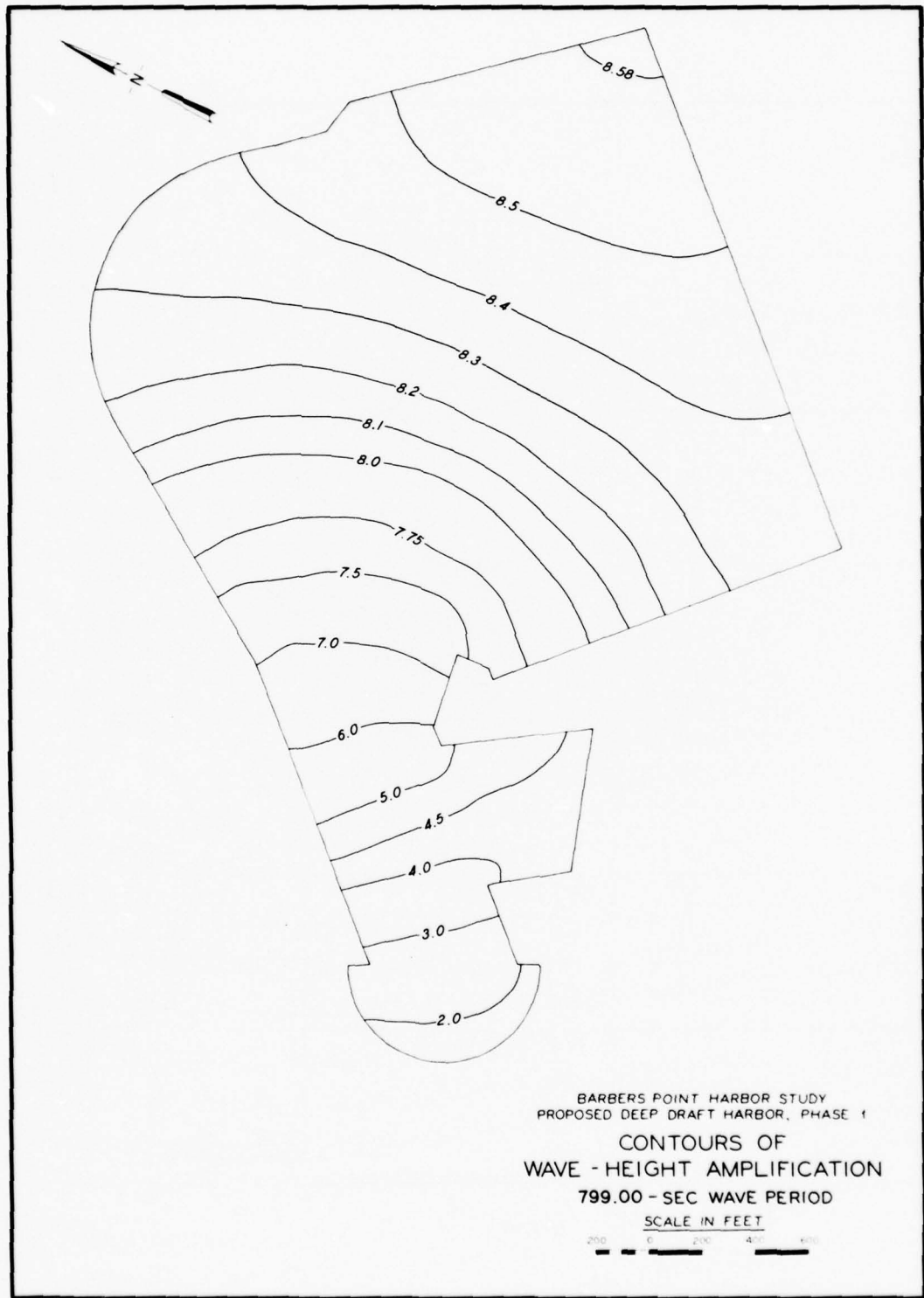
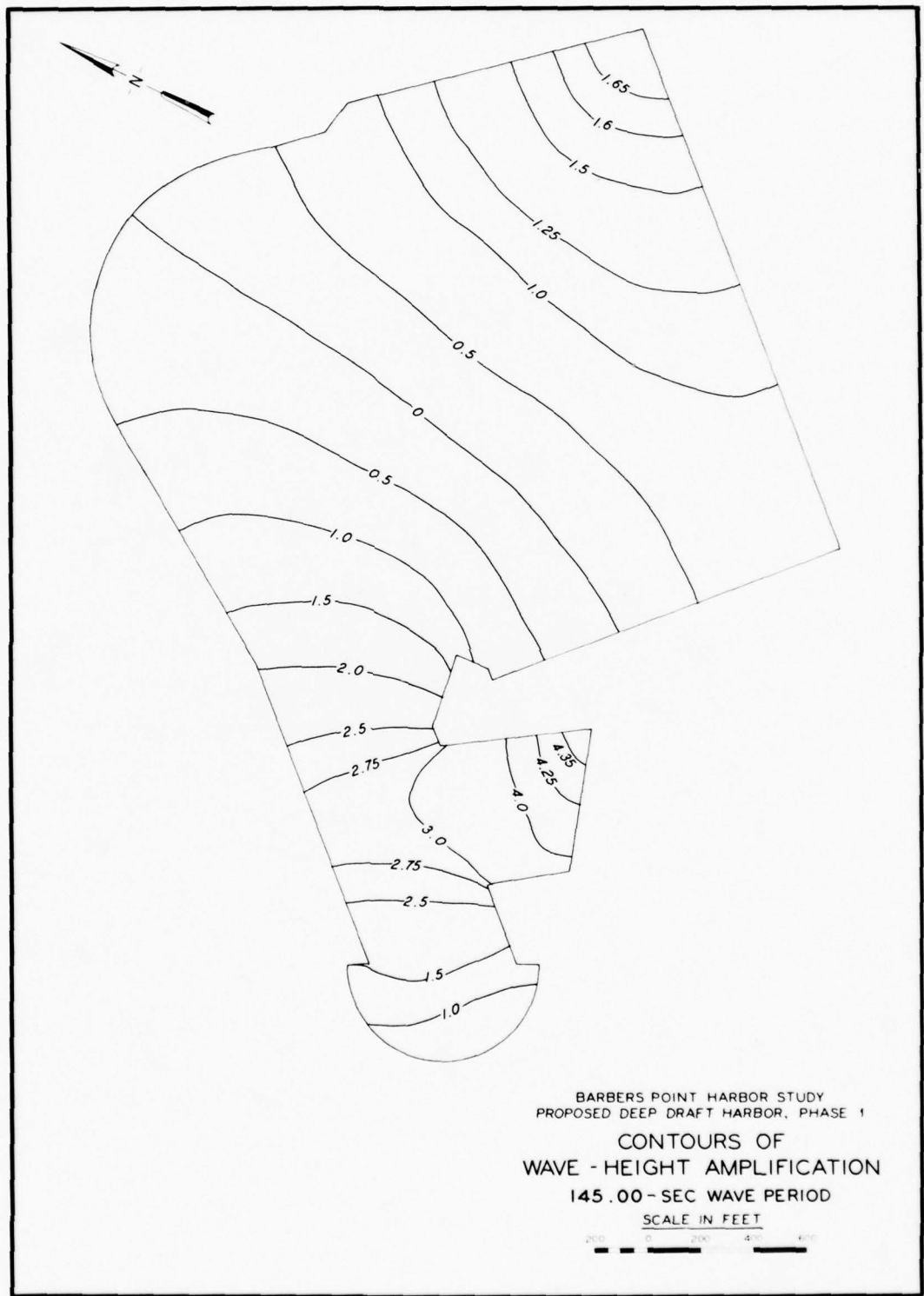


PLATE 124





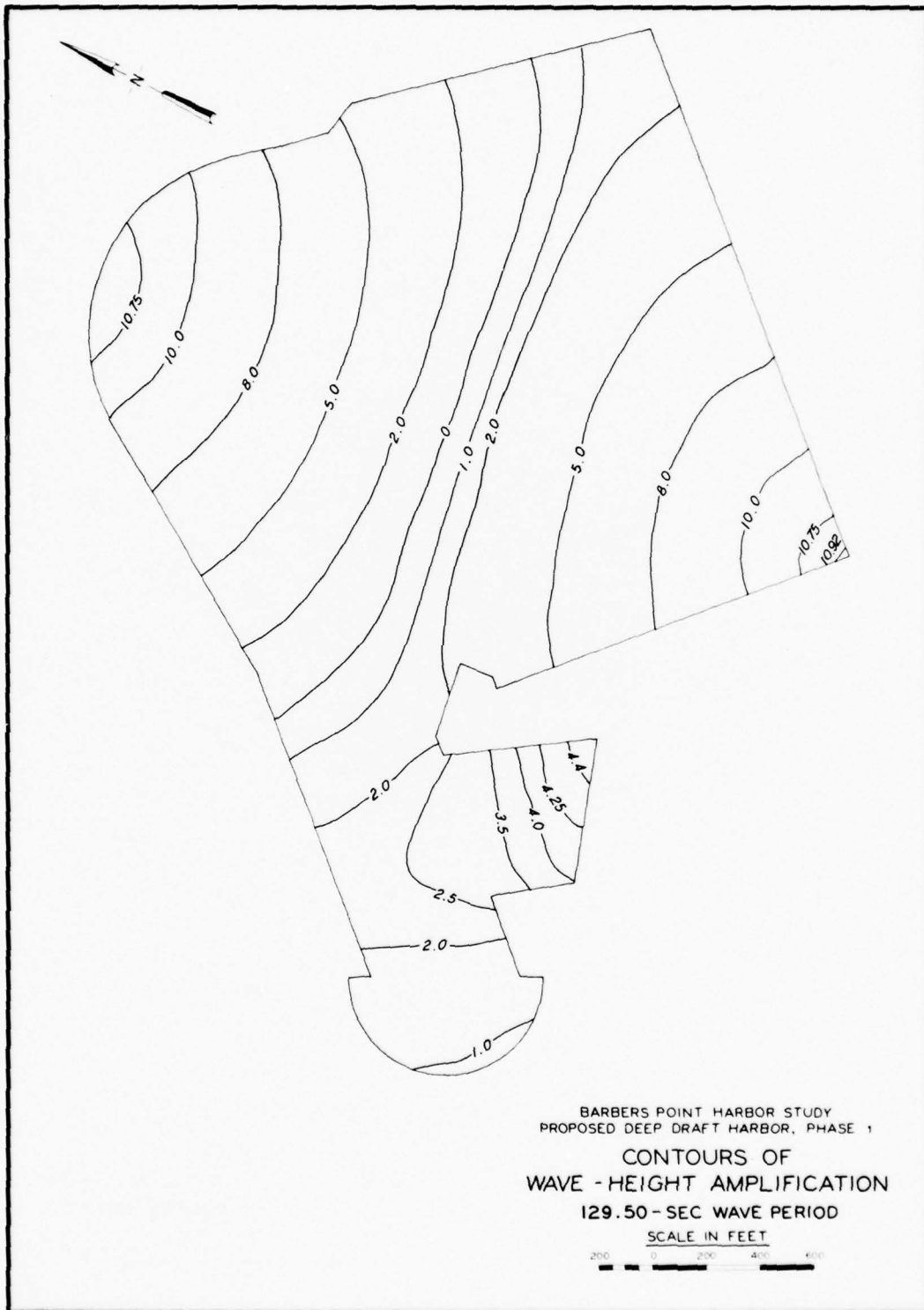
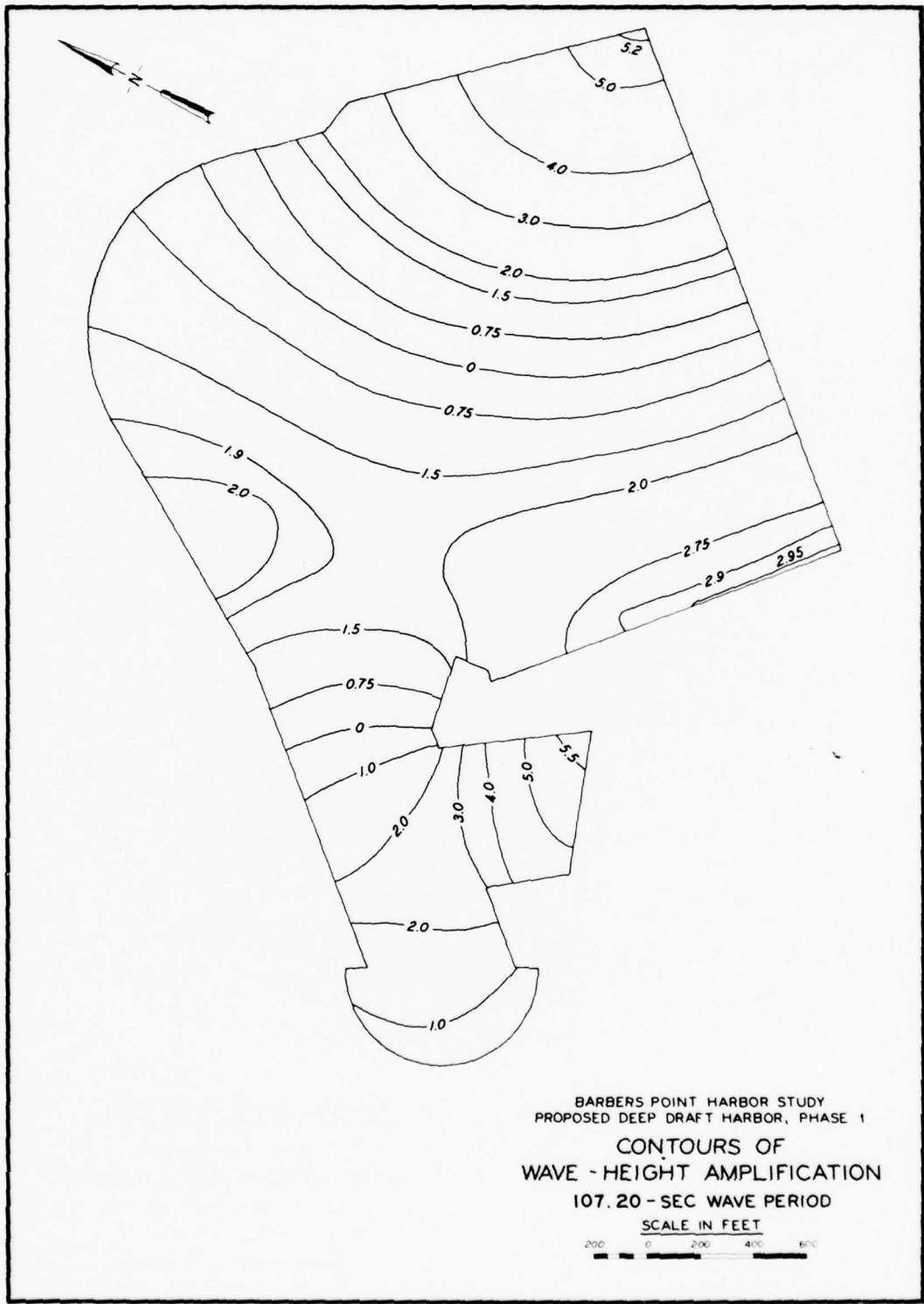


PLATE 126



BARBERS POINT HARBOR STUDY  
 PROPOSED DEEP DRAFT HARBOR, PHASE 1

CONTOURS OF  
 WAVE - HEIGHT AMPLIFICATION  
 107.20 - SEC WAVE PERIOD

SCALE IN FEET  
 200 0 200 400 600

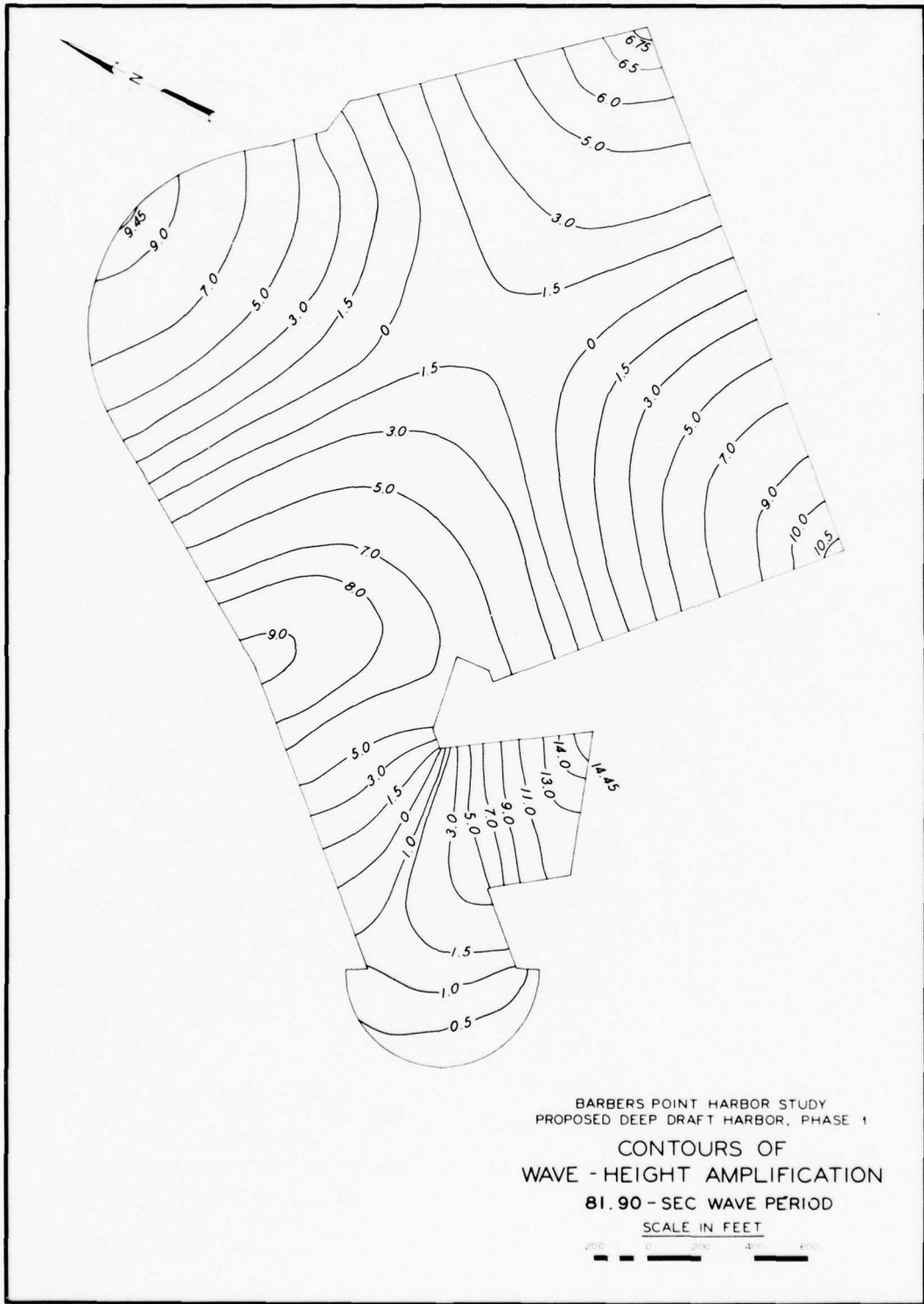
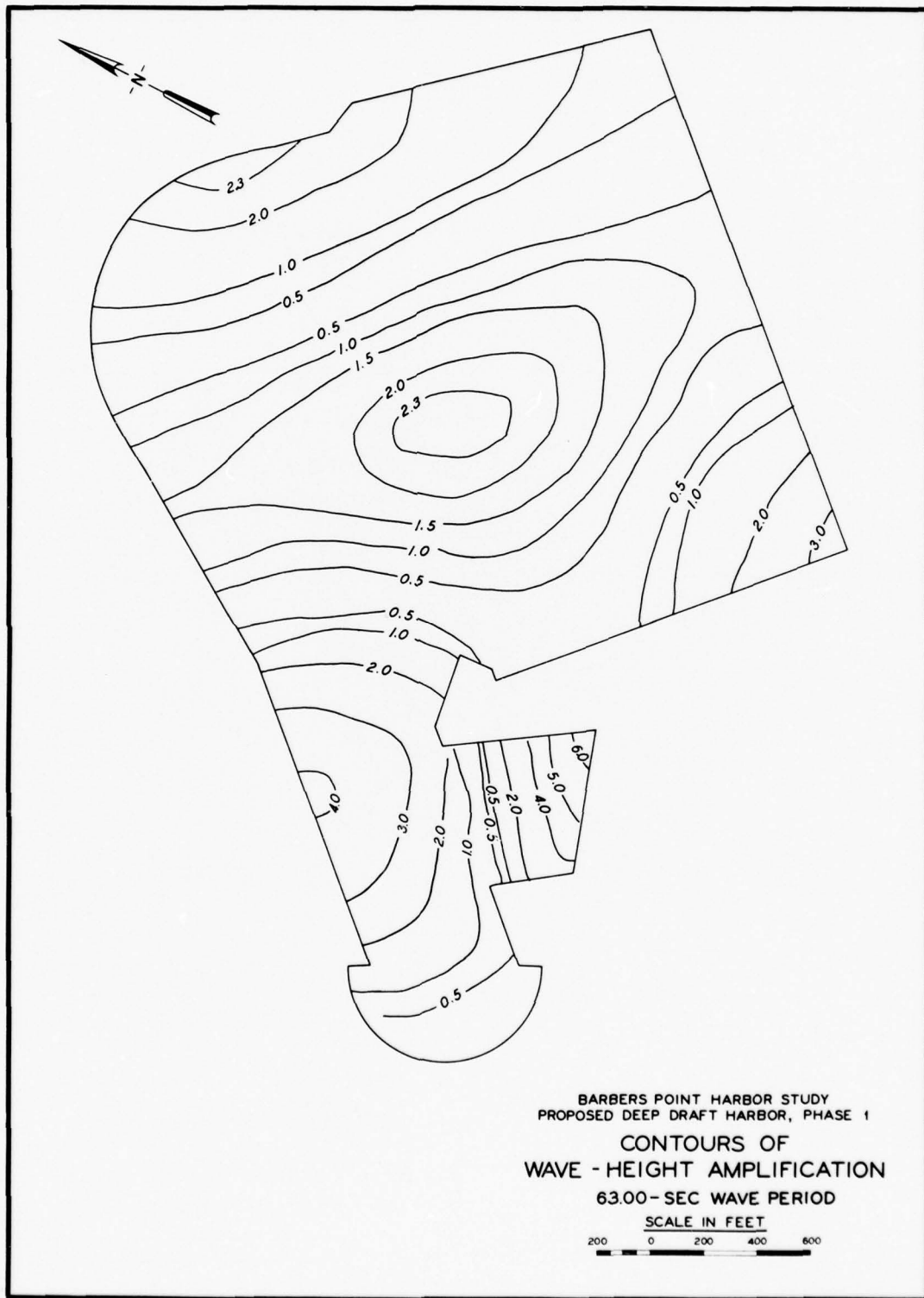


PLATE 128



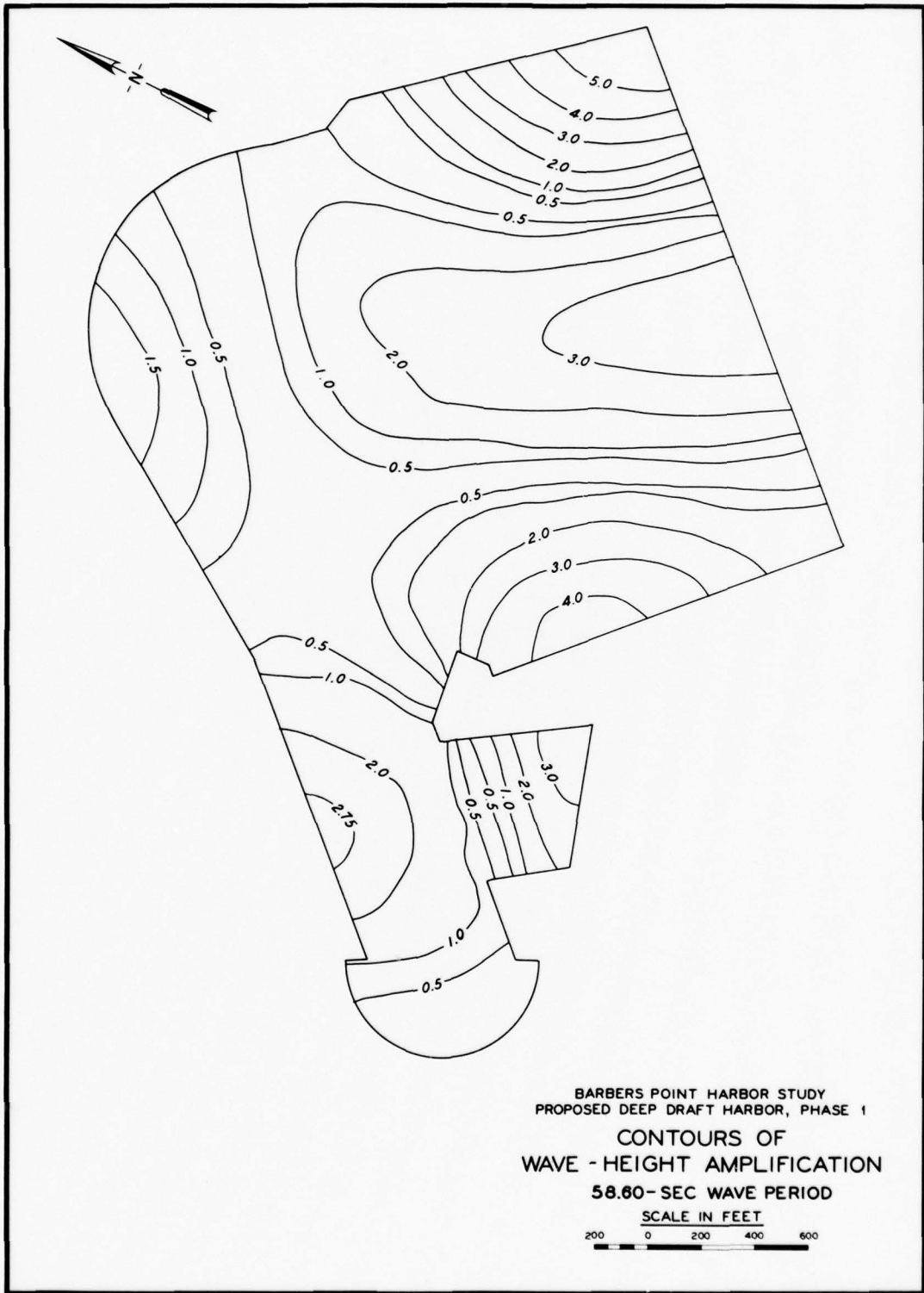
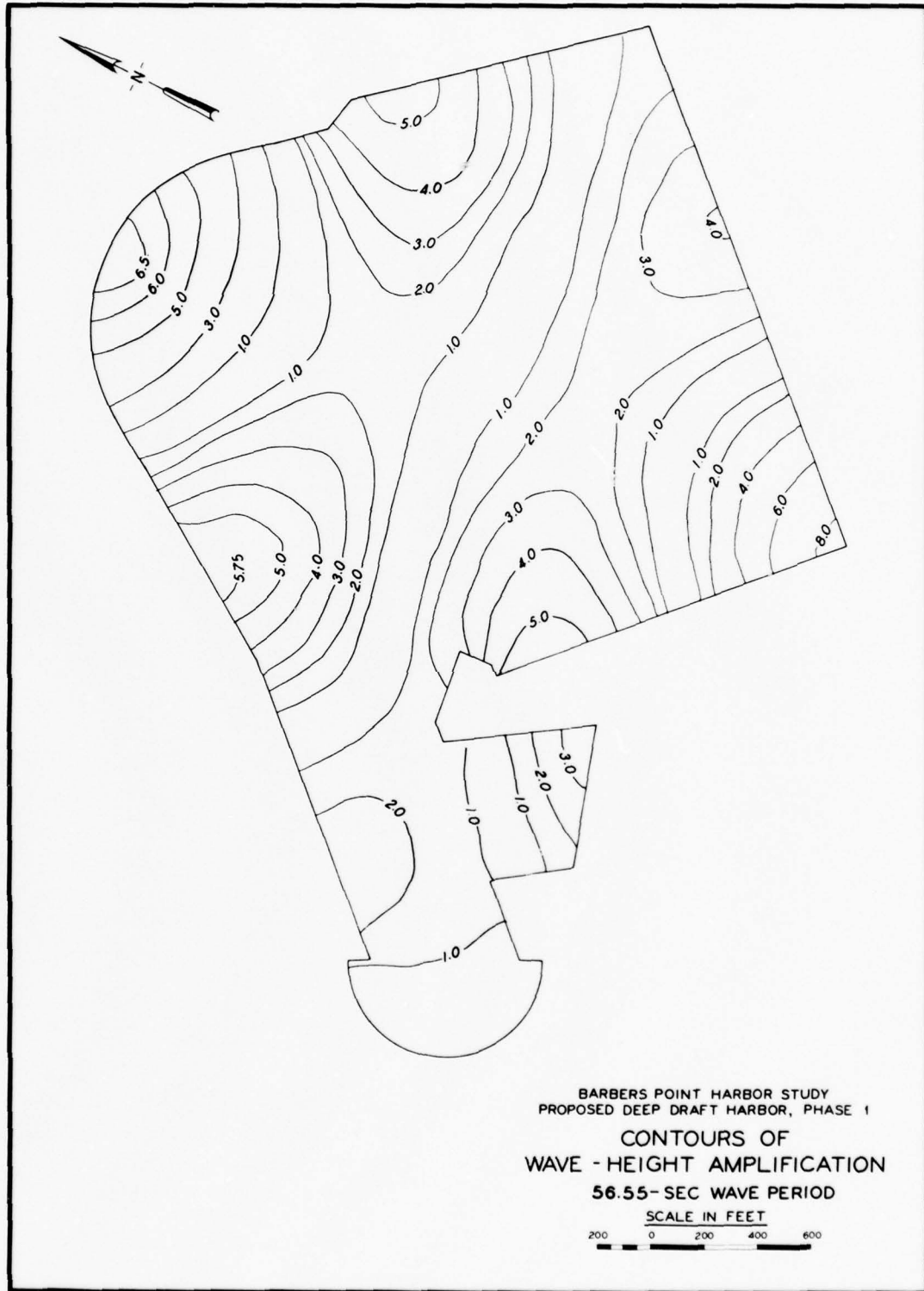


PLATE 130



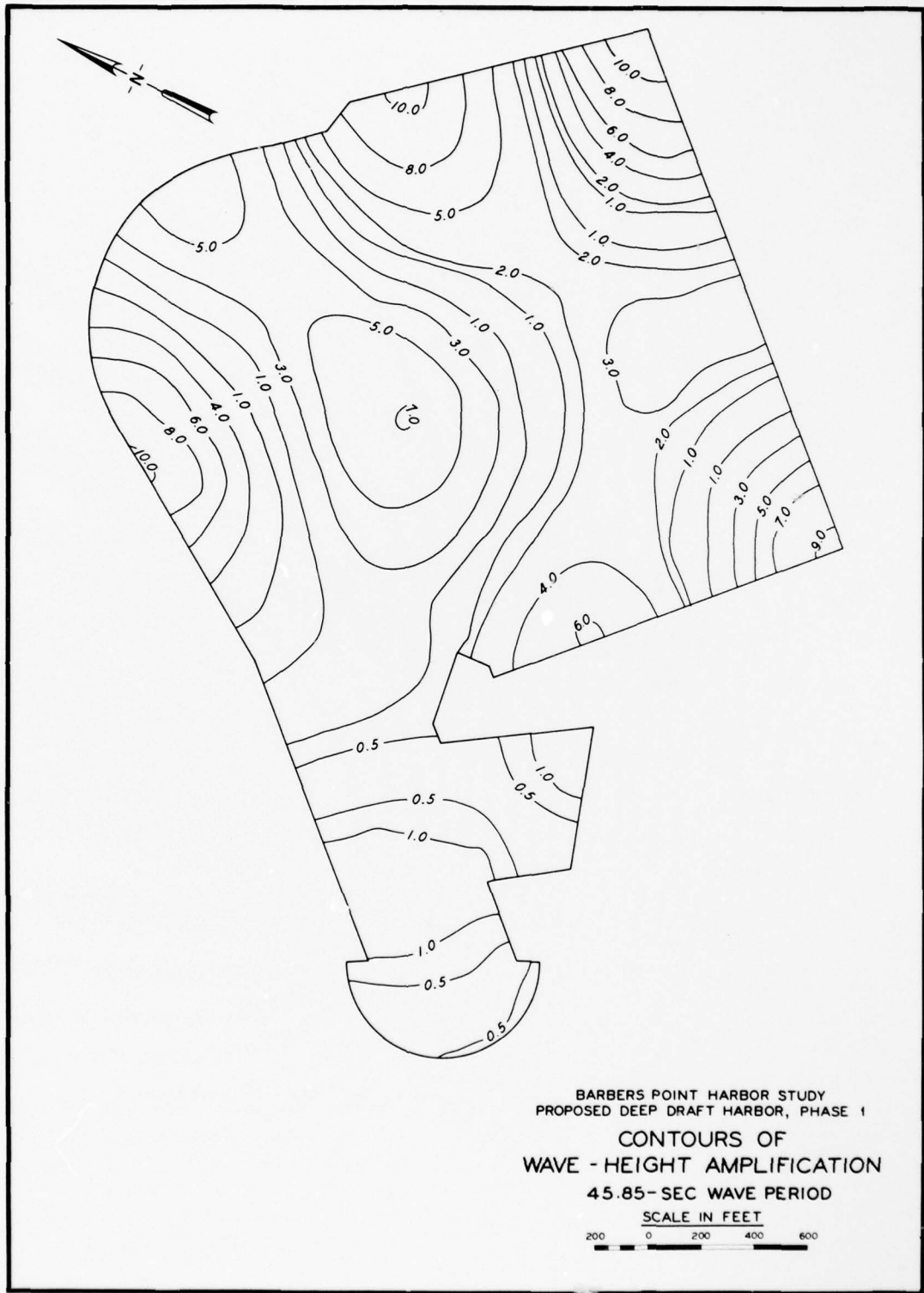
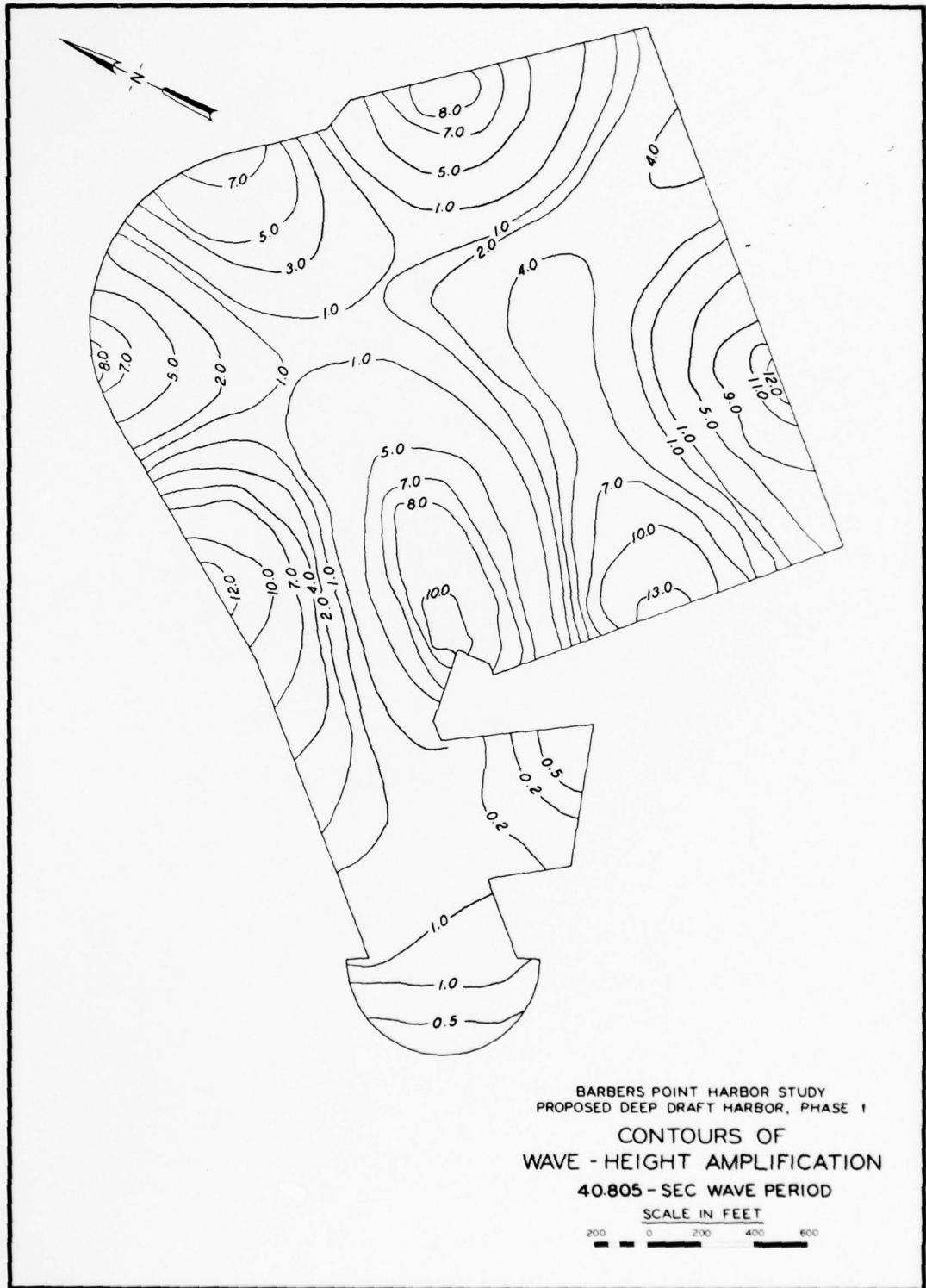


PLATE 132





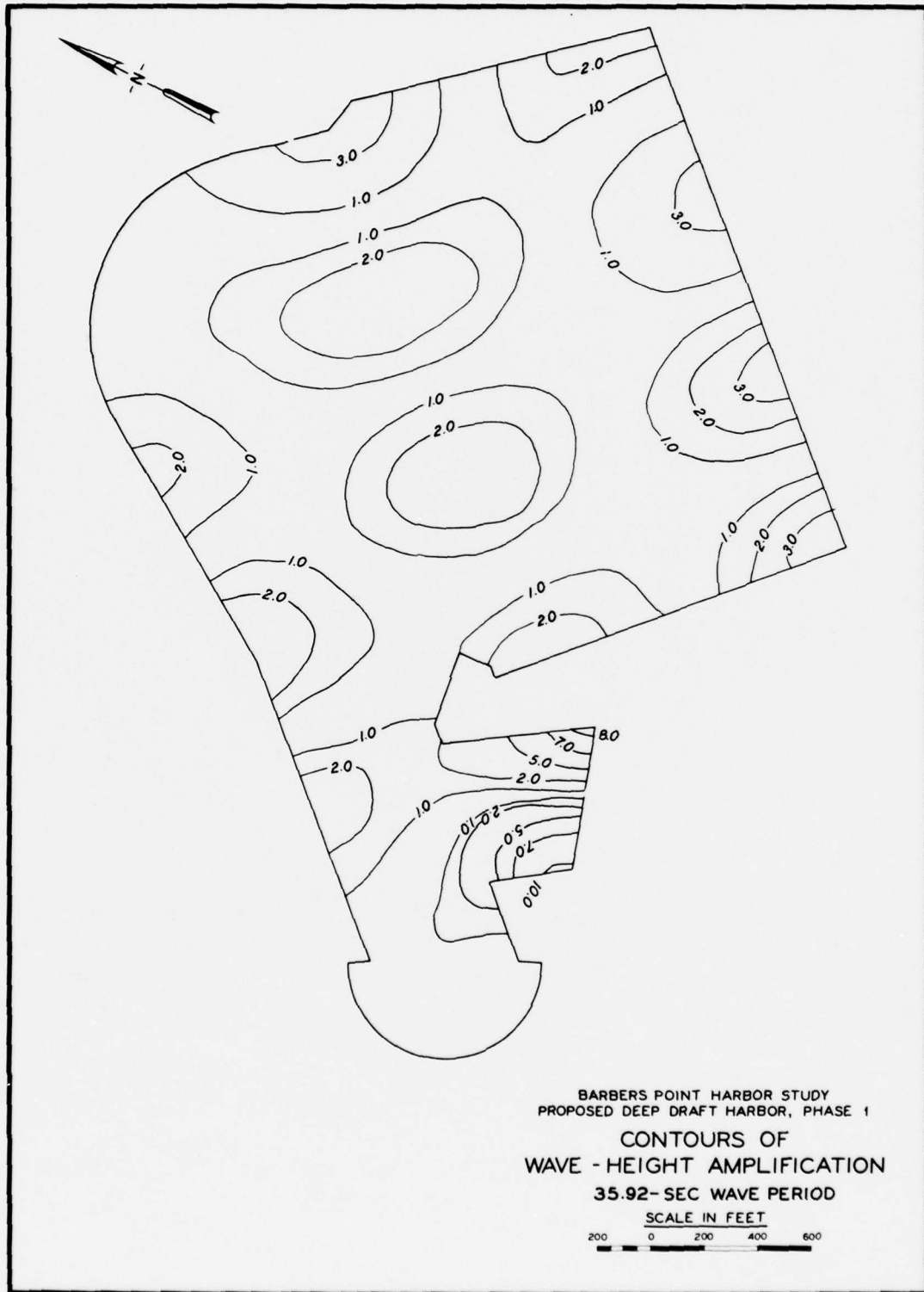
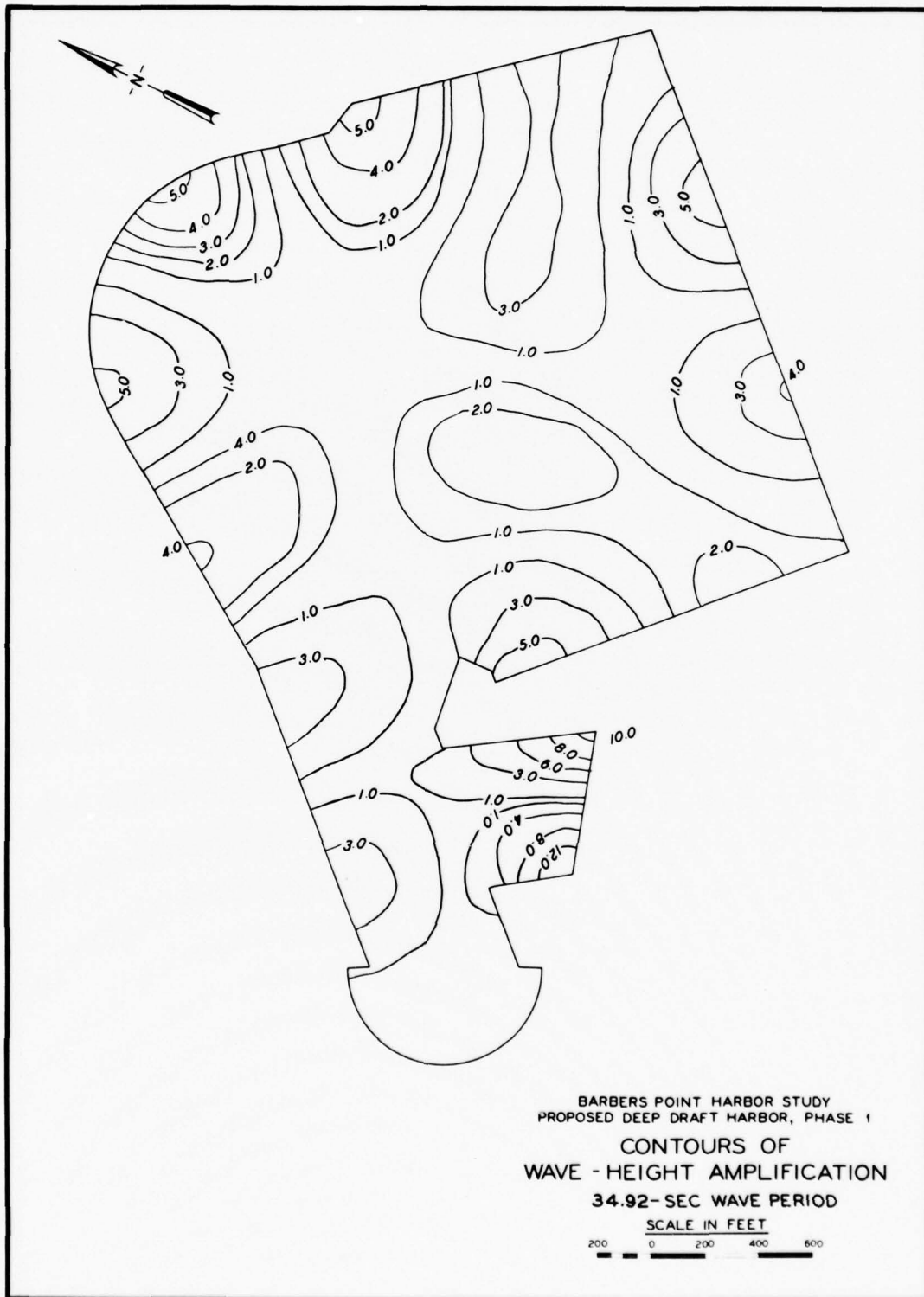


PLATE 134



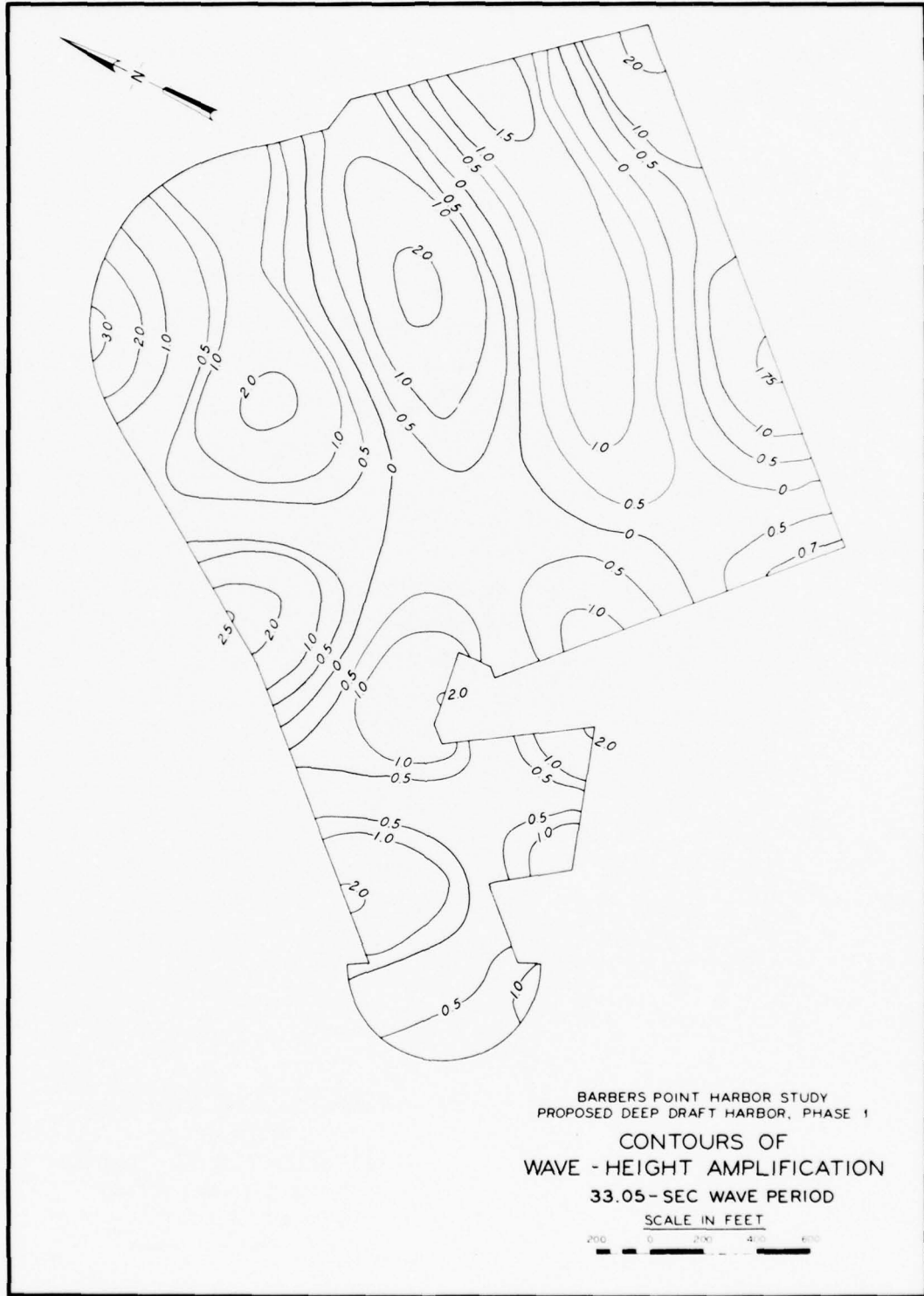
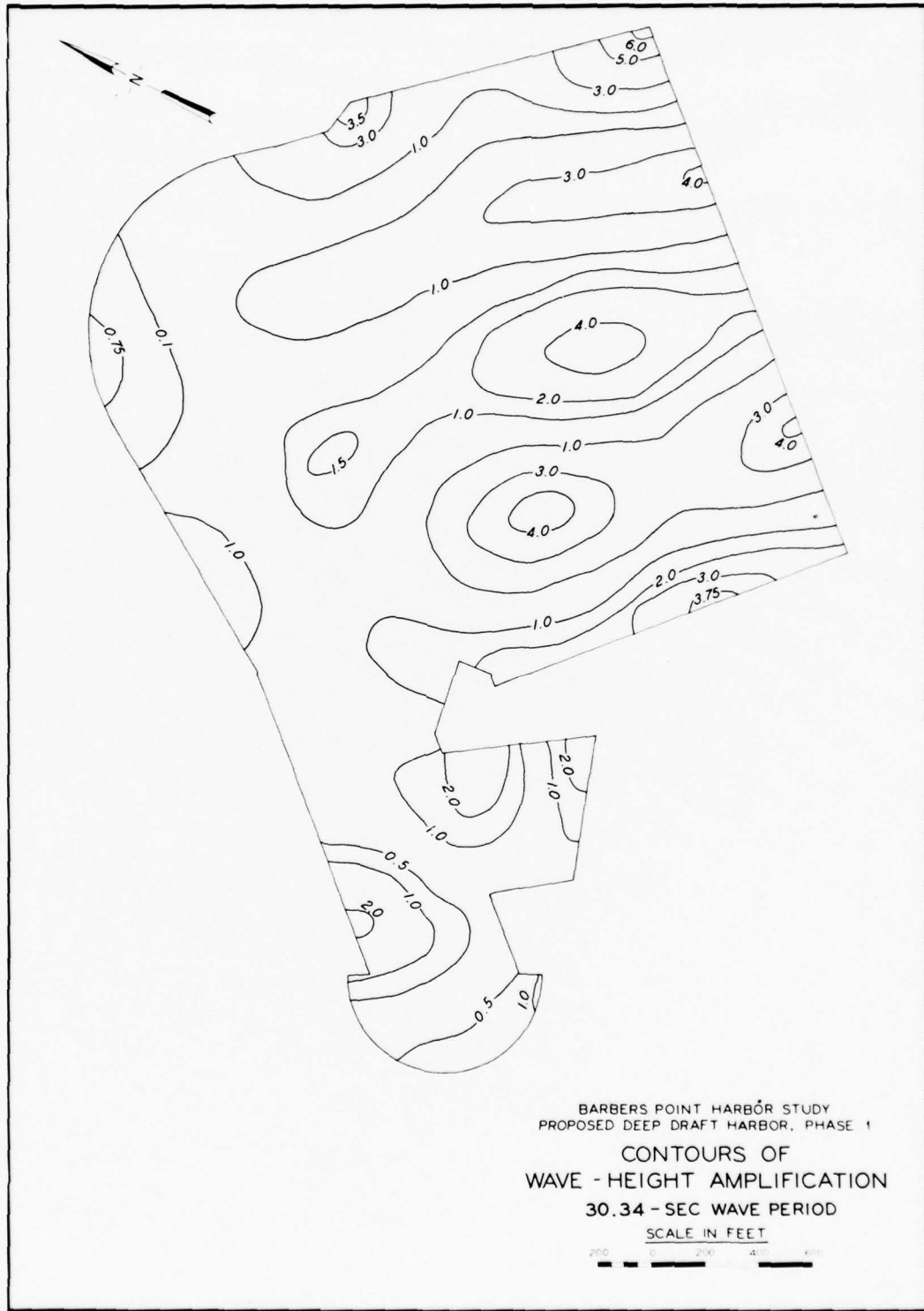


PLATE 136



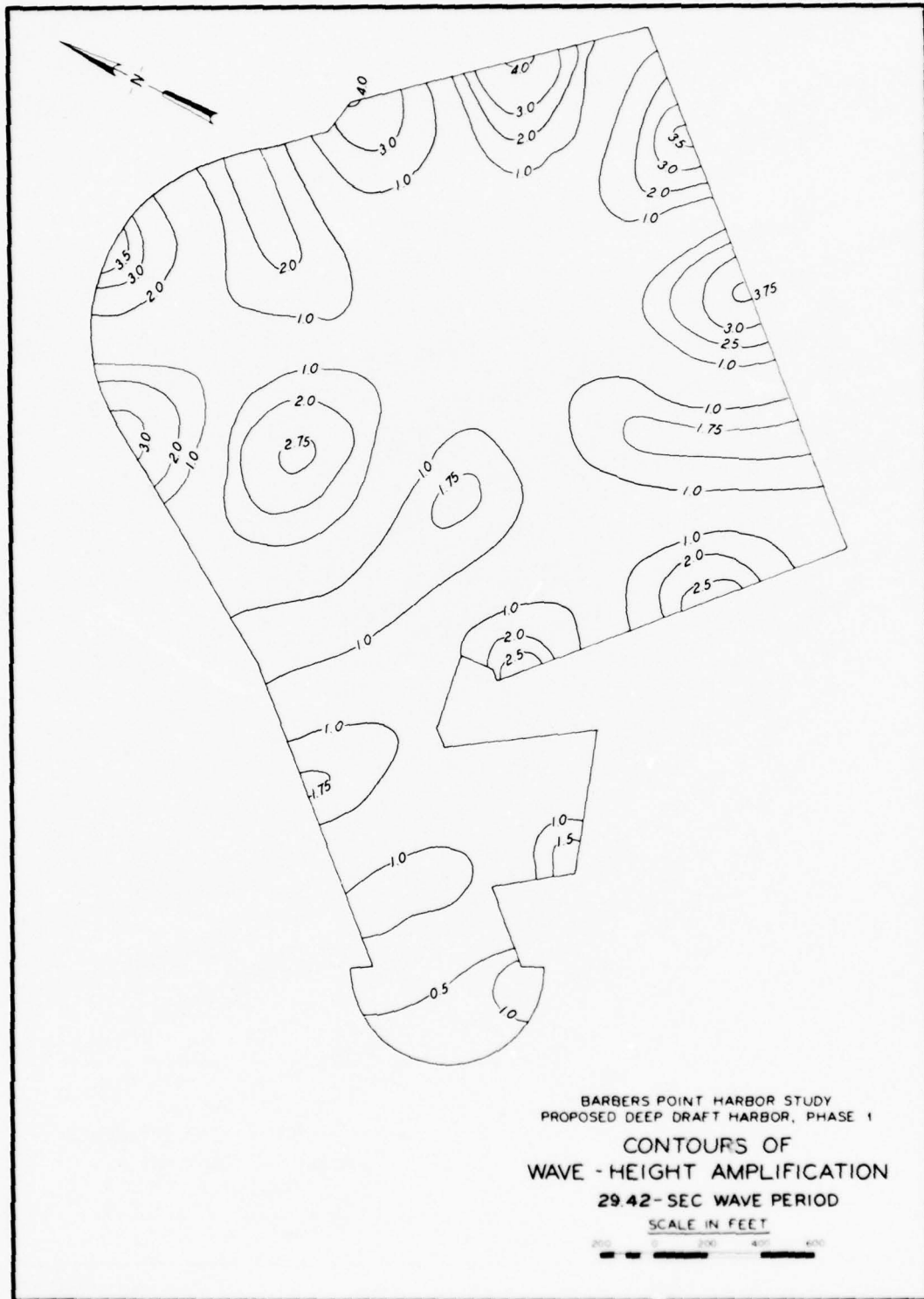
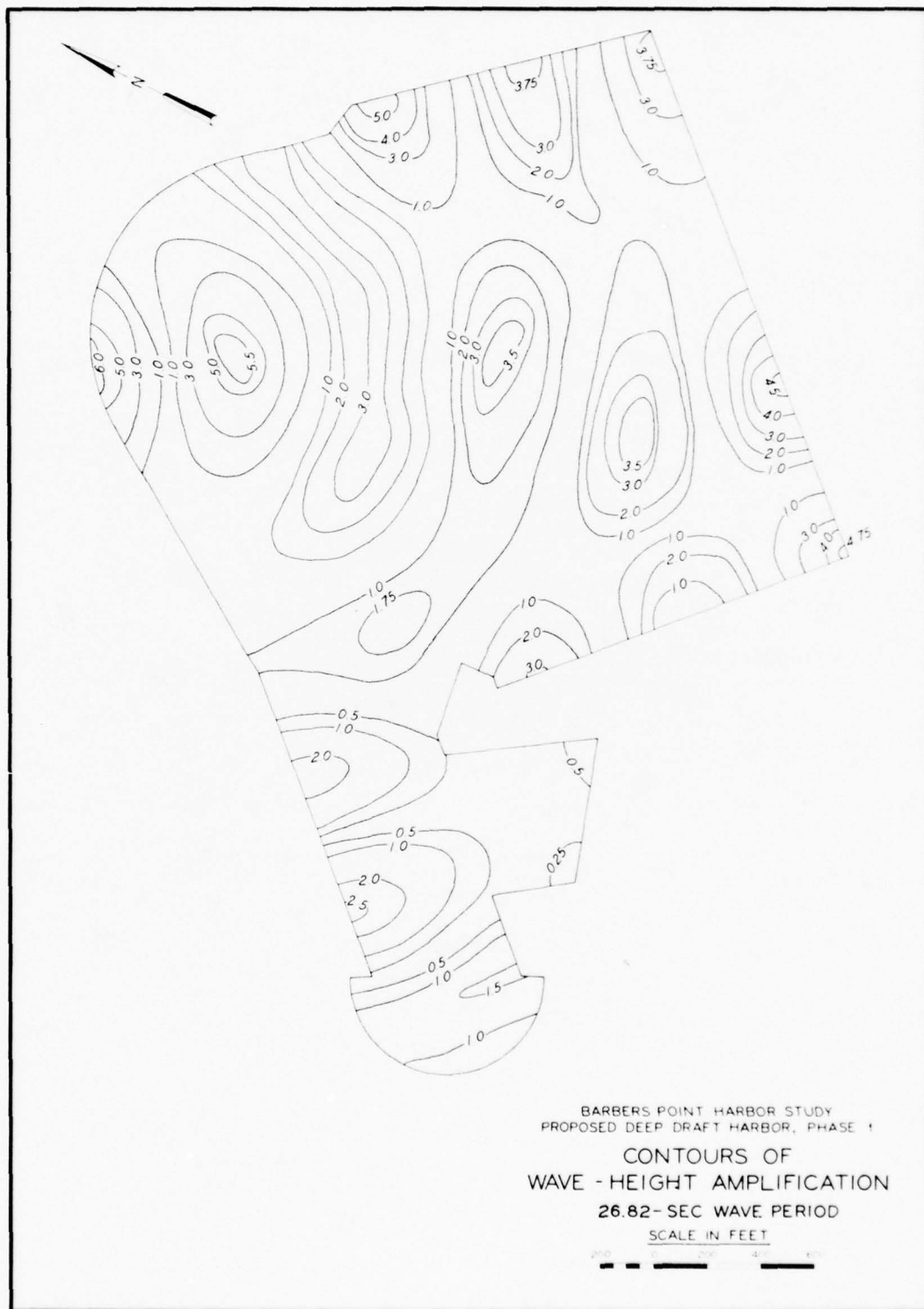


PLATE 138



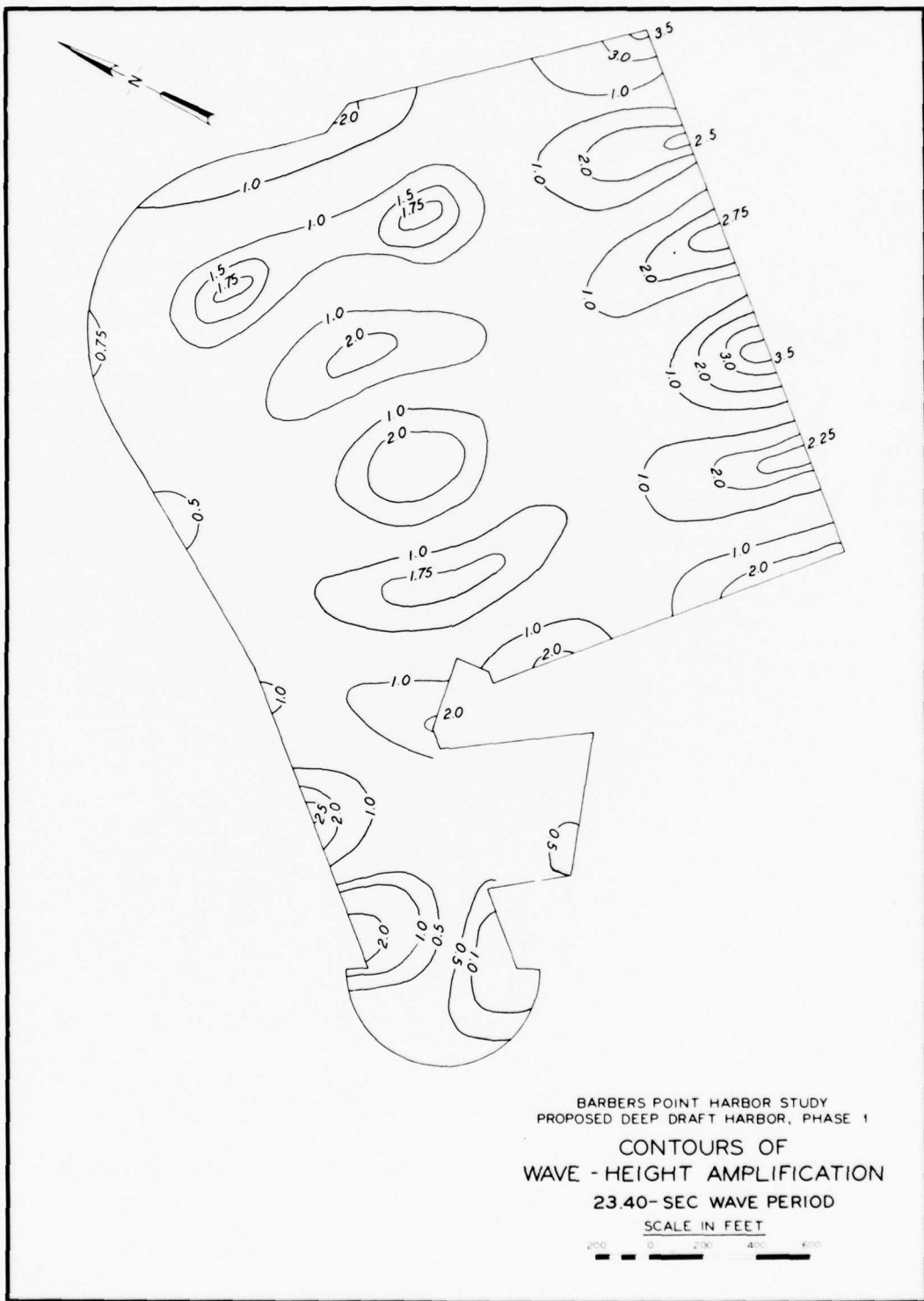
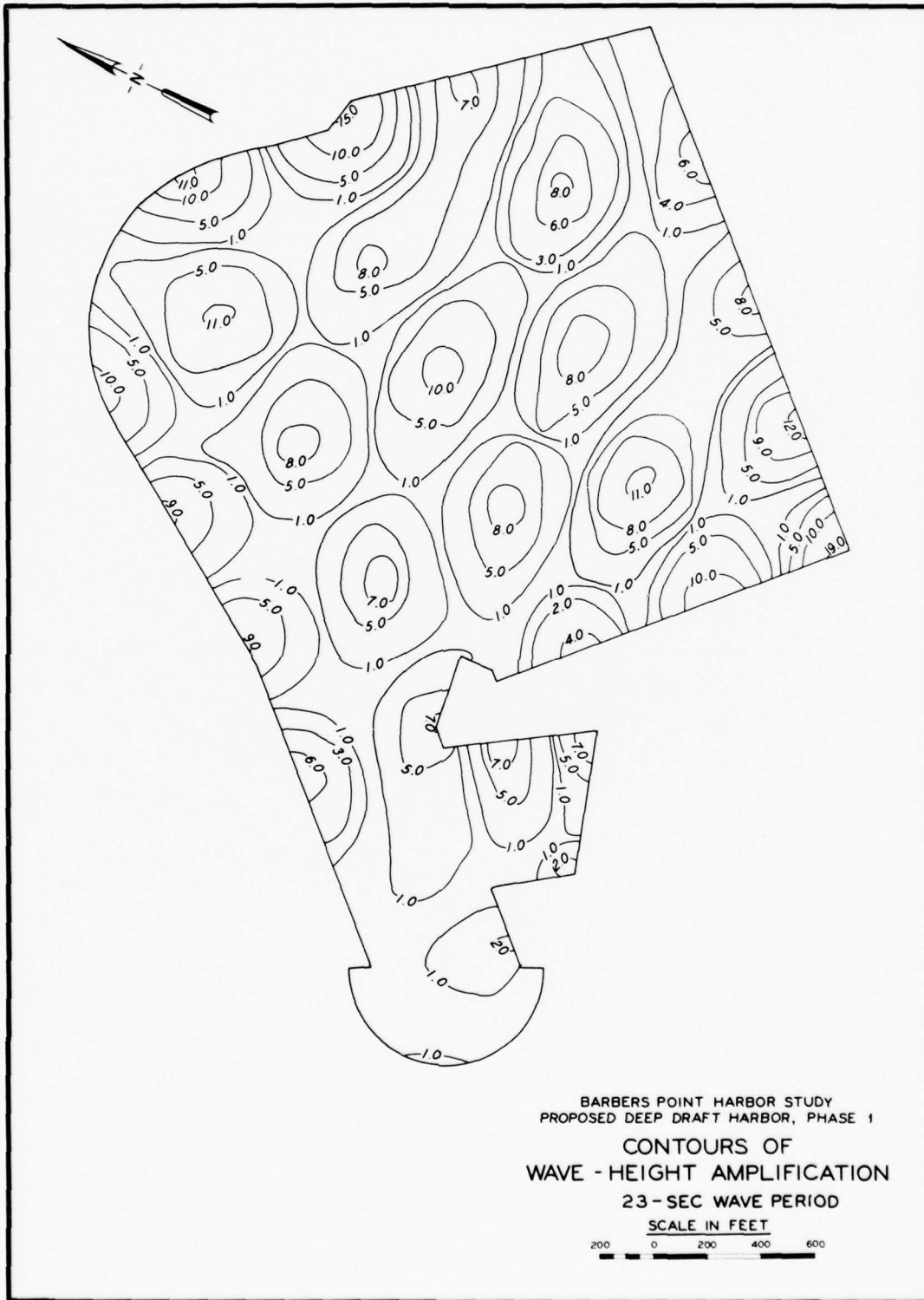


PLATE 140





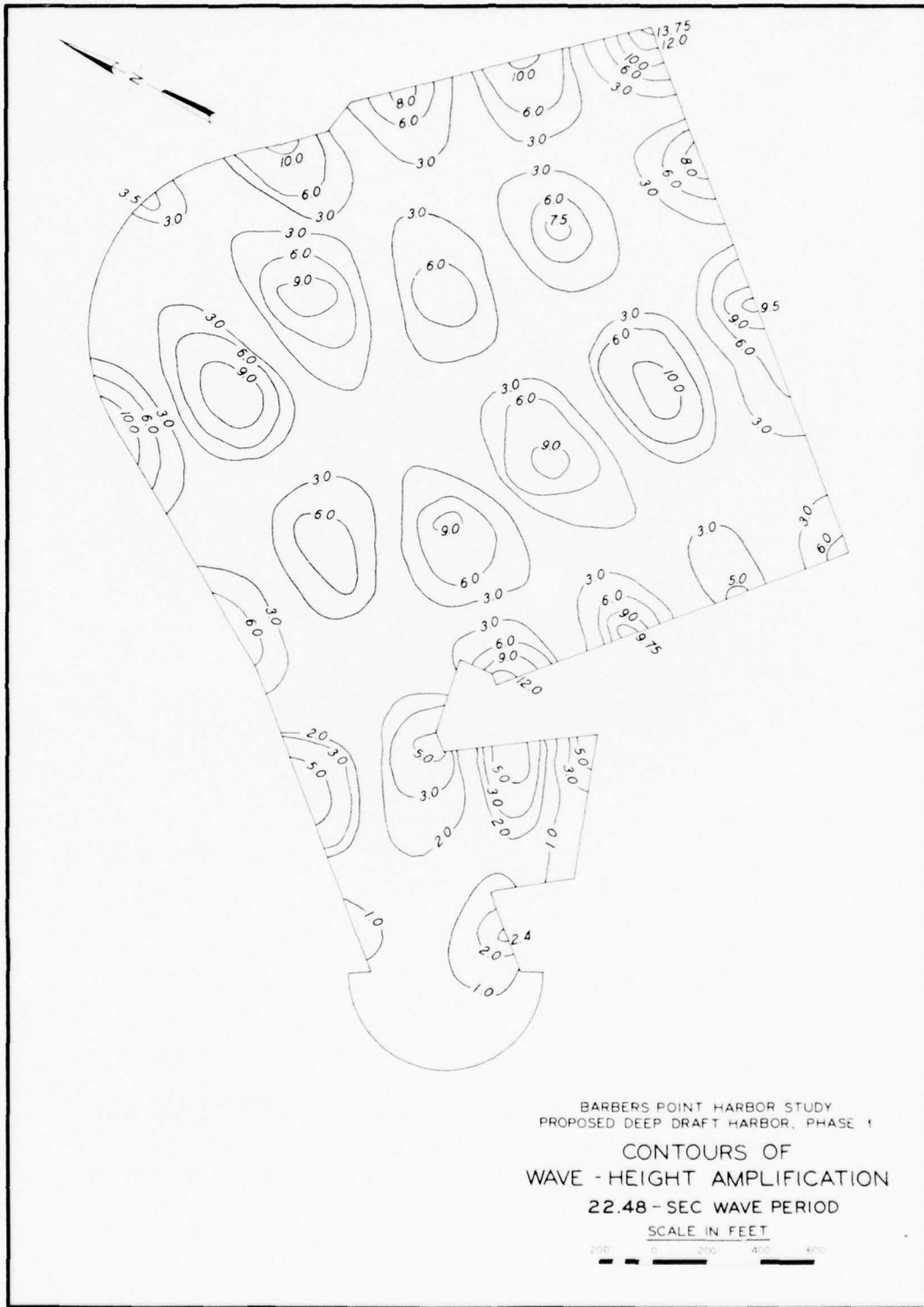
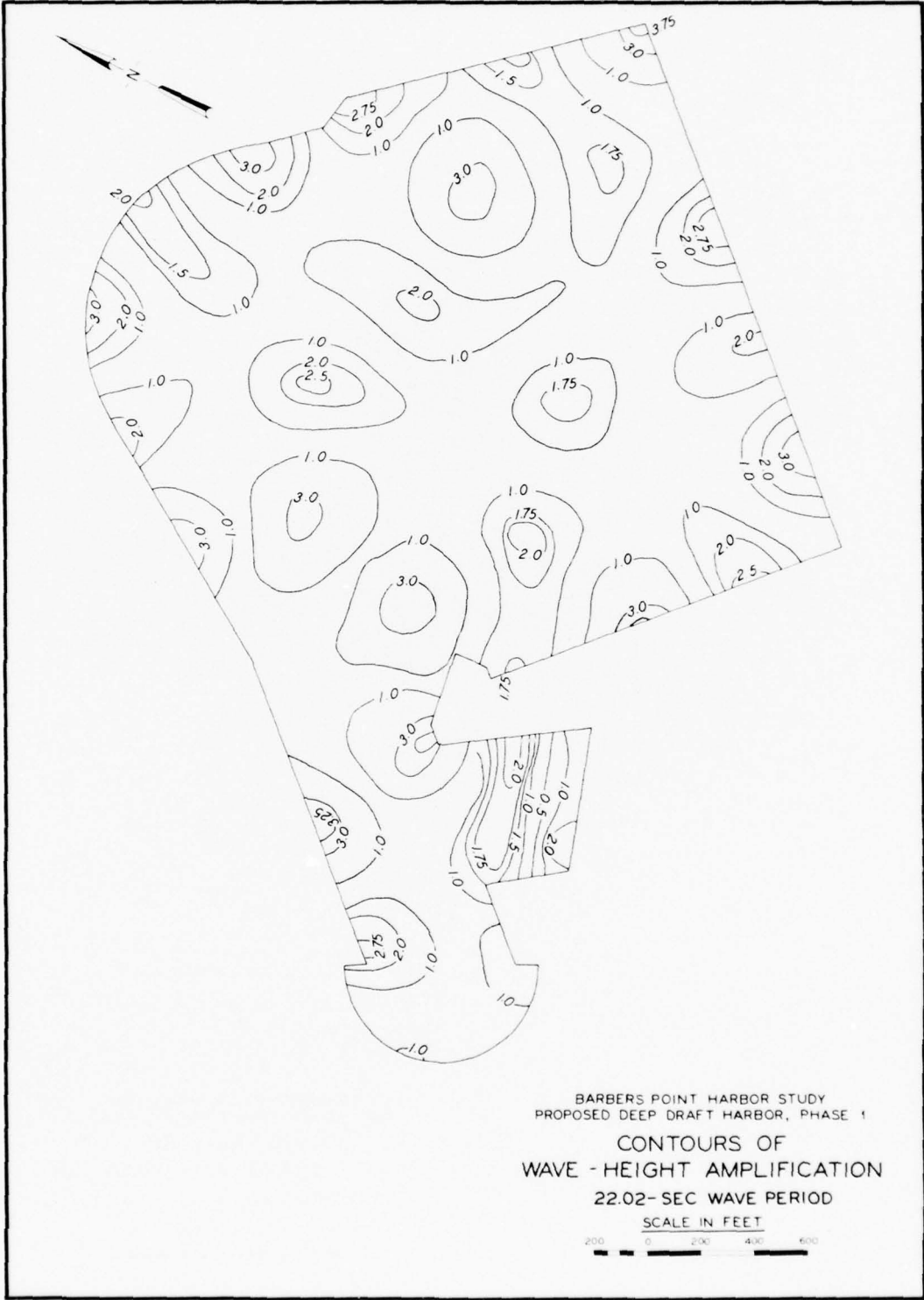


PLATE 142



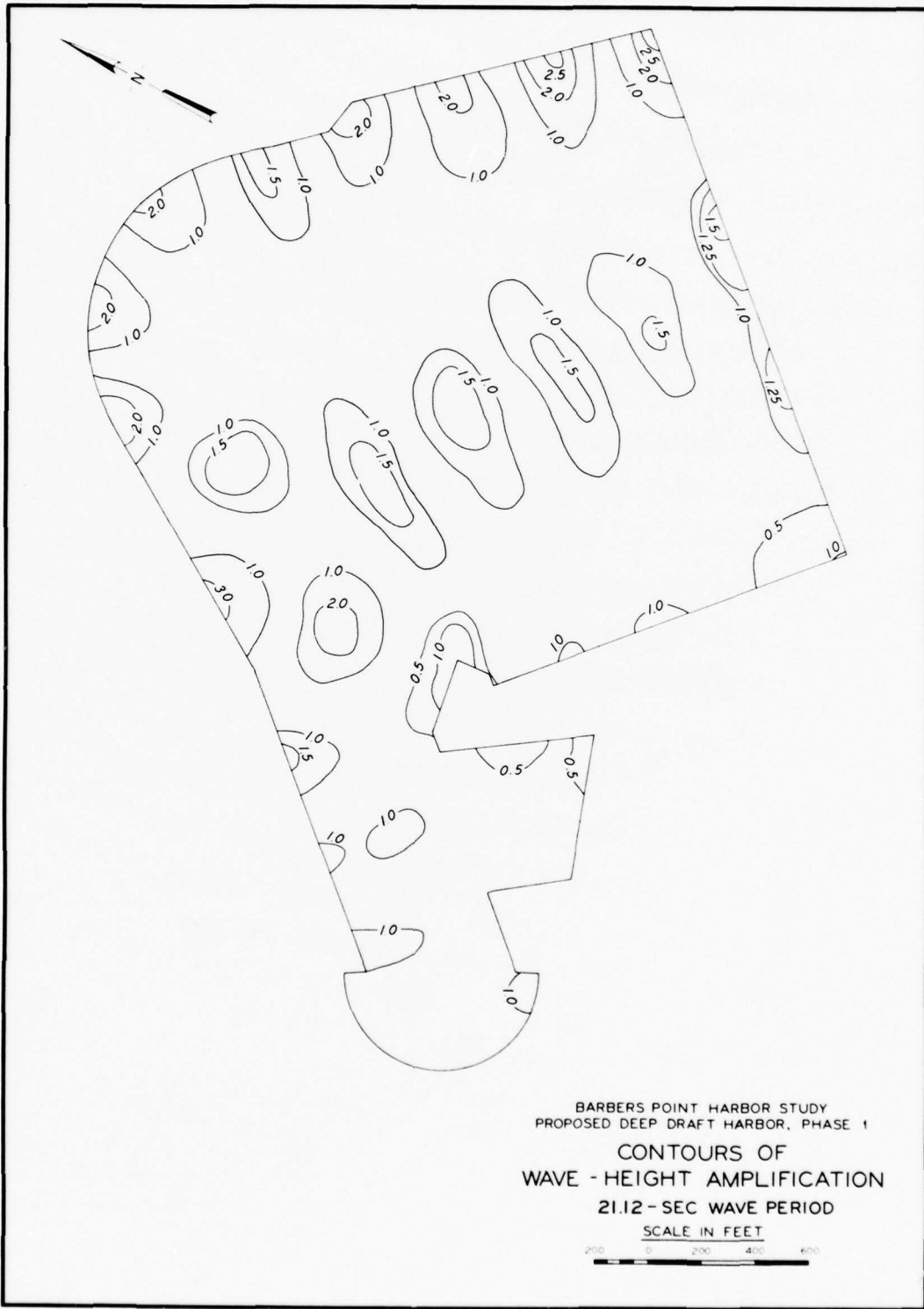


PLATE 144

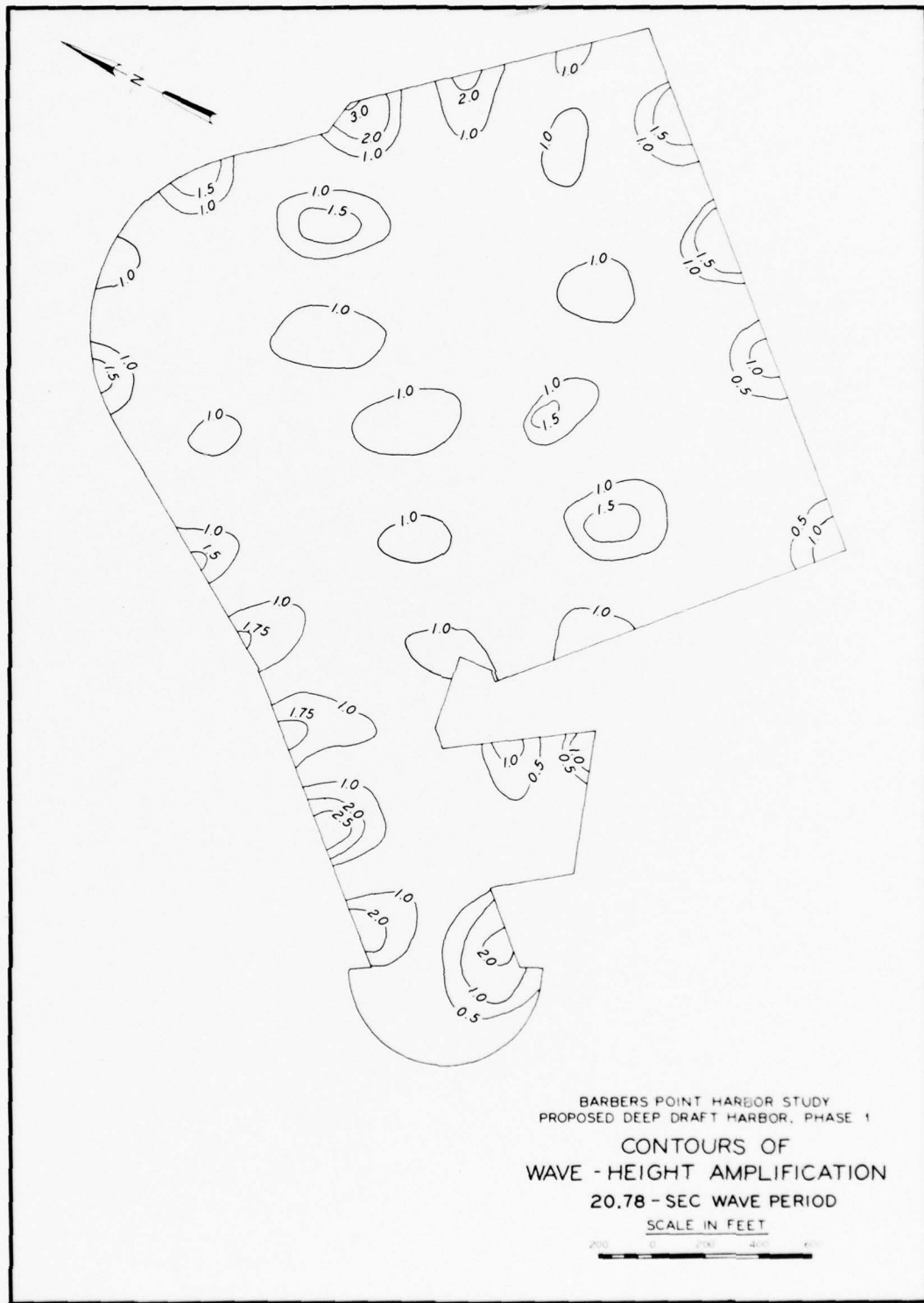


PLATE 145

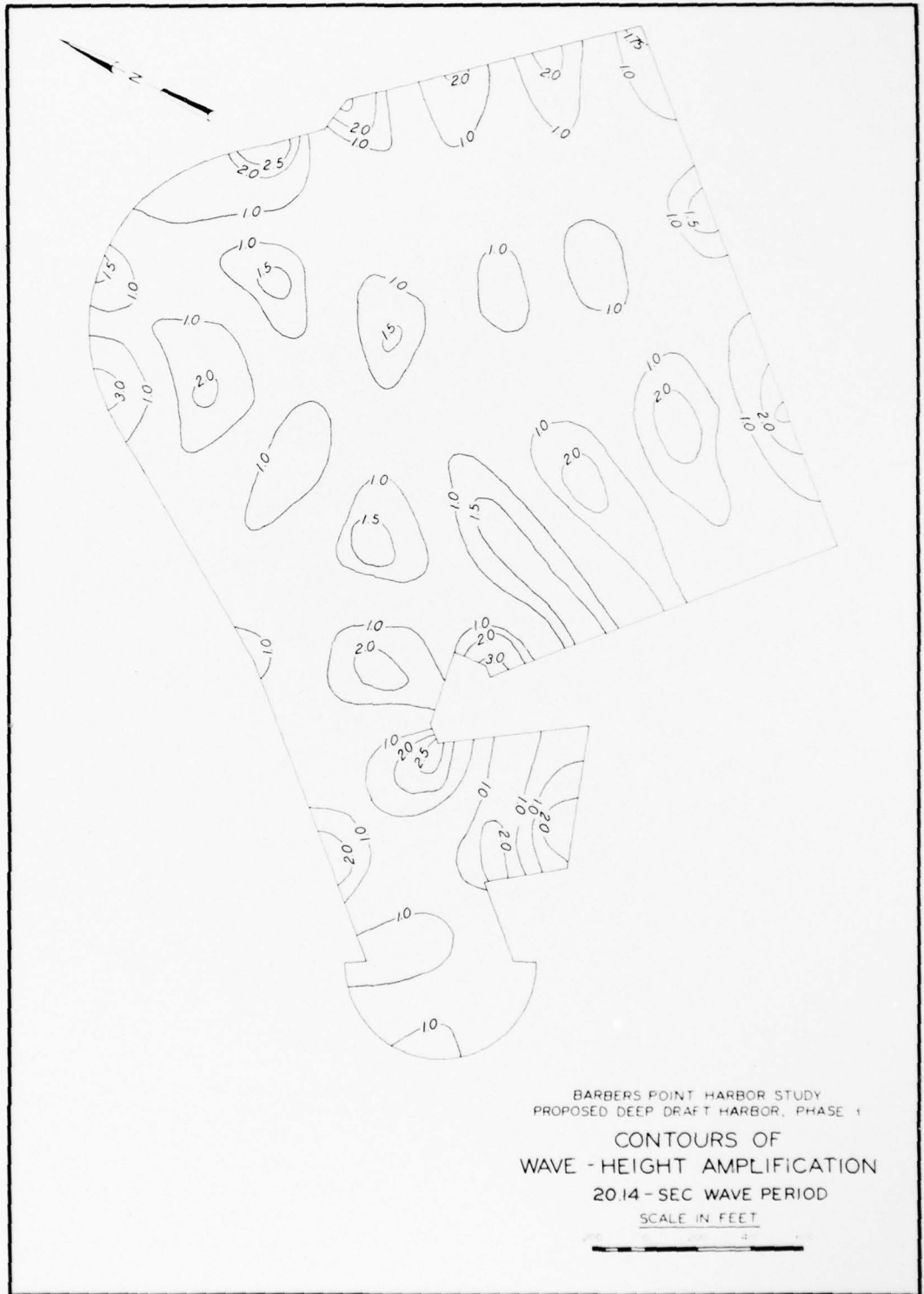
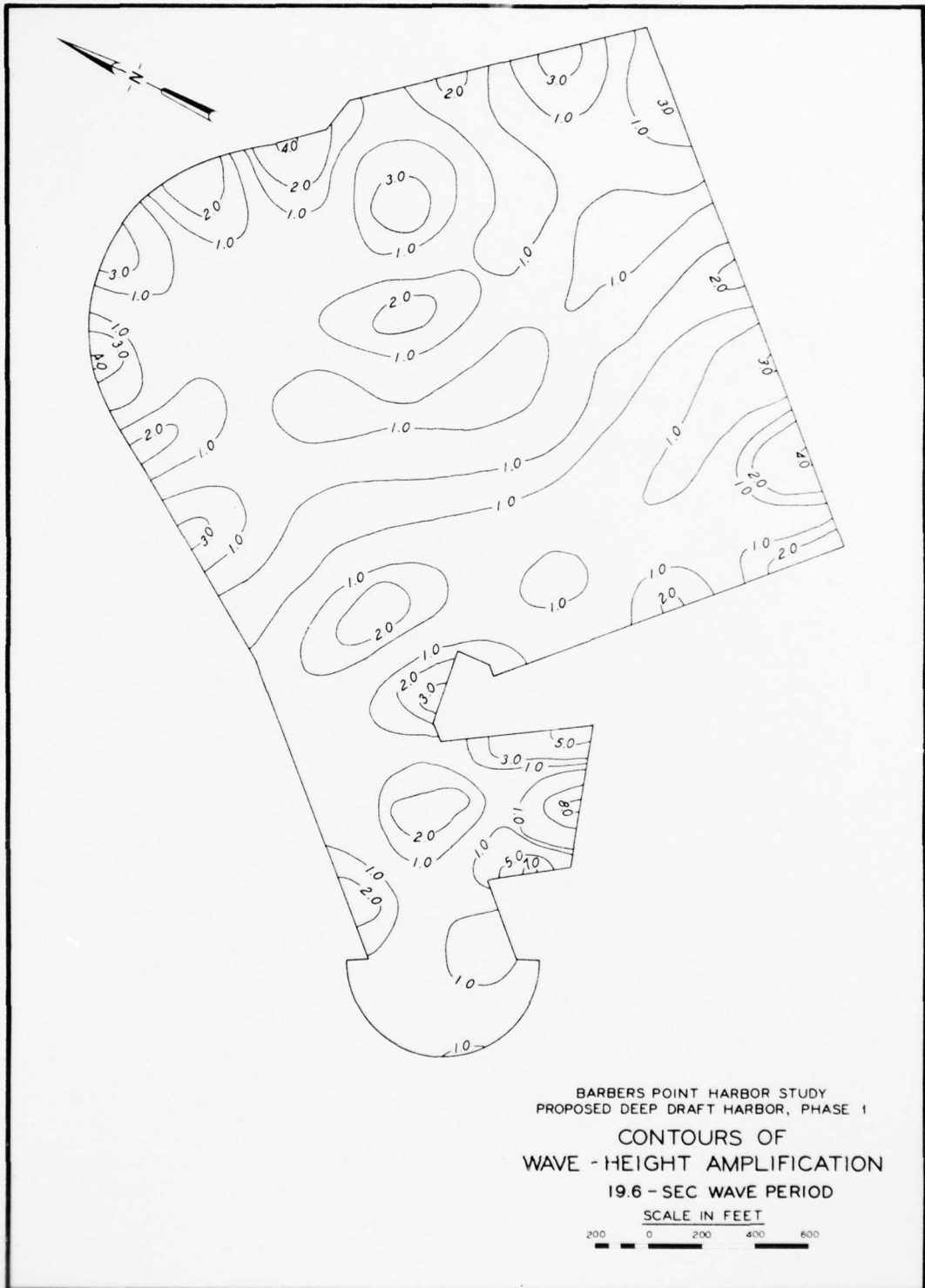
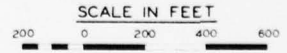


PLATE 146



BARBERS POINT HARBOR STUDY  
PROPOSED DEEP DRAFT HARBOR, PHASE I  
CONTOURS OF  
WAVE - HEIGHT AMPLIFICATION  
19.6 - SEC WAVE PERIOD  
SCALE IN FEET



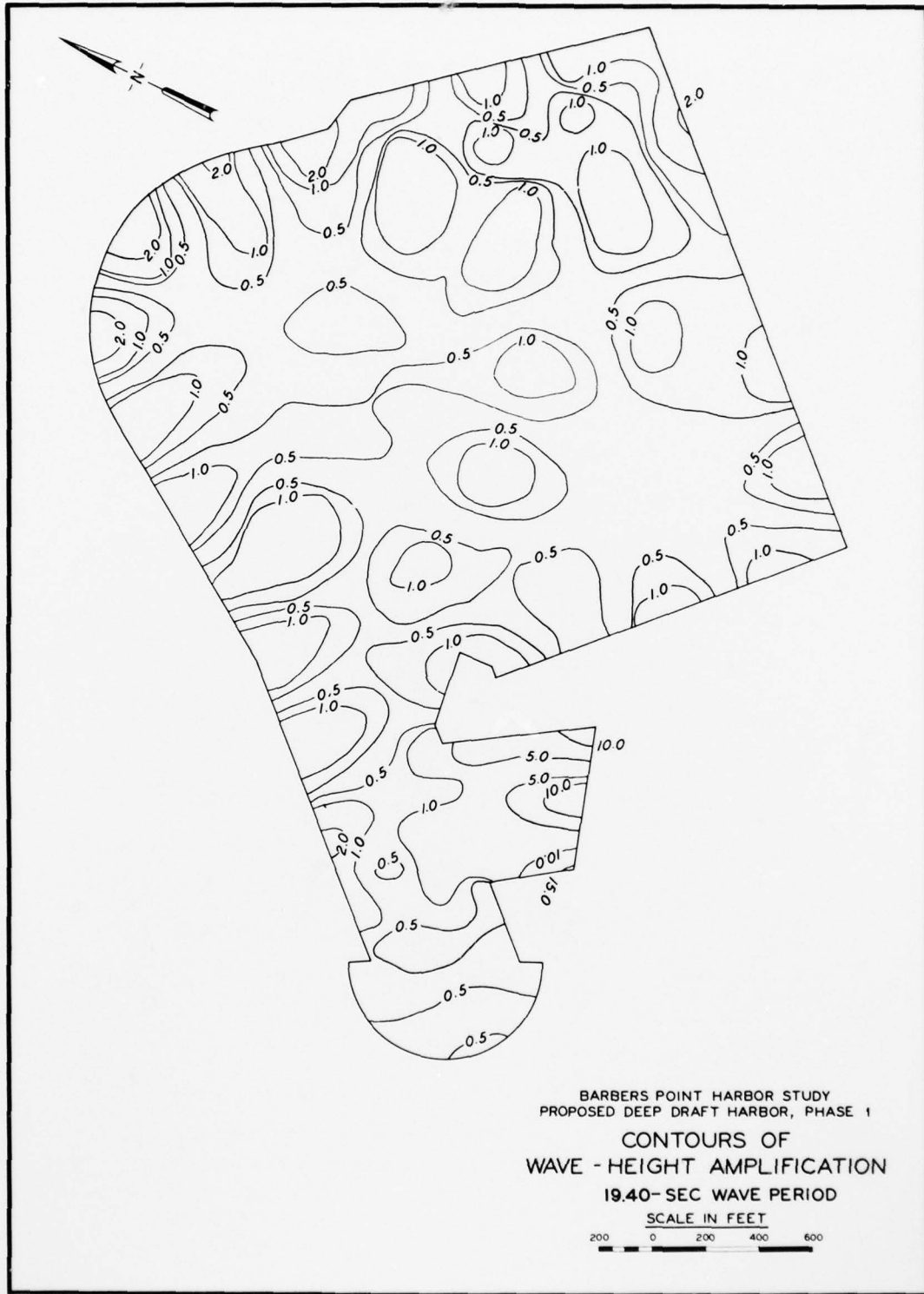
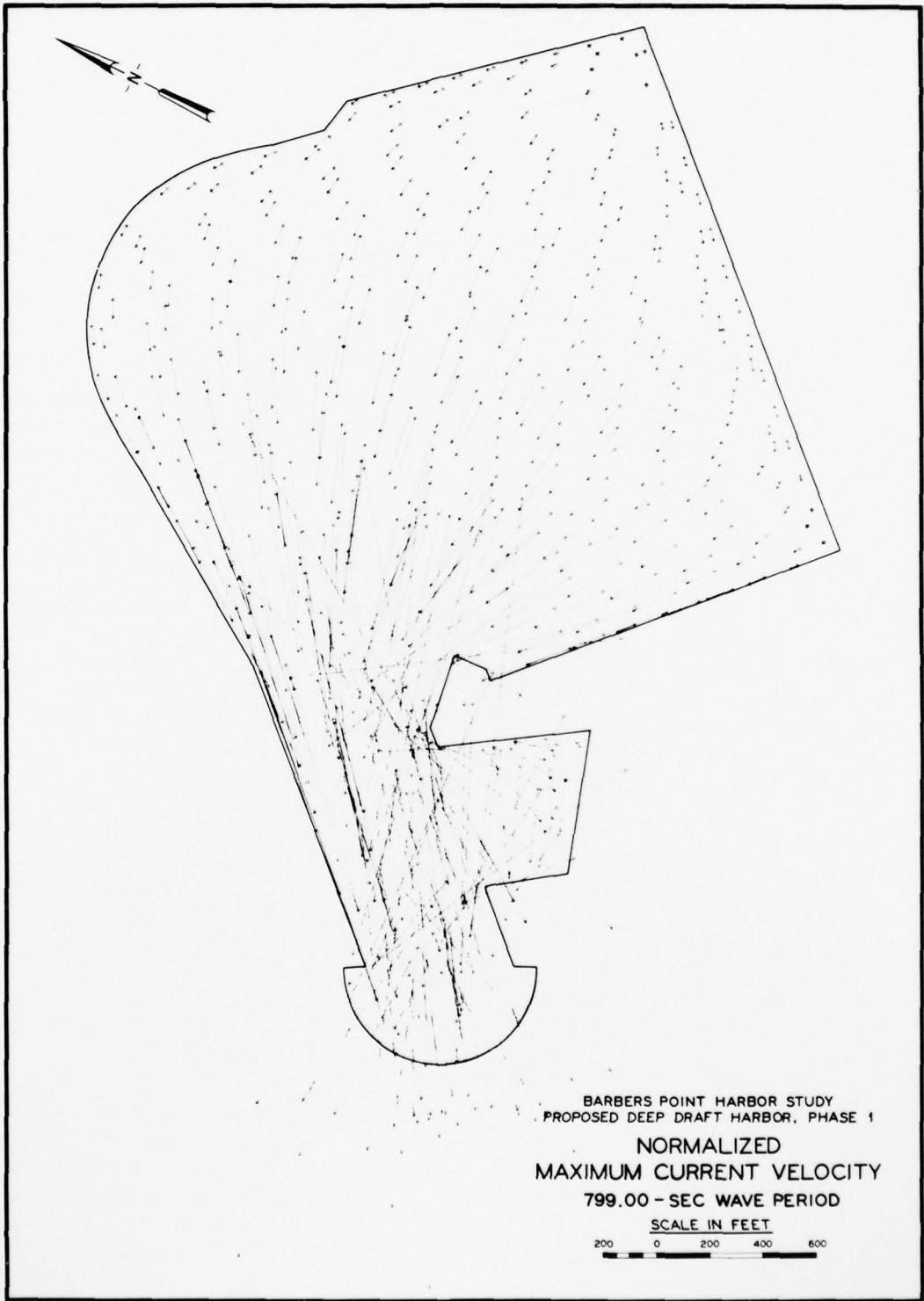


PLATE 148





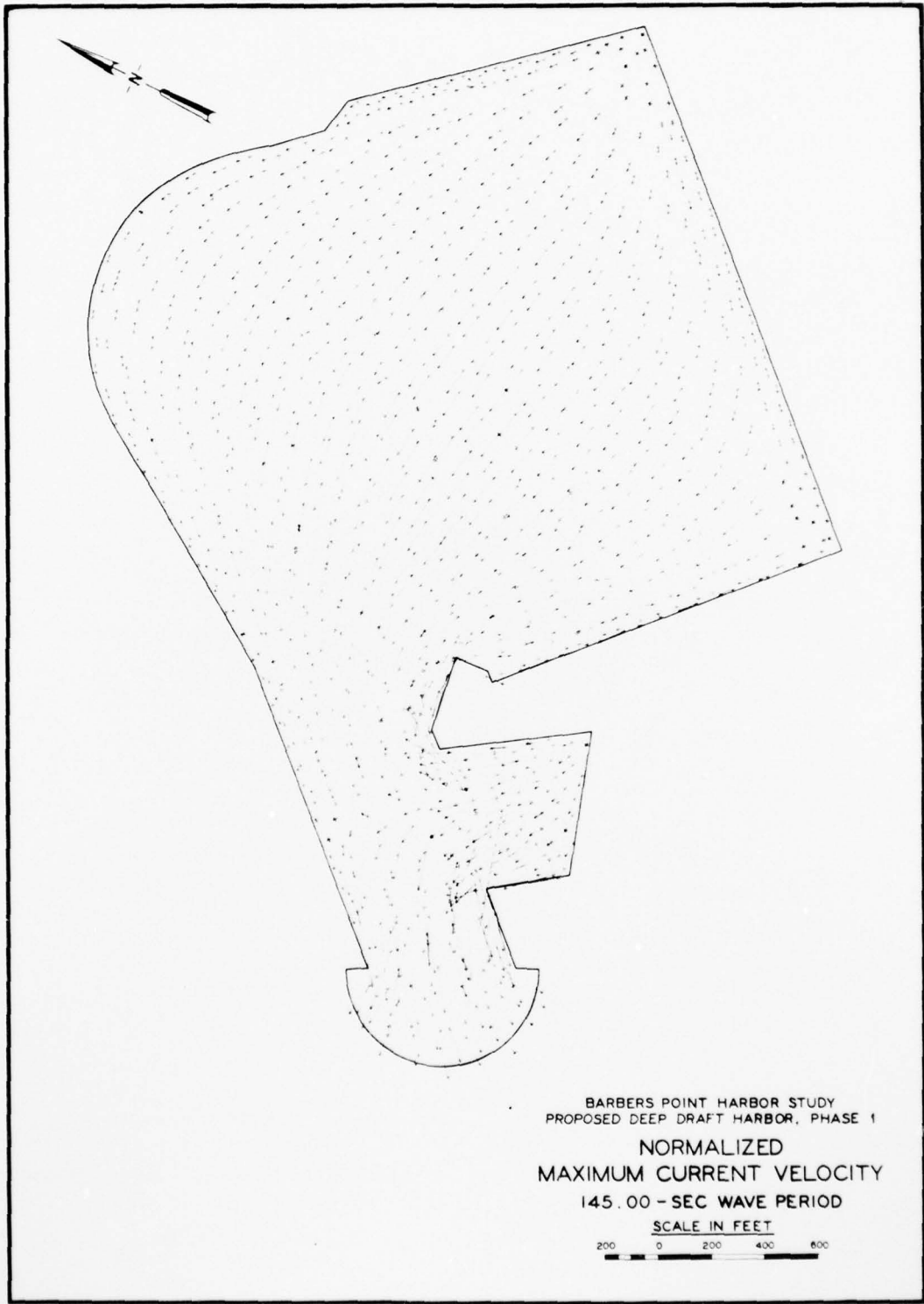
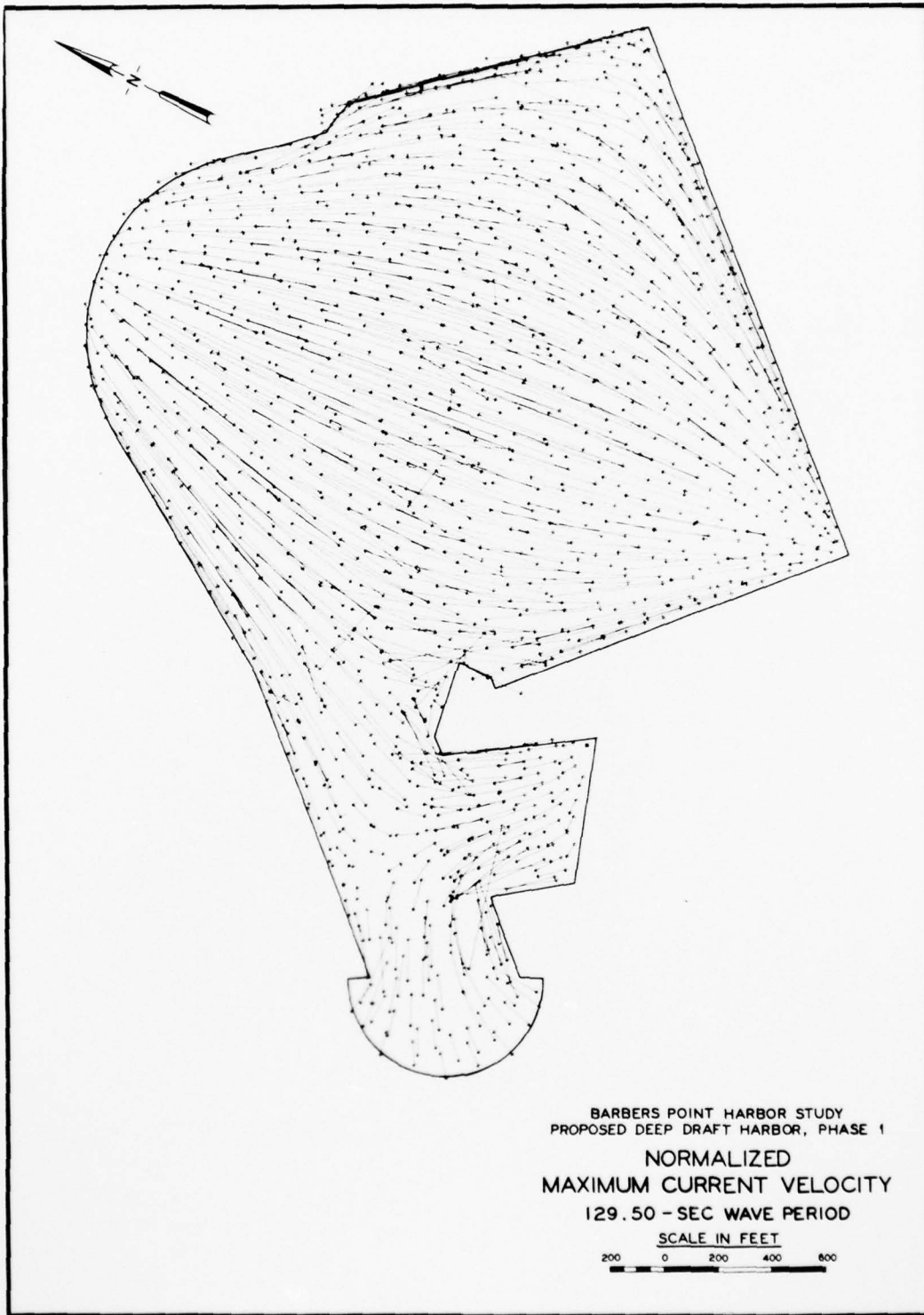


PLATE 150



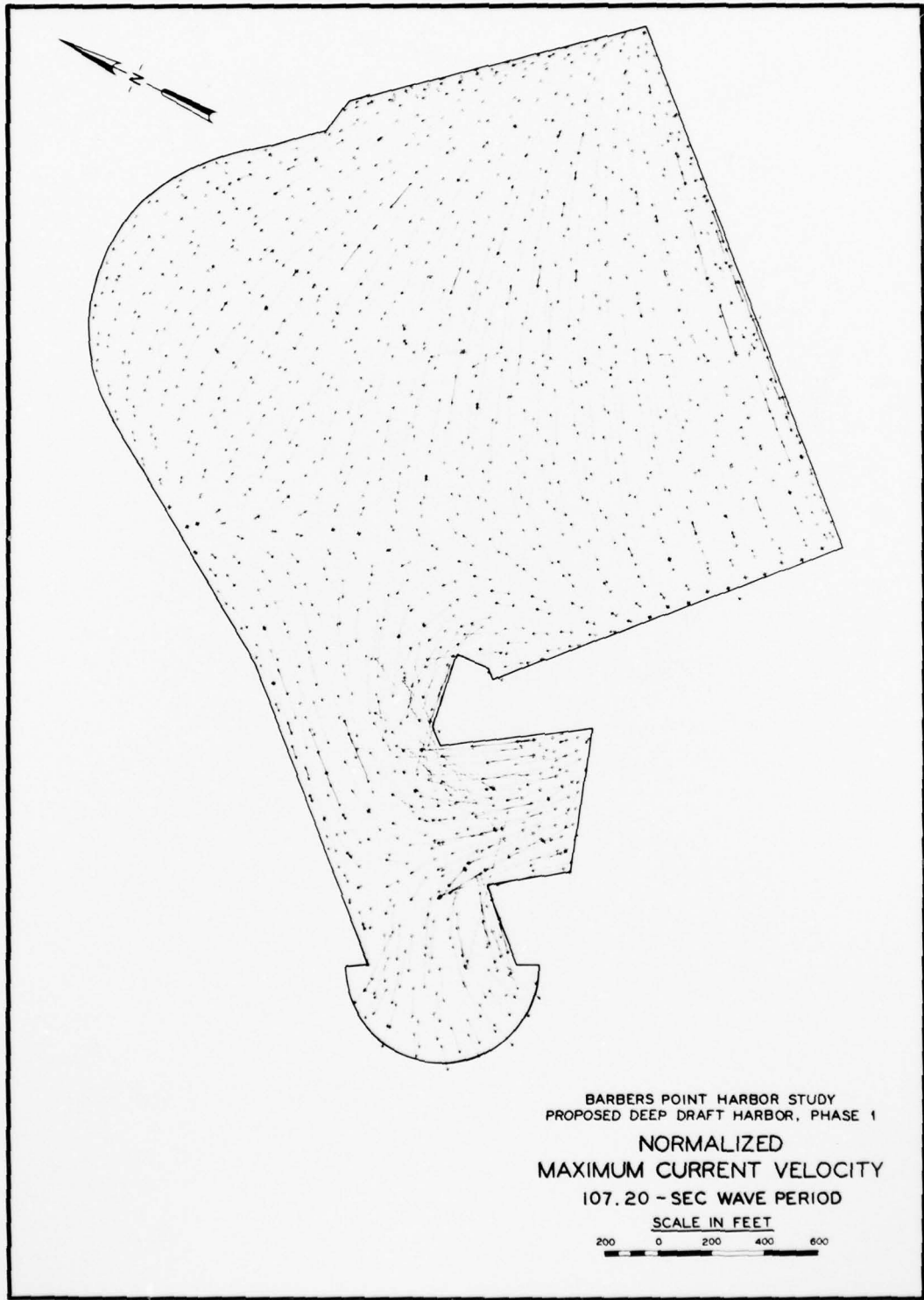
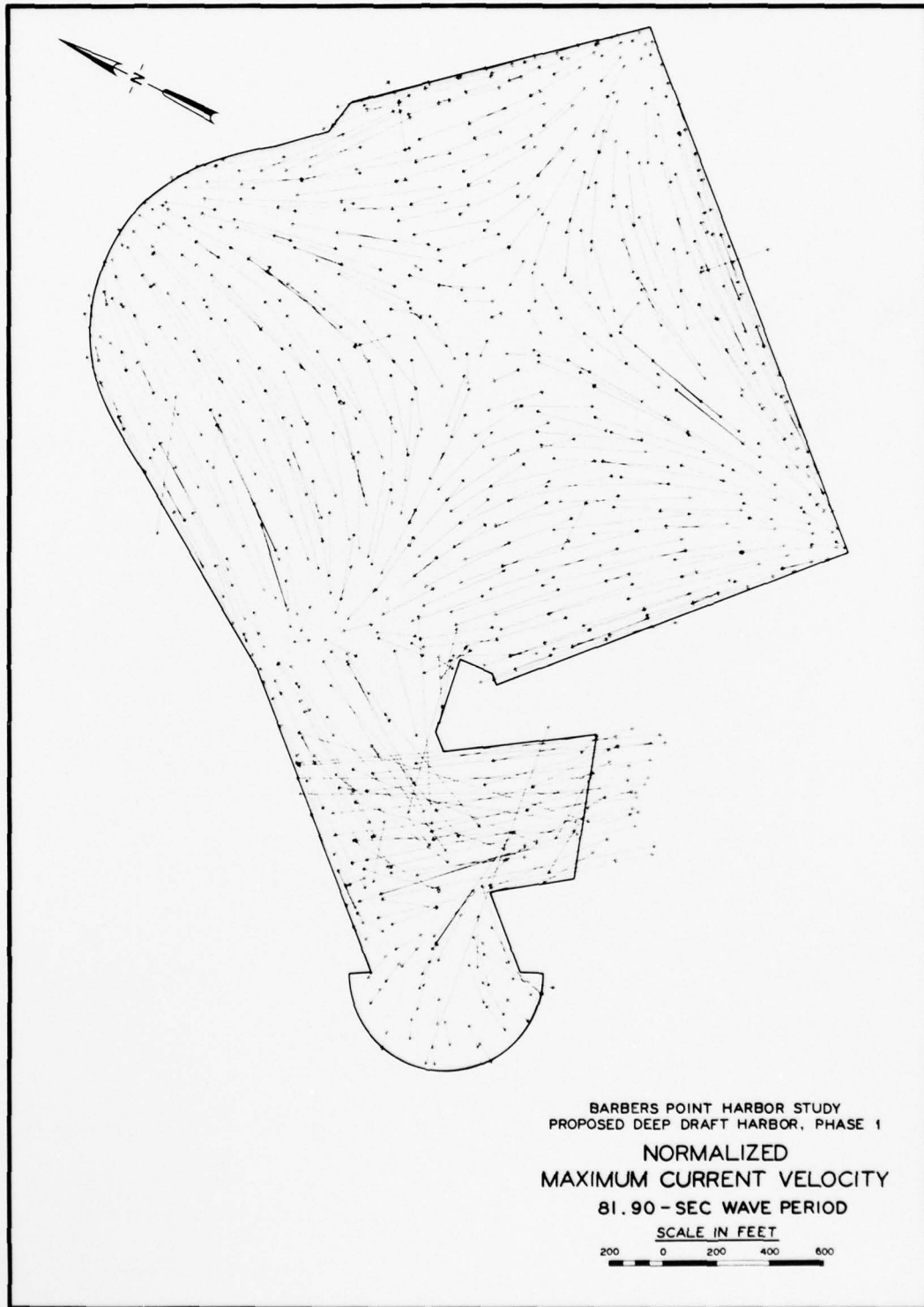


PLATE 152



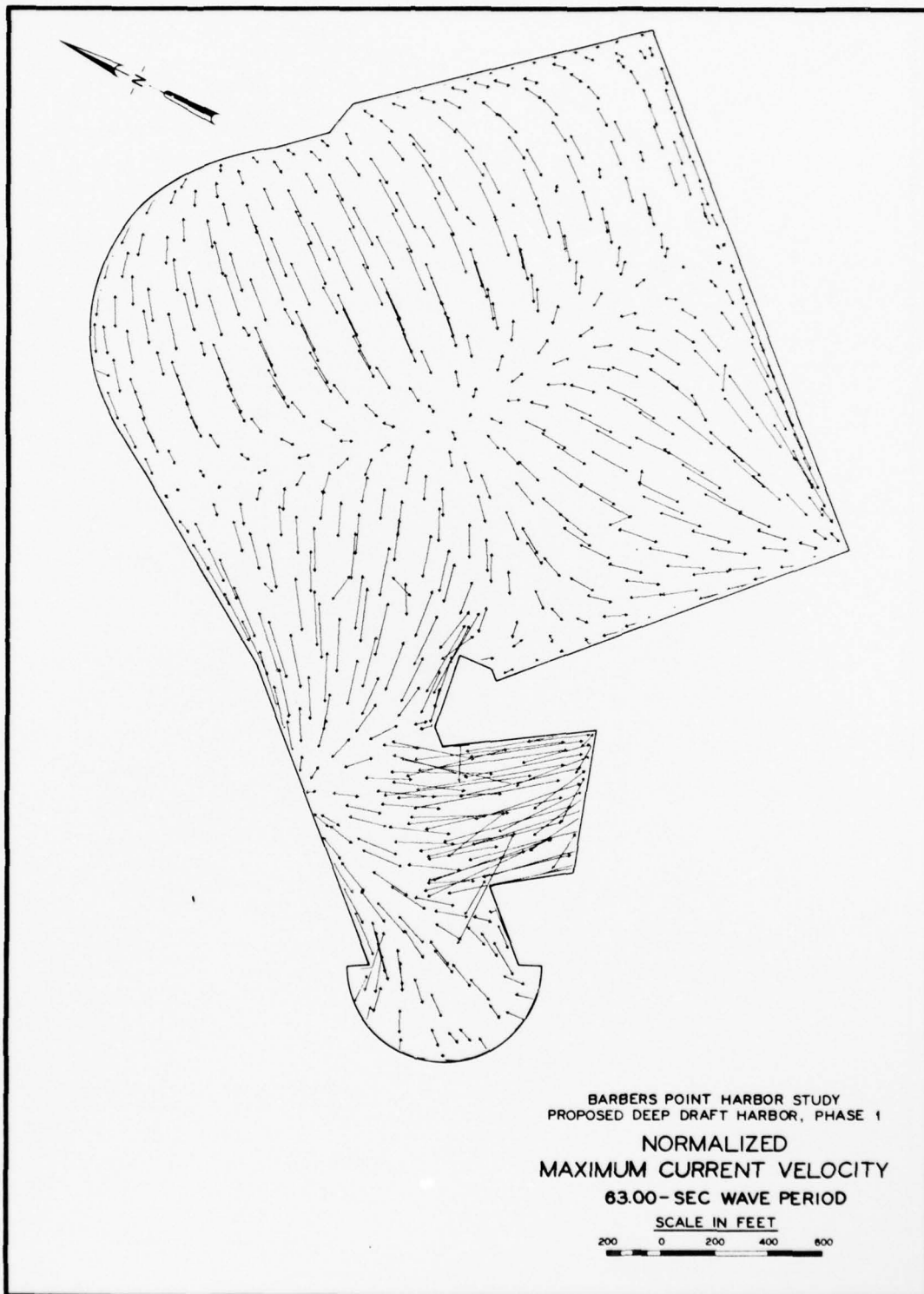
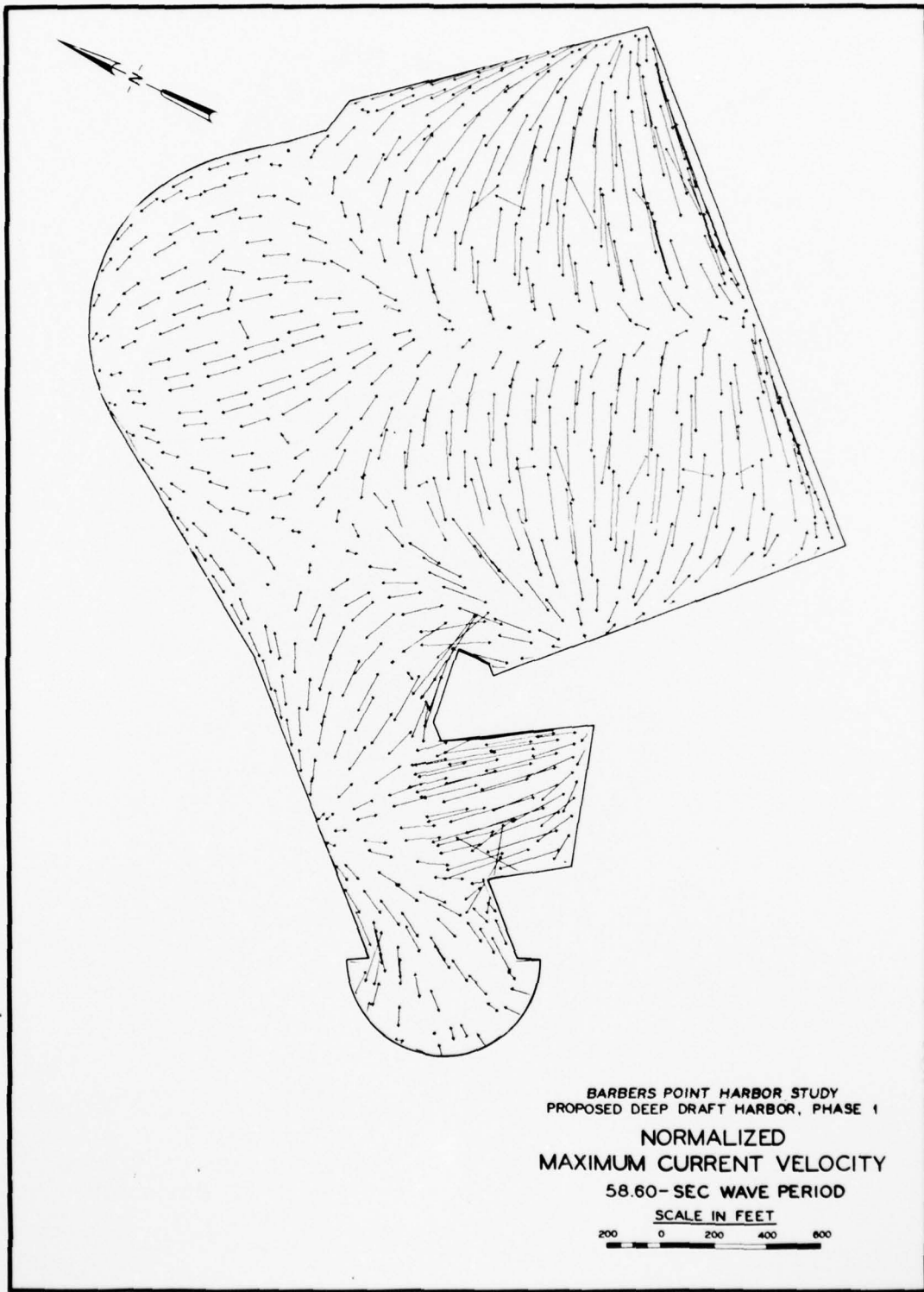


PLATE 154



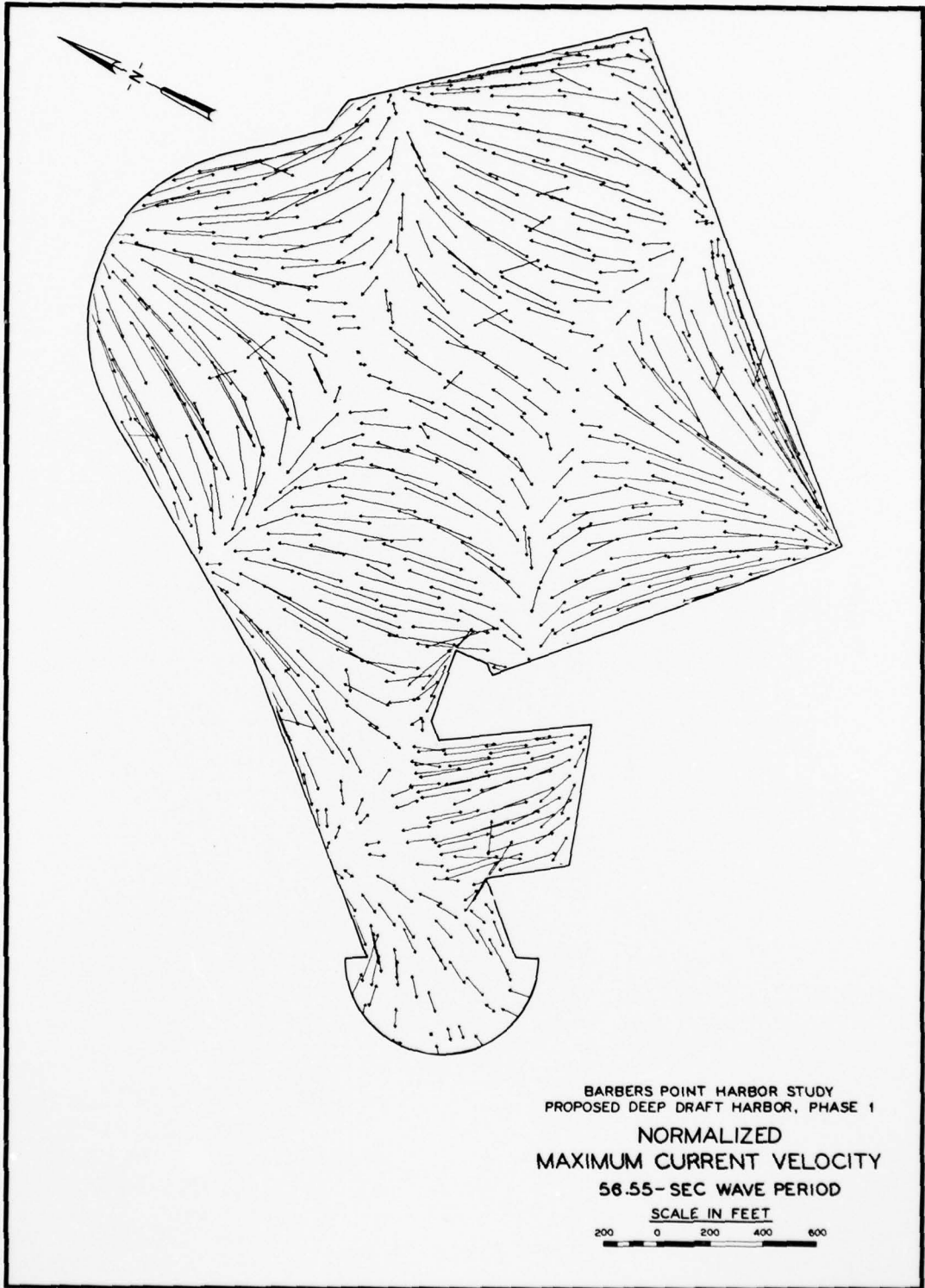


PLATE 156



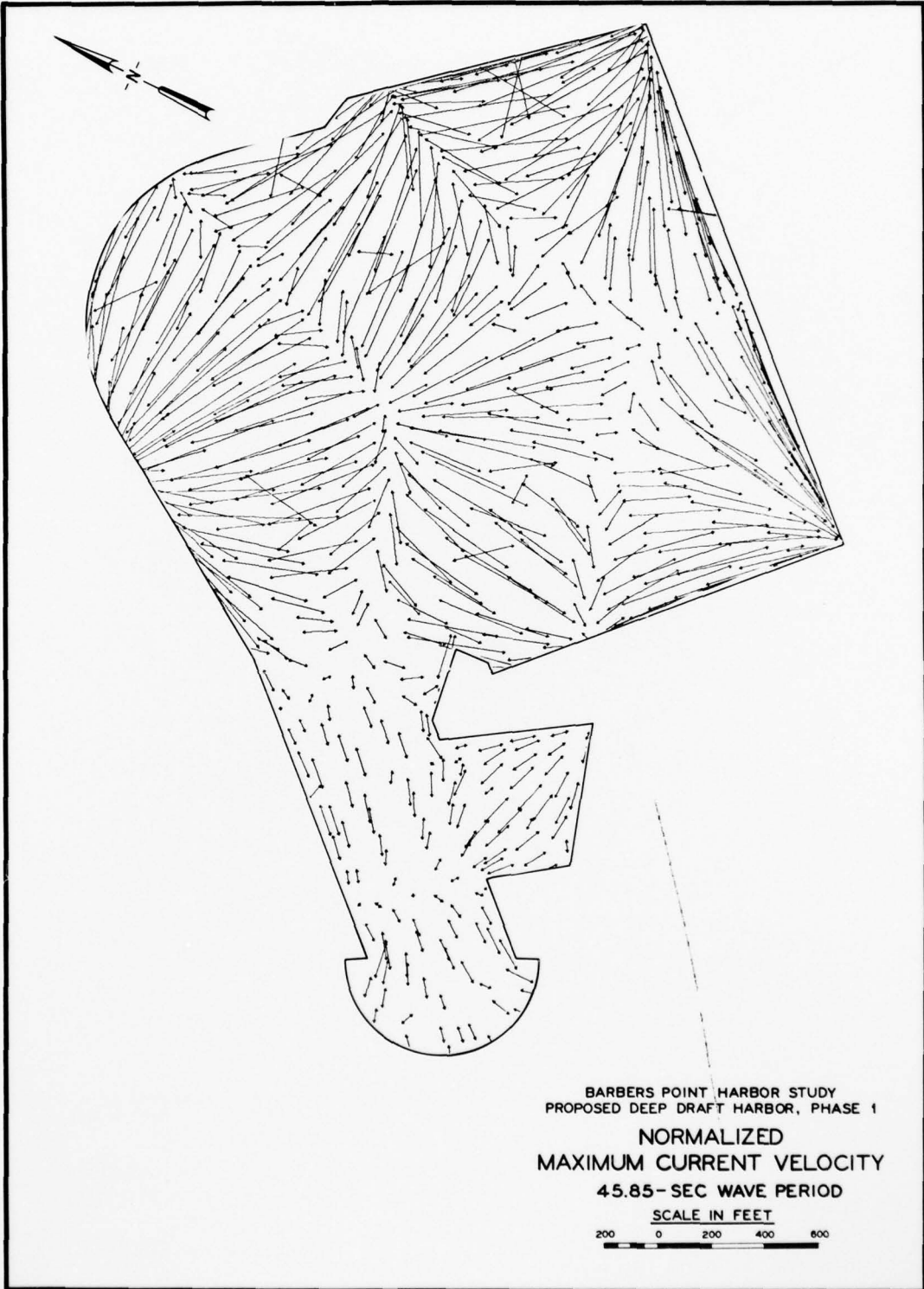


PLATE 157

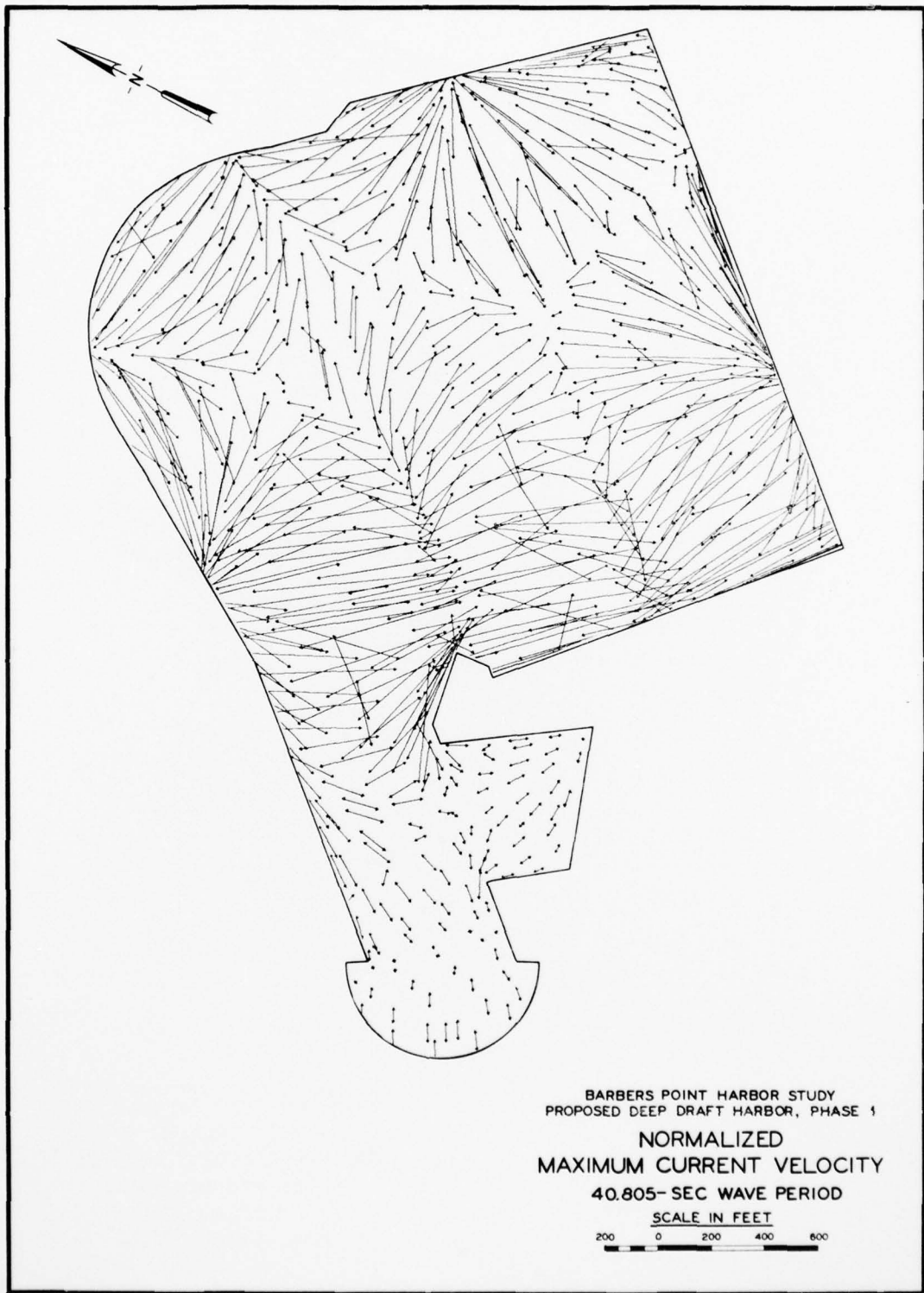
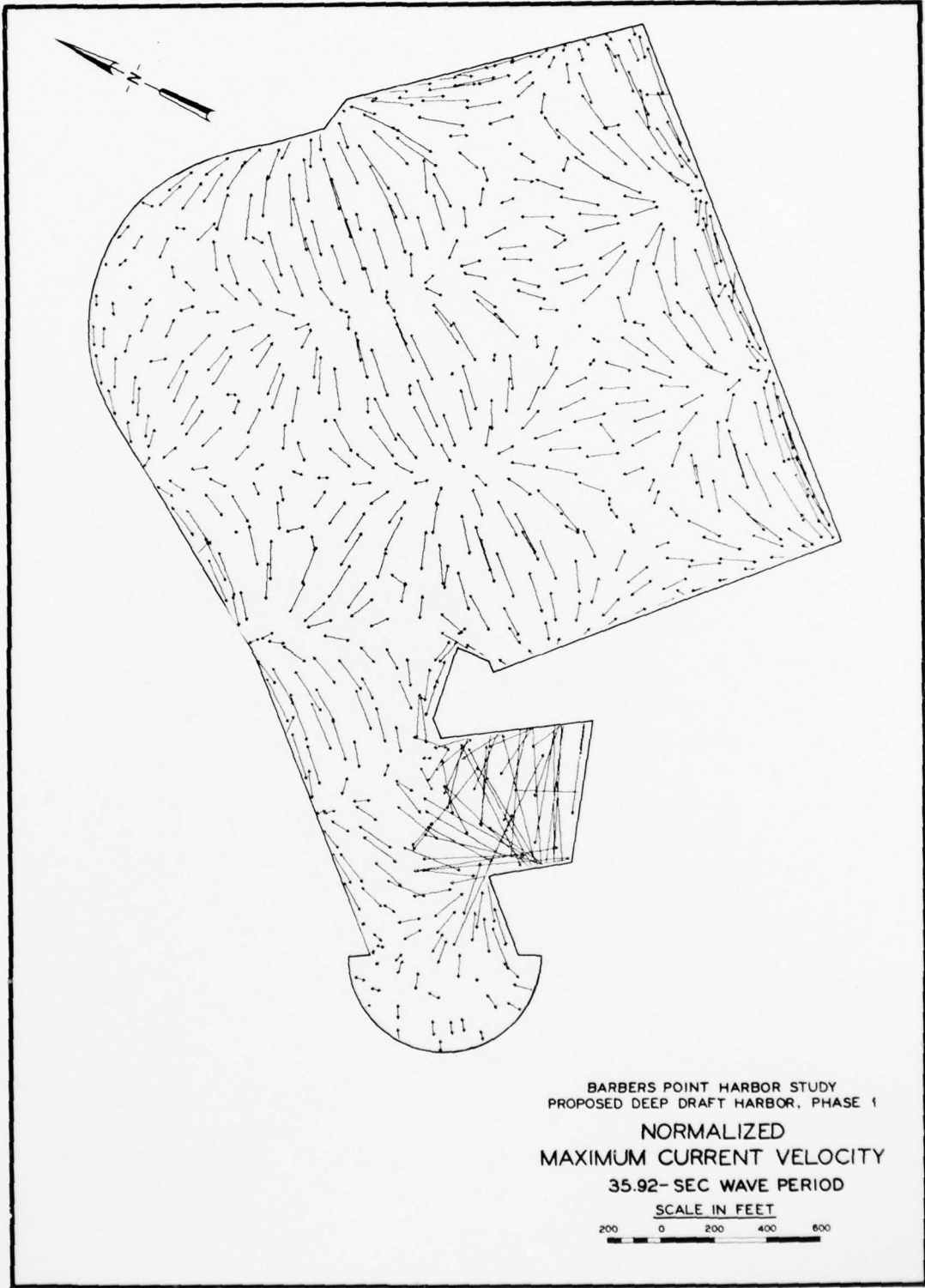


PLATE 158



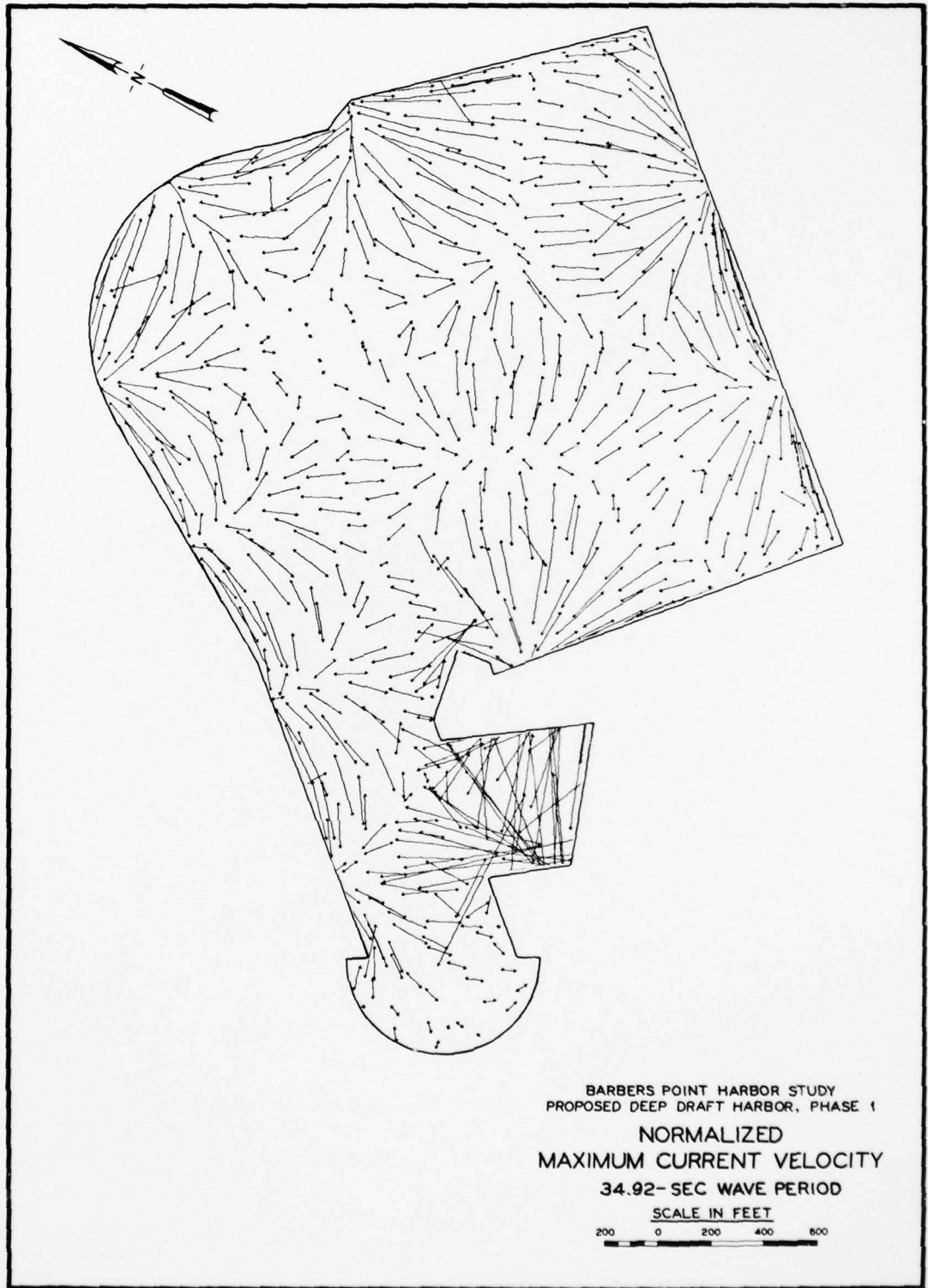


PLATE 160

AD-A063 795

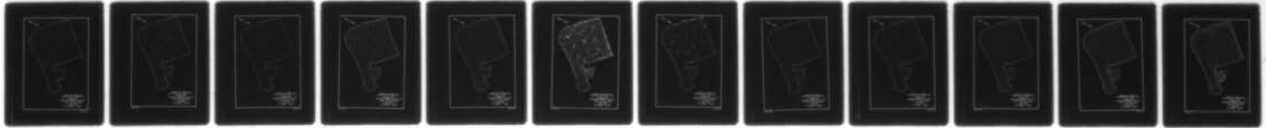
ARMY ENGINEER WATERWAYS EXPERIMENT STATION VICKSBURG MISS F/G 8/3  
NUMERICAL ANALYSIS OF HARBOR OSCILLATIONS FOR BARBERS POINT DEE--ETC(U)  
SEP 78 D L DURHAM  
WES-TR-H-78-20

NL

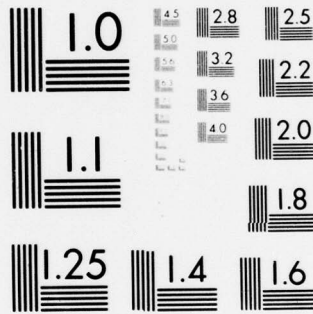
UNCLASSIFIED

3 OF 3

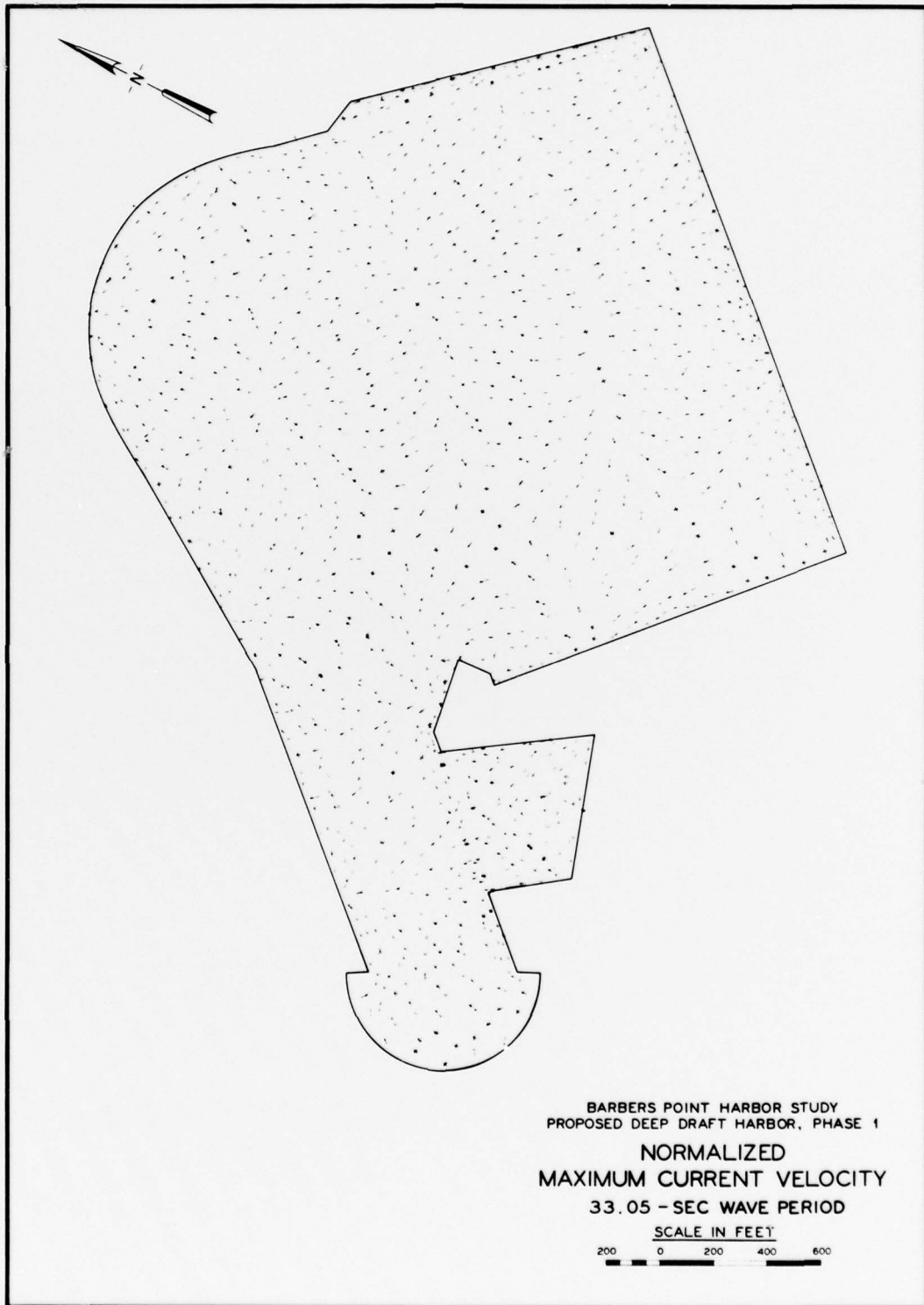
AD  
A063795



END  
DATE  
FILMED  
3-79  
DDC



MICROCOPY RESOLUTION TEST CHART  
NATIONAL BUREAU OF STANDARDS-1963-A



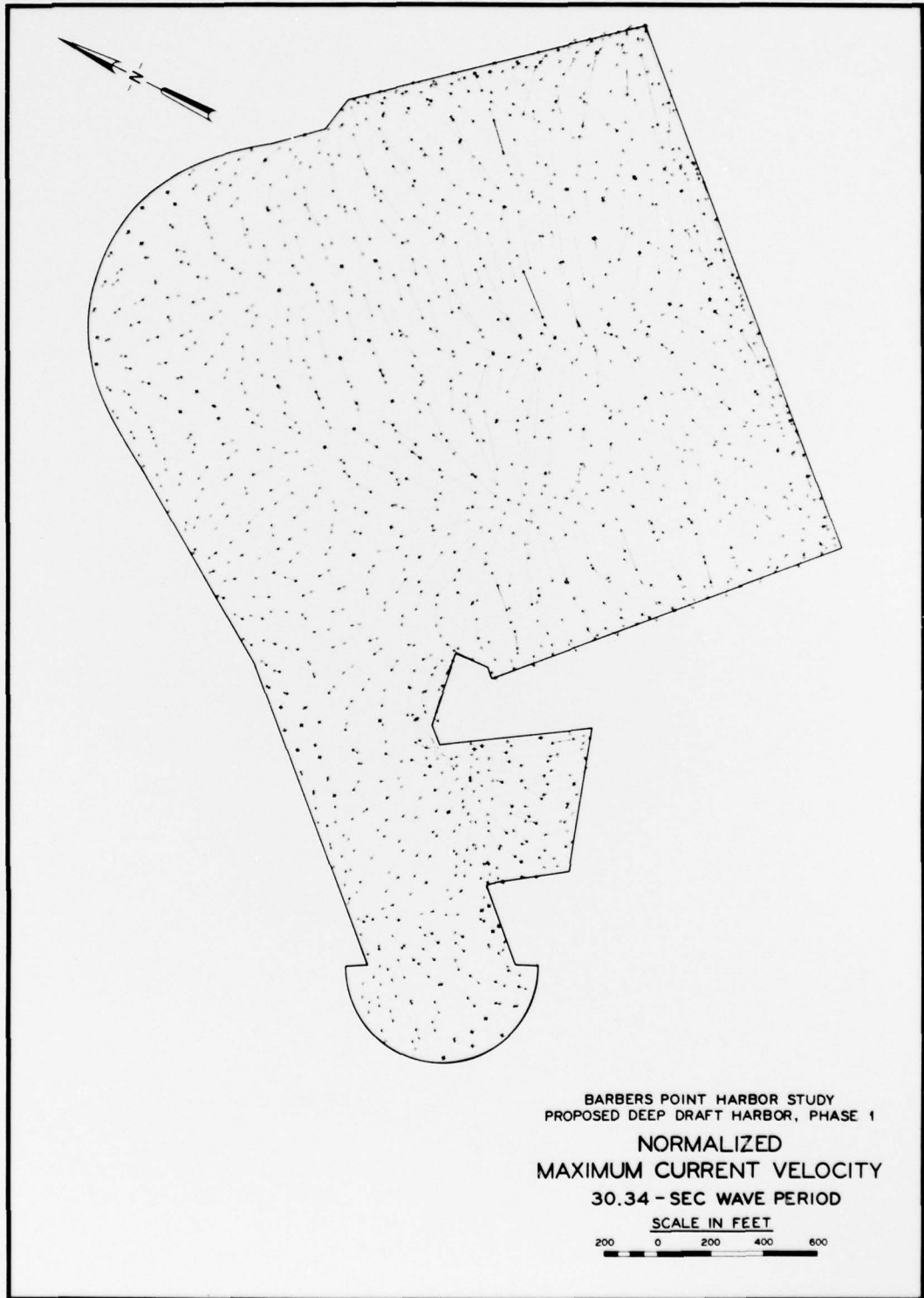
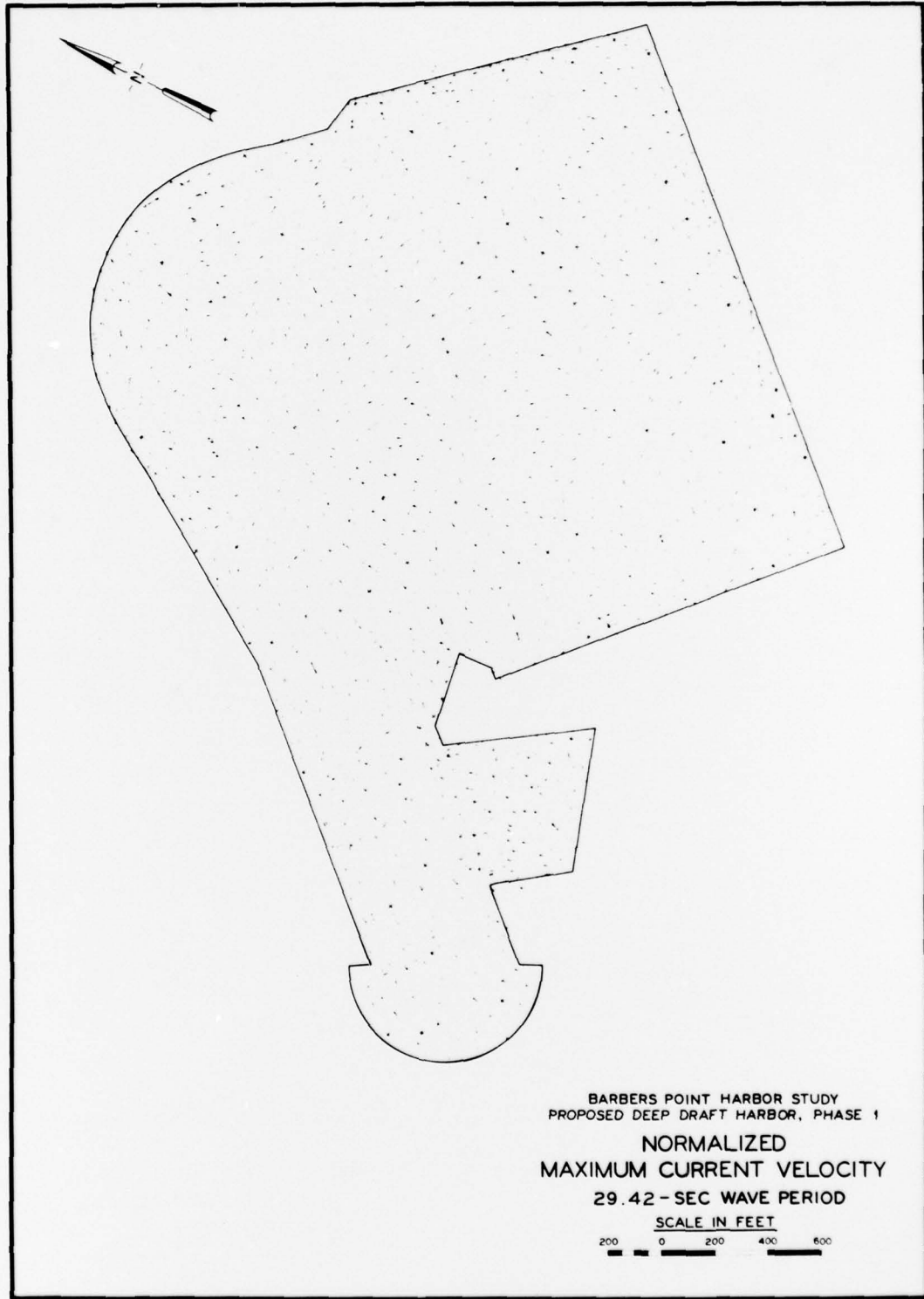


PLATE 162





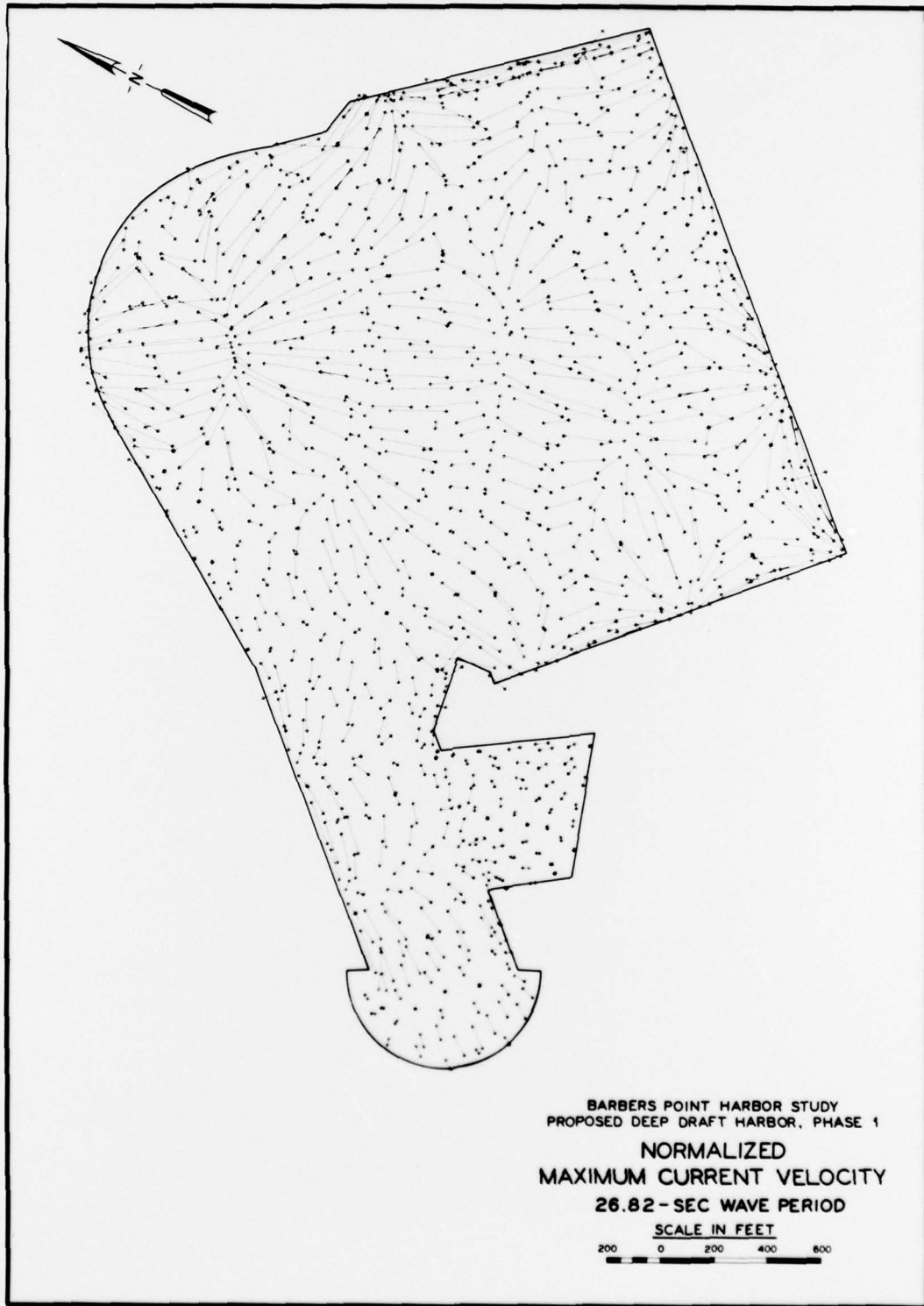
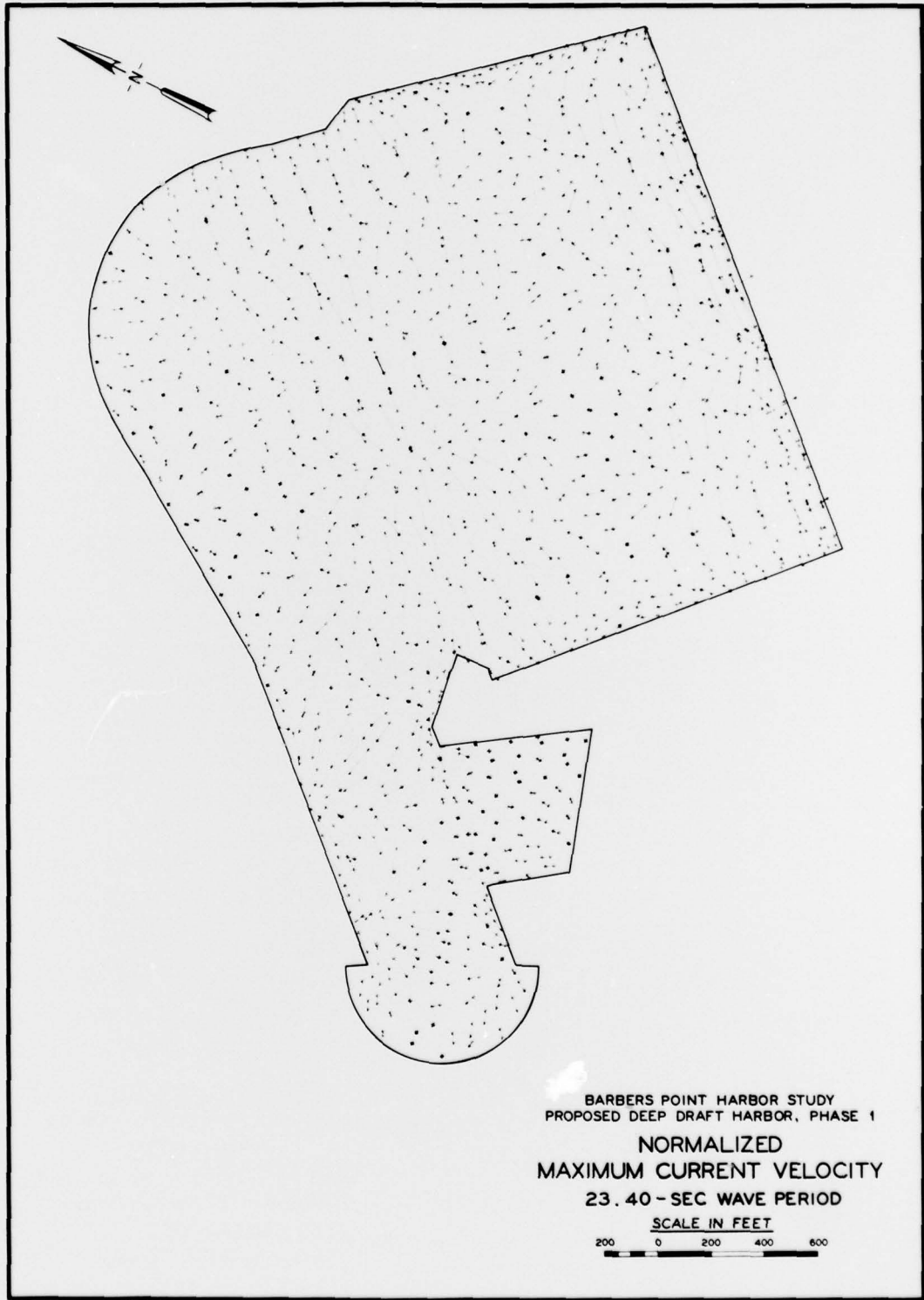


PLATE 164



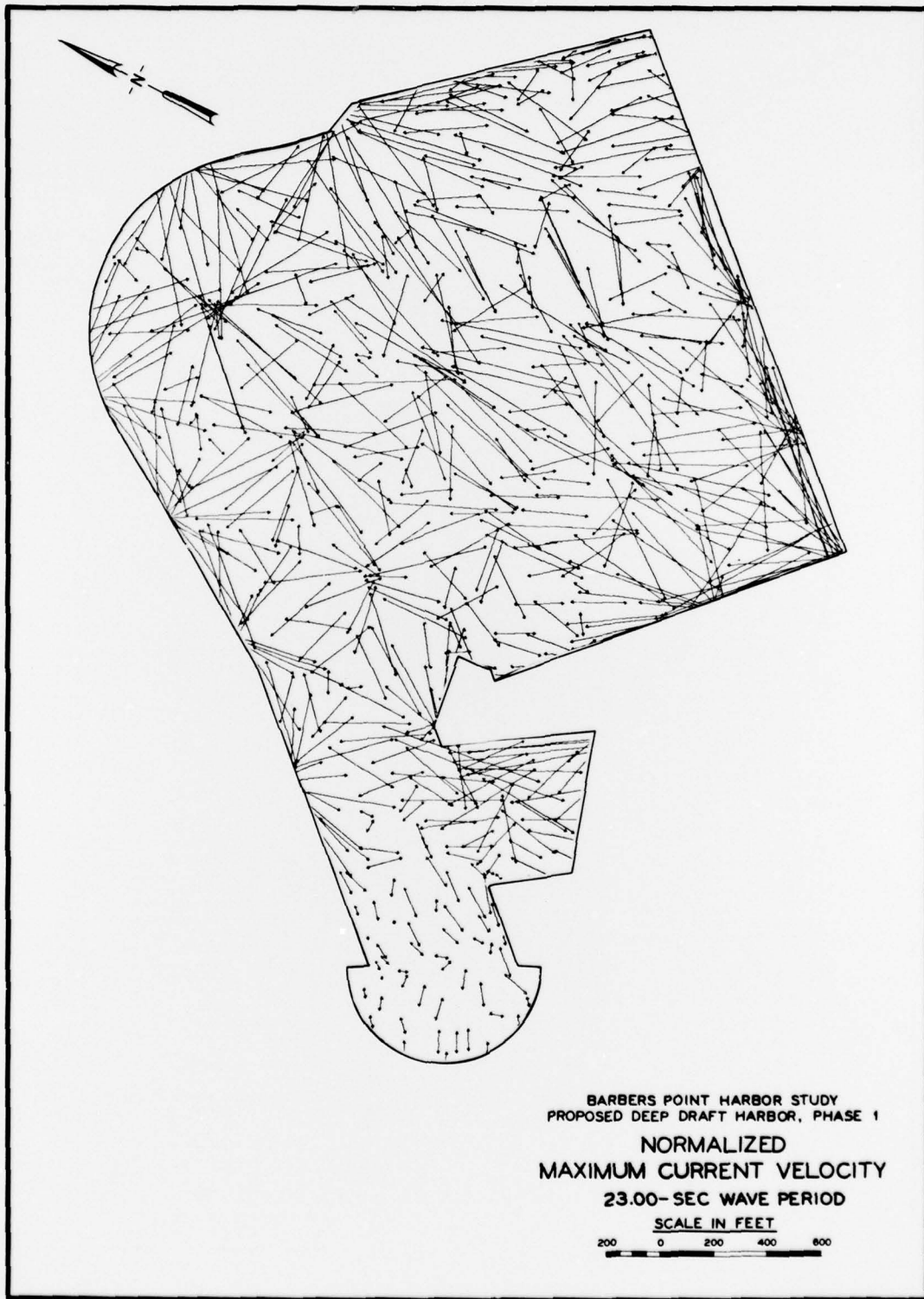


PLATE 166

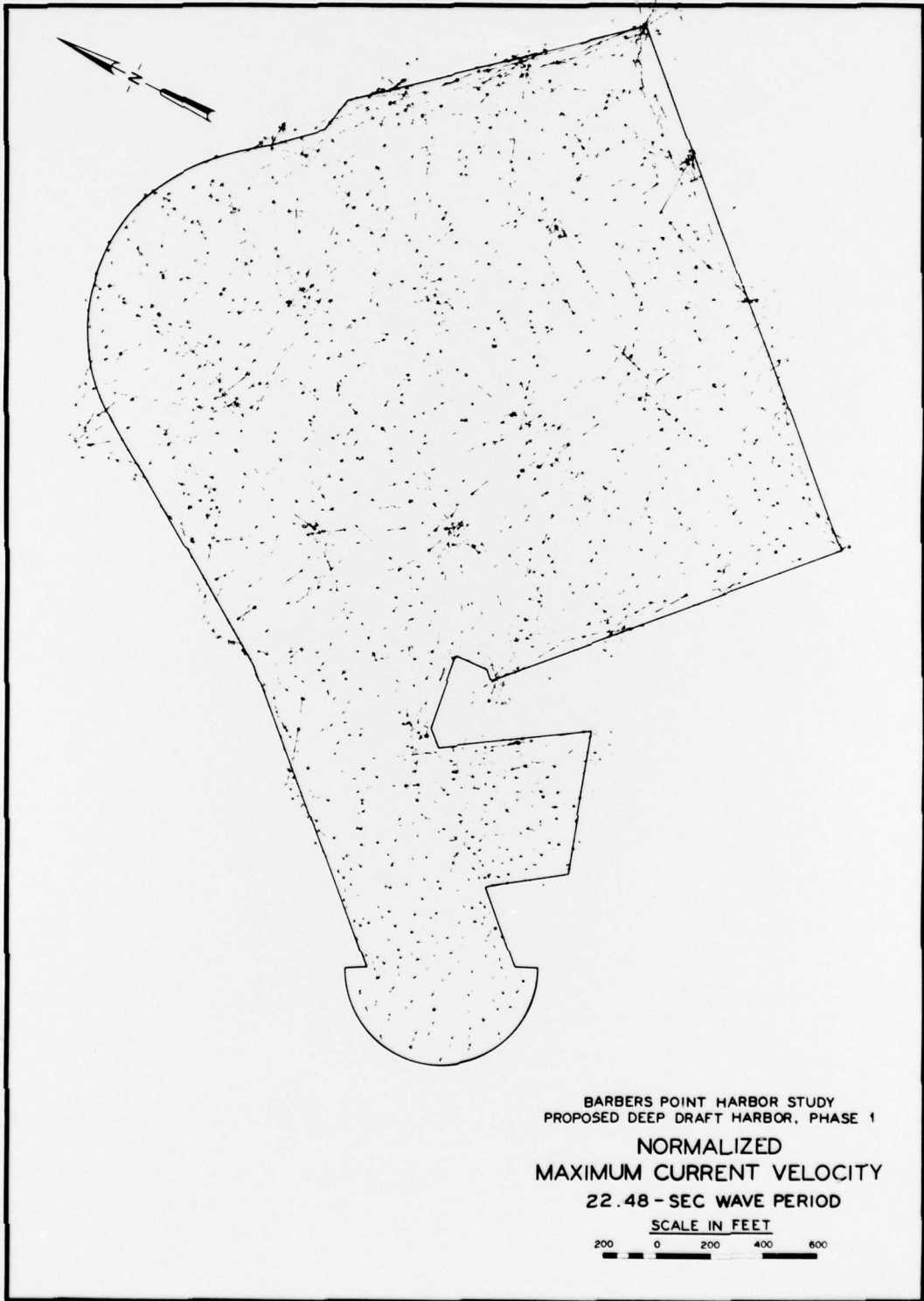


PLATE 167

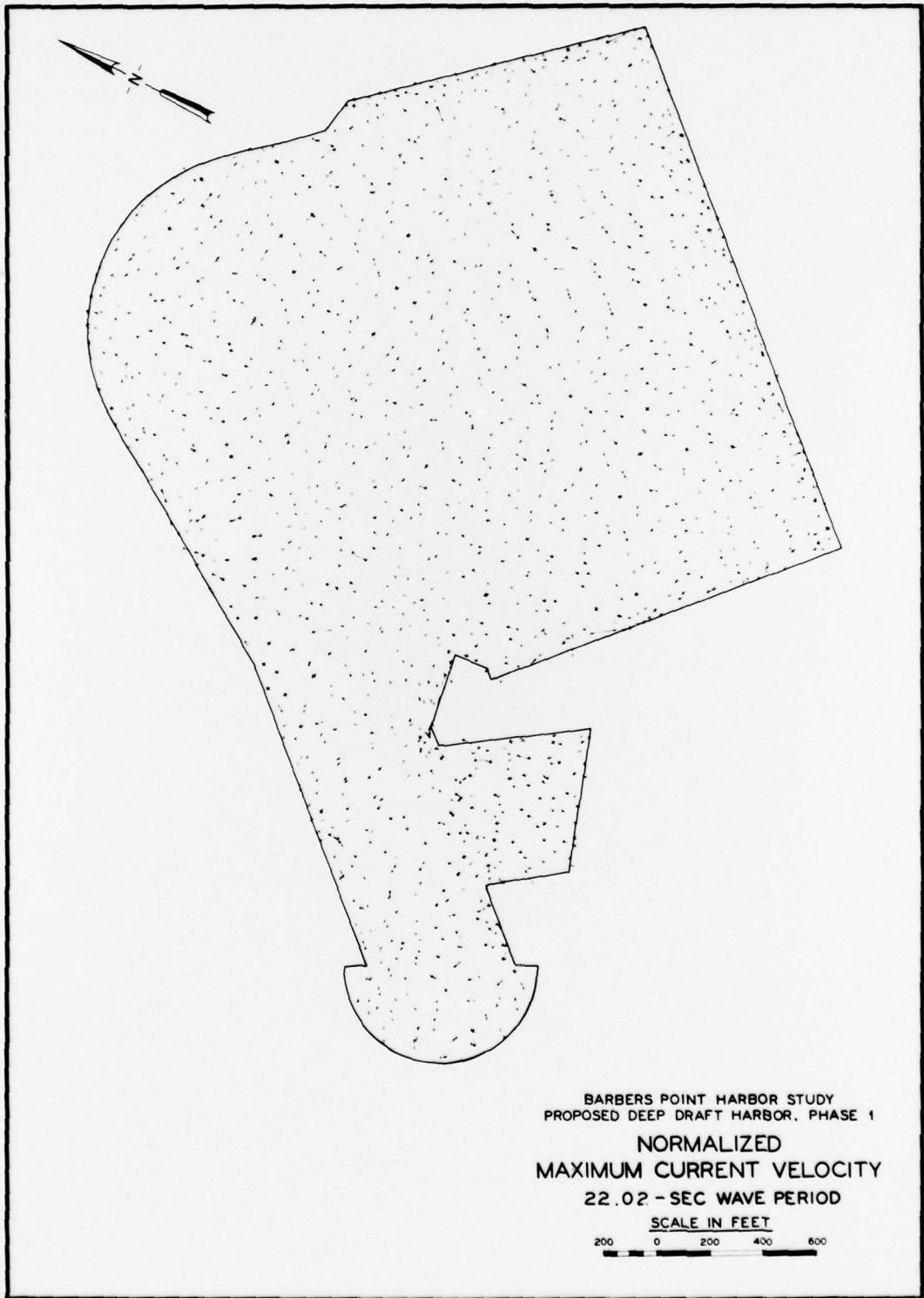
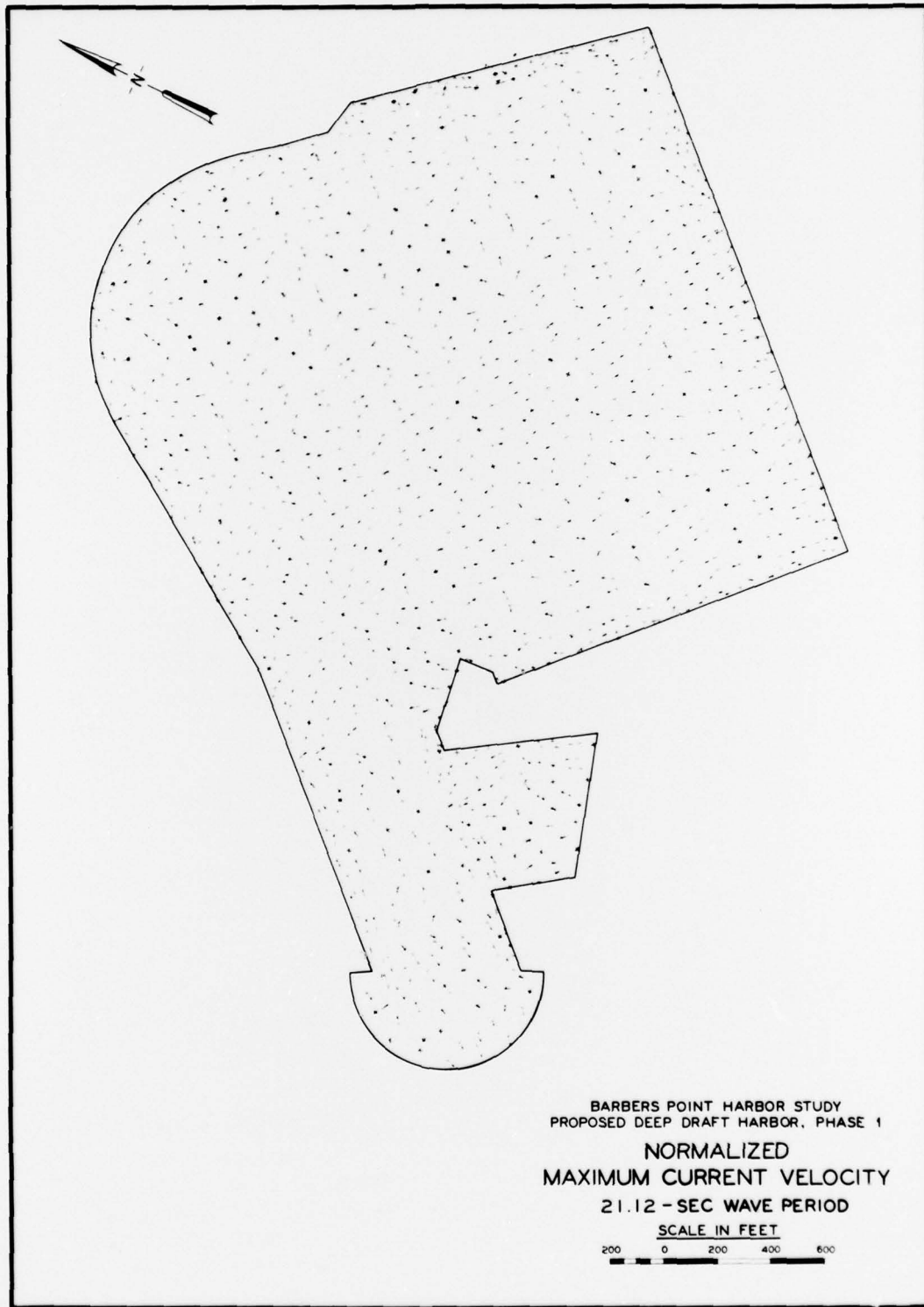


PLATE 168



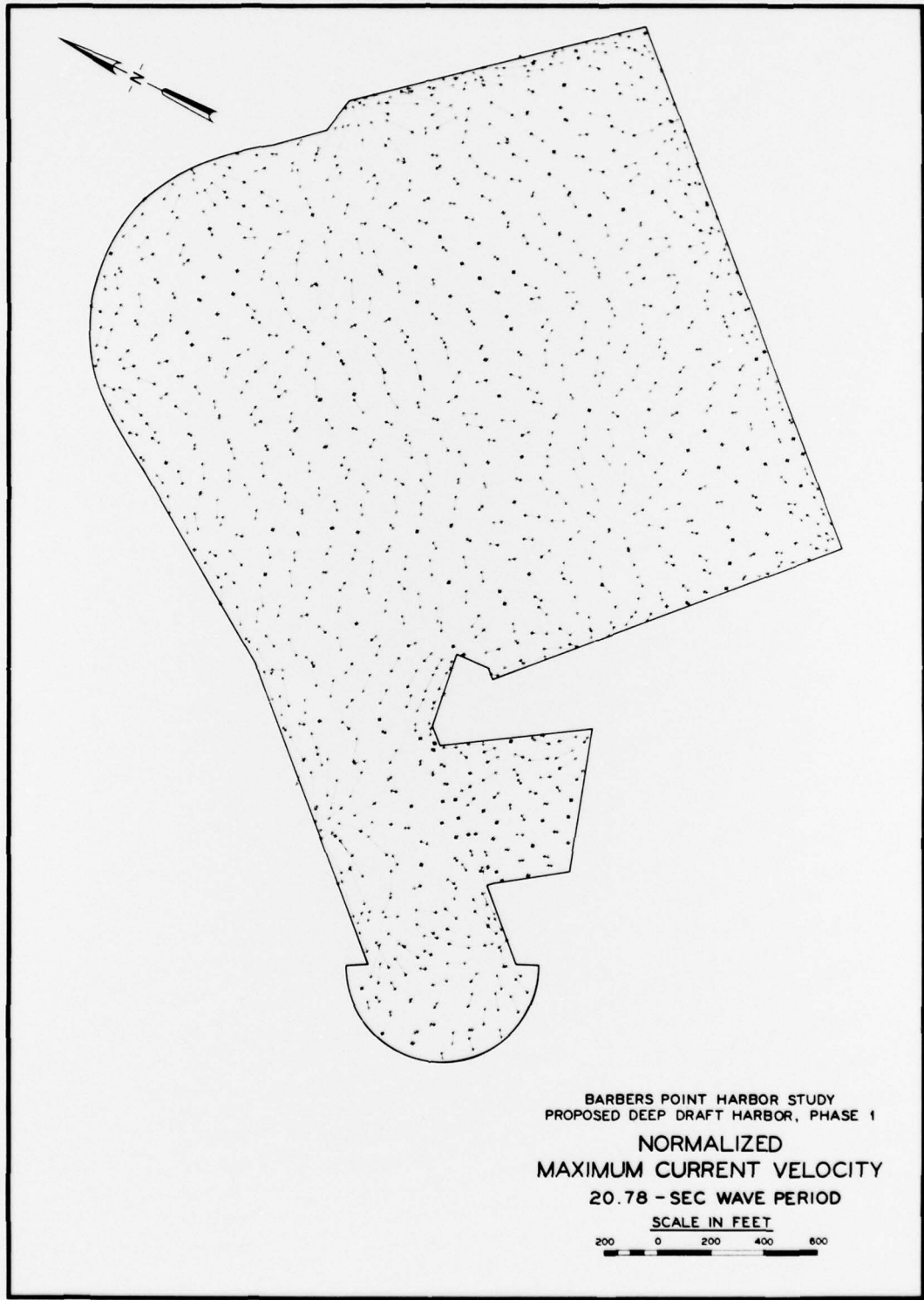
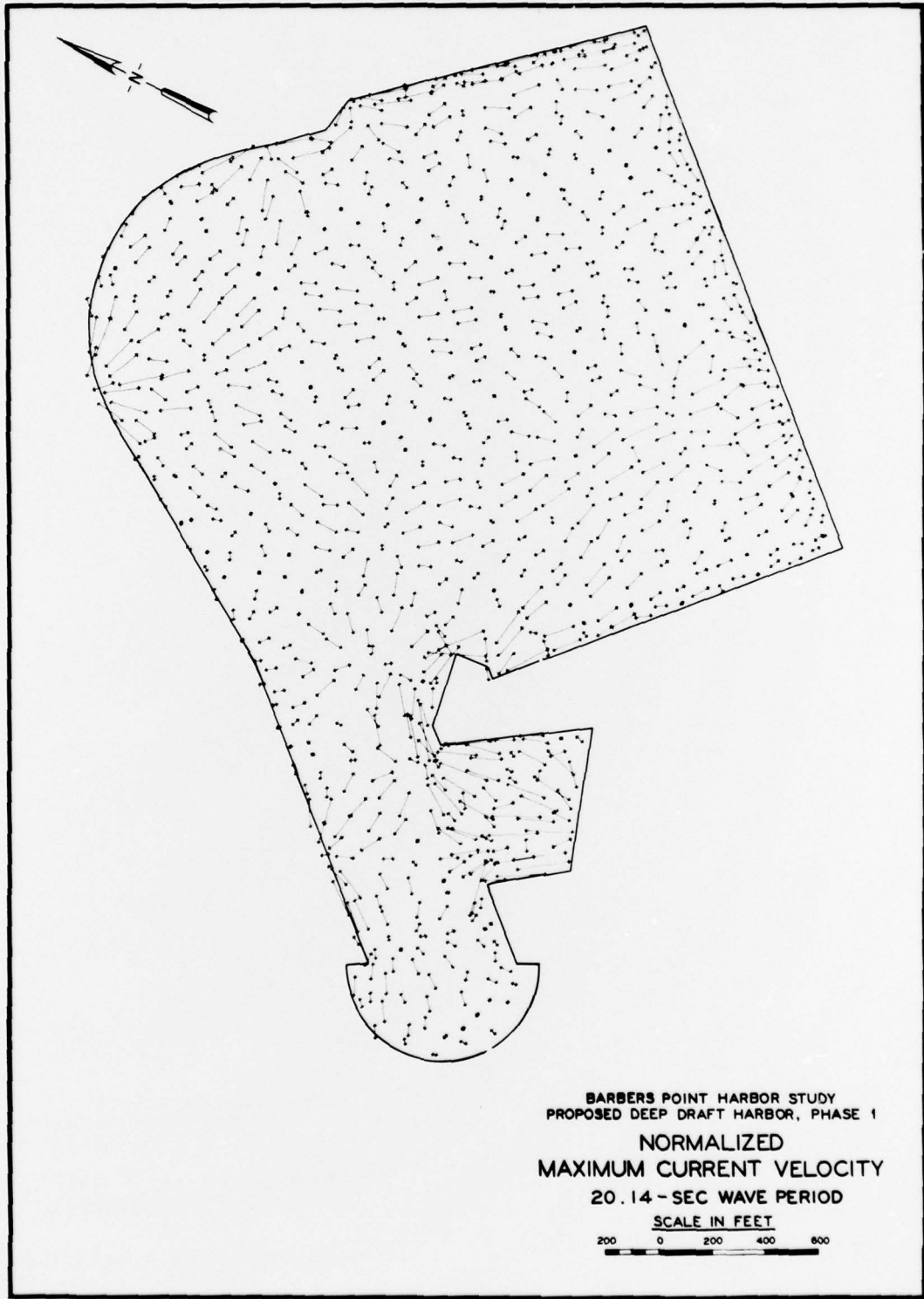


PLATE 170





BARBERS POINT HARBOR STUDY  
PROPOSED DEEP DRAFT HARBOR, PHASE 1  
NORMALIZED  
MAXIMUM CURRENT VELOCITY  
20.14 - SEC WAVE PERIOD  
SCALE IN FEET  
200 0 200 400 600

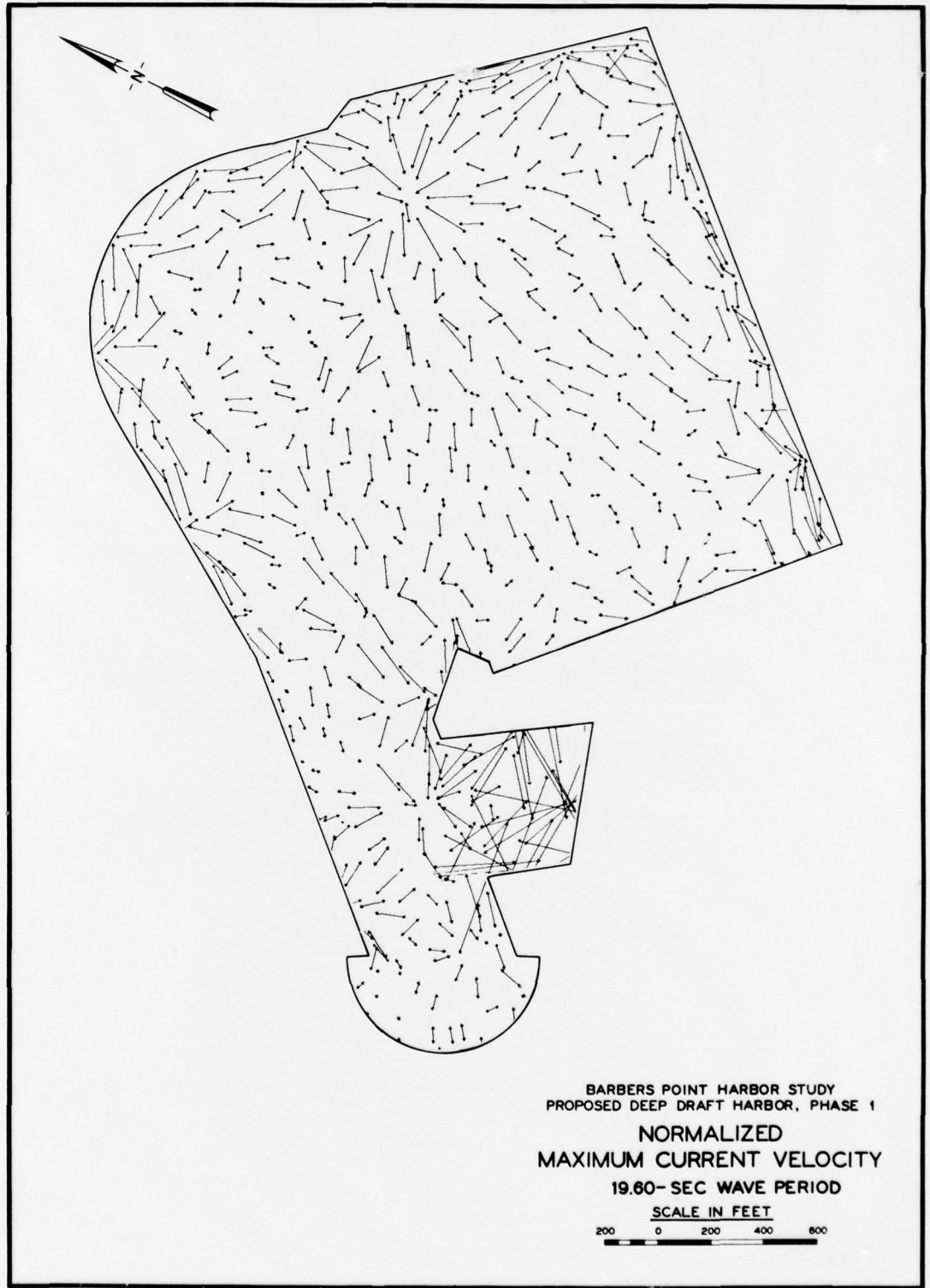
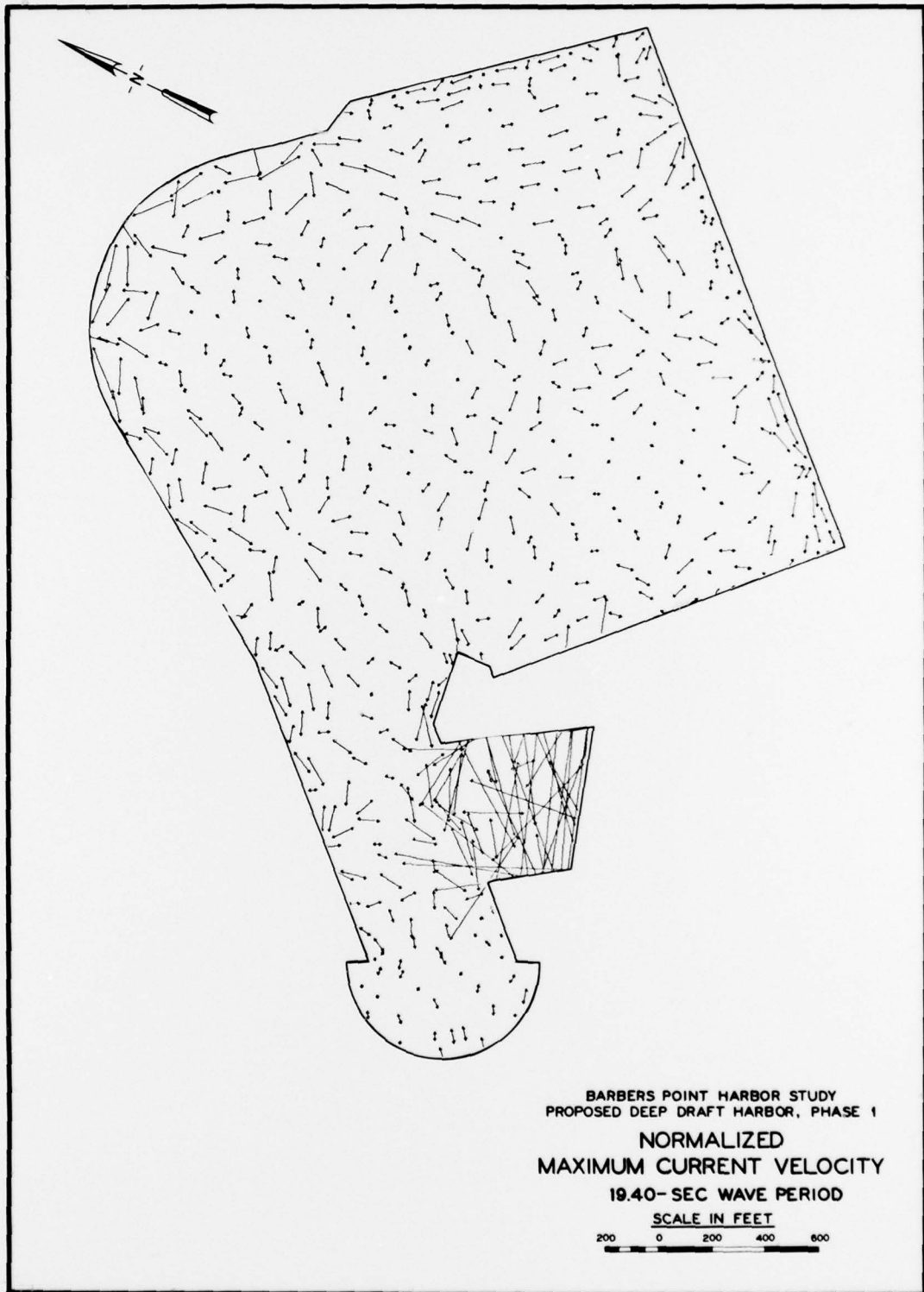


PLATE 172



APPENDIX A: NOTATION

$a$	Boundary of region
$A$	Region inside harbor
$b(\omega)$	Amplitude of frequency component $\omega$
$b_0$	Incident wave amplitude
$g$	Acceleration due to gravity, 32.2 ft/sec <sup>2</sup>
$G$	Element slope matrix
$h$	Water depth, ft
$H_n$	Hankel function of the first kind of order $n$
$i$	Imaginary number
$k$	Wave number
$n$	Integer
$N$	Interpolation function
$n_a$	Unit normal vector outward from region $A$
$r$	Spherical coordinate, ft
$R_e$	Real number
$t$	Time, sec
$u$	Velocity in x-direction, fps
$U$	Total horizontal velocity, fps
$v$	Velocity in y-direction, fps
$x$	Cartesian coordinate, ft
$y$	Cartesian coordinate, ft
$\alpha_n$	Unknown coefficient
$\Delta$	Area of element
$\nabla$	Gradient operator, ft <sup>-1</sup>

$\theta$	Spherical coordinate, radians
$\xi$	Response of harbor
$\phi$	Total velocity potential, $\text{ft}^2/\text{sec}$
$\phi_a$	Total velocity potential evaluated on boundary $a$ , $\text{ft}^2/\text{sec}$
$\phi_I$	Velocity potential of incident wave, $\text{ft}^2/\text{sec}$
$\phi_R$	Far-field velocity potential, $\text{ft}^2/\text{sec}$
$\phi_S$	Scattered wave velocity potential, $\text{ft}^2/\text{sec}$
$\omega$	Angular frequency, radians/sec

In accordance with letter from DAEN-RDC, DAEN-ASI dated 22 July 1977, Subject: Facsimile Catalog Cards for Laboratory Technical Publications, a facsimile catalog card in Library of Congress MARC format is reproduced below.

Durham, Donald L

Numerical analysis of harbor oscillations for Barbers Point deep-draft harbor / by Donald L. Durham. Vicksburg, Miss. : U. S. Waterways Experiment Station ; Springfield, Va. : available from National Technical Information Service, 1978.

26, [4] p., 173 leaves of plates : ill. ; 27 cm.  
(Technical report - U. S. Army Engineer Waterways Experiment Station ; H-78-20)

Prepared for U. S. Army Engineer Division, Pacific Ocean, Fort Shafter, Hawaii.

References: p. 26.

1. Barbers Point, Hawaii -- Harbor. 2. Deep draft harbors. 3. Harbor oscillations. 4. Harbors. 5. Mathematical models. I. United States. Army. Corps of Engineers. Pacific Ocean Division. II. Series: United States. Waterways Experiment Station, Vicksburg, Miss. Technical report ; H-78-20.  
TA7.W34 no.H-78-20